AD_____

GRANT NUMBER DAMD17-94-J-4111

TITLE: Breast Cancer Predoctoral Training Program

PRINCIPAL INVESTIGATOR: Stuart A. Aaronson, M.D.

CONTRACTING ORGANIZATION: Mount Sinai School of Medicine
New York, New York 10029-6574

REPORT DATE: June 1998

TYPE OF REPORT: Final

PREPARED FOR: Commander
U.S. Army Medical Research and Materiel Command
Fort Detrick, Frederick, Maryland 21702-5012

REPORT DOCUMENTATION PAGE

Form Approved
OMB No. 0704-0188

1. AGENCY USE ONLY *(Leave blank)*	2. REPORT DATE	3. REPORT TYPE AND DATES COVERED
	June 1998	Final (1 Jul 94 - 30 Jun 98)

4. TITLE AND SUBTITLE
Breast Cancer Predoctoral Training Program

5. FUNDING NUMBERS
DAMD17-94-J-4111

6. AUTHOR(S)
Stuart A. Aaronson, M.D.

7. PERFORMING ORGANIZATION NAME(S) AND ADDRESS(ES)
Mount Sinai School of Medicine
New York, New York 10029-6574

8. PERFORMING ORGANIZATION REPORT NUMBER

9. SPONSORING/MONITORING AGENCY NAME(S) AND ADDRESS(ES)
Commander
U.S. Army Medical Research and Materiel Command
Fort Detrick, MD 21702-5012

10. SPONSORING/MONITORING AGENCY REPORT NUMBER

11. SUPPLEMENTARY NOTES

12a. DISTRIBUTION / AVAILABILITY STATEMENT
Approved for public release; distribution unlimited

12b. DISTRIBUTION CODE

13. ABSTRACT *(Maximum 200*

The USAMRMC-sponsored Breast Cancer Predoctoral Training Program at the Mount Sinai School of Medicine is completing its fourth and final year with six students currently supported. The training program has served the dual function of encouraging the predoctoral students to focus on the issues of breast cancer in their research and training and at the same time has served as a focal point to bring various Mount Sinai faculty together to stimulate collaborations and research in the area of breast cancer. Support for a given student was limited to a two year period. This strategy encouraged the widest participation in the program and made it possible to support students whose preceptors hold faculty appointments in six different departments/centers within the medical school. The elements of the training program were designed to educate the students concerning important questions in breast cancer research and to stimulate pursuit of careers that involve research into the underlying mechanisms responsible for human breast cancer.

14. SUBJECT TERMS	15. NUMBER OF PAGES
Training, Multidisciplinary, Oncogenes, Growth Factors, Signal Transduction, Epidemiology, Humans, Anatomical Samples, Breast Cancer	90
	16. PRICE CODE

17. SECURITY CLASSIFICATION OF REPORT	18. SECURITY CLASSIFICATION OF THIS PAGE	19. SECURITY CLASSIFICATION OF ABSTRACT	20. LIMITATION OF ABSTRACT
Unclassified	Unclassified	Unclassified	Unlimited

FOREWORD

Opinions, interpretations, conclusions and recommendations are those of the author and are not necessarily endorsed by the U.S. Army.

SA Where copyrighted material is quoted, permission has been obtained to use such material.

SA Where material from documents designated for limited distribution is quoted, permission has been obtained to use the material.

SA Citations of commercial organizations and trade names in this report do not constitute an official Department of Army endorsement or approval of the products or services of these organizations.

___ In conducting research using animals, the investigator(s) adhered to the "Guide for the Care and Use of Laboratory Animals," prepared by the Committee on Care and use of Laboratory Animals of the Institute of Laboratory Resources, national Research Council (NIH Publication No. 86-23, Revised 1985).

___ For the protection of human subjects, the investigator(s) adhered to policies of applicable Federal Law 45 CFR 46.

SA In conducting research utilizing recombinant DNA technology, the investigator(s) adhered to current guidelines promulgated by the National Institutes of Health.

SA In the conduct of research utilizing recombinant DNA, the investigator(s) adhered to the NIH Guidelines for Research Involving Recombinant DNA Molecules.

SA In the conduct of research involving hazardous organisms, the investigator(s) adhered to the CDC-NIH Guide for Biosafety in Microbiological and Biomedical Laboratories.

PI - Signature 3/14/98 Date

TABLE OF CONTENTS

- Somasundaram, K., Zhang, H., Zeng, Y. X., **Houvras, Y.**, Peng, Y., Zhang, H., Wu, G. S., Licht, J. D., Weber, B. L., and El-Deiry, W. S. (1997) Arrest of the cell cycle by the tumour-suppressor BRCA1 requires the CDK-inhibitor p21WAF1/CIP1. Nature 389: 187-190.
- Kimmelman, A., Tolkacheva, T., Lorenzi, M.V., **Osada, M.**, and Chan, A.M.-L. (1997) Identification and characterization of R-ras3: a novel member of the RAS gene family with a non-ubiquitous pattern of tissue distribution Oncogene 15: 2675 - 2686.
- **Santagata, S.**, Aidinis, V., and Spanopoulou, E. (1998) The effect of Me2+ cofactors at the initial stages of V(D)J recombination. J. Biol. Chem. 273:16325-16331.
- Villa, A., **Santagata, S.**, Bozzi, F., Giliani, S., Frattini, A., Imberti, L., Benerini Gatta, L., Ochs, H.D., Schwarz, K., Notarangelo, L.D., Vezzoni, P., and Spanopoulou, E. (1998) Partial V(D)J recombination activity leads to Omenn syndrome. Cell 93: 885-896
- Chen, J., Bander, J. A., **Santore, T. A.**, Chen, Y., Ram, P. T., Smit, M. J., and Iyengar, R. (1998) Expression of Q227L-galphas in MCF-7 human breast cancer cells inhibits tumorigenesis. Proc Natl Acad Sci USA 95: 2648-2652.
- Resnick-Silverman, L., **St. Clair, S.**, Maurer, M., Zhao, K., and Manfredi, J.J. (1998) Identification of a novel class of genomic DNA binding sites suggests a mechanism for selectivity in target gene activation by the tumor suppressor protein p53. Genes Dev., in press.

ANNUAL REPORT - YEAR 4
BREAST CANCER PREDOCTORAL TRAINING PROGRAM
(07/01/97-06/30/98)

INTRODUCTION

The USAMRMC-sponsored Breast Cancer Predoctoral Training Program (BCPTP) at the Mount Sinai School of Medicine is completing its fourth and final year with six students currently supported. The training program has served the dual function of encouraging the predoctoral students to focus on the issues of breast cancer in their research and training and at the same time has served as a focal point to bring various Mount Sinai faculty together to stimulate collaborations and research in the area of breast cancer. As this program was initiated during a phase of dynamic growth in the cancer research enterprise at Mount Sinai, efforts were made to attract as many as possible of Mount Sinai's breast cancer research oriented students and growing number of newly recruited faculty. Thus, support for a given student was limited to a two year period, unless exceptional performance warranted an additional year. This strategy encouraged the widest participation in the program and made it possible to support students whose preceptors hold faculty appointments in six different departments/centers within the medical school. The elements of the training program were designed to educate the students concerning important questions in breast cancer research and to stimulate pursuit of careers that involve research into the underlying mechanisms responsible for human breast cancer.

BODY

Program Direction

Dr. Stuart Aaronson, the Director of the Derald H. Ruttenberg Cancer Center, serves as the Director of the Breast Cancer Training Program. He was responsible for the overall direction of the program and was assisted by a Steering Committee, composed of senior and junior faculty from both the basic science and clinical departments. The composition of the steering committee reflected the multidisciplinary nature of the training program. Members of the steering committee (Appendix A) include senior scientists with extensive mentoring experience (Drs. Johnson, Wang, and Woo), a junior investigator with a relevant research program (Dr. Manfredi), and investigators involved in translational research (Drs. Gabrilove, Wolff, and Woo). The Steering Committee met in the spring to review progress through reports prepared by each trainee.

Research Progress of Trainees

Six students were supported by the BCPTP in Year 3 of the program and the same six students were supported in Year 4. A summary of the trainees supported to date by the BCPTP is shown in Appendix B. A total of eight students who were involved in the BCPTP continue their predoctoral study at Mount Sinai (Maxim Fonarev and Wei Li have since chosen not to continue their Ph.D. studies). A list of

those students, their research topic, and the name of their preceptor is show in Appendix C. The research progress of the six currently supported students is examined in detail here.

Jessica Feinlieb

Jessica and her colleagues in the laboratory of Dr. Robert Krauss in the Department of Biochemistry recently isolated a novel gene designated *cdo* (CAM-related *d*own regulated by *o*ncogenes) from the rat and the human. Sequence analysis of cdo indicates that it is a 1242 amino acid protein containing 5 Ig domains, 3 FN type-III domains, a single pass transmembrane domain and a 256 amino acid cytoplasmic tail. Based on its sequence, *cdo* is a member of the immunoglobulin superfamily and a founding member of a new immunoglobulin/fibronectin type-III repeat subfamily. It is suspected that this gene acts as a negative growth regulator or as a possible tumor suppressor gene. This is supported by the circumstances under which *cdo* was isolated, and human *cdo*'s chromosomal location, 11q23-24, which is known to sustain loss of heterozygosity in breast, ovarian and lung carcinomas. *cdo* is expressed in primary breast cell cultures and is dramatically down-regulated or undetectable in multiple breast tumor cell lines. Additionally, *cdo* is highly expressed in the developing nervous system and the limb bud of the rat embryo. To further examine *cdo*'s possible role in differentiation, *cdo* was ectopically expressed in B104 cells, a neuroblastoma derived cell line, and PC-12 cells. This expression induced neurite outgrowth in these cells in the absence of additional differentiation-inducing stimuli. Furthermore, exposure of these cells to soluble, unclustered *cdo* also induced differentiation. This preliminary evidence suggests that *cdo* may play a substantial and pivotal role in neuronal differentiation. A role in differentiation is consistent with a possible role for *cdo* as a tumor suppressor gene.

Albert Fliss

The hsp90 chaperone machine plays a vital role in steroid receptor hormone binding as well as downstream transcriptional activation. However to date, no conclusive study has been performed to determine the role of the hsp90 chaperone machine in high affinity hormone binding to the estrogen receptor. Albert and his colleagues in Dr. Avrom Caplan's laboratory in the Department of Cell Biology and Anatomy have used the yeast *Saccharomyces cerevisiae* was developed as a model system to address this question. Previous studies have demonstrated that yeast is an appropriate *in vivo* model system, which enables the researcher to study the activation of steroid hormone receptors in a convenient *in vivo* setting. In order to address the above question, hormone binding, 4-hydroxytamoxifen competition, and reporter gene transactivation assays were performed on yeast strains containing either a mutant hsp90 or Ydj1 (yeast homologue of E. coli dnaJ). The results from hormone binding studies demonstrated that both hsp90 and Ydj1 are required for high affinity hormone binding to the estrogen receptor. 4-hydroxytamoxifen competition assays suggest that hsp90 and Ydj1 are required for tamoxifen to act as a competitive inhibitor of hormone binding to the estrogen receptor. Interestingly, in the hsp90 mutant 4-hydroxytamoxifen potentiated hormone binding to the estrogen receptor, however, this did not result in a downstream potentiation of transactivation. In addition, results from lacZ reporter gene assays performed on the

hsp90 mutant demonstrated a moderate decrease in downstream transactivation when compared to the isogenic wild type. Taken together these results suggest that both hsp90 and Ydj1 play vital roles in estrogen receptor hormone binding and downstream transactivation. Further studies will be performed in order to determine the mechanism of hsp90 and Ydj1 action in hormone-dependent estrogen receptor action. In addition, studies will be performed to determine the role of the other components of the hsp90 chaperone machine including hsp70, Sti1, CDC37, p23 and the cyclophilins in hormone dependent estrogen receptor activation. The results from the above and future studies should help further the understanding of the role played by the hsp90 chaperone machine in estrogen receptor activation.

Yariv Houvras

BRCA1 is a tumor suppressor gene mutated in hereditary breast and ovarian cancer. Approximately 45% of women with hereditary breast cancer and 75% of women with hereditary breast/ovarian cancer have mutations in BRCA1. In the laboratory of Dr. Jonathan Licht in the Brookdale Center for Molecular Biology, Yariv has focused his efforts in the past year towards understanding the biological function of the BRCA1 protein. He hypothesized that BRCA1 must interact with other proteins to carry out its function and began a yeast two hybrid screen to identify BRCA1 partner proteins. His search led him to a recently identified protein which functions as a phosphatase inhibitor as a potential partner protein for BRCA1. This phosphatase inhibitor fails to interact with tumor derived missense mutant forms of BRCA1, which suggests that this interaction has biological relevance. Studies are currently underway to verify this interaction by biochemical methods in human cells. Yariv is designing experiments to assess whether BRCA1 regulates the function of this partner protein and whether this interaction has effects in regulating the cell cycle.

Masako Osada

R-ras, a member of Ras subfamily of G-protein, was first isolated by low stringency hybridization using v-H-ras as a probe by the colleagues of Masako in the laboratory of Dr. Andrew Chan in the Derald H. Ruttenberg Cancer Center. Since this gene has been isolated, multiple biological phenotypes have been described for R-ras. These include transformation of NIH3T3 cells, promoting cell adhesion, and regulation of apoptotic responses. However, whether these events were mediated through common or distinct signaling pathways have not been characterized. The major focus of Masako's research is to understand the signaling mechanisms responsible for biological phenotypes elicited by R-ras. Given the relationship between Ras and R-ras downstream signaling cascade, she is currently addressing the importance of the known Ras effector pathways in mediating R-ras induced biological functions.

Sandro Santagata

Genomic rearrangement of antigen receptor gene segments is driven by two lymphoid specific proteins, Rag-1 and Rag-2 which recognize recombination signals and mediate double strand DNA cleavage. These proteins are the focus of the

research in the laboratory of Dr. Eugenia Spanopoulou in the Ruttenberg Cancer Center. Aberrant recognition of cryptic recombination sites by Rags can result in chromosomal translocations, activation of oncogenes and subsequent cellular transformation. Null mutations in either Rag-1 or Rag-2 has been shown to eliminate initiation of V(D)J recombination and to result in severe combined immunodeficiency with a total absence of T and B lymphocytes. Sandro has recently identified that Omenn syndrome, a severe immunodeficiency characterized by the presence of activated, anergic, oligoclonal T lymphocytes, elevated IgE levels and hypereosinophilia results from mutations in either Rag-1 or Rag-2 that render the proteins only partially active. He is currently undertaking functional analysis of the mutant proteins in terms of their ability to bind DNA, multimerize and form a productive recombination competent complex.
Identification of the precise step at which the mutant proteins are deficient will elucidate the contribution of various domains in both Rag-1 and Rag-2 to the recombination process. An understanding of the normal physiology of Rag-1/Rag-2 function will ultimately define the aberrant events leading to chromosomal translocation.

Selvon St. Clair

Selvon St. Clair is performing his thesis research in the laboratory of DR. James Manfredi in the Ruttenberg Cancer Center. The tumor suppressor protein p53 has previously been shown to repress transcription, but this activity did not appear to involve DNA binding. Selvon has demonstrated p53-dependent repression via an element derived from the *cdc25C* gene, indicating, for the first time, a role for p53 in sequence-specific repression of a cellular promoter. Previous studies from Dr. Manfredi's laboratory have demonstrated that there are two classes of genomic DNA binding sites for p53 which are differentially regulated by the binding of a monoclonal antibody, 421. The binding of p53 to most of its characterized DNA binding sites is enhanced by incubation with monoclonal antibody 421. In contrast, the binding of p53 to the element from the *cdc25C* promoter is inhibited by 421 and thus puts it in a novel class of genomic sites that includes one of the p53 response elements in the promoter of the human gene that encodes the cyclin-dependent kinase inhibitor, p21. Thus, Selvon's results demonstrate that p53 mediates transcriptional repression in a sequence-specific manner and that this repression involves a p53 binding site that belongs to a novel class of p53 response elements. His current research is focussed on understanding the underlying molecular mechanism of that repression and the physiologically significance if an interaction between p53 and the cdc25C promoter.

Selection of Trainees

As the six students which were funded in Year 3 continued in the program through Year 4, no selection of new trainees was necessary.

Description of Training Program

BCPTP Trainee Biweekly Meetings

To focus the training program specifically on breast cancer, the biweekly luncheon meeting was continued. All trainees were expected to attend. To stimulate discussion and create an informal atmosphere, lunch was served at these meetings. The purpose of these meetings was twofold. First, Mount Sinai faculty with expertise in the area of breast cancer were invited to give didactic lectures presenting an overview of their area of expertise. Second, these meetings were used as a forum for the students to present their own research. The schedule for these meetings for 1997 and 1998 is shown in Appendix H.

Since the ongoing research experience of the trainees has been primarily grounded in basic laboratory science, the invited lecture portion of these meetings was designed to give the trainees a better understanding of clinical aspects of breast cancer and to stimulate their thinking as to how their own research may help to answer some of the important questions that are currently relevant in the diagnosis and treatment of breast cancer. To that end, Dr. Mira-y-Lopez (Neoplastic Diseases) discussed the basic cell biology of the human mammary gland as a background for a presentation by Dr. Ira Bleiweis (Pathology) on the pathology of the human breast and the pathological techniques that are used in the diagnosis of breast cancer. Dr. James Holland (Neoplastic Diseases) lectured on the clinical care of breast cancer patients with a particular emphasis on his area of expertise: combination chemotherapy. Dr. Christine Eng (Human Genetics) led a lively discussion of the ethical issues involved in the genetic testing for BRCA1 and BRCA2 mutations. Drs. Mary Wolff and Jonine Bernstein (Community Medicine) discussed the environmental and genetic epidemiology, respectively, of human breast cancer. Other speakers have addressed the areas of Cancer Prevention and Control (Drs. Kate DuHamel and William Redd, Cancer Center), radiation treatment and breast cancer (Dr. Brenda Shank, Radiation Oncology), molecular biological aspects of breast cancer (Drs. Avrom Caplan, Paolo Fedi, James Manfredi, and Jonathan Licht). This series has been very well-received by the students and participating faculty.

Didactic lectures alternated with presentations of research by each of the trainees. Thus, this forum provides the opportunity for each student to present his/her current research at least twice during the academic year. These presentations were attended by members of the steering committee as well as the preceptors of all of the trainees. Students were requested to submit a short written report for evaluation by the steering committee. In summary, these biweekly meetings provided a sense of cohesion and unity to the group of trainees and their preceptors, fostered interactions and potential collaboration between the various training laboratories, and gave faculty and students alike an opportunity to become better educated about the important issues in clinical breast cancer.

Molecular Oncogenesis Research Colloquia

To foster interactions between laboratories within the Mount Sinai cancer research community and to keep both the students and faculty aware of

opportunities for collaboration, a monthly Molecular Oncogenesis Research Colloquium is held. Two participating laboratories present their current research each month. The Colloquia were held in the early evening. Pizza and soda was served to maintain an informal atmosphere and allow for interactive discussions. All trainees were required to attend these monthly events.

Molecular Basis of Disease Journal Club

The interdisciplinary graduate training program, Molecular Basis of Disease, sponsors a weekly journal club. Presentation at this journal club is required of all students in the program

Cancer Center Seminar Series

There is a full and varied schedule of research seminars presented at the Mount Sinai School of Medicine. All trainees were required to attend the seminar series sponsored by the Ruttenberg Cancer Center. A list of speakers for the last year is shown in Appendix I.

Courses

Two relevant cancer-related courses are offered by the Graduate School at Mount Sinai. The BCPTP trainees were expected to complete both of these courses. These courses were Advanced Topics in Cancer Biology, organized by the Derald H. Ruttenberg Cancer Center, and Advanced Signal Transduction, organized by the Department of Pharmacology.

Advanced Topics in Cancer Biology. In previous years, the Advanced Topics in Cancer Biology course was organized as a series of didactic lectures covering relevant topics in cancer. In 1997, a new Molecular Basis of Disease overview course was organized in which ten lectures are dedicated to cancer and cancer-related topics. The Advanced Topics in Cancer Biology course was therefore reorganized to consist of journal article-based student presentations in particular topics that are relevant to cancer biology. The topics chosen for 1997 were (1) Growth Factors and Receptors, (2) DNA Recombination and Repair, and (3) Apoptosis. The topics for 1998 were (1) Intracellular Signal Transduction, (2) Cell Cycle, and (3) Novel Tumor Suppressors. A course offering is included in Appendix J.

Advanced Signal Transduction. The Advanced Signal Transduction course is an inter-departmental effort organized by the Department of Pharmacology. It is a lecture-based course which covers a wide range of topics, many of which are relevant to cancer.

Evaluation of Training

Advisory Committee. Entering students were assigned an initial Advisory Committee (usually 3 members) chosen in consultation with the entering student and aligned with the research interests of the student. As soon as the student formally entered the BCPTP, a new Advisory Committee including the preceptor and at least two other members of the BCPTP faculty was chosen. Students met with their Advisory Committees twice each year and filed a Progress Report with the

Graduate School. Advisory Committees for each trainee are listed in Appendix D.

Trainee Luncheons. Trainees presented their research twice a year to members of the steering committee and preceptors during the trainee luncheons. As part of these meetings, students were encouraged to discuss how their research may potentially impact on the diagnosis and treatment of cancer patients and to express what interest they have in pursuing careers involving cancer research. Trainees were required to submit a written summary of their research to be evaluated by the steering committee.

Faculty Collaboration

The participation of the faculty in the USAMRMC-sponsored BCPTP has greatly stimulated interactions. Dr. Aaronson sponsors periodic meetings of a Breast Cancer Study Group in which laboratory and clinical faculty present their work with the intent of stimulating collaborations and new initiatives (Appendix K). A program project initiative which includes a major component involving breast cancer has been submitted involving Drs. Aaronson, Licht, Manfredi, Pan, Ronai, and Wu. Dr. Wolff has organized monthly luncheon meetings to discuss research initiatives involving the role of environmental and genetic influences in the development of cancer. A collaboration between Drs. Wolff and Fedi involving expression of erbB family members in primary human breast tumors has led to the award of a grant. Another collaboration between Drs. Wolff and Manfredi on the role of p53 expression in the chemotherapeutic responsiveness of human breast tumors has also led to a grant award from the National Cancer Institute.

Budget

In the current reporting period, Year 4, six trainees were supported by the BCPTP grant for a full year. A summary of the budget for Year 4 is shown in Appendix G.

Adherence to Statement of Work

Review progress of trainees

The academic progress of trainees is evaluated by advisory committees that are set up by the Graduate School at Mount Sinai. The progress of the trainees as it specifically relates to the BCPTP is reviewed by the steering committee through the oral presentations of the trainees at the biweekly luncheon meetings and through an annual written report. This has continued to be done for Year 4.

Select additional trainees and set up advisory committees for new trainees

As the six students which were funded in Year 3 continued in the program through Year 4, no selection of new trainees was necessary. The composition of the advisory committees were maintained.

Review training program/Evaluate impact of seminars and journal club

Two years ago, the steering committee decided that more attention needed to

be paid to educating the trainees specifically in the area of breast cancer. The biweekly luncheon meetings were initiated to perform this task. These meetings were enthusiastically received by students and faculty alike and were continued. A regular Cancer Center seminar series was established (see Appendix I). The Molecular Basis of Disease journal club continued and proved to be an important component of the BCPTP.

Organize breast cancer seminars, a journal club for trainees, with modifications if necessary

The biweekly luncheon meetings were organized to meet this goal and have been met with enthusiasm. The format of alternating invited lectures with student presentations worked well and were continued.

Continue to recruit and advertise program

The program has completed its fourth and final year of funding. The satisfaction and interest of both faculty and students in the training program has prompted an effort to apply for funding from the National Cancer Institute in the form of a training grant as well as an application to the USAMRMC to continue the BCPTP in the future.

Continue encouragement of breast cancer research among Mount Sinai faculty

The organization of monthly meetings by Dr. Mary Wolff to encourage interactions between basic science researchers and those involved in more clinical approaches were continued and resulted in two newly funded grants specifically focussed on breast cancer. The program project initiative of Dr. Ze'ev Ronai resulted in a submission that is currently under review. In addition, many new breast cancer initiatives have been submitted or are being formulated by the faculty. A list of the currently funded research grants of the training faculty that are specifcially focussed on breast cancer is shown in Appendix L.

CONCLUSIONS

The BCPTP has been instrumental in focusing our faculty and students toward breast cancer-relevant research areas. During the initial four years of the program, our training faculty has greatly expanded. Direct costs funding for breast cancer research has increased from $372,600 to $2,300,236, annually and funded cancer investigations have increased from $1,827,223 to $5,999,644. The Training Program in Cancer Biology which began just prior to the award of the original training grant has become one of the most popular training areas at Mount Sinai with more than one third of our students being mentored by our faculty. The dynamic, interactive, intellectual environment, superb laboratory facilities, and major new emphasis on cancer initiatives over the past four years along with the BCPTP have all contributed to this success.

REFERENCES

Currently supported students have been successful in their research as demonstrated by their publications records which includes papers in Cell, Genes and Development, Molecular and Cellular Biology, and the Journal of Cell Biology (see Appendix F and M).

APPENDIX A
BCPTP Program Direction

Role	Name	Academic Rank	Department or Center Affiliation
Program Director	Stuart Aaronson, M.D.	Professor	Cancer Center
Training Coordinator	James Manfredi, Ph.D.	Assistant Professor	Cancer Center
Steering Committee	Janice Gabrilove, M.D.	Professor	Neoplastic Diseases
	Edward Johnson, Ph.D.	Professor	Pathology
	Lu-Hai Wang, Ph.D.	Professor	Microbiology
	Mary Wolff, Ph.D.	Professor	Community Medicine
	Savio Woo, Ph.D.	Professor	Gene Therapy
Graduate School Liaison	Terry Krulwich, Ph.D.	Professor and Dean	Biochemistry

APPENDIX B
Summary of Trainees Supported to Date

Trainee	Dates of Support				Total Months of Support
	Year One	Year Two	Year Three	Year Four	
Jessica Feinlieb		7/1/95-6/30/96	7/1/96-6/30/97	7/1/97-6/30/98	36
Albert Fliss			10/1/96-6/30/97	7/1/97-6/30/98	21
Maxim Fonarev	7/1/94-6/30/95	7/1/95-6/30/96			24
Ulrich Hermanto	7/1/94-6/30/95	7/1/95-6/30/96	7/1/96-8/31/96		26
Yariv Houvras			7/1/96-6/30/97	7/1/97-6/30/98	24
Wei Li		7/1/95-6/30/96	7/1/961/31/97		19
Masako Osada			9/1/96-6/30/97	7/1/97-6/30/98	22
Selvon St. Clair			2/1/97-6/30/97	7/1/97-6/30/98	17
Sandro Santagata			7/1/96-6/30/97	7/1/97-6/30/98	24
Tara Santore	7/1/94-6/30/95	7/1/95-6/30/96	7/01/96-9/30/96		27

APPENDIX C
BCPTP Trainees, Research Project Titles, and Preceptors

Trainee	Research Project Title	Preceptor
Jessica Feinlieb (MD/PhD, Year Six)	Cdo, a novel CAM-related gene and differentiation	Robert Krauss, Ph.D. Department of Biochemistry
Albert Fliss (PhD, Year Four)	Hsp90 and estrogen receptor activation	Avrom Caplan, Ph.D. Department of Cell Biology and Anatomy
Ulrich Hermanto (MD/PhD, Year Seven)	Receptor tyrosine kinases in breast cancer	Lu-Hai Wang, Ph.D. Department of Microbiology
Yariv Houvras (MD/PhD, Year Five)	Identification of BRCA1 partner proteins	Jonathan Licht, M.D. Brookdale Center for Molecular Biology
Masako Osada (PhD, Year Four)	R-ras and transformation	Andrew Chan, Ph.D. Derald H. Ruttenberg Cancer
Selvon St. Clair (PhD, Year Three)	p53 and cdc25C	James J. Manfredi, Ph.D. Derald H. Ruttenberg Cancer
Sandro Santagata (MD/PhD, Year Five)	Mechanisms of genomic DNA rearrangements	Eugenia Spanopoulou, Ph.D. Derald H. Ruttenberg Cancer
Tara Santore (PhD, Year Seven)	cAMP signalling in breast cancer	Srinivas R.V. Iyengar, Ph.D. Department of Pharmacology

APPENDIX D
BCPTP Trainee Advisory Committees

Trainee	Advisory Committee	
	Name	Department or Center Affiliation
Jessica Feinlieb	Jonathan Licht, M.D. Steven Salton, M.D.	Molecular Biology Neurobiology
Albert Fliss	Gillian Small, Ph.D. Jeanne Hirsch, Ph.D.	Cell Biology and Anatomy Cell Biology and Anatomy
Ulrich Hermanto	Robert Krauss, Ph.D. Irwin Gelman, Ph.D.	Biochemistry Microbiology
Yariv Houvras	Stuart A. Aaronson, M.D. James J. Manfredi, Ph.D. David Sassoon, Ph.D.	Cancer Center Cancer Center Molecular Biology
Masako Osada	Sandra Masur, Ph.D. Edward Johnson, Ph.D.	Cell Biology and Anatomy Pathology
Selvon St. Clair	Adolfo Garcia-Sastra, Ph.D. Stave Kohtz, Ph.D. Ze'ev Ronai, Ph.D.	Microbiology Pathology Cancer Center
Sandro Santagata	Thomas Lufkin, Ph.D. Francisco Ramirez, Ph.D. David Colman, Ph.D.	Molecular Biology Molecular Biology Molecular Biology
Tara Santore	Lui-Hai Wang Irwin Gelman	Microbiology Microbiology

APPENDIX E
BCPTP Trainee Prior Academic History

Trainee	Undergraduate Training					GRE or MCAT Scores
	Degree	Institution	Year Awarded	Major	GPA	
Jessica Feinlieb	A.B.	University Of Chicago	1992	Biology	3.00	MCAT: VB-9, PH-9, WR-O, BS-11, TOT-29
Albert Fliss	B.S.	University of Central Florida	1982	Microbiology	3.06	GRE: VRB-580, QUA-690 ANA-500
Ulrich Hermanto	B.A.	Boston University	1992	Chemistry	3.52	MCAT: VB-11, PH-10, WR-N, BS-12 , TOT-33
Yariv Houvras	B.S.	University of Michigan	1992	Biology	3.22	MCAT: VB-11, PH-10, WR-S, BS-11 , TOT-32
Masako Osada	B.S.	City College of New York	1994	Biology	3.60	GRE: VRB-350, QUA-560 ANA-510, ADV-590
Sandro Santagata	B.A.	Amherst College	1993	Neuroscience	3.55	MCAT: VB-10, PH-12, WR-R, BS-13 , TOT-35
Selvon St. Clair	B.Sc.	University of West Indies	1993	Chemistry	3.76	GRE: VRB-520, QUA-540 ANA-520
Tara Santore	B.S.	St. Francis College	1990	Biology	3.94	GRE: VRB-460, QUA-460, ANA-610, ADV-660

APPENDIX F
Publications of Current and Past Trainees

Name of Trainee	Preceptor	Publications
Feinlieb, Jessica	Krauss	**Feinleib, J. L.**, and Krauss, R. S. (1996) Dissociation of ras oncogene-induced gene expression and anchorage- independent growth in a series of somatic cell mutants. Mol Carcinog 16: 139-148. Kang, J. S., Gao, M., **Feinleib, J. L.**, Cotter, P. D., Guadagno, S. N., and Krauss, R. S. (1997) CDO: an oncogene-, serum-, and anchorage-regulated member of the Ig/fibronectin type III repeat family. J Cell Biol 138: 203-213.
Fliss, Albert	Caplan	Fang, Y., **Fliss, A. E.**, Robins, D. M., and Caplan, A. J. (1996) Hsp90 regulates androgen receptor hormone binding affinity in vivo. J Biol Chem 271: 28697-28702. **Fliss, A. E.**, Fang, Y., Boschelli, F., and Caplan, A. J. (1997) Differential In Vivo Regulation of Steroid Hormone Receptor Activation by Cdc37p. Mol Biol Cell 8: 2501-2509. Fang, Y., **Fliss, A.E.**, Rao, J., and Caplan, A.J. (1998) SBA1 encodes a yeast hsp90 cochaperone that is homologous to vertebrate p23 proteins. Mol. Cell. Biol. 18:3727-3734.
Hermanto, Ulrich	Wang	none
Houvras, Yariv J.	Licht	Somasundaram, K., Zhang, H., Zeng, Y. X., **Houvras, Y.**, Peng, Y., Zhang, H., Wu, G. S., Licht, J. D., Weber, B. L., and El-Deiry, W. S. (1997) Arrest of the cell cycle by the tumour-suppressor BRCA1 requires the CDK-inhibitor p21WAF1/CIP1. Nature 389: 187-190.
Osada, Masako	Chan	Kimmelman, A., Tolkacheva, T., Lorenzi, M.V., **Osada, M.**, and Chan, A.M.-L. (1997) Identification and characterization of R-ras3: a novel member of the RAS gene family with a non-ubiquitous pattern of tissue distribution Oncogene 15: 2675 - 2686.
Santagata, Sandro	Spanopoulou	Spanopoulou, E., Zaitseva, F., Wang, F. H., **Santagata, S.**, Baltimore, D., and Panayotou, G. (1996) The homeodomain region of Rag-1 reveals the parallel mechanisms of bacterial and V(D)J recombination. Cell 87: 263-276. **Santagata, S.**, Aidinis, V., and Spanopoulou, E. (1998) The effect of Me2+ cofactors at the initial stages of V(D)J recombination. J. Biol. Chem., in press. Villa, A., **Santagata, S.**, Bozzi, F., Giliani, S., Frattini, A., Imberti, L., Benerini Gatta, L., Ochs, H.D., Schwarz, K., Notarangelo, L.D., Vezzoni, P., and Spanopoulou, E. (1998) Partial V(D)J recombination activity leads to Omenn syndrome. Cell 93: 885-896
Santore, Tara	Iyengar	Chen, J., Bander, J. A., **Santore, T. A.**, Chen, Y., Ram, P. T., Smit, M. J., and Iyengar, R. (1998) Expression of Q227L-galphas in MCF-7 human breast cancer cells inhibits tumorigenesis. Proc Natl Acad Sci U S A 95: 2648-2652.
St. Clair, Selvon	Manfredi	Resnick-Silverman, L., **St. Clair, S.**, Maurer, M., Zhao, K., and Manfredi, J.J. (1998) Identification of a novel class of genomic DNA binding sites suggests a mechanism for selectivity in target gene activation by the tumor suppressor protein p53. Genes Dev., in press.

Appendix G
Budget Summary for Current Reporting Period

Trainee	Dates of Support	Stipend	Tuition and Fees	Supply Allowance	Total
Jessica Feinlieb	07/01/97-06/30/98	14,708	1,385	350	16,450
Albert Fliss	07/01/97-06/30/98	14,708	1,385	350	16,450
Yariv Houvras	07/01/97-06/30/98	14,708	1,385	350	16,450
Masako Osada	07/01/97-06/30/98	14,708	1,385	350	16,450
Selvon St. Clair	07/01/97-06/30/98	14,708	1,385	350	16,450
Sandro Santagata	07/01/97-06/30/98	14,708	1,385	350	16,450
	TOTALS	**88,248**	**8,310**	**2,100**	**98,700**

APPENDIX H

Breast cancer training grant biweekly group luncheons

The Army breast cancer training grant biweekly group luncheons will be held on Tuesdays beginning Tuesday, February 18, 1997 from 12:00-1:00 PM. The meeting will be held in Annenberg 25-51 until May 13th. The May 13th meeting and thereafter will be held in the Cancer Center's conference room, East Building 15-84. Lunch will be served.

Annenberg 25-51

February 18	Organizational meeting	
March 4	Cell Biology I: basic biology	Rafael Mira-y-Lopez (4-3194)
March 18	Research talks I	Yariv Houvras Jessica Feinlieb
April 1	Cell Biology II: pathology	Ira Bleiweis (4-9159)
April 15	Research talks II	Albert Fliss Masako Osada
April 29	Patient care I: diagnosis and treatment	Jim Holland (4-6361)

East Building 15-84

May 13	Patient care II: genetic testing and ethical isses	Christine Eng (4-3150)
May 27	Research talks III	Selvon St. Clair Sandro Santagata
June 10	Epidemiology II: environmental factors	Mary Wolff (4-6183)
June 24	Epidemiology I: genetic factors	Jonine Bernstein (4-8495)

1997-1998 BCPTP Luncheon Meetings
Tuesdays, 12 noon-1 PM
East Building, Room 15-84

Date	Topic	Speaker
October 14	Prevention and control I	Kate DuHamel (5-9039) *Cancer Center*
October 28	Treatment I: surgery	Paul Tartter (4-8027) *Surgery*
~~November 4~~	(USAMRMC Breast Cancer meeting)	
November 11	Treatment II: radiotherapy	Brenda Shank (4-7500) *Radiation Oncology*
November 18	Breast Cancer meeting review	James Manfredi Yariv Houvras
November 25	Prevention and control II	William Redd (5-8186) *Cancer Center*
December 2	Epidemiology I	Lauren Lipworth (4-0591) *Community Medicine*
December 16	Research Talks I	Sandro Santagata (5-8121) Albert Fliss (4-6564)
January 6	Epidemiology II: genetic factors	Jonine Bernstein (4-8495) *Community Medicine*
January 20	Research Talks II	Yariv Houvras (4-9428) Masako Osada (5-8101)
February 3	Advocate's Viewpoint (tentative)	
February 17	Research Talks III	Selvon St. Clair (5-8113) Jessica Feinlieb (4-6436)
March 3	Molecular Biology I: estrogen receptor	Avrom Caplan (4-6563) *Cell Biology*
March 17	Molecular Biology II: *erb*B receptor tyrosine kinases	Paolo Fedi (5-8205) *Cancer Center*
March 31	Molecular Biology III: p53	James Manfredi (5-8110) *Cancer Center*

1998 BCPTP Luncheon Meetings
Wednesdays, 12 noon-1 PM
East Building, Room 15-84

Date	Topic	Speaker
January 21	Research Talks II	Yariv Houvras (4-9428)
February 4	Molecular Biology I: p53	James Manfredi (5-8110) *Cancer Center*
February 18	Research Talks III	Masako Osada (5-8101)
March 4	Molecular Biology II: estrogen receptor	Avrom Caplan (4-6563) *Cell Biology*
March 18	Research Talks IV	Albert Fliss (4-6564)
April 1	Molecular Biology III: *erb*B receptor tyrosine kinases	Paolo Fedi (5-8205) *Cancer Center*
April 15	Research Talks V	Jessica Feinlieb (4-6436)
April 29	Molecular Biology IV: BRCA1	Jonathan Licht (4-9427) *Molecular Biology*
May 13	Research Talks VI	Selvon St. Clair (5-8113)

APPENDIX I

DHRCC Seminars

August '97 - June '98

Seminar Date	Speaker	Affiliation	Seminar Title
8/1/97	Zhijun Luo, M.D., Ph.D.	Harvard Medical School	Activation of Raf1, a complex process
8/15/97	Curt Horvath, Ph.D.	Rockefeller University	Signal transduction to the nucleus through stat proteins
9/4/97	Marc Symons, Ph.D.	Onyx Pharmaceuticals	Pole of Rho Family GTPases in cell proliferation and migration
10/7/97	Nikos Yannoutsos, Ph.D.	Erasmus University, Rotterdam	Complement and Xenotransplantation
10/17/97	Jan Vijg, Ph.D.	Harvard Medical School	Mutatuion and detection in aging and disease
10/22/97	Takashi Fujita, Ph.D.	Tokyo Metropolitan Institute	Direct triggering of the type I interferon sustem by virus infection: activation of a transcription factor complex containing IRF-3 and CBP/300
10/27/97	Walter Birchmeier, Ph.D.	Max-Delbrueck-Center, Berlin	The role of armadillo beta-catenin in cell adhesion and signalling
11/5/97	Judith Jacobson, Ph.D.	Columbia University School of Public Health	Reproductive risk factors for colorectal neoplasia
11/13/97	Louise Prakash, Ph.D.	University of Texas	The Dna repair, chromatin silencing and protein degradation roles of yeast Rad6 ubiquitin-conjugating enzyme
11/14/97	Satya Prakash, Ph.D.	University of Texas	Nucleotide excision repair in yeast and human
12/3/97	Michael Nerenberg, M.D.	Nanogen	Genetic analysis by electric field manipulation on a microship array
12/8/97	Ira Pastan, M.D.	NCI/NIH	Bioengineering of immunotoxins
12/19/97	Marcus Kretzchmar, Ph.D.	Memorial Sloan-Kettering Cancer Center	Regulation of Smad proteins in TGF-beta family signalling

DHRCC Seminars
August '97 - June '98

Seminar Date	Speaker	Affiliation	Seminar Title
1/6/98	Kornelia Polyak, M.D., Ph.D.	John Hopkins Oncology Center	P53 and cell death
1/13/98	Thomas Daniel, M.D.	Vanderbilt University	Eph receptor discriminatory switches and signal diversification in vascular cell assembly
1/30/98	Othon Iliopoulos, M.D.	Dana Farber Cancer Institute	Functional analysis of the von Hippel-Lindau tumor suppressor protein
2/3/98	E. Premkumar Reddy, Ph.D.	Fels Institute	Myb oncogene in breast development and carcinogenesis
3/5/98	Tom Kelly, Ph.D.	John Hopkins University Medical School	A replication switch: regulation of the replication initiator protein Cdc18 by cyclin-dependent kinase
3/9/98	Hidetoshi Tahara, Ph.D.	Hiroshima University	Telomerase, cellular senescence and cancer diagnosis
3/23/98	Moshe Oren, Ph.D.	The Weizmann Institute	P53, Mdm2 and cell Fate
5/14/98	Thomas Guadagno, Ph.D.	Stanford University School of Medicine	Two signalling pathways that regulate aspects of mitosis
5/19/98	Igor Roninson, Ph.D.	University of Illinois	Genetic suppressor elements in the analysis of drug response in tumor cell
5/26/98	Jim Woodgett, Ph.D.	University of Toronto	Regulation of differentiation and apoptosis by the Wnt and pI3K signalling pathways
6/9/98	Nicole Schreiber-Agus, Ph.D.	Albert Einstein College of Medicine	The Myc antagonist Mxi1: committing Sin and controlling cellular growth
6/23/98	Karen Vousden, Ph.D.	NCI	The rise and fall of p53
6/25/98	Steven Grant, Ph.D.	Medical College of Virginia Virginia Commonwealth U.	Regulation of drug-induced apoptosis in leukemia by Bcl-2 and p21WAF1/CIP1, basic considerations and clinical implications

APPENDIX J

Advanced Topics in Cancer Biology Spring, 1997

Advanced Topics in Cancer Biology will be offered in the Spring semester, 1997. Three modules will be offered. Students may take either one, two, or all three modules for credit. Each module is 1 credit. Classes meet on Tuesday and Thursday, 1:30-3:00 PM in Annenberg 18-85. This is a journal article-based class in which students take turns leading discussion of assigned journal articles. Each module will have one invited speaker who will present a research seminar that is relevant to the topic of the module. For general information, students should contact Jim Manfredi (5-8110). For details concerning the topics to be covered in each module, students should contact each of the instructors directly. An organizational meeting for the first module will be held on Tuesday, January 28 at 1:30 PM in Annenberg 18-85.

Module I: Biology of Growth Factors and Receptors (P. Finch, 4- 8351 and P. Fedi, 4-8369)

Dates: February 4-March 6, 1997

The focus will be on the role of various growth factors and their receptors in normal biological processes as well as particular pathological states, most notably cancer. The approach to the topics will emphasize the biology of the systems being examined and thus will attempt to avoid overlap with the signal transduction course being offered concurrently.

Module II: DNA Recombination and Repair (E. Spanopoulou, 5-8120 and Z. Pan, 5-8115)

Dates: March 11-April 10, 1997

Molecular mechanisms of DNA recombination and repair will be studied utilizing where appropriate examples of physiological or developmental relevance.

Module III: Apoptosis (X. Wu, 4-8320 and J. Manfredi, 5-8110)

Dates: April 15-May 15, 1997

The biochemistry and molecular biology of apoptosis will be emphasized. In particular, the molecular mechanisms underlying programmed cell death will be examined, including signal transduction pathways leading to apoptosis, the bcl-2 family of proteins, and the involvement of the tumor suppressor protein p53.

Advanced Topics in Cancer Biology
Spring, 1998

Advanced Topics in Cancer Biology will be offered in the Spring semester, 1998. Three modules will be offered. Students may take either one, two, or all three modules for credit. Each module is 1 credit. Classes meet on Tuesday and Thursday, 1:30-3:00 PM in East Building 15-84. This is a journal article-based class in which students take turns leading discussion of assigned journal articles. For general information, students should contact James Manfredi (5-8110). For details concerning the topics to be covered in each module, students should contact each of the instructors directly.

Module I: Novel Tumor Suppressors
(Jonathan Licht, 4-9427 and James Manfredi, 5-8110)
Dates: January 13-February 12, 1998

The purpose of this module is to examine the growing number of tumor suppressor proteins that have been recently identified. The retinoblastoma protein, pRb, and p53 will expressly not be included. Topics will include BRCA1, BRCA2, APC, the VHL gene product, and others.

Module II: Biology of Intracellular Signal Transduction
(Andrew Chan, 5-8106 and Ze'ev Ronai, 5-8183)
Dates: February 17-March 19, 1998

This module will cover a variety of topics including redox signal transduction, phosphoinositide 3-kinases, the Ras-MAPK-Erk pathway, stress-activated protein kinases (SAPK/JNK), and the WNT/wingless pathway.

Module III: Cell Cycle Control and Cancer
(Jeanne Hirsch, 4-0224 and Robert Krauss, 4-2177)
Dates: March 31-April 30, 1998

This module will deal with a general study of cell cycle controls in lower eukaryotes, particularly, yeast and an examination of mammalian systems with an emphasis on how cell cycle control is altered in cancer.

PLEASE NOTE THE ORDER OF THE MODULES.

THE FIRST CLASS IS JANUARY 13 IN THE EAST BUILDING, ROOM 15-84.

APPENDIX K

THE MOUNT SINAI MEDICAL CENTER

LECTURE

Date of Posting: February 24, 1998

THE DERALD H. RUTTENBERG CANCER CENTER
BREAST CANCER WORKING GROUP

March 17, 1998

"ERB2/HER/NEU AND ITS ROLE IN HUMAN CANCER"
presented by

PAOLO FEDI, M.D., PH.D.
RUTTENBERG CANCER CENTER
and
JONINE BERNSTEIN, PH.D.
DEPARTMENT OF COMMUNITY MEDICINE

EAST BUILDING SEMINAR ROOM
12:00 NOON

June 2, 1998

"ESTROGEN AND BREAST CANCER"
presented by

AVROM CAPLAN, PH.D.
CELL BIOLOGY AND ANATOMY
and
MARY WOLFF, PH.D.
DEPARTMENT OF COMMUNITY MEDICINE

EAST BUILDING SEMINAR ROOM
12:00 NOON

FOR MORE INFORMATION, CALL 46470

Lunch will be served.

APPENDIX L
Breast Cancer-Specific Support of Training Faculty

Faculty Name	Source of Support	Grant Title
Aaronson	NIH/NCI	SPORE in breast cancer
Aaronson	NIH/NCI	Cloning and analysis of wnt receptors in breast cancer
Fedi	NIH/NCI	Validation of erbB-3 immunostaining in breast tumor
Bernstein	NIH/NCI	The prevalence of BRCA1: a population-based study
Bernstein	NIH/NCI	The molecular epidemiology of breast cancer
Bernstein	USAMRMC Breast Cancer Program	Role of the ATM gene in bilateral breast cancer following radiotherapy
Eng	NIH/NCI	BRCA1 and BRCA2 testing in Ashkenazi Jewish breast cancer families
Eng	USAMRMC Breast Cancer Program	Inherited susceptibility to breast cancer in health women: mutations in breast cancer genes, immune surveillance, and psychological distress
Fedi	NIH/NCI	Validation of erbB-3 immunostaining in breast tumor
Manfredi	USAMRMC Breast Cancer Program	Mechanisms of breast carcinogenesis involving wild-type p53
Manfredi	USAMRMCBreast Cancer program	Regulation of the tumor suppressor activity of p53 in human br cancer
Manfredi	NIH/NCI	Role of p53 in breast cancer chemotherapeutic response
Mira-y-Lopez	NIH/NCI	Aberrant retinoid signaling in breast cancer
Small	USAMRMCBreast Cancer Program	Peroxisomal oxidation in normal and tumoral human breast
Woo	USAMRMCBreast Cancer Program	Phase I trial of adenoviral mediated interleukin-12 gene thera for metastatic breast cancer
Wolff	NIH/NCI	Breast cancer and the environment on Long Island
Wolff	NIH/NCI	Metropolitan New York Breast Cancer Registry

Appendix M
Manuscripts Published by Trainees during Current Reporting Period

1. Fang, Y., **Fliss, A.E.**, Rao, J., and Caplan, A.J. (1998) SBA1 encodes a yeast hsp90 cochaperone that is homologous to vertebrate p23 proteins. Mol. Cell. Biol. 18:3727-3734.

2. Somasundaram, K., Zhang, H., Zeng, Y. X., **Houvras, Y.**, Peng, Y., Zhang, H., Wu, G. S., Licht, J. D., Weber, B. L., and El-Deiry, W. S. (1997) Arrest of the cell cycle by the tumour-suppressor BRCA1 requires the CDK-inhibitor p21WAF1/CIP1. Nature 389: 187-190.

3. Kimmelman, A., Tolkacheva, T., Lorenzi, M.V., **Osada, M.**, and Chan, A.M.-L. (1997) Identification and characterization of R-ras3: a novel member of the RAS gene family with a non-ubiquitous pattern of tissue distribution Oncogene 15: 2675 - 2686.

4. **Santagata, S.**, Aidinis, V., and Spanopoulou, E. (1998) The effect of Me2+ cofactors at the initial stages of V(D)J recombination. J. Biol. Chem. 273:16325-16331.

5. Villa, A., **Santagata, S.**, Bozzi, F., Giliani, S., Frattini, A., Imberti, L., Benerini Gatta, L., Ochs, H.D., Schwarz, K., Notarangelo, L.D., Vezzoni, P., and Spanopoulou, E. (1998) Partial V(D)J recombination activity leads to Omenn syndrome. Cell 93: 885-896

6. Chen, J., Bander, J. A., **Santore, T. A.**, Chen, Y., Ram, P. T., Smit, M. J., and Iyengar, R. (1998) Expression of Q227L-galphas in MCF-7 human breast cancer cells inhibits tumorigenesis. Proc Natl Acad Sci USA 95: 2648-2652.

7. Resnick-Silverman, L., **St. Clair, S.**, Maurer, M., Zhao, K., and Manfredi, J.J. (1998) Identification of a novel class of genomic DNA binding sites suggests a mechanism for selectivity in target gene activation by the tumor suppressor protein p53. Genes Dev., in press.

MOLECULAR AND CELLULAR BIOLOGY, July 1998, p. 3727–3734 Vol. 18. No. 7
0270-7306/98/$04.00+0

SBA1 Encodes a Yeast Hsp90 Cochaperone That Is Homologous to Vertebrate p23 Proteins

YIFANG FANG, ALBERT E. FLISS, JIE RAO, AND AVROM J. CAPLAN*

Department of Cell Biology and Anatomy, Mount Sinai Medical Center, New York, New York 10029

Received 26 November 1997/Returned for modification 20 January 1998/Accepted 31 March 1998

The *Saccharomyces cerevisiae SBA1* gene was cloned by PCR amplification from yeast genomic DNA following its identification as encoding an ortholog of human p23, an Hsp90 cochaperone. The *SBA1* gene product is constitutively expressed and nonessential, although a disruption mutant grew more slowly than the wild type at both 18 and 37°C. A double deletion of *SBA1* and *STI1*, encoding an Hsp90 cochaperone, displayed synthetic growth defects. Affinity isolation of histidine-tagged Sba1p (Sba1^{His6}) after expression in yeast led to coisolation of Hsp90 and the cyclophilin homolog Cpr6. Using an in vitro assembly assay, purified Sba1^{His6} bound to Hsp90 only in the presence of adenosine 5′-*O*-(3-thiotriphosphate) or adenyl-imidodiphosphate. Furthermore, interaction between purified Sba1^{His6} and Hsp90 in yeast extracts was inhibited by the benzoquinoid ansamycins geldanamycin and macbecin. The in vitro assay was also used to identify residues in Hsp90 that are important for complex formation with Sba1^{His6}, and residues in both the N-terminal nucleotide binding domain and C-terminal half were characterized. In vivo analysis of known Hsp90 substrate proteins revealed that Sba1 loss of function had only a mild effect on the activity of the tyrosine kinase v-Src and steroid hormone receptors.

Polypeptide folding occurs in vivo with the aid of molecular chaperones. Members of this diverse protein family have been proposed to function by protecting nascent chains from off-pathway interactions that might otherwise lead to aggregation and to stabilize conformations from which productive folding can proceed (25, 29). The two major classes of molecular chaperone that exist in the eukaryotic cytosol under normal growth conditions are Hsp70 and Hsp90. Both of these chaperones function in protein folding reactions with the aid of several factors that act as cochaperones or modulators. In the case of eukaryotic Hsp70, the cochaperones include members of the DnaJ family, p48/Hip, p60/Sti1p, and Bag1 (10, 21, 26, 50). Each of these cochaperones has been reported to modulate the ATPase activity of Hsp70 by either stimulating ATP hydrolysis or regulating nucleotide exchange (10, 21, 24, 26). The Hsp70 chaperone machine also appears to function in association with Hsp90 via the action of the p60 gene, an ortholog of the yeast *STI1*, which binds to both chaperone proteins (9, 11, 36, 46). Hsp90 is an abundant and highly conserved molecular chaperone. It exists in several discrete subcomplexes that together comprise the Hsp90 chaperone machine. One of these subcomplexes contains Hsp90/Hsp70/Hip and p60/Sti1 (46), while another contains one of several immunophilins and the acidic protein p23 (31).

The p23 protein was first identified in association with the progesterone receptor (PR) (45) and was later shown to be an Hsp90 binding protein (30, 32, 49). In addition to being found in protein complexes with several unliganded steroid hormone receptors, p23 has been found to associate via Hsp90 with several proteins including transcription factors, protein kinases, and a viral reverse transcriptase (27, 37, 56). In all of these interactions, p23 is thought to be indirectly associated via Hsp90. There is also evidence, however, that p23 can bind independently to polypeptides and prevent them from aggregating (5, 20, 27).

Purified p23 binds to Hsp90 in a manner that is stabilized by nonhydrolyzable ATP and by molybdate ions (49). In addition, complex formation between p23 and Hsp90 is inhibited by geldanamycin, a benzoquinoid ansamycin that was originally defined as a tyrosine kinase inhibitor but was recently shown to specifically interact with Hsp90 (54). Geldanamycin negatively affects the activity of steroid hormone receptors and protein kinases and stimulates their degradation (43, 44, 47, 53). By contrast, p23 appears to be important for stabilizing a high-affinity hormone binding conformation of the glucocorticoid receptor (GR) and PR (14, 47).

Recent studies have demonstrated the conserved nature of yeast and animal cell Hsp90 protein complexes (8, 9; see reference 6 for a review), but to date there has been no report of a yeast p23 homolog. In this report, we present a genetic and biochemical characterization of a p23 homolog from the yeast *Saccharomyces cerevisiae.*

MATERIALS AND METHODS

Materials. Geldanamycin and macbecin were obtained from the Drug Synthesis & Chemistry Branch, Developmental Theraputics Program, Division of Cancer Treatment, National Cancer Institute. Both compounds were stored at 2 mg/ml in dimethyl sulfoxide at −20°C. Monoclonal antibodies to phosphotyrosine (4G10) and v-Src (GD11) were purchased from Upstate Biotechnology (Lake Placid, N.Y.). Antiserum to Hsp90 was described previously (12). and antiserum to Hsp70 was purchased from Affinity Bioreagents. Antisera to Cpr6 and Sti1 were the kind gifts of D. Picard and D. Toft, respectively. Isogenic yeast strains encoding wild-type and G170D mutant forms of *HSP82* were the kind gifts of S. Lindquist. Plasmids encoding the A97I (pts38RV), T101I (pcs2-3RV), and S485Y (pts33BE) *hsp82* mutants were the kind gift of Y. Kimura (33), and those encoding the E431K (pTCA/hsp82 E431K) and T525I (pTCA/hsp82 T525I) mutants of *hsp82* were the gift of K. Yamamoto (3). Plasmid pGVSRC (*CEN/ARS URA3* v-*src*) was the kind gift of Frank Boschelli.

Yeast methods and strains. The genotypes of *S. cerevisiae* strains used in this study are shown in Table 1. Standard genetic methods were used for growth and manipulation. Yeast strains were grown in either rich medium (YPD) or selective minimal medium (0.67% yeast nitrogen base) with 2% glucose (or raffinose or galactose) and supplemented with adenine, uracil, and amino acids, depending on auxotrophy. Transformation of yeast strains was performed as described previously (22). Strain ACY77 was constructed from W3031b by one-step gene

* Corresponding author. Mailing address: Department of Cell Biology and Anatomy, Mount Sinai Medical Center, One Gustave L. Levy Place, New York, NY 10029. Phone: (212) 241-6563. Fax: (212) 860-1174. E-mail: caplan@msvax.mssm.edu.

TABLE 1. Yeast strains used in this study

Strain	Genotype	Reference
W3031b	α *ade2-1 leu2-3,112 his3-11,15 trp1-1 ura3-1 can1-100*	51
CN11	**a** *Δtrp1 lys1 lys2 ura3-52 leu2-3,112 his3-11,15 sti1-1::HIS3*	39
ACY77	α *ade2-1 leu2-3,112 his3-11,15 trp1-1 ura3-1 can1-100 sti1-1::HIS3*	This study
YF233	α *ade2-1 leu2-3,112 his3-11,15 trp1-1 ura3-1 can1-100 sba1-1::URA3*	This study
YF240	α *ade2-1 leu2-3,112 his3-11,15 trp1-1 ura3-1 can1-100 sba1-1::ura3*	This study
YF256	α *ade2-1 leu2-3,112 his3-11,15 trp1-1 ura3-1 can1-100 sba1-1::ura3* pGAL-SBA1	This study
YF257	α *ade2-1 leu2-3,112 his3-11,15 trp1-1 ura3-1 can1-100 sti1-1::HIS3 sba1-1::URA3*	This study
YF265	α *ade2-1 leu2-3,112 his3-11,15 trp1-1 ura3-1 can1-100* pRS426	This study
YF266	α *ade2-1 leu2-3,112 his3-11,15 trp1-1 ura3-1 can1-100* pJR10	This study
AFY200	α *ade2-1 leu2-3,112 his3-11,15 trp1-1 ura3-1 can1-100* pGVSRC	This study
AFY202	α *ade2-1 leu2-3,112 his3-11,15 trp1-1 ura3-1 can1-100 sba1-1::ura* 3 pGVSRC	This study
YF267	α *ade2-1 leu2-3,112 his3-11,15 trp1-1 ura3-1 can1-100* pARH, pPGKarelacZC	This study
YF268	α *ade2-1 leu2-3,112 his3-11,15 trp1-1 ura3-1 can1-100 sba1-1::ura3* pARH, pPGKarelacZC	This study
p82a	**a** *ade2-1 leu2-3,112 his3-11,15 trp1-1 ura3-1 can1-100 (hsc82::LEU2) (hsp82::LEU2)* pTGPDHsp82	38
G170Da	**a** *ade2-1 leu2-3,112 his3-11,15 trp1-1 ura3-1 can1-100 (hsc82::LEU2) (hsp82::LEU2)* pTGPpd/T1-101	38
ACY 2W	**a** *ade2-1 leu2-3,112 his3-11,15 trp1-1 ura3-1 can1-100 (hsc82::LEU2) (hsp82::LEU2)* pTGPDHsp82, pJR1	This study
ACY 1WU	**a** *ade2-1 leu2-3,112 his3-11,15 trp1-1 ura3-1 can1-100 (hsc82::LEU2) (hsp82::LEU2)* pJR1	This study
AFYA97I	**a** *ade2-1 leu2-3,112 his3-11,15 trp1-1 ura3-1 can1-100 (hsc82::LEU2) (hsp82::LEU2)* pts38RV	This study
AFYT101I	**a** *ade2-1 leu2-3,112 his3-11,15 trp1-1 ura3-1 can1-100 (hsc82::LEU2) (hsp82::LEU2)* pcs2-3RV	This study
AFYE431K	**a** *ade2-1 leu2-3,112 his3-11,15 trp1-1 ura3-1 can1-100 (hsc82::LEU2) (hsp82::LEU2)* pTCA/hsp82 E431K	This study
AFYS485Y	**a** *ade2-1 leu2-3,112 his3-11,15 trp1-1 ura3-1 can1-100 (hsc82::LEU2) (hsp82::LEU2)* pts33BE	This study
AFYT525I	**a** *ade2-1 leu2-3,112 his3-11,15 trp1-1 ura3-1 can1-100 (hsc82::LEU2) (hsp82::LEU2)* pTCA/hsp82 T525I	This study

replacement (42) using a DNA fragment containing the *sti1-1::HIS3* allele that was amplified by PCR from the genomic DNA of strain CN11 (38), using the primers 5′ GCGCGCAAGCTTAATATTCTATGTCTGGCAACT 3′ and 5′ GCGCGCTCTAGACTTATTATCTTCAAGTTCCGA 3′ in a 30-cycle reaction at an annealing temperature of 50°C. *sti1-1*/*sba1-1* double mutants were prepared from ACY77 by one-step gene replacement using the 2.4-kb *sba1-1::URA3* fragment as described below.

The *hsp82* mutant strains (except for G170D, which was the gift of S. Lindquist) were constructed from strain p82a (38). This strain was transformed with pJR1 (*CEN6*/*ARS4*/*HSP82*/*URA3*), and the resulting strain (AFY2W) was grown in rich medium to deselect for pTGPD (*HSP82*/*TRP1*). Resulting Trp auxotrophs were designated AFY1WU. This strain was transformed with plasmids containing different *hsp82* mutant genes (see above) and subsequently plated on 5-fluoro-orotic acid to select for loss of pJR1. The resulting strains all contained a single mutant *hsp82* allele (Table 1).

***SBA1* cloning and gene disruption.** *SBA1* was cloned by a 30-cycle PCR amplification (using *Taq* polymerase; annealing temperature of 37°C) from *S. cerevisiae* W3031b genomic DNA, using the primers 5′ GCGCGCCTCGAGGATA ATCATCCAGCA 3′ and 5′ GCGCGCTCTAGAACTGCCTTTTATGAA 3′. The 1,269-bp product was gel purified and cloned into the pCR-Script vector (Stratagene) to generate the clone designated p2323. The *SBA1* disruption allele was generated by insertion of a 1.1-kb blunt-ended DNA fragment containing the *URA3* gene into *Hpa*I-digested p2323, which linearized the plasmid in the *SBA1* open reading frame (ORF). A 2.4-kb DNA fragment containing the *sba1-1::URA3* disruption allele (called *sba1-1* hereafter) was released from this plasmid (pΔ23URA3) by digestion with restriction endonucleases *Xho*I and *Xba*I. This linear 2.4-kb fragment was transformed into haploid wild-type yeast (W3031b) for one-step gene replacement of *SBA1*.

A gene encoding His_6-tagged Sba1 ($Sba1^{His6}$) under control of the yeast *GAL1* promoter was cloned by PCR amplification (using *Pfu* polymerase at an annealing temperature of 55°C) from p2323 by using the primers 5′ ATAGTCATGC ACCACCATCACCACCACTCCGATAAAGTTATTAAC 3′ and 5′ GCGCGC CTCGAGGATAATCATCCAGCA 3′. This amplification resulted in addition of six histidine residues just downstream of the N-terminal methionine. The 1-kb product was first cloned into pCR-Script (Stratagene) and then released from this vector by *Bam*HI and *Sac*I digestion before ligation into pRS316.GAL (*CEN*/*ARS URA3 GAL1-10* promoter) digested with the same restriction endonucleases. The resulting plasmid (pGAL-SBA1) was transformed into an *sba1-1* strain that had been plated on medium containing 5-fluoro-orotic acid (2) to select for reversion to uracil auxotrophy (YF240).

Purification of $Sba1^{His6}$ and preparation of Sba1 antiserum. A gene encoding recombinant $Sba1^{His6}$ for expression in *Escherichia coli* was generated by PCR amplification from p2323 (as above), using the primers 5′ GCGCGCCATATG TCCGATAAAGTTATTAAC 3′ and 5′ GCGCGCGGATCCAAGTTACTCA TTCTAGCA 3′. The 1-kb product was cloned into pCR-Script (Stratagene), excised by using *Nde*I and *Bam*HI, and subcloned into similarly digested pET15b (Novagen). Construction of *SBA1* in this vector resulted in an N-terminal sequence extension juxtaposed to wild-type *SBA1* sequence as follows: MGSSHH HHHHSSGLVPRGSH (single-letter amino acid code). The resulting plasmid, p23ET, was transformed into *E. coli* BL21(DE3). Expression of $Sba1^{His6}$ was induced as follows. BL21(DE3) containing p23ET was grown overnight at 37°C in 100 ml of LB medium plus 50 μg of ampicillin per ml. The culture was diluted 1:10 into fresh LB medium and incubated for 1 h at 37°C before addition of isopropyl-β-D-thiogalactopyranoside to a final concentration of 1 mM. The culture was incubated for a further 2 h before harvesting the cells. The cells were resuspended in 5 ml of BL buffer (10 mM Tris-HCl [pH 7.5], 50 mM Sba1, 50 mM KCl, 10 mM $MgCl_2$, 1 mM EDTA, 5 mM dithiothreitol, 1 mM phenylmethylsulfonyl fluoride [PMSF], protease inhibitor cocktail containing equimolar amounts of aprotinin, chymostatin, leupeptin, and pepstatin [each at 2 μg/ml]) and broken by sonication (10 times, 10-s bursts with cooling on ice for 30 s between bursts). The lysate was cleared by centrifugation at 14,000 × *g* for 30 min at 4°C. The protein concentration was adjusted to 10 mg/ml with lysis buffer.

$Sba1^{His6}$ was purified by a two-step procedure. First, $Sba1^{His6}$ present in the crude bacterial lysate was bound to Ni-nitrilotriacetic acid (NTA) resin (Qiagen) in batch. This was performed by adding 2 ml of Ni-NTA resin (equilibrated in lysis buffer) to 20 ml of crude lysate (at 10 mg/ml) supplemented with 5 mM imidazole (Sigma); this mixture was incubated on a nutator for 30 min at 4°C. The resin was collected by centrifugation at 1,000 × *g* and washed twice in lysis buffer plus 10 mM imidazole and twice with lysis buffer plus 20 mM imidazole. Bound proteins were eluted in lysis buffer plus 150 mM imidazole in a 3-ml volume for 10 min at 4°C. The eluate was dialyzed overnight against 20 mM HEPES (pH 7.2)–0.2 mM EDTA–0.5 mM PMSF. The dialyzed eluate was concentrated in a Centricon-10 centrifugal concentrator before loading onto a 5-ml Mono-Q column. Bound proteins were eluted with a 0 to 500 mM KCl gradient.

Antiserum to $Sba1^{His6}$ was prepared by resolving crude bacterial lysate as described above in a denaturing 10% polyacrylamide gel. The band containing $Sba1^{His6}$ was identified after Coomassie blue staining and excised with a razor blade. Antiserum to $Sba1^{His6}$ was prepared from these gel slices in rabbits by Covance Research Products Inc. (Denver, Pa.).

Affinity isolation of Sba1 from yeast. One-step affinity chromatography of $Sba1^{His6}$ expressed in yeast was performed by a modification of the procedure of Fang et al. (18). Briefly, 100-ml yeast cultures were harvested, the pellet was washed once with water and once with YL buffer (10 mM Tris-HCl [pH 7.5], 50 mM NaCl, 50 mM KCl, 10 mM $MgCl_2$, 1 mM EDTA, 1 mM PMSF, and protease inhibitor cocktail [2 μg/ml] as described above). The pellet was resuspended in 0.8 ml of lysis buffer plus 20 mM sodium molybdate, and the cells were broken in the presence of 1.5 g of 0.4-mm-diameter glass beads by 5 30-s bursts in a mini-BeadBeater (Biospec Products) at 4°C, with cooling on ice for 30 s between bursts. The crude lysate was cleared at 14,000 × *g* for 30 min at 4°C. The protein concentration was adjusted to 3 mg/ml, and 0.5 ml of protein extract was incubated with 50 μl of Ni-NTA resin (equilibrated in lysis buffer) for 15 min at 4°C on a nutator. The resin was collected at 500 × *g* and washed three times in 1 ml of lysis buffer plus 20 mM sodium molybdate and 10 mM imidazole. The resin was incubated with 50 μl of elution buffer (lysis buffer plus 150 mM imidazole) at 4°C for 10 min. The eluted protein was resolved by sodium dodecyl sulfate-polyacrylamide gel electrophoresis (SDS-PAGE) and analyzed by Coomassie blue staining or by Western blotting.

In vitro assembly assay. $Sba1^{His6}$ purified from *E. coli* was bound to Ni-NTA resin (30 μl of packed beads, equilibrated in YL buffer as described above) by

```
Sba1  MSDKVINPQV AWAQRSSTT.D PERNYVLITV SIADCDAPEL TIKPSYIELK  50
Cp23  *......... ...*PA*AKWY DR*D**F*EF CVE*SKDVNV NFEK*KLTF.  38
Hp23  *......... ...*PA*AKWY DR*D**F*EF CVE*SKDVNV NFEK*KLTF.  38

Sba1  AQSKPHVGDE NVHHYQLHID LYKEIIPEKT MHKVANGQHY FLKLYKKDLE  100
Cp23  SCLGGSD... *FK*LN.E** *FNN*D*NES K**RT..DRS I*CCLR*GES   82
Hp23  SCLGGSD... *FK*LN.E** *FHC*D*NDS K**RT..DRS I*CCLR*GES   82

Sba1  SEYWPRLTKE KVKYPYIKTD FDKWVDEDEQ DEVEAEGNDA AQGM.DFSQM  149
Cp23  GQA******* RA*LNWLSV* *NN*K*WEDD SD........ .ED*SN*DRF  123
Hp23  GQS******* RA*LNWLSV* *NN*K*WEDD SD........ .ED*SN*DRF  123

Sba1  MGGAGGAGGA GGMDFSQMMG GAGGAGSPDM AQLQQLLAQS GGNLDMGDFK  199
Cp23  SE........ ........**N NM**D..... .......... ..........  133
Hp23  SE........ ........**N NM**D..... .......... ..........  133

Sba1  .......... ENDEEDEEEE IEPEVKA                           216
Cp23  DDVDLPEVDG AD*DSPDSDD EKMPDLE                            160
Hp23  EDVDLPEVDG AD*DSQDSDD EKMPDLE                            160
```

FIG. 1. Sequence comparison of Sba1 with chicken (Cp23) and human (Hp23) p23 proteins. Identical matches are denoted by asterisks; gaps in the sequence are denoted by periods.

direct addition and incubation for 15 min at 4°C. Beads containing 1 μg of $Sba1^{His6}$ were added to 100 μl of desalted yeast whole-cell extract (at a concentration of 1 mg/ml; prepared by using a 5-ml HiTrap desalting column [Pharmacia]). The volume was adjusted to 250 μl with YL buffer, and the mixture was incubated for 30 min at 30°C. The beads were collected by centrifugation at 1,000 × *g* and washed three times with 1 ml of YL buffer plus 10 mM imidazole. Protein was eluted from the beads YL buffer plus 150 mM imidazole in a 30-μl volume for 10 min at 4°C and analyzed by SDS-PAGE and Western blotting.

v-Src expression, immunoblot analysis, and steroid hormone receptor assays. Lysates of yeast expressing v-Src were prepared as follows. Yeast cultures were grown at 30°C in minimal medium containing 2% (wt/vol) raffinose to late log phase. v-Src expression was induced by the addition of 2% (wt/vol) galactose to the medium. Induction was continued for 6 h, at which time cells were harvested, resuspended in YLS buffer (20 mM Tris-HCl [pH 7.4], 0.14 M NaCl, 5 mM EDTA, 1% Nonidet P-40, 1 mM sodium vanadate, 5 mM dithiothreitol, 1 mM PMSF, a mixture of aprotinin, chymostatin, leupeptin, and pepstatin [each at 2 μg/ml]), and lysed with glass beads as described above. Lysates were cleared of broken cell debris at 14,000 × *g*.

The levels of tyrosine phosphorylation and v-Src protein were assayed by immunoblot analysis using either antiphosphotyrosine or anti-v-Src monoclonal antibodies (see Materials and Methods). Lysates (100 μg of total protein) were resolved by SDS-PAGE and transferred to nitrocellulose membranes (0.45 μm; MSI). Filters were washed briefly with TTBS (20 mM Tris-HCl [pH 7.5], 0.5 M NaCl, 0.05% Tween 20) and blocked overnight with TTBS containing 5% nonfat dry milk. Filters were incubated with antibodies to v-Src or phosphotyrosine (diluted 1:1,000 in antibody dilution buffer [1× phosphate-buffered saline, 3% bovine serum albumin, 0.05% Tween 20, 0.1% thimerosal) for 2 h. Filters were washed three times for 10 min each in TTBS. Filters were incubated with secondary antibody (horseradish peroxidase-conjugated goat anti-mouse immunoglobulin G, diluted 1:10,000 in antibody dilution buffer) for 1 h, and subsequently washed as for the primary antibody. Filters were then treated with the chemiluminescence reagent (Pierce) and exposed to X-ray film for detection.

Immunoblots for detecting Sba1, Cpr6, Sti1, and Hsp90 were processed by standard procedures after transfer of the proteins in denaturing gels to nitrocellulose membranes. The filters were typically blocked overnight in TTBS plus 5% nonfat dried milk and incubated with primary and secondary antibodies for 1 to 2 h. Filters were washed between antibody incubations with TTBS (three times, 5 min each), and proteins were detected as described above. Assays for steroid hormone receptor activation were performed as previously described (7, 18).

RESULTS

YKL117W is orthologous to vertebrate p23 genes. A BLAST search of the GenBank database with the sequence of human p23 protein revealed a single orthologous ORF in *S. cerevisiae* displaying 24% identical amino acids (28). This gene (YKL117W) encodes a putative protein of 24.1 kDa, which is 5.4 kDa larger than the human p23 protein (18.7 kDa) (Fig. 1 shows protein sequence alignments). YKL117W resides on the left arm of chromosome XI between coordinates 219970 and 220620, just downstream of a $tRNA^{Ala}$ gene and upstream of a hypothetical ORF, YKL116C.

The YKL117W protein sequence displays weak identity and similarity throughout its length with human and chicken p23

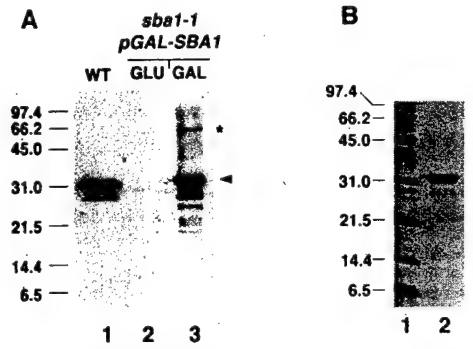

FIG. 2. Characterization of Sba1 by gel electrophoresis. (A) Western blot analysis of Sba1 in yeast whole-cell extracts using polyclonal anti-Sba1. Lane 1, 50 μg of whole-cell extract from wild-type (WT) cells; lane 2, 50 μg of whole-cell extract from *sba1-1* cells containing pGAL-SBA1 (YF256) grown in glucose-containing medium; lane 3, 5 μg of whole-cell extract from *sba1-1* cells containing pGAL-SBA1 grown in galactose-containing medium. The arrowhead shows positions of Sba1 (lane 1) and $Sba1^{His6}$ (lane 3). The asterisk shows the band at 60 kDa that reacts with anti-Sba1 in cells overexpressing $Sba1^{His6}$. (B) Coomassie blue-stained gel of 2 μg of $Sba1^{His6}$ (lane 2) after overexpression in *E. coli* and protein purification. Molecular size markers (in kilodaltons) shown in lane 1.

proteins. The strongest region of identity is between seven identical consecutive amino acids starting at position 104 of the yeast sequence: Trp Pro Arg Leu Thr Lys Glu (three-letter code). The sequences of vertebrate and yeast p23 proteins diverge toward the C-terminal end, with the yeast protein having additional sequence that is rich in hydrophobic amino acids. This region contains the motif Gly Gly Ala repeated five times from amino acids 150 to 174. Like human and chicken p23 proteins, YKL117W has an acidic C terminus. We have named this yeast gene *SBA1* because the binding of Sba1 to Hsp90 is sensitive to benzoquinoid ansamycins, as will be shown below.

***SBA1* is nonessential and constitutively expressed.** The *SBA1* gene was cloned by PCR amplification from wild-type yeast genomic DNA. Northern blot analysis revealed that *SBA1* is constitutively expressed as previously found (17) but not heat shock inducible under the same conditions when *STI1* mRNA is induced (reference 38 and data not shown). Sba1 protein was detected in wild-type yeast whole-cell extracts by Western blot analysis using antisera prepared from recombinant $Sba1^{His6}$ expressed in *E. coli*. Wild-type Sba1 migrates anomalously at 32 kDa, approximately 8 kDa larger than the predicted size (Fig. 2A, lane 1). $Sba1^{His6}$ also migrated anomalously at 32 kDa after inducible expression in yeast or after purification (to approximately 90%) from *E. coli* (Fig. 2).

A disruption allele was constructed by inserting the *URA3* gene into the *SBA1* ORF. Replacement of wild-type genomic *SBA1* with the disruption allele (*sba1-1*) resulted in complete loss of Sba1 protein expression as assessed by Western blotting (Fig. 2A), although this did not result in a very severe growth phenotype. Using a plate assay to determine the relative growth rate of wild-type and *sba1-1* cells, there was very little difference in the growth rate at 30 or 37°C, although the *sba1-1* cells grew noticeably more slowly at 18°C (Fig. 3). In liquid media, *sba1-1* cells had a doubling time similar to that of the wild type at 30°C but grew 1.6 times more slowly than the wild type at 37°C. Thus, deletion of Sba1 protein resulted in mild growth defects at both low and high temperatures but not at 30°C.

To investigate the relationship between Sba1 and other components of the molecular chaperone machinery, we constructed a double mutant that was deleted for *SBA1* and also

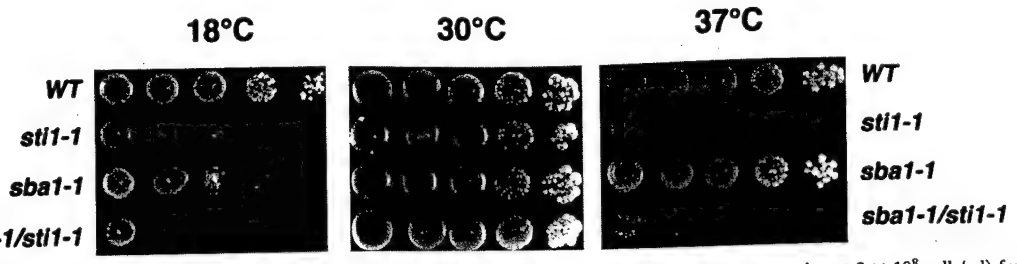

FIG. 3. Growth phenotype of *sba1-1* cells. Each panel shows a serial dilution of yeast cells spotted (3 μl of culture starting at 2×10^8 cells/ml) from left to right of each plate, using wild-type (WT), *sti1-1*, *sba1-1*, and double-mutant (*sba1-1/sti1-1*) strains. Each plate was incubated at the indicated temperature for either 4 days (30 and 37°C) or 7 days (18°C).

for *STI1*, a gene encoding an Hsp90 cochaperone that is orthologous to p60 of vertebrate cells (8, 9, 36, 38, 46). As previously shown, *STI1* deletion results in reduced growth at both low and high temperatures (38) (Fig. 3). While the double mutant grew normally at 30°C, it exhibited synthetic defects by having more restrictive growth at both 18 and 37°C compared with either mutant alone (Fig. 3). These synthetic defects suggest that Sba1 and Sti1 either interact with each other or function in the same or redundant processes. Expression of wild-type *SBA1* on a low-copy-number plasmid in the double mutant resulted in a growth phenotype similar to that of the *sti1-1* mutant (data not shown). The temperature-sensitive growth phenotype of *sba1-1/sti1-1* double mutants was somewhat strain dependent, being more severe in the W303 background having the *ade2* mutation than in strains that were *ADE2* wild type.

Sba1 interacts with Hsp90. Vertebrate p23 proteins bind to Hsp90 in a nucleotide-dependent manner (49). To determine whether Sba1 also interacts with Hsp90, $Sba1^{His6}$ was inducibly expressed from the yeast *GAL1* promoter at 30°C in the *sba1-1* disruption strain (Fig. 2A). $Sba1^{His6}$ was isolated from whole-cell extracts by affinity chromatography using Ni-NTA resin. Examination of the protein profiles after affinity chromatography revealed that many yeast proteins bound nonspecifically to the Ni-NTA resin. However, comparison of the eluates from induced and noninduced cells revealed the presence of two major bands at 32 and 86 kDa that were observed only after $Sba1^{His6}$ induction (Fig. 4A; compare lanes 4 and 5). The band at 32 kDa corresponds to $Sba1^{His6}$ itself and reacted with Sba1 antiserum (data not shown), while the 86-kDa protein (which appears as a very tight doublet in Fig. 4A) reacted with antiserum to Hsp90 (Fig. 4B). The isolation of Hsp90 with Ni-NTA resin was dependent on the presence of $Sba1^{His6}$, since it was not isolated from extracts of wild-type cells not containing plasmid pGAL-SBA1 (Fig. 4B). Complex formation between Hsp90 and $Sba1^{His6}$ was stabilized by the presence of sodium molybdate in the binding and wash buffers; omission of sodium molybdate from the wash buffer destabilized the complex and Hsp90 dissociated from $Sba1^{His6}$ (Fig. 4C).

In vertebrate cells, p23 binds to Hsp90 in a complex with immunophilins such as cyclophilin 40. *S. cerevisiae* contains cyclophilin homologs encoded by the *CPR6* and *CPR7* genes that also bind to Hsp90 (16, 52). We therefore analyzed whether one of these proteins (Cpr6) was present in the $Sba1^{His6}$-Hsp90 complexes isolated by the affinity chromatography procedure described above. Cpr6 was identified in this experiment by using specific antisera (52), and as shown in Fig. 4C, it is highly enriched in the eluates containing $Sba1^{His6}$ and Hsp90. We also observed a small amount of Sti1p to coisolate with $Sba1^{His6}$ (Fig. 4D, lower panel), although the amount is very small compared with Cpr6, as judged by the relative band intensity of the eluted sample (Fig. 4D, lane 3) compared with the corresponding extract sample (Fig. 4D, lane 1).

The formation of $Sba1^{His6}$-Hsp90 complexes was further investigated by an in vitro assembly assay. Purified recombinant $Sba1^{His6}$ was first bound to Ni-NTA resin and then incubated at 30°C with desalted whole-cell extracts from a wild-type yeast strain. Complex formation with Hsp90 was assayed after reisolation of the resin bound $Sba1^{His6}$, several rounds of washing, and subsequent protein elution with a high concentration of imidazole. The presence of Hsp90 was determined after SDS-PAGE and Western blot analysis. As shown in Fig. 5, complex formation between Hsp90 and $Sba1^{His6}$ was extremely weak in the absence of nucleotide or in the presence of AMP, ADP, or ATP. Complex formation between Hsp90 and $Sba1^{His6}$ was readily observed, however, when the extracts were supplemented with adenyl-imidodiphosphate (AMP-PNP) or adenosine 5′-*O*-(3-thiotriphosphate) (ATPγS), suggesting that this interaction is strongest when ATP is unable to be hydrolyzed. The binding of $Sba1^{His6}$ to Hsp90 is apparently specific since there was no interaction with Hsp70 under any of the conditions used, as revealed by reprobing the Western blot with antiserum to Hsp70 as shown in Fig. 5A. The interaction between $Sba1^{His6}$ and Hsp90 can also occur with either the Hsc82 or the Hsp82 isoform, as judged by the formation of complexes in strains having deletions in either the *HSC82* or *HSP82* gene (data not shown). This interaction with both isoforms may account for the presence of a doublet at 86 kDa (4) after affinity isolation of $Sba1^{His6}$ from wild-type yeast cell extracts after in vivo expression (Fig. 5A).

We also tested whether binding of $Sba1^{His6}$ to Hsp90 was sensitive to benzoquinoid ansamycins, which have been shown to inhibit complex formation between p23 and Hsp90 (23, 32, 47). Similar inhibition occurs between yeast Hsp90 and Sba1. As shown in Fig. 5B, both geldanamycin and the related compound macbecin inhibit the association of purified Sba1 with Hsp90 in yeast extracts supplemented with AMP-PNP. The inhibition by macbecin is 5- to 10-fold less sensitive than was found for geldanamycin.

The in vitro binding assay was used to identify residues in Hsp90 that are critical to Sba1 binding. This experiment was performed by incubating purified $Sba1^{His6}$ with extracts from yeast cells expressing different mutant forms of Hsp90 (specifically the Hsp82 isoform expressed from a constitutive promoter). Six different point mutants were used in this experiment (Fig. 5C), and in the presence of AMP-PNP, only two of these mutant forms of Hsp90 (T101I and E431K) were able to bind to $Sba1^{His6}$. Of those that failed to bind $Sba1^{His6}$, two have their mutations in the N-terminal nucleotide binding domain and two (S485Y and T525I) reside in the C-terminal half of Hsp90, suggesting that this region is also important for $Sba1^{His6}$ binding.

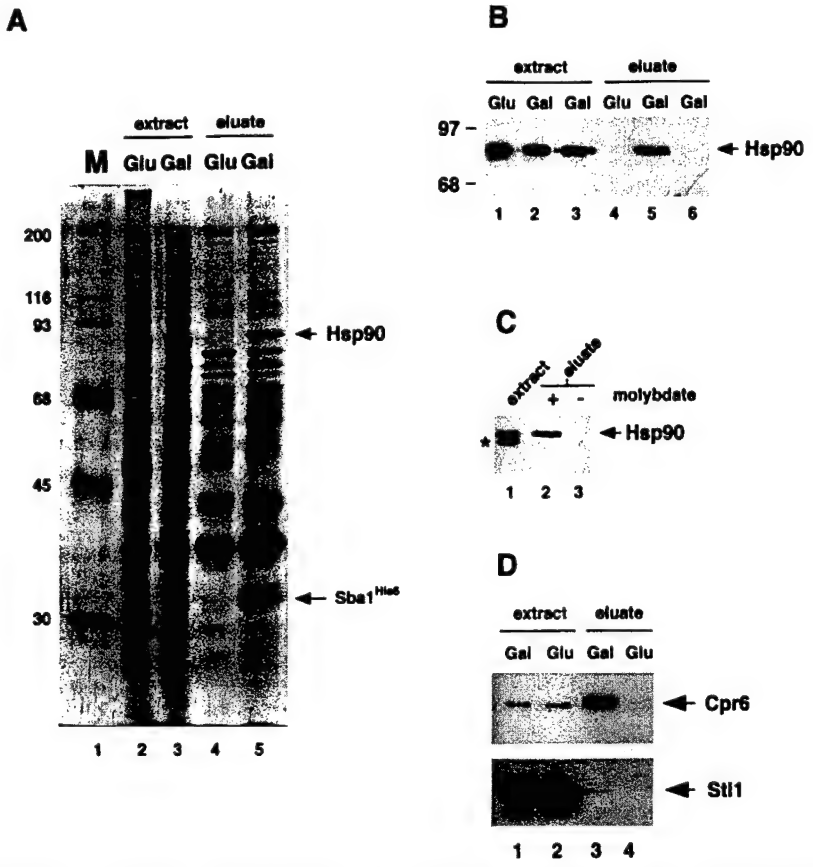

FIG. 4. Sba1^{His6} binding to Hsp90. (A) Coomassie blue-stained gel of whole-cell extracts from strain YF256 (*sba1-1* pGAL-SBA1) (lanes 2 and 3) and eluates after affinity chromatography with Ni-NTA resin (lanes 4 and 5). Extracts were prepared from cells grown in glucose-containing medium (lanes 2 and 4) or galactose-containing medium (lanes 3 and 5). Molecular size markers (M, in kilodaltons) are shown in lane 1. Bands corresponding to Sba1^{His6} and Hsp90 are indicated by arrows. (B) Detection of Hsp90 by Western blot analysis in whole-cell extracts (lanes 1 to 3) and eluates after Ni-NTA resin affinity chromatography (lanes 4 to 6). Extracts and eluates were prepared from strain YF256 grown in glucose (lanes 1 and 4)- or galactose (lanes 2 and 5)-containing medium and wild-type strain W3031b grown in galactose-containing medium (lanes 3 and 6). (C). Western blot analysis of Hsp90 after isolation of Sba1^{His6} protein complexes on Ni-NTA resin and washing in buffers plus (lane 2) or minus (lane 3) sodium molybdate. A Western blot of the whole-cell extract is shown in lane 1; the band labeled with an asterisk is an Hsp90 degradation product. Data are from nonconsecutive lanes of the same gel and Western blot. (D) Western blot analysis of Cpr6 (upper panel) and Sti1 (lower panel) after isolation of Sba1^{His6} protein complexes on Ni-NTA resin. Lanes 1 and 2, whole-cell extracts of cells grown in galactose or glucose; lanes 3 and 4, eluates after affinity chromatography on Ni-NTA resin.

These combined results demonstrate the similarity in structure and function between Sba1 and vertebrate p23 proteins. We next performed a functional analysis in yeast to determine whether Sba1 loss of function affected processes known to require the Hsp90 chaperone machine: the activity of the tyrosine kinase v-Src and steroid hormone receptors.

Role of Sba1 in v-Src maturation and steroid hormone receptor activation. After heterologous expression in yeast, the tyrosine kinase v-Src is active in a manner that is dependent on Hsp90 and its cochaperones. In wild-type cells, expression of v-Src from a galactose-inducible promoter leads to greatly increased levels of phosphotyrosine (Fig. 6A) which result in a lethal phenotype (reference 19 and data not shown). Previous studies have shown that mutation or deletion of yeast genes encoding Hsp90 or other components of the Hsp90 chaperone machine resulted in decreased levels of v-Src activity, often suppressing the lethal phenotype accompanying it (9, 12, 13, 16, 34, 35, 55). Disruption of the *SBA1* gene, however, did not suppress this lethal phenotype upon inducible expression of v-Src. Furthermore, v-Src gene induction from a *GAL1* promoter led to similar accumulation of v-Src protein (Fig. 6A, lower panel), and the level of protein tyrosine phosphorylation, as assessed by Western blotting with antiphosphotyrosine, revealed significant v-Src activity in *sba1-1* cells (Fig. 6A), although the levels were approximately twofold lower in this strain than in the wild type (Fig. 6B).

We also tested whether Sba1 was important for signaling by steroid hormone receptors. For these experiments, androgen receptors (AR) were assayed for hormone-dependent transactivation of a *lacZ* reporter gene in wild-type and *sba1-1* strains. However, there was only a slight decrease in signaling in the mutant compared to the wild type (Fig. 6C), corresponding to a mean of 82% of wild-type activity in the *sba1-1* mutant. Similar results were obtained by assaying GR activity in the same strains (data not shown). Thus, Sba1 loss of function did not significantly affect the activity of proteins known to require other components of the Hsp90 chaperone machine.

DISCUSSION

Molecular chaperones are thought to play a major role in the folding and assembly of newly synthesized polypeptide chains in both prokaryotes and eukaryotes. Hsp70 and Hsp90 are the most abundant molecular chaperones in the eukaryotic cytosol and are probably responsible for the majority of chaperoning events taking place in this compartment. These ac-

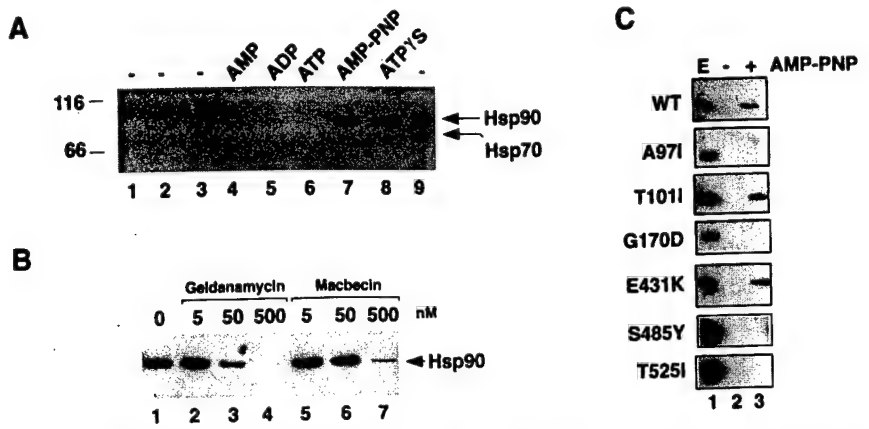

FIG. 5. In vitro association of Sba1^{His6} with Hsp90. (A) Purified Sba1^{His6} was prebound to Ni-NTA resin and added to desalted whole-cell extracts from wild-type yeast cells and incubated at 30°C for 30 min. Hsp90 binding to Sba1^{His6} (lanes 1 to 8; lane 9 is whole-cell extract loaded directly onto the gel) was determined after reisolation of Sba1^{His6} and Western blotting using anti-Hsp90. Lane 1, Ni-NTA-Sba1^{His6} incubated in buffer; lane 2, Ni-NTA resin without prebound Sba1^{His6} incubated with extract; lane 3; Ni-NTA-Sba1^{His6} incubated with extract but without further addition; lane 4, Ni-NTA-Sba1^{His6} incubated with extract plus 5 mM AMP; lane 5, Ni-NTA-Sba1^{His6} incubated with extract plus 5 mM ADP; lane 6, Ni-NTA-Sba1^{His6} incubated with extract plus 5 mM ATP; lane 7, Ni-NTA-Sba1^{His6} incubated with extract plus 5 mM AMP-PNP; lane 8, Ni-NTA-Sba1^{His6} incubated with extract plus 5 mM ATPγS; lane 9, 2.5 μg of desalted whole-cell extract. The blot was first probed with anti-Hsp90 and subsequently reprobed with anti-Hsp70. Molecular size markers are shown in kilodaltons at left. (B) Binding of Hsp90 to Sba1^{His6} is competed by benzoquinoid ansamycins. Ni-NTA-Sba1^{His6} resin was incubated with desalted extracts as described above plus 5 mM AMP-PNP in the presence of solvent (dimethyl sulfoxide; lane 1), geldanamycin (lanes 2 to 4), or macbecin (lanes 5 to 7) at the concentrations indicated. After 30 min at 30°C, the resin was reisolated and washed, and bound proteins were resolved by SDS-PAGE. Hsp90 was detected by Western blotting. (C) Binding of wild-type (wt) and different mutant forms of Hsp90 to Ni-NTA-Sba1^{His6} resin. Lane 1, whole-cell extract (E); lane 2, incubation of Ni-NTA-Sba1^{His6} resin with extracts in the absence of AMP-PNP; lane 3, incubation of Ni-NTA-Sba1^{His6} resin with extracts in the presence of AMP-PNP. The Western blots were probed with anti-Hsp90.

tivities occur in association with various cochaperones that modulate Hsp70 or Hsp90 action and may also function as molecular chaperones themselves.

The Sba1 protein has properties similar to those of the vertebrate Hsp90 cochaperone, p23. These proteins display several regions of conserved sequence similarity, although the overall amino acid sequence identity between Sba1 and p23 is only 24% (Fig. 1). In addition, both p23 and Sba1 migrate more slowly in denaturing gels than would be predicted from their size, suggesting some shared structural feature (30).

Sba1 and p23 also have functional similarities. Both bind to Hsp90 in a manner that is stabilized by nonhydrolyzable ATP or by molybdate ions (32, 49). This nucleotide requirement is likely to represent the binding of ATP to Hsp90 itself, which has recently been shown to have a nucleotide binding pocket in its N-terminal domain (41). Indeed, two mutations in the *HSP82* gene (A97I and G170D) that alter amino acids adjacent to those directly interacting with the nucleotide prevent binding of Sba1p to Hsp90 in vitro (Fig. 5C). Similar inhibition has also been observed between human Hsp90 and p23 when the G170 equivalent (G182 in human Hsp90) is mutated to aspartate (23). Residues at the C-terminal domain of Hsp90 also appear to be important for its interaction with Sba1, since no complex formation was observed with the S485Y or T525I

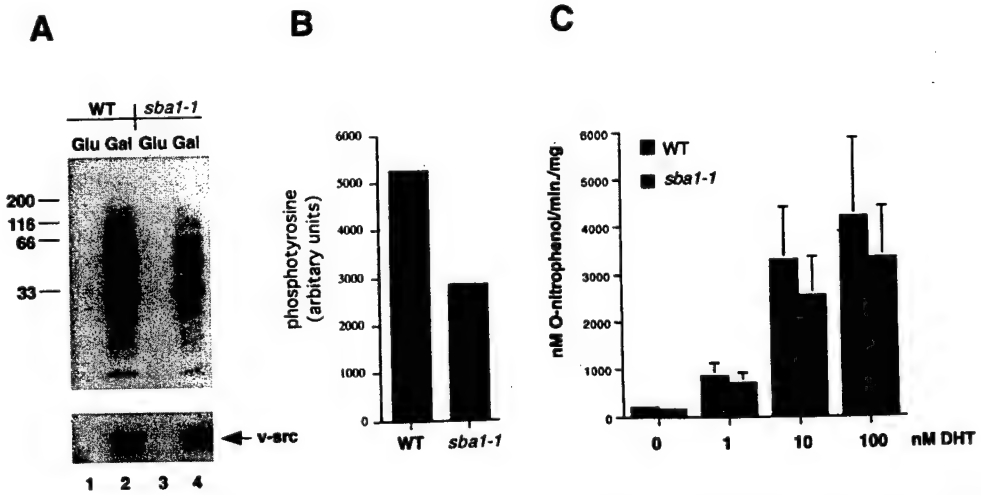

FIG. 6. v-Src and AR activities in wild-type and *sba1-1* mutant yeast cells. (A) Western blot analysis of phosphotyrosine activity (upper panel) and the level of v-Src protein (lower panel) in wild-type (WT; strain AFY200; lanes 1 and 2) or *sba1-1* (strain AFY202; lanes 3 and 4) cells after growth in glucose (lanes 1 and 3) or galactose (lanes 2 and 4) for 6 h. Molecular size markers are shown in kilodaltons at the left. (B) Quantitation of the level of phosphotyrosine in wild-type and *sba1-1* cells from the Western blot shown in panel A. (C) *lacZ* gene expression in wild-type (strain YF267) and *sba1-1* cells (strain YF268) after addition of dihydrotestosterone (DHT) as indicated. Cells were assayed for β-galactosidase 2 h after addition of hormone. Data are means of three independent assays.

mutant (Fig. 5C). A further similarity between vertebrate and yeast p23 proteins derives from the finding that Sba1 association with Hsp90 is inhibited by geldanamycin and by the related compound macbecin, which has been shown to affect the activity of p53 expressed in yeast (1). Geldanamycin binds in the nucleotide binding pocket of human Hsp90 (48) and also inhibits complex formation with p23 (23, 47, 49). The effect of N-terminal mutations in Hsp90 and the effect of geldanamycin or macbecin may therefore be related to nucleotide-dependent conformations that may allosterically affect the binding of Sba1 elsewhere in Hsp90. The most likely candidate region for Sba1 binding is therefore the C-terminal half of Hsp90, since two of three mutations in this region (S485Y and T525I) blocked complex formation.

The complex between p23 and Hsp90 in animal cells also contains one of several immunophilins, such as cyclophilin 40 (31). Similar interactions also occur in yeast, since the cyclophilin Cpr6 is highly enriched in eluates after affinity chromatography of $Sba1^{His6}$. By contrast, the Sti1 cochaperone was present in these complexes in much smaller amounts. Previous biochemical studies have concluded that p60 and p23 reside independently of each other on different Hsp90 subcomplexes (30, 46) and that immunophilins and p60 compete with each other for the same binding site on Hsp90 (40). The relationship between p23 and p60/Sti1 may not be so discrete, however, since purified p23 can interact with the Hsp90-Hsp70-p60 complex, suggesting that these proteins may indeed function together, if only in a temporary manner (14, 32). Our results are consistent with there being a functional interaction between Sti1 and Sba1, based on the biochemical evidence that they coexist in the same complexes (albeit to a very small degree) in addition to the synthetic growth defects of the *sba1/sti1* double mutant.

Together, these combined data indicate that Sba1 is a yeast homolog of vertebrate p23 proteins. *SBA1* disruption did not result in any major growth phenotype, however, although the *sba1-1* cells grew more slowly at both low and high temperatures compared to the wild type. These data contrast with the relative importance of Hsp90 for cell growth (4) and suggest that Sba1 is dispensable for general chaperone-mediated protein folding under normal conditions, although it may have a more specific role under nonoptimal growth conditions.

The vertebrate p23 protein has been characterized as a component of Hsp90 containing heterocomplexes with steroid hormone receptors and with v-Src. However, loss of Sba1 function resulted in only mild defects in steroid receptor signaling or v-Src activity. These data contrast with the relative importance of other yeast Hsp90 or Hsp70 cochaperones to both steroid receptor signaling and v-Src activity, such as Ydj1, Cdc37, Cpr7, and Sti1 (9, 12, 13, 16, 34, 35, 55). The results from the *sba1-1* strain are especially surprising given the relative importance attributed to p23 for stable complex formation between Hsp90 and steroid hormone receptors (14, 31). However, the near-wild-type activity of AR and GR in the *sba1-1* strain is consistent with the recent finding that while p23 is important to stabilize Hsp90-GR complexes in a high-affinity hormone binding state (14), it is not responsible for generating this conformation (15), through which receptor activation is likely to occur in yeast. In the absence of p23, the GR can attain the high-affinity hormone binding state via the action of Hsp90/Hsp70 and p60, although its ability to maintain it is severely compromised. But as observed by Dittmar and Pratt (15), heterocomplex instability does not preclude hormone binding if the ligand is incubated during heterocomplex assembly. Thus, Sba1 may be dispensable for AR and GR signaling because it stabilizes the activatable state rather than generates it. In this manner, Sba1 may contribute to the efficiency with which chaperone-mediated folding of steroid receptors and v-Src take place and hence the relatively mild reductions in activity resulting from its loss of function.

ACKNOWLEDGMENTS

We thank Jie Jin for help with protein purification, Alex Shorstein for help with *SBA1* gene cloning, and Robert J. Donnelly (Molecular Resource Facility, New Jersey Medical School, UMDNJ) for DNA sequencing. We also thank F. Boschelli and E. Craig, Y. Kimura, S. Lindquist, D. Picard, D. Toft, and K. Yamamoto for the gifts of reagents, Sean Bohen for discussions and communication of results prior to publication, and Jeanne Hirsch for comments on the manuscript.

This work was supported by grants from the NIH (R01-DK49065) and the Sinsheimer Foundation to A.J.C.

REFERENCES

1. **Blagosklonny, M. V., J. Toretsky, S. Bohen, and L. Neckers.** 1996. Mutant conformation of p53 translated in vitro or in vivo requires functional HSP90. Proc. Natl. Acad. Sci. USA **93:**8379–8383.
2. **Boeke, J. D., J. Trueheart, G. Natsoulis, and G. R. Fink.** 1987. 5-Fluoroorotic acid as a selective agent in yeast molecular genetics. Methods Enzymol. **154:**164–175.
3. **Bohen, S. P., and K. R. Yamamoto.** 1993. Isolation of Hsp90 mutants by screening for decreased steroid receptor function. Proc. Natl. Acad. Sci. USA **90:**11424–11428.
4. **Borkovich, K. A., F. W. Farrelly, D. B. Finkelstein, J. Taulien, and S. Lindquist.** 1989. Hsp82 is an essential protein that is required in higher concentrations for growth of cells at higher temperatures. Mol. Cell. Biol. **9:**3919–3930.
5. **Bose, S., T. Weikl, H. Bügl, and J. Buchner.** 1996. Chaperone function of Hsp90-associated proteins. Science **274:**1715–1717.
6. **Caplan, A. J.** 1997. Yeast molecular chaperones and the mechanism of steroid hormone action. Trends Endocrine Metab. **8:**271–276.
7. **Caplan, A. J., E. Langley, E. M. Wilson, and J. Vidal.** 1995. Hormone dependent transactivation by the human androgen receptor is regulated by a dnaJ protein. J. Biol. Chem. **270:**5251–5257.
8. **Chang, H.-C. J., and S. Lindquist.** 1994. Conservation of Hsp90 macromolecular complexes in Saccharomyces cerevisiae. J. Biol. Chem. **269:**24983–24988.
9. **Chang, H.-C. J., D. F. Nathan, and S. Lindquist.** 1997. In vivo analysis of the Hsp90 cochaperone Sti1 (p60). Mol. Cell. Biol. **17:**318–325.
10. **Cheetham, M. E., and A. J. Caplan.** 1998. Structure, function and evolution of dnaJ: conservation and adaptation of chaperone function. Cell Stress Chap. **3:**28–36.
11. **Chen, S., V. Prapapanich, R. A. Rimerman, B. Honoré, and D. F. Smith.** 1996. Interactions of p60, a mediator of progesterone receptor assembly, with heat shock proteins Hsp90 and Hsp70. Mol. Endocrinol. **10:**682–693.
12. **Dey, B., A. J. Caplan, and F. Boschelli.** 1996. The YDJ1 molecular chaperone facilitates formation of active $p60^{v\text{-}src}$ in yeast. Mol. Biol. Cell **7:**91–100.
13. **Dey, B., J. J. Lightbody, and F. Boschelli.** 1996. CDC37 is required for $p60^{v\text{-}src}$ activity in yeast. Mol. Biol. Cell **7:**1405–1417.
14. **Dittmar, K. D., D. R. Demady, L. F. Stancato, P. Krishna, and W. B. Pratt.** 1997. Folding of the glucocorticoid receptor by the heat shock protein (hsp) 90-based chaperone machinery. J. Biol. Chem. **272:**21213–21220.
15. **Dittmar, K. D., and W. B. Pratt.** 1997. Folding of the glucocorticoid receptor by the reconstituted hsp90-based chaperone machinery. J. Biol. Chem. **272:**13047–13054.
16. **Duina, A. A., H.-C. J. Chang, J. A. Marsh, S. Lindquist, and R. F. Gaber.** 1996. A cyclophilin function in Hsp90-dependent signal transduction. Science **274:**1713–1715.
17. **Fairhead, C., and B. Dujon.** 1994. Transcript map of two regions from chromosome XI of Saccharomyces cerevisiae for interpretation of systematic sequencing results. Yeast **10:**1403–1413.
18. **Fang, Y., A. E. Fliss, D. M. Robins, and A. J. Caplan.** 1996. Hsp90 regulates androgen receptor hormone binding affinity in vivo. J. Biol. Chem. **271:**28697–28702.
19. **Florio, M., L. K. Wilson, J. B. Trager, J. Thorner, and G. S. Martin.** 1994. Aberrant protein phosphorylation at tyrosine is responsible for the growth-inhibitory action of pp60v-src expressed in the yeast Saccharomyces cerevisiae. Mol. Biol. Cell **5:**283–296.
20. **Freeman, B. C., D. O. Toft, and R. I. Morimoto.** 1996. Molecular chaperone machines: chaperone activities of the cyclophilin Cyp-40 and the steroid aporeceptor-associated protein p23. Science **274:**1718–1720.
21. **Frydman, J., and J. Höhfeld.** 1997. Chaperones get in touch: the Hip-Hop connection. Trends Biochem. Sci. **22:**87–92.
22. **Geitz, R. D., R. H. Schiestl, A. R. Willems, and R. A. Woods.** 1995. Studies

on the transformation of intact yeast cells by the LiAc/SS-DNA/PEG procedure. Yeast **11**:355–360.
23. **Grenert, J. P., W. P. Sullivan, P. Fadden, T. A. J. Haystead, J. Clark, E. Mimnaugh, H. Krutzsch, H.-J. Ochel, T. W. Schulte, E. Sausville, L. M. Neckers, and D. O. Toft.** 1997. The amino-terminal domain of heat shock protein 90 (hsp90) that binds geldanamycin is an ATP/ADP switch domain that regulates hsp90 conformation. J. Biol. Chem. **272**:23843–23850.
24. **Gross, M., and S. Hessefort.** 1996. Purification and characterization of a 66-kDa protein from rabbit reticulocyte lysate which promotes the recycling of Hsp70. J. Biol. Chem. **271**:16833–16841.
25. **Hartl, F. U.** 1996. Molecular chaperones in cellular protein folding. Nature **381**:571–580.
26. **Höhfeld, J., and S. Jentsch.** 1997. GrpE-like regulation of the Hsc70 chaperone by the anti-apoptotic protein BAG-1. EMBO J. **16**:6209–6216.
27. **Hu, J., D. O. Toft, and C. Seeger.** 1997. Hepadnavirus assembly and reverse transcription require a multi-component chaperone complex which is incorporated into nucleocapsids. EMBO J. **16**:59–68.
28. **Jacquier, A., P. Legrain, and B. Dujon.** 1992. Sequence of a 10.7 kb segment of yeast chromosome XI identifies the APN1 and the BAF1 loci and reveals one tRNA gene and several new open reading frames including homologs to RAD2 and kinases. Yeast **8**:121–132.
29. **Johnson, J. L., and E. A. Craig.** 1997. Protein folding in vivo: unraveling complex pathways. Cell **90**:201–204.
30. **Johnson, J. L., T. G. Beito, C. J. Krco, and D. O. Toft.** 1994. Characterization of a novel 23-kilodalton protein of unactive progesterone receptor complexes. Mol. Cell. Biol. **14**:1956–1963.
31. **Johnson, J. L., and D. O. Toft.** 1994. A novel chaperone complex for steroid receptors involving heat shock proteins, immunophilins, and p23. J. Biol. Chem. **269**:24989–24993.
32. **Johnson, J. L., and D. O. Toft.** 1995. Binding of p23 and hsp90 during assembly with the progesterone receptor. Mol. Endocrinol. **9**:670–678.
33. **Kimura, Y., S. Matsumoto, and I. Yahara.** 1994. Temperature-sensitive mutants of hsp82 of the budding yeast Saccharomyces cerevisiae. Mol. Gen. Genet. **242**:517–527.
34. **Kimura, Y., I. Yahara, and S. Lindquist.** 1995. Role of the protein chaperone YDJ1 in establishing Hsp90 mediated signal transduction pathways. Science **268**:1362–1365.
35. **Kimura, Y., S. L. Rutherford, Y. Miyata, I. Yahara, B. C. Freeman, L. Yue, R. I. Morimoto, and S. Lindquist.** 1997. Cdc37 is a molecular chaperone with specific functions in signal transduction. Genes Dev. **11**:1775–1785.
36. **Lässle, M., G. L. Blatch, V. Kundra, T. Takatori, and B. R. Zetter.** 1997. Stress inducible, murine protein mSTI1. J. Biol. Chem. **272**:1876–1884.
37. **Nair, S. C., E. J. Toran, R. A. Rimerman, S. Hjermstad, T. E. Smithgall, and D. F. Smith.** 1996. A pathway of multi-chaperone interactions common to diverse regulatory proteins; estrogen receptor, fes tyrosine kinase, heat shock transcription factor HSF1 and the arylhydrocarbon receptor. Cell Stress Chap. **1**:237–249.
38. **Nathan, D. F., and S. Lindquist.** 1995. Mutational analysis of Hsp90 function: interactions with a steroid hormone receptor and protein kinase. Mol. Cell. Biol. **15**:3917–3925.
39. **Nicolet, C. M., and E. A. Craig.** 1989. Isolation and characterization of STI1, a stress inducible gene from *Saccharomyces cerevisiae*. Mol. Cell. Biol. **9**:3638–3646.
40. **Owens-Grillo, J. K., M. J. Czar, K. A. Hutchison, K. Hoffmann, G. H. Perdew, and W. B. Pratt.** 1996. A model of protein targeting mediated by immunophilins and other proteins that bind to hsp90 via tetratricopeptide repeat domains. J. Biol. Chem. **271**:13468–13475.
41. **Prodromou, C., S. M. Roe, R. O'Brien, J. E. Ladbury, P. W. Piper, and L. H. Pearl.** 1997. Identification and structural characterization of the ATP/ADP-binding site in the Hsp90 molecular chaperone. Cell **90**:65–75.
42. **Rothstein, R.** 1991. Targeting, disruption, replacement and allele rescue: integrative DNA transformation in yeast. Methods Enzymol. **194**:281–301.
43. **Schulte, T. W., M. V. Blagosklonny, C. Ingui, and L. Neckers.** 1995. Disruption of the raf-1-hsp90 molecular complex results in destabilization of raf-1 and loss of raf-1-ras association. J. Biol. Chem. **270**:24585–24588.
44. **Segnitz, B., and U. Gehring.** 1997. The function of steroid hormone receptors is inhibited by the hsp90-specific compound geldanamycin. J. Biol. Chem. **272**:18694–18701.
45. **Smith, D. F., L. E. Faber, and D. O. Toft.** 1990. Purification of unactivated progesterone receptor and identification of novel receptor-associated proteins. J. Biol. Chem. **265**:3996–4003.
46. **Smith, D. F., W. P. Sullivan, T. N. Marion, K. Zaitsu, B. Madden, D. J. McCormick, and D. O. Toft.** 1993. Identification of a 60-kilodalton stress-related protein, p60, which interacts with Hsp90 and Hsp70. Mol. Cell. Biol. **13**:869–876.
47. **Smith, D. F., L. Whitesell, S. C. Nair, S. Chen, V. Prapapanich, and R. A. Rimmerman.** 1995. Progesterone receptor structure and function altered by geldanamycin, an Hsp90-binding agent. Mol. Cell. Biol. **15**:6804–6812.
48. **Stebbins, C. E., A. A. Russo, C. Schneider, N. Rosen, F. U. Hartl, and N. P. Pavletich.** 1997. Crystal structure of an Hsp90-geldanamycin complex: targeting of a protein chaperone by an antitumor agent. Cell **89**:239–250.
49. **Sullivan, W., B. Stensgard, G. Caucutt, B. Bartha, N. McMahon, E. S. Alnemri, G. Litwack, and D. O. Toft.** 1997. Nucleotides and two functional states of hsp90. J. Biol. Chem. **272**:8007–8012.
50. **Takayama, S., D. N. Bimston, S. Matsuzawa, B. C. Freeman, C. Aime-Sempe, Z. Xie, R. I. Morimoto, and J. C. Reed.** 1997. BAG-1 modulates the chaperone activity of Hsp70/Hsc70. EMBO J. **16**:4887–4896.
51. **Thomas, B. J., and R. Rothstein.** 1989. Elevated recombination rates in transcriptionally active DNA. Cell **56**:619–630.
52. **Warth, R., P.-A. Briand, and D. Picard.** 1997. Functional analysis of the yeast 40 kDa cyclophilin Cyp40 homologue and its role for viability and steroid receptor regulation. Biol. Chem. **387**:381–391.
53. **Whitesell, L., and P. Cook.** 1996. Stable and specific binding or heat shock protein 90 by geldanamycin disrupts glucocorticoid receptor function in intact cells. Mol. Endocrinol. **10**:705–712.
54. **Whitesell, L., E. G. Mimnaugh, B. De Costa, C. E. Myers, and L. M. Neckers.** 1994. Inhibition of heat shock protein Hsp90-pp60$^{v\text{-}src}$ heteroprotein complex formation by benzoquinone ansamycins: essential role for stress proteins in oncogenic transformation. Proc. Natl. Acad. Sci. USA **91**:8324–8328.
55. **Xu, Y., and S. L. Lindquist.** 1993. Heat-shock protein hsp90 governs the activity of pp60v-src. Proc. Natl. Acad. Sci. USA **90**:7074–7078.
56. **Xu, Z., J. K. Pal, V. Thulasiraman, H. P. Hahn, J. J. Chen, and R. L. Matts.** 1997. The role of the 90-kDa heat-shock protein and its associated cohorts in stabilizing the heme-regulated eIF-2alpha kinase in reticulocyte lysates during heat stress. Eur. J. Biochem. **246**:461–470.

Arrest of the cell cycle by the tumour-suppressor BRCA1 requires the CDK-inhibitor p21$^{WAF1/CiPI}$

Kumaravel Somasundaram*†¶, Hongbing Zhang†¶, Yi-Xin Zeng*†, Yariv Houvras‡, Yi Peng†, Hongxiang Zhang†, Gen Sheng Wu*†, Jonathan D. Licht‡, Barbara L. Weber†§‖ & Wafik S. El-Deiry*†§‖

** Laboratory of Molecular Oncology and Cell Cycle Regulation, Howard Hughes Medical Institute, Departments of † Medicine and § Genetics, and ‖ Cancer Center, University of Pennsylvania School of Medicine, Philadelphia, Pennsylvania 19104, USA*

‡ Brookdale Center for Developmental and Molecular Biology and Department of Medicine, The Mount Sinai School of Medicine, New York, New York 10029, USA

¶ These authors contributed equally to this study.

Much of the predisposition to hereditary breast and ovarian cancer has been attributed to inherited defects in the *BRCA1* tumour-suppressor gene[1–3]. The nuclear protein BRCA1 has the properties of a transcription factor[4–7], and can interact with the recombination and repair protein RAD51 (ref. 8). Young women with germline alterations in *BRCA1* develop breast cancer at rates 100-fold higher than the general population[3], and *BRCA1*-null mice die before day 8 of development[9,10]. However, the mechanisms of *BRCA1*-mediated growth regulation and tumour suppression remain unknown. Here we show that BRCA1 transactivates expression of the cyclin-dependent kinase inhibitor p21$^{WAF1/CIP1}$ in a p53-independent manner, and that BRCA1 inhibits cell-cycle progression into the S-phase following its transfection into human cancer cells. BRCA1 does not inhibit S-phase progression in p21$^{-/-}$ cells, unlike p21$^{+/+}$ cells, and tumour-associated, transactivation-deficient mutants of BRCA1 are defective in both transactivation of p21 and cell-cycle inhibition. These data suggest that one mechanism by which BRCA1 contributes to cell-cycle arrest and growth suppression is through the induction of p21.

Because several known tumour-suppressor genes interact with or negatively regulate the cell-cycle machinery[11], we investigated the effect of BRCA1 on cell-cycle progression (Fig. 1, Table 1). By using green fluorescent protein (GFP) to mark specific transfected cells[12], we examined the effects of *BRCA1* transfection on new DNA synthesis in SW480 and HCT116 human colon cancer cells (Figs 1, 4 and Table 1). We found fewer BrdU(+)/GFP(+) SW480 cells following transfection of either BRCA1 or p53 than with their control vectors (Fig. 1). A quantitative summary of the percentage of BrdU(+)/GFP(+) cells from three independent experiments in SW480 cells is shown in Fig. 1 and Table 1. BRCA1 inhibited new DNA synthesis in SW480 cells by approximately 50% compared with the pCR3 vector. The extent of inhibition of BrdU incorporation following BRCA1 transfection was similar to p53 transfection (Fig. 1i). BRCA1 also inhibited S-phase progression in HCT116 cells (Fig. 4). These results suggest that BRCA1 can inhibit S-phase progression and thus negatively regulate the cell cycle in human cancer cells.

We investigated cyclin-dependent kinase (CDK) inhibition of cell-cycle progression as a potential mechanism by which BRCA1 may control cell proliferation. Induction of p21$^{WAF1/CIP1}$ expression has been linked to growth inhibition by p53 (ref. 13), and p21 expression also has been found to signal growth arrest, independent of p53, in cells undergoing differentiation[14]. The protein p21 is a universal cell-cycle inhibitor that specifically binds cyclin–CDK complexes and proliferating cell nuclear antigen, thereby serving as a potent growth inhibitor and effector of cell-cycle checkpoints[11]. As

Table 1 Cell cycle effects of tumour-derived BRCA1 mutants

	GFP(+) cells	BrdU(+) cells	BrdU(+)/GFP(+) (%)
pCR3	43	27	62.8
BRCA1	55	19	34.6
P1749R	59	31	52.5
Y1853insA	56	32	57.1

These BRCA1 mutants are defective at inhibiting DNA synthesis. GFP was used as a marker for transfection of SW480 cells. GFP(+) cells were examined for BrdU incorporation (BrdU(+)) by anti-BrdU staining. BrdU(+)/GFP(+) cells represents the fraction of GFP(+) cells with active DNA synthesis.

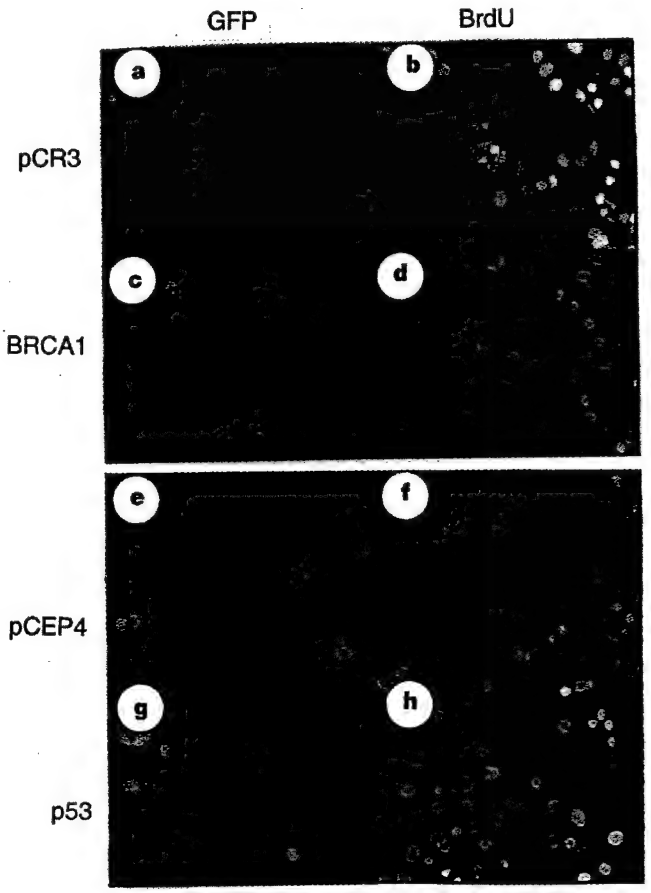

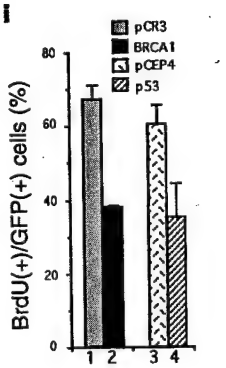

Figure 1 BRCA1 transfection inhibits DNA synthesis in human cancer cells. SW480 cells were co-transfected with pCR3 (**a**, **b**), pCR3–BRCA1 (**c**, **d**), pCEP4 (**e**, **f**), or pCEP4–p53 (**g**, **h**) and pGreen Lantern-1. The same fields were examined for GFP expression (**a**, **c**, **e**, **g**) and BrdU incorporation (**b**, **d**, **f**, **h**). White arrows indicate the GFP(+) cells that are positive for BrdU incorporation; black arrows indicate the GFP(+) cells that are negative for BrdU incorporation. **i**, The proportion of BrdU(+)/GFP(+) cells was determined by analysing at least 75 GFP(+) cells for each transfection in three fields, in two independent experiments.

BRCA1 contains a carboxy-terminal transactivation domain[6], we hypothesized that BRCA1 may transcriptionally induce p21 expression and thus negatively regulate cell-cycle progression. We examined the effect of BRCA1 on p21-promoter reporter gene expression following transfection into SW480, HCT116, COS-7, HeLa and CV1 cells (Figs 2, 3, and data not shown). BRCA1 activated the human p21 promoter luciferase-reporter by 5- to greater than 20-fold in SW480 (Fig. 2A), HCT116 (Fig. 2A), HeLa (data not shown) and COS-7 (Fig. 3B) cells, as compared to transfection of the pCR3 vector. BRCA1 also transactivated the mouse p21-promoter by more than 10-fold in CV1 cells (Fig. 2B).

Deletion mapping within the human p21 promoter identified a control region of 50 base pairs (between −143 and −93) within the proximal promoter that seems to mediate activation of p21 by BRCA1 (Fig. 2C). The two p53-binding sites are not required for BRCA1 transactivation of p21. Whether p21 activation by BRCA1 is a direct consequence of BRCA1 binding to the p21 promoter or is an indirect effect is not known. We also investigated whether BRCA1 could activate endogenous p21 mRNA and protein expression. Figure 3D shows that p21 mRNA levels were elevated in HeLa cells after BRCA1 transfection. By using immunochemical methods, we also found increased levels of endogenous p21 protein in SW480 cells transfected with BRCA1, compared with cells transfected with vector alone (Fig. 2D). These results strengthen the hypothesis that transcriptional activation of p21 by BRCA1 is functionally relevant.

To further investigate the biological importance of p21 regulation by BRCA1, we studied the effect of various synthetic and tumour-associated mutant BRCA1 proteins on p21 expression and cell-cycle progression (Figs 3, 4 and Table 1). Mutants of BRCA1 lacking a functional nuclear localization signal, the C-terminal transactivation domain, the RAD51-interacting domain or all three domains were deficient in activating p21 expression (Fig. 3A, B, D). Similarly, three different tumour-associated transactivation-deficient[6,7] BRCA1 mutants were defective in activating the human p21-promoter luciferase-reporter gene (Fig. 3C). The expression of the synthetic deletion and tumour-derived point mutant BRCA1 proteins is shown in Fig. 3E, F. The two tumour-associated transactivation-deficient BRCA1 mutants tested for cell-cycle inhibition were also found to be deficient in cell-cycle inhibition in SW480 cells (Table 1). These results suggest that transactivation by BRCA1 may be required for its cell-cycle inhibitory effect, and that tumour-derived BRCA1 mutants may be defective in cell-cycle inhibition.

To determine whether p21 is required for the cell-cycle inhibitory effect of BRCA1, we examined the extent of new DNA synthesis following BRCA1 transfection into $p21^{+/+}$ and $p21^{-/-}$ HCT116 cells. BRCA1 inhibited new DNA synthesis in $p21^{+/+}$ HCT116 cells, but there was no evidence of DNA synthesis inhibition resulting from BRCA1 in the $p21^{-/-}$ cells (Fig. 4). These observations suggest that p21 induction may be required for cell-cycle inhibition by BRCA1 in HCT116 cells. Expression of p21 has previously been shown to be required for cell-cycle arrest following γ-irradiation of these cells[15].

These results demonstrate that BRCA1 can negatively regulate the mammalian cell cycle, and suggest that this effect is at least partly mediated by the ability of BRCA1 to induce p21. Although previous studies have reported that expression of BRCA1 is cell-cycle dependent[16–18], our results demonstrate that BRCA1 can inhibit cell-cycle progression. The absence of this inhibition in $p21^{-/-}$ cells indicates that p21 expression may be essential for BRCA1 to inhibit new DNA synthesis. Decreased cell-cycle inhibition by transactivation-deficient tumour-derived BRCA1 mutants is consistent with the idea that regulation of p21 by BRCA1 may contribute to growth control. In support of this hypothesis, recent observations in the yeast *Saccharomyces cerevesiae* demonstrate that the C-terminal 303 amino acids of BRCA1 are sufficient to inhibit yeast colony formation, and that tumour-associated mutations in the context of the 303 amino-acid region fail to inhibit colony growth[19].

There is a fundamental discrepancy between our results and recent observations that cells from BRCA1-null mouse embryos have increased levels of p21 mRNA, which suggest that BRCA1 may suppress p21 expression during development to allow cell growth[10]. However, p21 protein level and its effect on the cell cycle have not been determined in BRCA1-null embryos, and the mechanism of increased p21 expression remains unclear[10]. It is conceivable that BRCA1 may serve different functions during development and adulthood. It also is possible that the absence of BRCA1 in these cells perturbs a feedback loop controlling expression of p21. Although our data do not provide a clear explanation for this

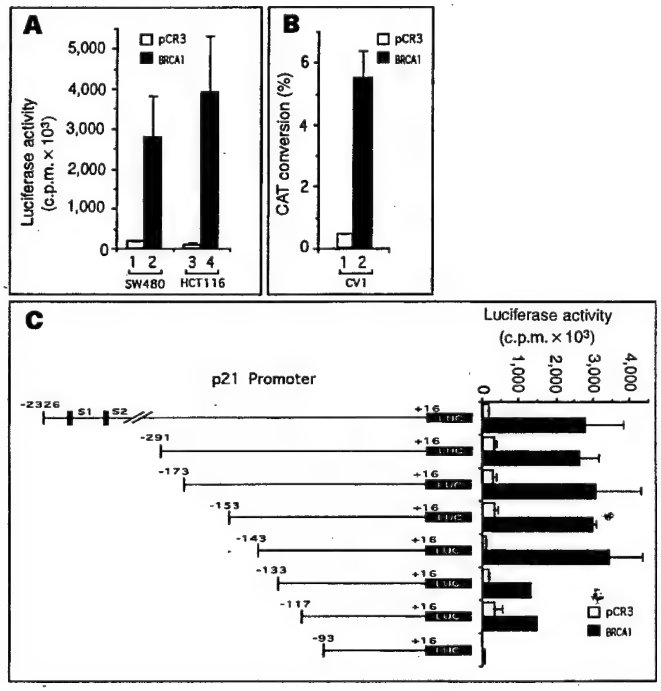

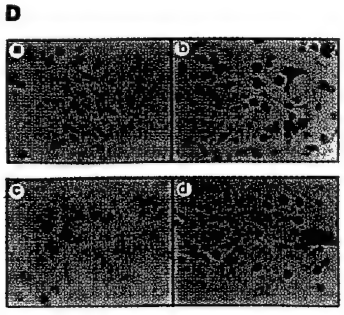

Figure 2 BRCA1 transactivates the human and mouse p21-promoter and upregulates endogenous p21 protein expression. **A**, SW480 or HCT116 cells were co-transfected with pWWP-Luc and either pCR3 or pCR3-BRCA1, and luciferase activity was measured 24 h later. **B**, CV1 cells were co-transfected with pCAT1 and pCR3 or pCR3-BRCA1, and CAT activity was measured 48 h later. **C**, Structure of the human p21-promoter luciferase reporter and several 5′-deletions are shown schematically (left). The 5′ end of each deletion is as indicated; the 3′ boundary is 16 bp downstream of the p21 transcription initiation site[13], fused to the luciferase reporter gene[21]. S1 and S2 indicate the relative locations of the two p53 DNA-binding sites within the 2.3-kb regulatory region upstream of the *WAF1/CIP1* gene[22]. pWWP-Luc or the 5′-deletion mutants were co-transfected with pCR3 or PCR3-BRCA1 into SW480 cells and luciferase activity was assayed as in **A**. **D**, Expression of endogenous p21 protein is increased in BRCA1- or p53-transfected SW480 cells. SW480 cells were transfected with pCEP4 (**a**), pCEP4-p53 (**b**), pCR3 (**c**), or pCR3-BRCA1 (**d**), and the cells were immunochemically probed for p21 expression.

difference, our results demonstrate that BRCA1 can transcriptionally induce p21 expression and negatively regulate the cell cycle. The identification of BRCA1 as an RNA polymerase II holoenzyme-associated protein provides additional evidence for the role of BRCA1 in transcriptional activation[20]. The importance of this role in tumour suppression is further supported by the fact that about 90% of the mutations in *BRCA1* result in C-terminal truncations that involve the transactivation domain. The loss of cell-cycle inhibition in $p21^{-/-}$ cancer cells and the deficiency in p21 activation and cell-cycle inhibition by tumour-derived BRCA1 mutants provides support for the hypothesis that p21 expression may lead to a quiescent or growth-inhibited state, which may contribute to BRCA1-dependent tumour suppression. □

Methods

Plasmid constructs. The pCEP4–p53 (ref. 13) and pWWP–Luc (ref. 13) plasmids were provided by B. Vogelstein. The construction of the p21-promoter deletions fused to the luciferase reporter gene has been described[21].

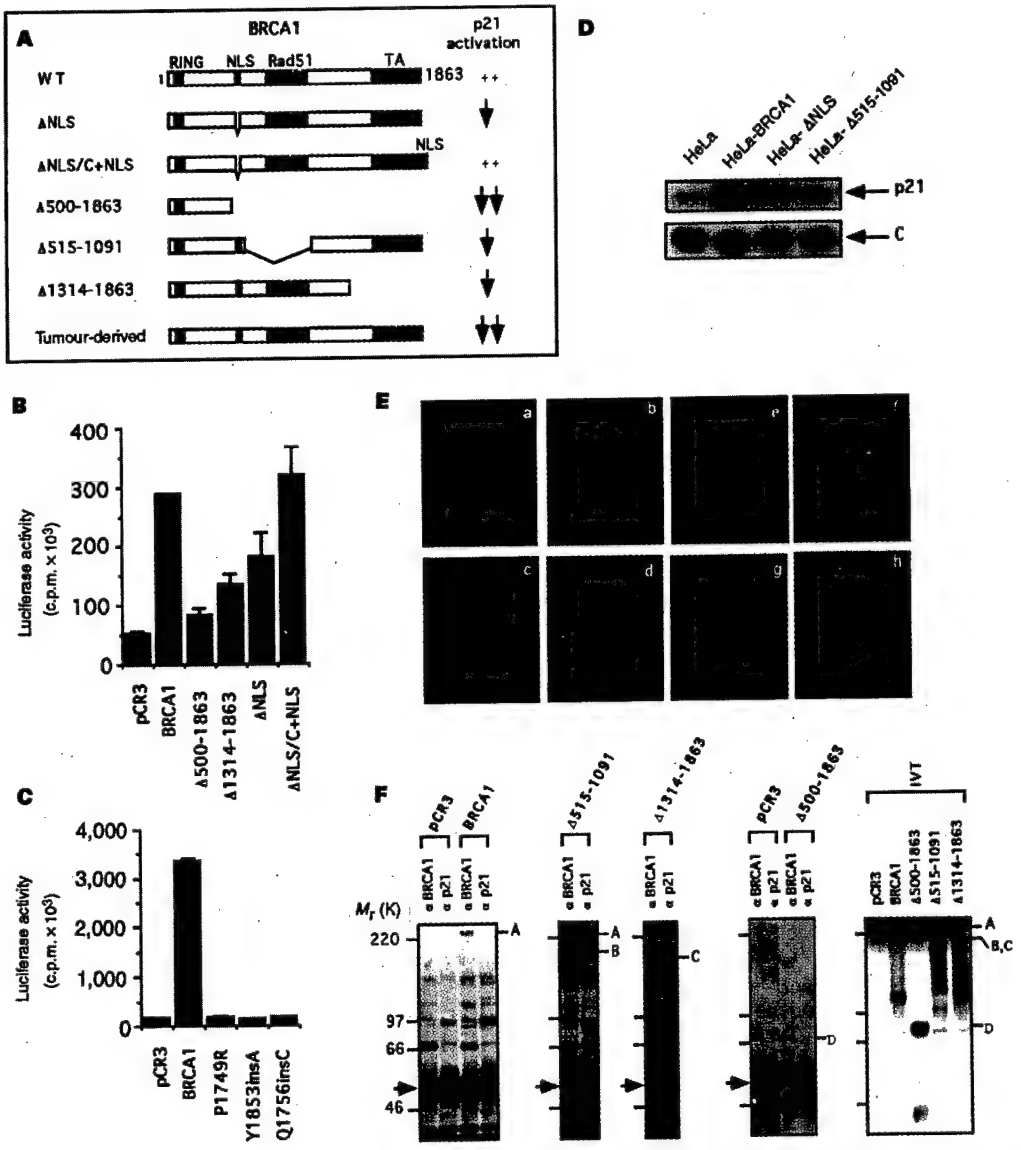

Figure 3 BRCA1 mutants are defective for activation of p21. **A**, Structure of wild-type BRCA1 (WT) and various mutants used is shown schematically. Synthetic mutants lacking the functional nuclear localization signal[23] (red, ΔNLS), a ΔNLS mutant with a C-terminal fused NLS (ΔNLS/C + NLS), mutants lacking the RAD51-interacting domain (blue, Δ515–1091), the C-terminal transactivation domain (green, Δ1314–1863) or both (Δ500–1863) are shown. Tumour-derived mutant BRCA1 is shown with an M within the green transactivation domain to signify the presence of point mutations as indicated in **C**. The corresponding extent of p21 induction (data from **B**–**D**) is shown (right; ++ indicates >5-fold induction; a single arrow, 1.5- to 2-fold reduction in p21 activation; double arrow, substantial decrease in p21 activation, corresponding to less than 1.5-fold induction). **B**, **C**, COS-7 (**B**) or SW480 (**C**) cells were co-transfected with pWWP-Luc and pCR3 or either WT or mutant BRCA1 expression plasmids as indicated, and luciferase activity was determined as in Fig. 2. **D**, Northern analysis of p21 expression in HeLa cells transfected with BRCA1 or various mutants as indicated. The same blot was reprobed with rpl32 (indicated by C). **E**, COS-7 cells (DAPI stain of permeabilized cells; **b**, **d**, **f**, **h**) transfected with WT BRCA1 (**a**, **b**) or the tumour-derived mutants P1749R (**c**, **d**), Y1853insA (**e**, **f**) and Q1756insC (**g** and **h**) were analysed by immunofluorescence (**a**, **c**, **e**, **g**) for BRCA1 expression. **F**, Expression of BRCA1 or various truncated mutant proteins (**A**). SW480 cells (left 4 panels) were transfected with the pCR3 control, BRCA1 or its mutant expression vectors, and lysates were analysed for BRCA1 expression at 24 h by immunoprecipitation and western blot analysis. A p21-specific monoclonal antibody was used as a negative control. Protein M_r (K) markers are shown on the left. A, position of (endogenous ± exogenous) WT BRCA1 protein; B, C and D indicate the position of the Δ515–1091, Δ1314–1863 and Δ500–1863 mutant BRCA1 proteins, respectively. Black arrows indicate the position of the immunoglobin heavy chain. *In vitro* translation of WT and truncated BRCA1 proteins without (right-hand panel, ^{35}S-labelled) or followed by western analysis (not shown) was performed to identify transfected BRCA1.

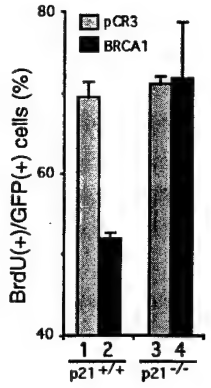

Figure 4 BRCA1 fails to inhibit DNA synthesis in $p21^{-/-}$ human cancer cells. The proportion of BrdU(+)/GFP(+) cells was determined following transfection of $p21^{+/+}$ (lanes 1, 2) or $p21^{-/-}$ (lanes 3, 4) HCT116 cells with pCR3 (lanes 1, 3) or pCR3-BRCA1 (lanes 2, 4), as described in Fig. 1.

The human p21-promoter luciferase-reporters with 5′-truncations at −153, −143 and −133 were constructed and sequenced as described[21]. The murine p21 promoter-CAT reporter, pCAT1, has been described[22]. The GFP expression vector pGreen Lantern-1 was obtained from Gibco. The pCR3–BRCA1 expression plasmid has been previously described[23]. pCR3 vectors encoding synthetic and tumour-associated BRCA1 mutants (Fig. 3A) were constructed as follows. The RAD51-interaction-deficient mutant plasmid (Δ515-1091) was constructed by digestion of pCR3–BRCA1 using *Bsu36I* to delete nucleotides 1661–3392 (ref. 1), followed by in-frame intramolecular ligation. The transactivation domain deletion mutant plasmid (Δ1314–1863) was prepared by digestion of pCR3–BRCA1 with *Bam*H1 (nucleotide 4058) and *Not*1 (nucleotide 5833), Klenow fill-in and subsequent intramolecular blunt-end ligation at 37 °C. The double mutant (Δ500–1863) was cloned by polymerase chain reaction (PCR) amplification of nucleotides 1–1616 using pCR3-BRCA1 as a template and the following primers: 5′-GCAAGCTTGC-CACCATGGATTT ATCTGCTCTTCGC-3′ and 5′-TTGTGAGGGGACGCTCTT-GTA-3′. The 1.6-kilobase PCR product was ligated into the pCR3 vector, and a clone expressing the N-terminal region of BRCA1 in the sense orientation downstream of the CMV-promoter was isolated. The ΔNLS/C + NLS vector was prepared as follows. A 488-bp DNA fragment containing a fusion between the extreme C terminus of BRCA1 and the NLS region (amino acids 499–510) was generated by PCR amplification of pCR3–BRCA1 using the following primers: 5′-AGGAGATGTGGTCAATGGAAG-3′ and 5′-TATCATGATGTAGGTCTCCTT TTACGCTTTAATTTATTGTAGTGGCTGTG-3′. This PCR product was sub-cloned into pCR3 and released as an *Apa*l fragment which was cloned in-frame into an *Apa*l-digested ΔNLS plasmid. pCR3 vectors encoding the transactivation-domain tumour-derived BRCA1 mutants[6,7] (P1749R, Y1853insA, Q1756insC) were constructed by amplification of a 1.8-kb C-terminal region containing the specific mutations and subcloning into pCR3–BRCA1 digested with *Bam*H1 and *Not*1. All mutant BRCA1 expression plasmids used were sequenced and shown to express protein (Fig. 3E, F, and data not shown). Deletion of the nuclear localization signal[23] (ΔNLS mutant) resulted in cytoplasmic staining, which reverted back to the nucleus upon addition of a C-terminal NLS (ΔNLS/C + NLS; unpublished data).

Cells, transfections and luciferase assays. The $p21^{+/+}$ parental and $p21^{-/-}$ HCT116 human colon cancer cells[15] were provided by T. Waldman and B. Vogelstein. SW480, HeLa, COS-7 and CV1 cells (ATCC) were transfected as described[13]. Luciferase and CAT assays were performed as described[13,22]. HeLa cells expressing BRCA1 or mutants were obtained following transfection of HeLa cells with BRCA1, ΔNLS or Δ515–1091 mutants (Fig. 3D) and continuous growth in 0.4 mg ml^{-1} G418.

Analysis of BrdU incorporation in transfected GFP(+) cells. SW480 or HCT116 cells were co-transfected with pGreen Lantern-1 and mammalian expression vectors (as indicated in Figs 1, 4 and Table 1) at a ratio of 1 : 3. At 12 h after transfection, BrdU (Sigma) was added at a final concentration of 20 μM and the cells incubated for 20 h at 37 °C. Cells were examined by fluorescence microscopy to identify GFP(+) cells. Cells were treated with a mouse anti-BrdU monoclonal antibody (BM 9318, Boehringer Mannheim) and Rhodamine-conjugated goat anti-mouse IgG (Pierce) as described[12]. The number of BrdU(+) cells was determined for all of the GFP(+) cells in three high-power fields, as described in Fig. 1.

Immunocytochemistry and immunofluorescence. SW480 cells, transfected with expression plasmids (as indicated in Fig. 2D), were stained 24 h later with an anti-human-WAF1 monoclonal antibody (Ab1; Calbiochem) as described[22]. Immunofluorescence analysis of BRCA1 expression was performed as described[23].

Northern blot analysis. Total RNA was isolated and northern blot analysis was performed as described[13], and p21 mRNA expression was detected using a 2.1-kb human p21 cDNA probe[13]. Equivalent loading of various RNA samples was demonstrated using a probe for rpl32, which encodes a ribosomal protein[24].

Immunoprecipitation and western blot analysis. Cells were lysed in a buffer containing 50 mM Tris-HCl, pH 7.5, 120 mM NaCl, 50 mM NaF, 0.5% NP-40, 1 mM EDTA, pH 8.0, 1 mM phenylmethylsulphonyl fluoride (Gibco), 1% antipain (Sigma), 1% leupeptin (Sigma), 1% pepstatin A (Sigma), 1% chymostatin (Sigma) and 1% AEBSF (Calbiochem). Immunoprecipitations were carried out in the lysis buffer using 2 μg of anti-BRCA1 monoclonal antibody (Ab1; Calbiochem) for 2 h at 4 °C, followed by the addition of 50% protein A-agarose beads (Sigma) and incubation for 1 h. After 3 washes with lysis buffer the immunoprecipitated proteins were analysed by western blotting as described[25] using a 1 : 250 dilution of the anti-BRCA1 monoclonal antibody, which was raised using the N-terminal portion of recombinant human BRCA1 (amino acids 1–304) as the immunogen (Calbiochem).

Received 9 July; accepted 28 July 1997.

1. Miki, Y. *et al.* A strong candidate for the breast and ovarian cancer susceptibility gene BRCA1. *Science* **266**, 66–71 (1994).
2. Futreal, P. A. *et al.* BRCA1 mutations in primary breast and ovarian carcinomas. *Science* **266**, 120–122 (1994).
3. Easton, D. F., Ford, D. & Bishop, D. T. Breast and ovarian cancer incidence in BRCA1-mutation carriers. *Am. J. Hum. Genet.* **56**, 265–271 (1995).
4. Chen, Y. *et al.* Aberrant subcellular localization of BRCA1 in breast cancer. *Science* **270**, 789–791 (1995).
5. Scully, R. *et al.* Location of BRCA1 in human breast and ovarian cancer cells. *Science* **272**, 123–125 (1996).
6. Chapman, M. S. & Verma, I. M. Transcriptional activation by BRCA1. *Nature* **382**, 678–679 (1996).
7. Monteiro, A. N., August, A. & Hanafusa, H. Evidence for a transcriptional activation function of BRCA1 C-terminal region. *Proc. Natl Acad. Sci. USA* **93**, 13595–13599 (1996).
8. Scully, R. *et al.* Association of BRCA1 with Rad51 in mitotic and meiotic cells. *Cell* **88**, 265–275 (1997).
9. Gowen, L. C. *et al.* Brca1 deficiency results in early embryonic lethality characterized by neuro-epithelial abnormalities. *Nature Genet.* **12**, 191–194 (1996).
10. Hakem, R. *et al.* The tumor suppressor gene Brca1 is required for embryonic cellular proliferation in the mouse. *Cell* **85**, 1009–1023 (1996).
11. Sherr, C. J. & Roberts, J. M. Inhibitors of mammalian G1 cyclin-dependent kinases. *Genes Dev.* **9**, 1149–1163 (1995).
12. Zeng, Y.-X., Somasundaram, K., Prabhu, N. S., Krishnadasan, R. & El-Deiry, W. S. Detection and analysis of living, growth-inhibited mammalian cells following transfection. *Biotechniques* **23**, 88–94 (1997).
13. El-Deiry, W. S. *et al.* WAF1, a potential mediator of p53 tumor suppression. *Cell* **75**, 817–825 (1993).
14. Zhang, W. *et al.* p53-independent induction of WAF1/CIP1 in human leukeumia cells is correlated with growth arrest accompanying monocyte/macrophage differentiation. *Cancer Res.* **55**, 668–674 (1995).
15. Waldman, T., Kinzler, K. W. & Vogelstein, B. p21 is necessary for the p53-mediated G1 arrest in human cancer cells. *Cancer Res.* **55**, 5187–5190 (1995).
16. Vaughn, J. P. *et al.* BRCA1 expression is induced before DNA synthesis in both normal and tumor-derived breast cells. *Cell Growth Differ.* **7**, 711–715 (1996).
17. Gudas, J. M. *et al.* Cell cycle regulation of BRCA1 messenger RNA in human breast epithelial cells. *Cell Growth Differ.* **7**, 717–723 (1996).
18. Chen, Y. *et al.* BRCA1 is a 220-kDa nuclear phosphoprotein that is expressed and phosphorylated in a cell cycle-dependent manner. *Cancer Res.* **56**, 3168–3172 (1996).
19. Humphrey, J. S. *et al.* Human BRCA1 inhibits growth in yeast: Potential use in diagnostic testing. *Proc. Natl Acad. Sci. USA* **94**, 5820–5825 (1997).
20. Scully, R. *et al.* BRCA1 is a component of the RNA polymerase II holoenzyme. *Proc. Natl Acad. Sci. USA* **94**, 5605–5610 (1997).
21. Zeng, Y.-X., Somasundaram, K. & El-Deiry, W. S. AP2 inhibits cancer cell growth and activates $p21^{WAF1/CIP1}$ expression. *Nature Genet.* **15**, 78–82 (1997).
22. El-Deiry, W. S. *et al.* Topological control of $p21^{WAF1/CIP1}$ expression in normal and neoplastic tissues. *Cancer Res.* **55**, 2910–2919 (1995).
23. Thakur, S. *et al.* Localization of BRCA1 and a splice variant identifies the nuclear localization signal. *Mol. Cell. Biol.* **17**, 444–452 (1997).
24. Meyuhas, O. & Perry, R. P. Construction and identification of cDNA clones for mouse ribosomal proteins: application for the study of r-protein gene expression. *Gene* **10**, 113–129 (1980).
25. Somasundaram, K. & El-Deiry, W. S. Inhibition of p53-mediated transactivation and cell cycle arrest by E1A through its p300/CBP-interacting region. *Oncogene* **14**, 1047–1057 (1997).

Acknowledgements. This work was supported by grants from the NIH and the Breast Cancer Research Foundation to B.L.W. W.S.E.-D. is an assistant investigator of the Howard Hughes Medical Institute.

Correspondence and requests for materials should be addressed to W.S.E.-D. (e-mail: weldeir@hhmi.upenn.edu).

Oncogene (1997) 15, 2675–2685

Identification and characterization of R-*ras3*: a novel member of the *RAS* gene family with a non-ubiquitous pattern of tissue distribution

Alec Kimmelman[1], Tatyana Tolkacheva[1], Matthew V Lorenzi[2], Masako Osada[1], and Andrew M-L Chan[1]

[1]The Derald H. Ruttenberg Cancer, Center, Mount Sinai School of Medicine, 1 Gustave Levy Place, Box#1130, New York, New York NY 10029; [2]Laboratory of Cellular & Molecular Biology, National Cancer Institute, National Institutes of Health, Building 37, Room 1E24, Bethesda, Maryland, MD 20892, USA

Members of the Ras subfamily of GTP-binding proteins, including Ras (H-, K-, and N-), *TC21*, and R-*ras* have been shown to display transforming activity, and activating lesions have been detected in human tumors. We have identified an additional member of the Ras gene family which shows significant sequence similarity to the human *TC21* gene. This novel human *ras*-related gene, R-*ras3*, encodes for a protein of 209 amino acids, and shows ~60–75% sequence identity in the N-terminal catalytic domain with members of the Ras subfamily of GTP-binding proteins. An activating mutation corresponding to the leucine 61 oncogenic lesion of the *ras* oncogenes when introduced into R-*ras3*, activates its transforming potential. R-*ras3* weakly stimulates the mitogen-activated protein kinase (MAPK) activity, but this effect is greatly potentiated by the co-expression of c-*raf*-1. By the yeast two-hybrid system, R-*ras3* interacts only weakly with known Ras effectors, such as Raf and RalGDS, but not with *Rgl*II. In addition, R-*ras3* displays modest stimulatory effects on trans-activation from different nuclear response elements which bind transcription factors, such as SRF, ETS/TCF, Jun/Fos, and NF-κB/Rel. Interestingly, Northern blot analysis of total RNA isolated from various tissues revealed that the 3.8 kilobasepair (kb) transcript of R-*ras3* is highly restricted to the brain and heart. The close evolutionary conservation between R-*ras3* and Ras family members, in contrast to the significant differences in its biological activities and the pattern of tissue expression, raise the possibility that R-*ras3* may control novel cellular functions previously not described for other GTP-binding proteins.

Keywords: Ras; TC21; R-ras; G-protein; transformation; MAPK

Introduction

The Ras superfamily of GTP-binding proteins are membrane-anchored, intracellular signal transducers responsible for a wide variety of cellular functions. The Ras subfamily of G-proteins consists of nine evolutionary conserved genetic elements widely implicated in controlling cell growth and differentiation (Lowy and Willumsen, 1993). The prototypic *ras* oncogenes, which are comprised of H-, K-, and N-*ras*, have been known to be oncogenically activated in a significant fraction of human tumors (Bos, 1989). RaplA (K-*rev*-1), together with RaplB, are *ras*-related molecules, with the former being shown to reverse the transformation caused by the K-*ras* oncogene (Kitayama *et al.*, 1989). RalA and its close relative, RalB, form a distinct subgroup, and recent evidence has suggested that RalA may be involved in v-*src*-induced activation of phospholipase D (Jiang *et al.*, 1995). More recently, two additional members of the Ras subfamily, *TC21*, and R-*ras*, have been demonstrated to display transforming activity when oncogenically activated (Graham *et al.*, 1994; Chan *et al.*, 1994; Saez *et al.*, 1994; Cox *et al.*, 1994). In the case of *TC21*, it has been shown to possess transforming activity comparable to that of *ras* oncogenes and mutations have been detected in human tumor samples (Chan *et al.*, 1994; Huang *et al.*, 1995). In contrast, R-*ras* induced cellular transformation is weaker and the resulting foci are morphologically distinct (Saez *et al.*, 1994; Cox *et al.*, 1994). Interestingly, R-*ras* has recently been shown to regulate cell adhesion by activating surface adhesion receptors, integrins (Zhang *et al.*, 1996). However, the relevance of cell adhesion in R-*ras* mediated cellular transformation has not been fully examined.

The prevailing mechanism of Ras transformation is characterized by a model which involves the participation of multiple downstream signaling cascades. Besides the ubiquitous Ras-Raf-MEK-MAPK pathway, numerous other signaling molecules have been shown to either directly interact with Ras or participate in its transforming signaling. These include phosphatidylinositol-3 kinase (PI3-K) (Rodriguez-Viciana *et al.*, 1997), Racl (Qiu *et al.*, 1995a), RhoA (Qiu *et al.*, 1995b), RhoB (Prendergast *et al.*, 1995), Cdc42 (Qiu *et al.*, 1997), RalGDS (White *et al.*, 1996), and Pak (Tang *et al.*, 1997). Codons 32–40 in Ras protein are important for its interaction with downstream effectors and constitute the effector-binding site (Lowy and Willumsen, 1993). Site-specific mutations introduced into this domain have led to the generation of partial-loss-of function mutants, in which the loss of specific biological properties is correlated with the loss of interaction with specific substrates (Rodriguez-Viciana *et al.*, 1997; White *et al.*, 1995; Joneson *et al.*, 1996; Khosravi-Far *et al.*, 1996). Paradoxically, members of the Ras subfamily all encode an identical effector-binding site and, therefore, would be expected to bind to common downstream effectors. This observation is in contrast with the highly diverse biological properties displayed by members of this subfamily.

Correspondence: AM-L Chan
Received 17 September 1997; revised 24 October 1997; accepted 24 October 1997

Ras proteins also play a crucial role in conveying upstream receptor mediated signaling events (Lowy and Willumsen, 1993). Various guanine nucleotide exchanger factors (GEF) have been isolated for the Ras subfamily members, such as SOS, GRF, GRF2, C3G, and RalGDS-related sequences (Quilliam *et al.*, 1995). SOS is known to stimulate the GTP exchange on Ras (Egan *et al.*, 1993), while GRF has been shown to activate both Ras (Farnsworth *et al.*, 1995) and R-*ras* GTP-loading (Gotoh *et al.*, 1997). Interestingly, C3G, which was first isolated based on its ability to interact with Crk *src*-homology domain 3 (SH3) (Tanaka *et al.*, 1994), has recently been shown to possess exchange activity on both K-*rev*-1/RaplA (Gotoh *et al.*, 1995), and R-*ras* (Gotoh *et al.*, 1997). Finally, several members of a group of exchange factors, including RalGDS, Rgl, *Rgl*II, and Rlf, have been found to induce exchange activities preferentially on the Ral-related GTPases (Albright *et al.*, 1993; Spaargaren and Bischoff, 1994; Peterson *et al.*, 1996; Wolthuis *et al.*, 1996). Interestingly, these RalGDS molecules possess in their C-terminal end, conserved domains which mediate the binding to the GTP-, but not the GDP-bound forms of Ras. This observation raises the possibility that RalGDS-related molecules are in fact downstream effectors of Ras and play a role in Ras-mediated transforming signaling events (Urano *et al.*, 1996).

The tremendous complexity of the intracellular signaling network would predict the existence of a diverse repertoire of signaling molecules in regulating these intricate events. In this study, we report the identification of a human cDNA sequence which shows considerable homology to the transforming oncogenes of the Ras subfamily. The distinct biological properties displayed by this novel *ras*-related gene and its unique pattern of tissue distribution may define a whole new class of G-proteins with an as of yet unidentified biological function.

Results

*Cloning of a human R-*ras3 *cDNA*

In an effort to identify additional novel human sequences closely related to either *TC21* (R-*ras*2) or R-*ras* oncogenes, we have performed Genebank database search using the full-length *TC21* (Drivas *et al.*, 1990) and R-*ras* (Lowe *et al.*, 1987) cDNA sequences as templates. We have identified a previously unpublished rat cDNA sequence (accession number – D89863), which showed considerable sequence similarity to the human *TC21* gene. Using the rat cDNA sequence to further search in the Expression Sequence Tag (EST) database, two human EST cDNA clones (accession numbers – AA324154 and W44458) were uncovered which displayed significant sequence identity to the 5′ and 3′ coding regions of the rat sequence, respectively.

PCR primers were then generated in regions of the human EST sequences which represent the translational start and termination regions of the *TC21*-related gene. Using DNA prepared from a human embryonic lung fibroblast cDNA library as template, we amplified a DNA fragment of ~630 basepairs (bp) in size and the PCR products were subsequently cloned into an eukaryotic expression vector, *pCEV29*. Nucleo-

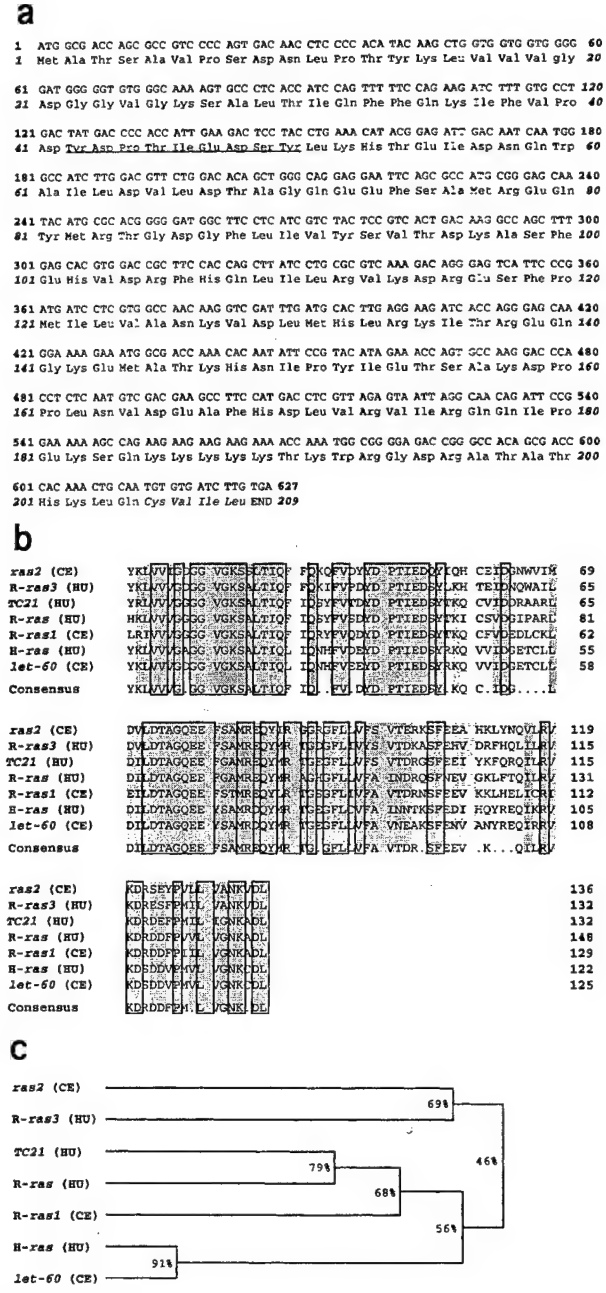

Figure 1 Sequence analysis of human R-*ras3*. (**a**) The nucleotide sequence of R-*ras3* and the predicted amino acid sequence are depicted. The 209 amino acid R-*ras* encoded protein contains functional domains that are found in other *ras*-related GTPases, including the effector-binding site (underlined), and the consensus sequence in the C-terminus for membrane-localization (CVIL, italicized). (**b**) Amino acid sequence alignment of R-*ras3* with the human (HU) Ras subfamily members and known ras-related sequences in *C. elegans* (CE). Only the N-terminal 117-amino acid catalytic domain (codon 14–132) of R-*ras3* was used in the alignment study. Residues with complete sequence identity are boxed and conserved amino acids are shaded. (**c**) Evolutionary tree of ras-related sequences was constructed based on the sequence alignment result generated in panel (b). Numbers represent the levels of sequence identity between the indicated two groups of GTPases. All computer-assisted sequence analyses were performed using GeneWork software. Accession numbers for sequences used in these analyses are: *ras2* (CE)-U80675, R-*ras3* (HU)-AF022080, *TC21* (HU)-M31468, R-*ras* (HU)-M14149, R-*ras1* (CE)-U56930, H-*ras* (HU)-131869, *let-60* (CE)-A36290

tide sequence analysis of the amplified cDNA revealed an open reading frame of 627 bp, encoding for a molecule of 209-amino acids with a predicted relative molecular mass ($\sim M_r$) of 23.8 kilodaltons (kDa) (Figure 1a). *In vitro* translation of the cloned cDNA in rabbit reticulocyte lysates has revealed a protein species of M_r 27 kDa in size (Figure 2a). The cloned cDNA was also fused in the N-terminus to a hemagglutinin (HA)-epitope, and transient transfection of this construct in COS7 cells has led to the expression of a readily detectable ~30 kDa protein species (Figure 2b). Since this novel sequence showed the highest sequence similarity among mammalian genes to *TC21* (R-*ras*2), we therefore designated this human cDNA, R-*ras3*, to reflect the potential expanding family of ras-related G-proteins with R-*ras* being the first identified member (Lowe *et al*., 1987).

Amino acid sequence alignment has revealed significant protein sequence similarity between R-*ras3* and members of the mammalian Ras family of GTPases. R-*ras3* shares with *TC21* the overall secondary structure in possessing an N-terminal extension of 10 amino acids which were not present in the prototypic *ras* oncogenes (Figure 1a). The N-terminal 117-amino acid catalytic domain of Ras has been shown to be important for its GTPase activity as well as in interacting with a host of downstream effectors (Lowy and Willumsen *et al*., 1993). In this region, human R-*ras3* was most related to *TC21*, displaying 75% sequence identity, which was followed by R-*ras* (65%) and H-*ras* (63%) (Figure 1b). Similarity between R-*ras3* and other *ras*-related G-proteins decreased dramatically in the C-terminal divergent region, resulting in an average of only ~30% sequence identity. Moreover, the R-*ras3* C-terminal sequence (CVIL) would predict the encoded protein to be post-translationally modified by the prenylation enzyme, geranyl-geranyl transferase I (Der and Cox, 1991).

Interestingly, sequences homologous to the human R-*ras3* gene were not only restricted to the vertebrate system. A recently identified *Caenorhabditis elegans ras*-related sequence, *ras*2 (accession number U80675), also showed significant sequence similarity to R-*ras*3 in the N-terminal catalytic domain (Figure 1b and c). In contrast, the two additional *C. elegans ras*-related sequences, *let-60* (Han and Sternberg, 1990) and R-*ras*1 (accession number U56930) are closer to mammalian Ras and R-*ras*/*TC21* genes, respectively (Figure 1b and c).

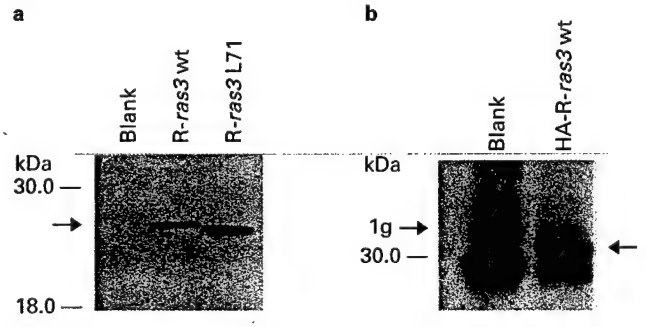

Figure 2 Expression of R-*ras3* by *in vitro* translation and transient transfection. (**a**) The wild-type and L71 activated mutant of R-*ras3* in the expression vector, *pCEV29*, were *in vitro* translated in rabbit reticulocyte lysates, and the ~27 kDa protein species synthesized are indicated. The R-*ras3* L71 encoded product displayed a faster mobility than the wild-type version which may due to conformational differences and has been previously reported for Ras L61 mutant (Reynolds *et al*., 1987). (**b**) R-*ras3* wild-type cDNA was tagged in the N-terminus by a hemagglutinin (HA) epitope, and was transiently transfected into COS7 cells. Following immunoprecipitation and Western blot analysis using an anti-HA antibody, the HA-R-*ras3* fusion product was detected as a ~30 kDa protein species. Ig: immunoglobulin

Transformation of NIH3T3 cells by R-ras3

We have previously reported the expression cloning of an activated *TC21* gene from a human ovarian carcinoma cell line, A2780 (Chan *et al*., 1994). The glutamine (CAA) to leucine (CTA) mutation in codon 72 (position 61 in human H-*ras*) of the *TC21* gene found in this tumor line confers striking transforming activity to the *TC21* proto-oncogenic sequence. The close similarity between R-*ras3* and *TC21* raises the possibility that these *ras*-related molecules may have evolutionary conserved biological properties. To examine if R-*ras3* also possesses transforming activity, the corresponding glutamine (CAG) to leucine (CTG) mutation was introduced in codon 71 of the R-*ras3* coding sequence. The resulting mutant, R-*ras3* L71, would be expected to be GTPase-deficient, and constitutively active.

Variable amounts of R-*ras3* L71 mutant were then introduced into NIH3T3 cells and parallel cultures were transfected with similar amounts of the oncogenic Ras (H-*ras* R12), *TC21*, (*TC21* L72), and R-*ras* (R-*ras* L87) cDNAs in order to assess their relative transforming activities. As shown in Figure 3, whereas transfection of wild-type R-*ras3* did not result in any detectable transformed phenotypes, the constitutively active R-*ras3* L71 mutant displayed readily detectable transformed foci, producing approximately ~400 foci per pmole of DNA. In addition, R-*ras3* transformed foci were reminiscent of the highly refractile, spindle-shaped morphology as observed in both H-*ras*- or *TC21*- transformed cells (Figure 3a).

Next, we sought to determine the ability of R-*ras3*-transformed cells in proliferating in an anchorage-independent manner. For this, marker-selected NIH3T3 cells transformed by H-ras, *TC21*, R-*ras* or R-*ras3* mutants were suspended in semi-solid agarose medium and continuously proliferating colonies were scored after 2 weeks in cultures. As shown in Figure 3, in contrast to its weak focus forming activity, R-*ras3*-transformed NIH3T3 cells were able to proliferate at a significantly higher frequency when compared with control cultures resulting in colonies exceeding 0.5 mm (>100 cells) in size (Figure 3c). In addition, R-*ras3*-induced cellular transformation was associated with an increased ability to proliferate under low-serum conditions when compared with control cells (data not shown). We conclude from these data that R-*ras3* represents a new transforming member of the Ras gene family with a readily detectable ability in inducing both morphological transformation and anchorage-independent growth.

Perturbation of the MAPK pathway by R-ras3

The observed quantitative and qualitative differences between R-*ras3* and other Ras family members in

inducing cellular transformation may reflect the potential divergence of R-*ras3* in its downstream signaling events. The ubiquitous Ras-Raf-MEK-MAPK signaling cascade has been widely implicated as one of the major pathways in mediating *ras* transformation in NIH3T3 cells (Cowley *et al*., 1994). To address whether the observed transforming activity of R-*ras3* was correlated with its ability to activate the MAPK signaling cascade, we sought to investigate the relative efficacy of various *ras*-related oncogenes in stimulating MAPK activity. For this, transient transfection experiments were performed in NIH3T3 cells using expression plasmids representing the oncogenic mutants of H-*ras*, *TC21*, R-*ras*, and R-*ras3*, together with a hemagglutinin (HA)-tagged MAPK (HA-erk2) cDNA construct.

As shown in Figure 4a, H-*ras* R12 mutant induced efficient MAPK activation (~21.0-fold), which was followed by *TC21* (~8.0-fold), and R-*ras* (~2.5-fold). In contrast, expression of R-*ras3* in NIH3T3 cells only

a

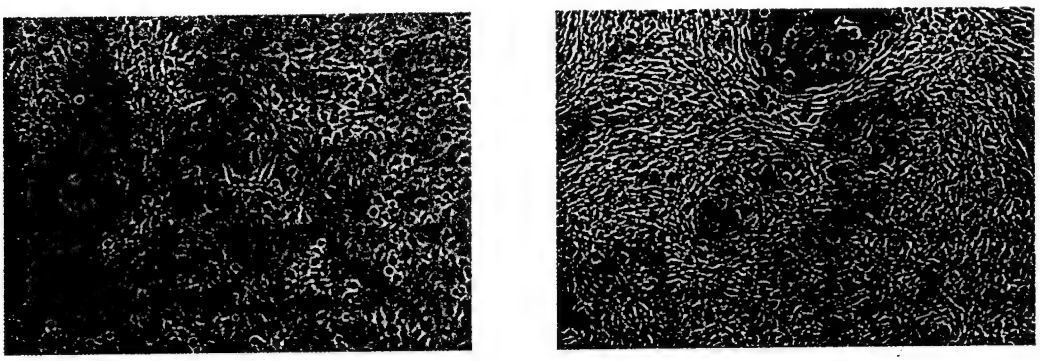

b

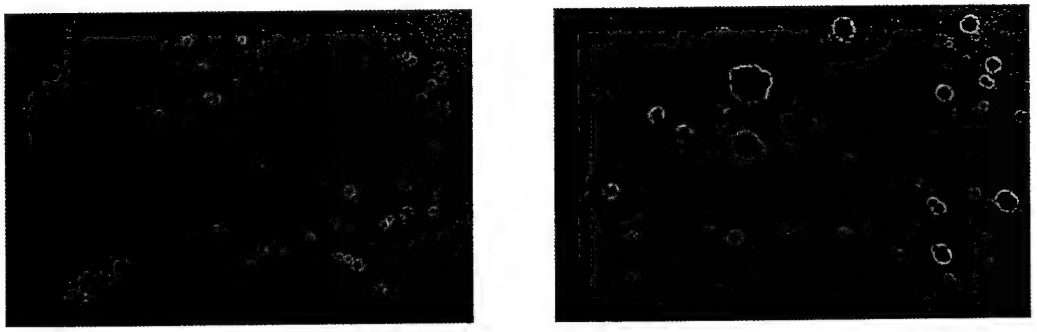

c

Plasmid construct	Transforming efficiency[a] ffu/pmol	Soft Agar growth[b] (relative cfu) >0.5 mm
pCEV29	$<1.0\times10^{0}$	0.13
pCEV29-H-*ras* R12	1.5×10^{4}	1.0
pCEV29-*TC21* L72	3.7×10^{4}	1.4
pCEV29-R-*ras* L87	0.3×10^{4}	0.44
pCEV29-R-*ras3* wt	$<1.0\times10^{0}$	ND
pCEV29-R-*ras3* L71	0.4×10^{3}	0.44

[a] NIH3T3 cells were transfected with different amounts of each plasmid DNA and the number of foci was scored after 3 weeks in culture.
[b] ~1×10^{3} NIH3T3 transfectants were suspended in 0.5% soft-top agarose and the relative colony formation units are indicated with all values normalized to H-*ras* R12.

Figure 3 Expression of R-*ras3* in NIH3T3 cells. (**a**) The constitutively active R-*ras3* L71 mutant was transfected into NIH3T3 cells and the resulting transforming foci composed of spindle-shaped, highly refractile transformed cells are shown. (**b**) Mass population of marker-selected R-*ras3* transformed cells were suspended in 0.5% semi-solid agar and continuously proliferating colonies induced are indicated. (**c**) Transforming properties of *ras*-related genes are summarized showing the relative transforming activity and the ability to proliferate in semi-solid medium. ND: not determined

resulted in a modest but reproducible 2.0-fold increase in MAPK activity. These results strongly suggested that the low transforming activity displayed by R-*ras3* was correlated with its weak intrinsic ability to stimulate the MAPK pathway. A potential explanation for this observation could be that R-*ras3* has differential effects on Ras downstream effectors. One likely candidate would be p74 Raf, which upon the activation of p21 Ras, stimulates the sequential phosphorylations of a downstream kinase cascade leading to the ultimate activation of the MAPK activity. To examine if overexpression of Raf could potentiate the ability of R-*ras3* to induce MAPK activity, transient transfection experiments were per-

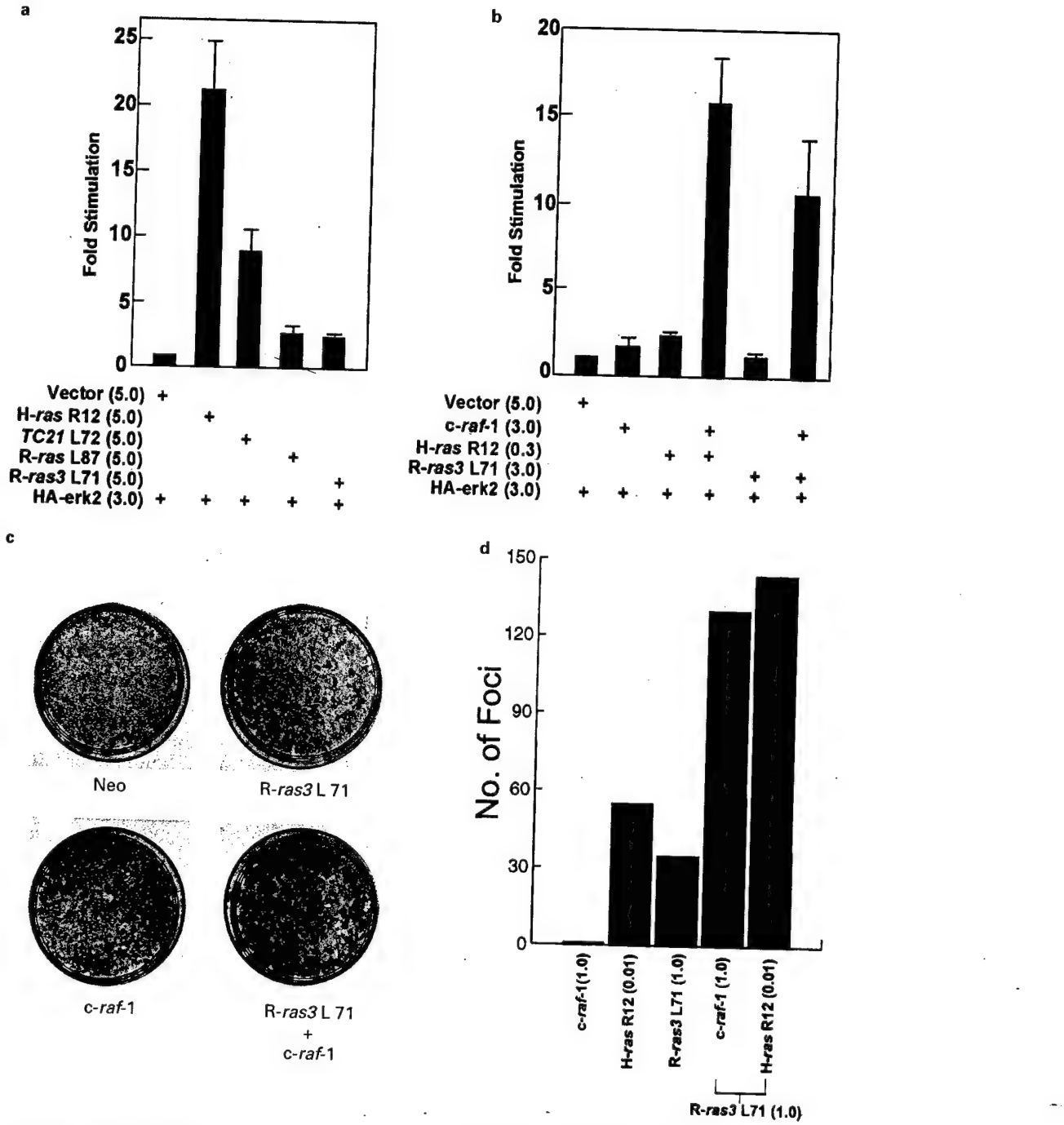

Figure 4 Activation of MAPK pathway by R-*ras3*. (**a**) The relative ability of R-*ras3* and various *ras*-related genes in activating the MAPK activity was measured by transient transfection assays in NIH3T3 cells. In addition, the ability of c-*raf*-1 in cooperating with Ras and R-*ras3* in activating MAPK was also examined (**b**). The amount of each expression plasmid used is parenthesized. Results represent fold stimulation with standard deviations (error bars) derived from triplicate plates of a typical experiment which has been repeated twice with very similar results being obtained. (**c**) The cooperative transformation of NIH3T3 cells by R-*ras3* L71 mutant and wild-type c-*raf*-1 is shown. Note the striking increase in the size of R-*ras3* transformed foci when co-transfected with the c-*raf*-1 plasmid. Similar results were also obtained when R-*ras3* L71 was co-transfected with H-*ras* R12. The results are summarized (right panel) showing the ~3–4-fold increase in focus forming units when R-*ras3* was co-transfected with components of the MAPK signaling pathway. Data represent averaged values from duplicate plates of a typical focus forming assay which has been repeated in 3 independent experiments

formed by introducing either R-*ras3* L71 mutant alone or co-transfected with a c-*raf*-1 plasmid in NIH3T3 cells. As positive control, we have reduced the amount of H-*ras* R12 mutant (0.3 μg) in order to produce a modest increase ($\sim$3.0-fold) in MAPK activity. As shown in Figure 4b, co-transfection of H-*ras* R12 with c-*raf*-1 resulted in an enhancement of the MAPK activity by $\sim$15.0-fold. Similarly, R-*ras3* L71 also displayed a similar cooperative effect with c-*raf*-1 producing in this case, a $\sim$10.0-fold increase in the MAPK activity.

To examine if the synergistic effect observed between R-*ras3* and Raf in stimulating MAPK would lead to a similar cooperative effect in cellular transformation, we co-transfected expression constructs of R-*ras3* activated mutant and c-*raf*-1 in NIH3T3 cells. As shown in Figure 4c, whereas c-*raf*-1 expression plasmid alone did not result in the formation of transformed foci, co-transfection with R-*ras3* L71 enhanced the number of transforming foci by $\sim$4.0-fold. More importantly, the resulting foci were strikingly larger in size and appeared much earlier than when they were transfected separately. Similarly, co-transfection of R-*ras3* with a low level of H-*ras* R12 mutant also resulted in a cooperative effect under similar experimental conditions (Figure 4d). We conclude from all these experiments that R-*ras3* possesses a weak intrinsic ability to induce MAPK activity, and its ability to cooperate with c-*raf*-1 in stimulating the MAPK pathway was correlated with their synergistic effect in cellular transformation.

Interactions of R-ras3 *with Ras downstream effectors*

To further explore the synergistic effect of R-*ras3* and Raf, we sought to compare the binding capacity of Ras or R-*ras3* with Raf utilizing the yeast two-hybrid system. Since both Ras and *TC21* have been shown to interact with additional common substrates, such as RalGDS and *Rgl*II (Spaargaren and Bischoff, 1994; Peterson *et al*., 1996), we therefore, included these molecules in our interaction analysis.

To facilitate the detection of potential subtle interactions between R-*ras3* and test effectors, we have created a R-*ras3* bait which lacked the C-terminal membrane-anchoring signal sequence, CVIL, in order to optimize targeting to the yeast nuclear compartment. As a positive control, a similar construct was generated with a H-*ras* cDNA which has been shown to mediate strong binding to the effectors being examined (Van Aelst *et al*., 1993). Since conserved regions referred to as the Ras-Binding Domains (RBD) have been delineated within the Raf, RalGDS, and *Rgl*II coding sequences, we PCR-amplified these regions and subcloned these fragments into the yeast expression vector, pJG4-5. As shown in Figure 5, binding of Ras to Raf, RalGDS and *Rgl*II was clearly demonstrated by the stimulation of transcriptional activity from the *lacZ* reporter gene, which was manifested by the intense blue color of yeast colonies grown on X-gal containing plates. In contrast, R-*ras3* displayed a considerably different pattern of interactions, with its binding to Raf and RalGDS being substantially less than that of Ras, and no detectable interaction was observed with *Rgl*II. We speculate from these results that the observed weaker transforming activity of R-*ras3* and the lower intrinsic ability to activate MAPK may be explained by its weak interaction with Raf.

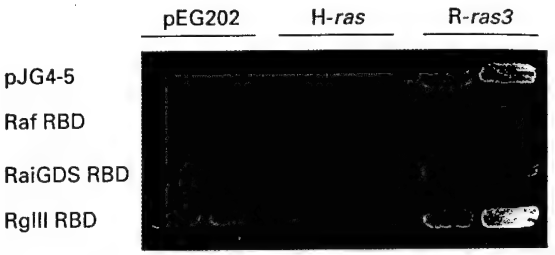

Figure 5 Interaction of R-*ras3* with Ras effectors. The wild-type versions of both H-*ras* and R-*ras3* were used in the yeast two-hybrid interaction tests based on the *LexA* transcription factor system, and the readout was provided by the *LexA* operon-*lacZ* reporter plasmid, pSH18-34. 'Bait' plasmids were co-transformed into yeast strain, EGY48, with interaction partners ('prey') representing the Ras-Binding Domains (RBDs) of Raf, RalGDS, and *Rgl*II. Next, two randomly selected co-transformants of each interaction test were then patched directly onto agar plates containing X-gal and the extent of blue color developed was recorded. In all cases, bait or prey plasmids when co-transformed with control plasmids, pJG4-5 and pEG202, respectively, did not result in any significant interactions

Effects of R-ras3 *on transcriptional responses*

To further characterize the observed differences between R-*ras3* and other Ras family members, we sought to determine if R-*ras3* could preferentially activate nuclear transcription events from different promoter elements previously known to be transactivated by Ras (Galang *et al*., 1994). For this, response elements representing the binding sites for different transcription factors, including SRF, ETS/TCF, Fos/Jun, and NF-κB/Rel, were constructed (Li *et al*., 1996). To assess if R-*ras3* could promote nuclear gene expression events, transient transcription reporter assays were performed in NIH3T3 cells. Following lysis of transfected cultures, the extent of gene transcription was quantitated by measuring the levels of transcriptional activity generated from the luciferase reporter gene, using β-luciferin as the substrate.

As shown in Figure 6, mutant forms of H-*ras*, *TC21*, R-*ras* and R-*ras3* activated transcription from different response elements with potency generally reflecting their relative ability in transforming NIH3T3 cells. However, whereas R-*ras3* stimulated transcriptional responses by $\sim$2.0-fold for ETS and NF-κB response elements, no significant stimulation of transcription was observed with SRF and TRE reporter constructs.

Tissue Distribution of R-ras3

Transforming oncogenes of the Ras subfamily, including Ras, *TC21* or R-*ras*, all displayed a broad tissue expression pattern, which may reflect their vital role in multiple cell types (Chan *et al*., 1994; Saez *et al*., 1994). To examine whether R-*ras3* has a similar pattern of tissue distribution, we performed Northern blot analysis using total RNAs derived from various human tissue origins. Using a ^{32}P-labeled R-*ras3* full-length cDNA as probe, we observed a $\sim$ 3.8 kb transcript expressed at high levels in both the brain and heart (Figure 7).

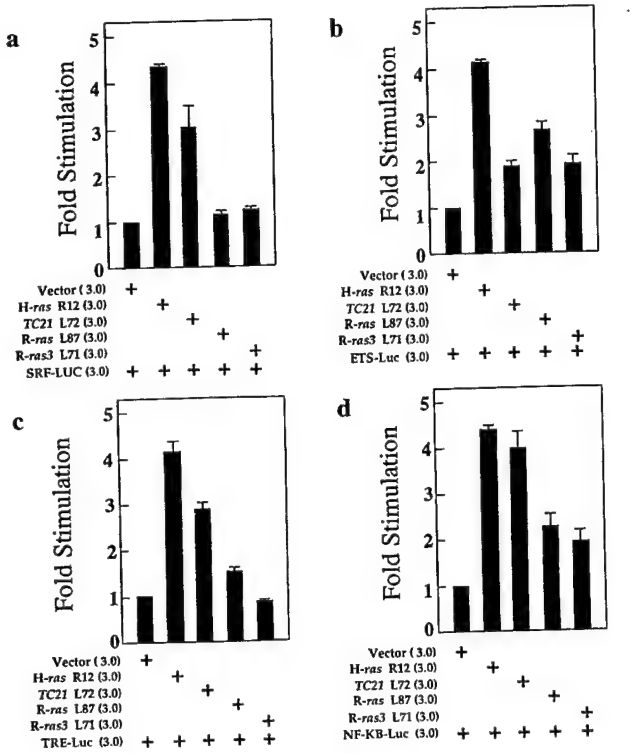

Figure 6 Activation of transcription responses by R-*ras3*. The relative ability of R-*ras3* and various *ras*-related genes in activating transcription responses by transcription factors: (**a**) SRF (SRF-LUC), (**b**) ETS (ETS-LUC), (**c**) Fos/Jun (TRE-LUC), and (**d**) NF-κB/Rel (NF-κB-LUC), was measured by transient transfection assays in NIH3T3 cells. The arbitrary luciferase activity for each sample was normalized with the amount of total cell protein being quantitated, and was expressed as fold-stimulation of the control. Data represent fold stimulation with standard deviations (error bars) derived from triplicate plates of a representative experiment which has been repeated at least three times with similar results being obtained

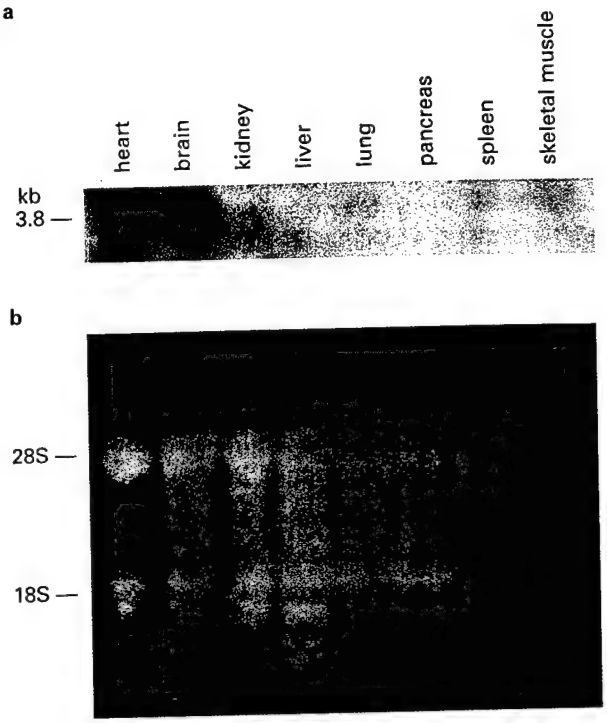

Figure 7 Tissue distribution of R-*ras3*. (**a**) Expression of R-*ras* transcripts were examined utilizing a nitrocellulose filter (Invitrogen, CA) containing around 10 μg of total RNAs derived from various human tissues. A ^{32}P-labeled R-*ras3* cDNA probe was hybridized to the filter and the amount of RNA loaded was visualized by ethidium bromide staining (**b**). The 3.8 kb transcripts of R-*ras3* are indicated

Similar size transcripts were not, however, detected in other tissues being examined. This strikingly restricted pattern of expression was in contrast with those previously reported for Ras, *TC21*, or R-*ras*, and would suggest a specific role of R-*ras3* in these tissues.

Discussion

Cellular responses to external stimuli in multicellular organisms are mediated by a diverse and complex intracellular signaling network for the control of regulated gene expression (Hunter, 1997). The present report describes the identification of R-*ras3* as an additional member of the Ras gene family. The gene product encoded by the human R-*ras3* is closely related to a *C. elegans ras*-related gene, *ras2*. Interestingly, the diversity of *ras*-related sequences in the mammalian system is clearly mirrored by the non-vertebrate organisms, since the human Ras and R-*ras* genes are closely related to the *C. elegans let-60*, and R-*ras1* genes, respectively. The high levels of evolutionary conservation among *ras*-related sequences would argue against these molecules representing redundant *ras* sequences. Rather, various *ras*-related genes may play a major role in regulating vital cellular functions found throughout evolution.

Among mammalian genes, although R-*ras3* is more closely related to *TC21* than to Ras or R-*ras*, protein sequence alignment studies suggest that R-*ras3* constitutes an evolutionarily distinct class of G-proteins. This is supported by the observation that in the N-terminal catalytic domain of Ras GTPases, cysteine residues among H-, K- and N-*ras*, or between *TC21* and R-*ras* are highly conserved. In contrast, R-*ras3* is completely devoid of cysteine residues suggesting that it may attain an unique tertiary conformation and thereby could display distinct biochemical properties.

R-*ras3* constitutes the sixth member of the Ras gene family to possess readily detectable transforming properties. However, the efficiency of R-*ras3* in inducing transformation is less than that of Ras, *TC21*, and R-*ras*. Interestingly, the hierarchy of transforming activity elicited by these *ras*-related genes shows a general correlation with their relative ability to stimulate the MAPK pathway. Consistent with these findings, R-*ras3*, also displays a substantially weaker interaction with Raf and has only modest effects on trans-activation from different transcription response elements. Our observations that wild-type Raf synergizes dramatically with R-*ras3* in both cellular transformation and MAPK activation, raises the possibility that Raf may be a rate-limiting step in R-*ras3* mediated transforming processes. However, whether R-*ras3* binds and activates Raf *in vivo* or that the observed synergistic effect is due to other mechanisms remains to be determined.

Ras has also been shown to activate several other signaling cascades known to be critical for its

transforming potential (Rodriguez-Viciana *et al*., 1997; Qiu *et al*., 1995a, b, 1997; Prendergast *et al*., 1995; Qiu *et al*., 1997; White *et al*., 1996; Tang *et al*., 1997). We have performed preliminary tests of the ability of R-*ras3* to activate the c-Jun N-terminal kinase (JNK) cascade, but failed to detect a significant perturbation of this particular pathway (data not shown). Given the fact that R-*ras3* only interacts modestly with Raf and RalGDS, we speculate that R-*ras3* induced biological effects may be coupled to a completely novel downstream signaling cascade. In this case, an effort to search for novel R-*ras3* interacting proteins would be highly warranted.

The region encompassing residues 32–40 (switch I) of Ras is important for its interactions with downstream substrates (Lowy and Willumsen, 1993). More recently, the switch II domain of Ras (codons 59–76), was also shown to be crucial in interacting with Raf (Drugan *et al*., 1996), and R-*ras3* shares 17 out of 18 amino acids in this domain. In addition, the regions immediately flanking the switch I effector loop have been reported to play a role in Ras functions. For example, in regions flanking the K-*rev*-1 effector loop, replacement of residues G26, I27, E30, K31, and E45, in K-*rev*-1 to those of Ras (N26, H27, D30 E31, V45) have been shown to confer Ras functions to K-*rev*-1 (Marshall *et al*., 1991). Interestingly, the corresponding residues in R-*ras3* (K36, I37, P40, D41, E55) are totally distinct from those of Ras, but share in two of these residues (I37 and E55) with K-*rev*-1 instead. These observations, once again, reinforce our earlier prediction that R-*ras3* may interact with a repertoire of effectors quite different from those described for Ras.

The carboxyl-terminal half of Ras constitutes the highly divergent region which has been considered as dispensable for Ras functions (Lowy and Willumsen, 1993). However, more recent findings indicate that sequences in this region could modulate Ras functions. For example, mutations introduced into the polybasic lysine residues in C-terminal region of K-ras4B have been shown to reduce the transforming activity and membrane-binding properties of this oncogene (Jackson *et al*., 1994). Incidentally, R-*ras3* possesses five lysine residues in the corresponding region, however, whether this polybasic domain plays a role in its biological functions is not known. Of note, we have also identified a tripeptide sequence, RGD, located immediately downstream of the polylysine domain, which resembles the consensus binding site for the extracellular matrix protein, fibronectin (Ruoslahti *et al*., 1996). Whether this sequence is fortuitously present in R-*ras3* or it mediates interaction with novel molecules is not clear.

The restricted nature of R-*ras3* gene expression in human brain and heart is intriguing. Obviously, the prospect of R-*ras3* in regulating nerve signal transmission or muscle cell functions would be exciting areas for future studies. Of note, several Ras regulators and effectors have been shown to be expressed predominantly in the brain. These include Ras guanine nucleotide exchange factors–GRF (Farnsworth *et al*., 1995), and GRF2 (Fam *et al*., 1997); GTPase activating proteins – NF1 (Hattori *et al*., 1992) and p98 R-*ras* GAP (Yamamoto *et al*., 1995); and a downstream effector – B-*raf* (Vossler *et al*., 1997). It is, therefore, of great interest to test the ability of these Ras regulators in interacting functionally with R-*ras3*.

Taking all these findings together, we have provided evidence that R-*ras3* possesses an intrinsic property of promoting cell growth. Given the distinct tissue expression pattern of R-*ras3*, it is plausible that R-*ras3* may serve as an important signal transducer for as of yet novel upstream stimuli in controlling cell proliferation.

Materials and methods

Cell lines

The NIH3T3 cell line, established in this laboratory was maintained in Dulbecco's Modified Eagle's Medium (DMEM) supplemented with 10% calf serum (CS). NIH3T3 cells carrying different plasmid constructs were derived by transfecting 1.5×10^5 cells with 1.0 μg of DNA by the standard calcium phosphate precipitation method (Wigler *et al*., 1977). Transfectants were selected in Geneticin (750 μg/ml) and were passaged once prior to characterization of growth properties *in vitro*.

NIH3T3 focus forming assay

Approximately 1.5×10^5 NIH3T3 cells were plated onto a 100 mm culture dish and DNA transfection was performed by the standard calcium phosphate precipitation method. In all cases, the amount of DNA added was normalized by the addition of a control expression vector, *pCEV29*. After transfection, cells were medium changed twice a week with 5% CS in DMEM and the number and quality of foci were scored every week for up to three weeks. All plates were then fixed in 70% cold methanol and stained with Giemsa solution for detailed quantitative analysis.

Plasmids

Expression plasmids representing the oncogenic mutants of H-*ras* (H-*ras* R12), *TC21* (*TC21* L72), and R-*ras* (R-*ras* L87) were all cloned into an eukaryotic expression vector, *pCEV29* (Chan et al., 1994). The full-length wild-type c-*raf*-1 construct was in the expression vector, pZIPneo (Saez *et al*., 1994). *pCEV29*-HA-R-*ras3* wt was constructed by cloning a *Bam*HI–*Bst*EII restriction fragment containing the entire full-length R-*ras3* cDNA into the expression vector, *pCEV29-HA*, which contains a hemagglutinin (HA) epitope.

Cloning and Site-directed mutagenesis

The human wild-type R-*ras3* coding region (nucleotide 1–627) was generated by polymerase chain reaction (PCR) method from a human embryonic lung fibroblast cDNA library (Rubin *et al*., 1991) with a *Bam*HI-tagged (+) primer (5′-AAAGGATCCATGGCGACCAGCGCCGTCC CCAGT-3′) and an *Eco*RI–*Xho*I-tagged (−) primer (5′-TTTGAATTCCTCGAGTCACAAGATCACACATTGCA GTTTGTG-3′). PCR amplified product was subcloned into the multiple cloning site of *pCEV29*, and was then subjected to sequencing analysis to confirm authenticity. The R-*ras3* L71 mutant was generated from the wild-type construct using a mutant oligonucleotide (5′-GCTgaat tcCTCCAGCCCAGCTGTGTC-3′) encompassing an internal *Eco*RI site (small letter) for PCR amplification with the *Bam*HI-containing 5′ primer at the translational start site. The resulting amplified product was digested with *Bam*HI and *Eco*RI and was used to replace the corresponding wild-type restriction fragment resulting in the generation of the CAG to CTG mutation (above, underlined) in codon 71 of

R-*ras3*. The authenticity of all constructs described in this study have been confirmed by nucleotide sequencing analysis.

In vitro *transcription/translation*

An *in vitro* transcription/translation kit was purchased from a commercial source (Promega, WI). Approximately 250 ng of circular plasmid was added to the rabbit reticulocyte lysate in the presence of 10 μCi of [^{35}S]methionine (NEN, Dupont, 10 mCi/ml; specific activity, 1078 Ci/mmol) and Sp6 RNA polymerase in a final volume of 10 μl. Reaction mixtures were incubated at 30°C for 90 min. Samples (5 μl) were then boiled in Lammili loading buffer and protein products were resolved by 14% polyacrylamide gel electrophoresis (SDS–PAGE). Gels were then fixed, treated with enhancer solution, dried and exposed to X-ray films at −70°C for 1–2 h.

Cell proliferation assays

For analysis of proliferation in semi-solid medium, 1×10^3, 1×10^4 and 1×10^5 cells were suspended in 0.5% agarose (Noble agar, Difco) in 10% CS as described elsewhere (DiFiore *et al*., 1987). Colonies were stained and scored after 2 weeks. For low serum proliferation, approximately 10^3 cells were plated onto 60 mm fibronectin (10 μg/ml, UBI, MA)-coated plates in the presence of full serum (10% CS). Twenty-four hours after plating, medium was changed to 10%, 2% and 0.5% and incubated for 2 weeks. Continuously proliferating colonies were then visualized by fixation in 70% methanol and staining with Giemsa solution.

MAPK kinase assay

For transient assays, 1×10^6 NIH3T3 cells were transfected singly or doubly by calcium phosphate precipitation method with the appropriate amount of each plasmid. The MAPK/erk2 was exogenously introduced by transfecting 3.0 μg of an HA-epitope-tagged MAPK/erk2 expression plasmid (Coso *et al*., 1995). One day after transfection, cells were placed in serum-depleted medium for 16 h and then lysed in 600 μl of 25 mM HEPES (pH 7.5), 0.3 M NaCl, 1.5 mM $MgCl_2$, 0.2 mM EDTA, 1% Triton-X100, 0.5 mM DTT, 20 mM β-glycerophosphate, 0.1 mM Na_3VO_4, 2 μg/ml leupeptin, 100 μg/ml PMSF, 0.1%SDS, and 0.5% sodium deoxycholate. Exogenously expressed HA-MAPK/erk2 was immunoprecipitated from total cell lysates with 1.0 μg of an anti-HA monoclonal antibody (Monoclonal Core Facility, The Mount Sinai School of Medicine), followed by coupling to 30 μl of γ-bind G-sepharose (Pharmacia, NJ). Immune complexes were washed three times with 1% NP-40 and 2 mM Na_3VO_4 in phosphate-buffered saline (PBS), followed by one wash in 0.5 mM LiCl and 100 mM Tris (pH 7.5). Beads were then resuspended in 30 μl of a kinase reaction buffer containing 12.5 mM HEPES pH 7.5, 12.5 mM β-glycerophosphate, 7.5 mM $MgCl_2$, 0.5 mM EGTA, 0.5 mM NaF, 0.5 mM Na_3VO_4, 1.0 μCi of [$^{\gamma 32}$P]ATP, 20 mM cold ATP, 3.3 mM DTT, and 60 μg of myelin basic protein (Sigma, MO) and incubated at 30°C for 30 min. Equal aliquots (8 μl) of the reaction mix were spotted in duplicate onto cellulose filters (Life Tech., MD) and washed three times in ice cold 1.0 % o-phosphoric acid. Filters were then dried and counted in a scintillation counter.

Immunoprecipitation and Western blotting analysis

Transiently transfected COS7 cells were lysed in 600 μl NP-40 solubilizer (50 mM Tris-HCl pH 7.5, 100 mM NaCl, 5 mM EDTA, and 1% NP-40) to obtain crude cell lysates. To detect HA-R-*ras3* protein, an anti-HA monoclonal antibody (2.0 μg/ml) was added to the total cell lysates and incubated for 1 h at 4°C. Antibodies were then absorbed onto 30 μl of γ-bind G sepharose beads (Pharmacia, NJ) for an additional 30 min at 4°C. Immunocomplexes were then washed three times with lysis buffer and bound proteins were eluted by boiling in Lammili buffer and resolved on a 14% SDS–PAGE gel. Following transfer onto Immobilon-P membrane (Millipore, MA), HA-R-*ras3* protein was detected by the sequential incubation with the same anti-HA antibody (1.5 μg/ml), a rabbit anti-mouse secondary antibody (1:2500 dilution, Jackson Lab, PA), and ^{25}I-labeled protein A (1:5000 dilution, ICN, CA).

Yeast two-hybrid interaction test

H-*ras* and X-*ras3* wild-type cDNAs lacking the C-terminal membrane targeting sequences were subcloned into the yeast 'bait' vector, pEG202, which contains the *LexA* DNA-binding domain. The Ras-Binding Domains (RBD) of human Raf (aa 48–176), mouse RalGDS (aa 727–853), and human *Rgl*II (aa 370–518) were generated by PCR amplification from cDNA plasmids and were subcloned into the yeast 'prey' vector, pJG4-5, which contains the *LexA* trans-activation domain (Golemis *et al*., 1997). Following co-transformation of the indicated interacting partners together with the *lacZ* reporter plasmid, pSH18-34, in the yeast strain, EGY48, transformants were selected on nutrient plates lacking the amino acids uracil, histidine and tryptophan. The extent of interactions between R-*ras3* and candidate effectors were investigated by streaking individual yeast colony onto X-gal (80 μg/ml)-containing plates, which measure the levels of expression from the reporter gene, *lacZ*.

Transcription reporter assay

With the exception of ETS response element which consists of a single copy of an inverted repeat of the ETS binding site in the polyoma enhancer, all the reporter constructs were synthesized with oligonucleotide adaptors incorporating 3 tandemly positioned response elements: ETS: [GCTAGC(GCAGGAAGTATACTTCCTGC)$_1$AGATCT]; NF-κB: [GCTAGC(TGGGGATTCCCCA)$_3$ AGATCT]; SRF: [GCTAGC(CCATATTAGG)$_3$ AGATCT]; TRE: [GCTAGC (TGAGTCA)$_3$AGATCT].

These oligonucleotides were then inserted into the *Nhe*I and *Bgl*II sites of a backbone reporter vector, pGL-2 (Promega) with a c-*fos* minimal promoter and a downstream reporter gene, luciferase (Li *et al*., 1996). Transient transfection of NIH3T3 cells was carried out in triplicate with 5×10^5 cells per 60 mm culture dish using 3.0 μg of the reporter plasmid, and 3.0 μg of each expression vector. Twelve hours after transfection, cultures were maintained in low serum (0.5% CS) for 24 h. Cells were solubilized in 250 μl of reporter lysis buffer (Promega, WI) and 25 μl of this extract was added to 80 μl of the luciferase substrate, β-luciferin (Promega, WI); emitted light was then measured using a luminometer (Turner, CA). The data were normalized for the amount of protein and expressed as an arbitrary luminescence unit per μg of total protein. Also, we have tested for background transcription responses from the backbone vector which contains the c-*fos* minimal promoter but without the response elements, and did not observe any significant trans-activation by Ras.

Northern analysis

A tissue RNA blot was purchased from a commercial source (Invitrogen, CA). The filter was hybridized at 42°C

for 12 h with [^{32}P]-labeled DNA probes in 40% formamide, 5× saline sodium citrate (SSC), 5× Denhardt's solution, 1% SDS, and sonicated salmon sperm DNA (100 μg/ml). After the hybridization reactions, the filter was washed twice in 1× SSC and 0.1% SDS at room temperature and in 0.1× SSC and 0.1% SDS at 50°C. The filter was dried and exposed to X-ray films at −70°C for 2 days.

Acknowledgements

We thank Drs Roger Brent (pEG202, pSH18-34, pJG4-5), Silvio Gutkind (*pCEV29-HA*, pLTR-HA-*erk2*), Toru Miki (*pCEV29*, M426 cDNA library), and Robert Weinberg (RalGDS) for the kind gift of reagents; Drs Toru Miki and Robert Krauss for careful reading of the manuscript. This work was supported by a grant from the NIH (CA66654) and a Career Scientist Award of the Irma T Hirschl Foundation to AMLC. R-*ras3* accession number: AF022080.

References

Albright CF, Giddings BW, Liu J, Vito M and Weinberg RA. (1993). *EMBO J.*, **12**, 339–347.

Bos, JL. (1989). *Cancer Res.*, **49**, 4682–4689.

Chan AML, Miki T, Meyers KA and Aaronson SA. (1994). *Proc. Natl. Acad. Sci. USA*, **82**, 2394–2398.

Coso OA, Chiariello M, Yu JC, Teramoto H, Crespo P, Xu N, Miki T and Gutkind JS. (1995). *Cell*, **81**, 1137–1146.

Cowley S, Paterson H, Kemp P and Marshall CJ. (1994). *Cell*, **77**, 841–852.

Cox AD, Brtva TR, Lowe DG and Der CJ. (1994). *Oncogene*, **9**, 3281–3288.

Der CJ and Cox AD. (1991). *Cancer Cells*, **3**, 331–340.

DiFiore PP, Pierce JH, Fleming TP, Hazan R, Ullrich A, King CR, Schlessinger, S and Aaronson SA. (1987). *Cell*, **51**, 1063–1070.

Drivas GT, Shih A, Coutavas E, Rush MG and D'eustachio P. (1990). *Mol. Cell. Biol.*, **10**, 1793–1798.

Drugan JK, Khosravi-Far R, White MA, Der CJ, Sung YJ, Hwang YW and Campbell SL. (1996). *J. Biol. Chem.*, **271**, 233–237.

Egan SE, Giddings BW, Brooks MW, Buday L, Sizeland AM and Weinberg RA. (1993). *Nature*, **363**, 45–51.

Fam NP, Fan WT, Wang Z, Zhang LJ, Chen H and Moran MF. (1997). *Mol. Cell. Biol.*, **17**, 1396–1406.

Farnsworth CL, Freshney NW, Rosen LB, Ghosh A, Greenberg ME and Feig LA. (1995). *Nature*, **376**, 524–527.

Galang CK, Der CJ and Hauser CA. (1994). *Oncogene*, **9**, 2913-2921.

Golemis EA, Serebriiskii I and Law SF. (1997). In *Gene Cloning and Analysis: Current Innovations*, (eds). Schaefer BC. (Horizon Scientific Press), **4**, pp 11–28.

Gotoh T, Niino Y, Tokuda M, Hatase O, Nakamura S, Matsuda M and Hattori S. (1997). *Biol. Chem.*, **272**, 18602–18607.

Gotoh T, Hattori S, Nakamura S, Kitayama H, Noda M, Takai Y, Kaibuchi K, Matsui H, Hatase O, Takahashi H, Kurata T and Matsuda M. (1995). *Mol. Cell. Biol.*, **15**, 6746–6753.

Graham SM, Cox AD, Drivas G, Rush MG, D'eustachio P and Der CJ. (1994). *Mol. Cell. Biol.*, **14**, 4108–4115.

Han M and Sternberg PW. (1990). *Cell*, **63**, 921–931.

Hattori S, Maekawa M and Nakamura S. (1992). *Oncogene*, **7**, 481–485.

Huang Y, Saez R, Chao L, Santos E, Aaronson SA and Chan AML. (1995). *Oncogene*, **11**, 1255–1260.

Hunter T. (1997). *Cell*, **88**, 333–346.

Jackson JH, Li JW, Buss JE, Der CJ and Cochrane CG. (1994). *Proc. Natl. Acad. Sci. USA*, **91**, 12730–12734.

Jiang H, Luo JQ, Urano T, Frankel P, Lu Z, Foster DA and Feig LA. (1995). *Nature*, **378**, 409–412.

Joneson T, White MA, Wigler MH and Bar-Sagi D. (1996). *Science*, **271**, 810–812.

Khosravi-Far R, White MA, Westwick JK, Solski PA, Chrzanowska-Wodnicka M, Van Aelst L, Wigler MH and Der CJ. (1996). *Mol. Cell. Biol.*, **16**, 3923-3933.

Kitayama H, Sugimoto Y, Matsuzaki T, Ikawa Y and Noda M. (1989). *Cell*, **56**, 77–84.

Li W, Michieli P, Alimandi M, Lorenzi MV, Wu Y, Wang LH, Heidaran MA and Pierce JH. (1996). *Oncogene*, **13**, 731–738.

Lowe DG, Capon DJ, Delwart E, Sakaguchi AY, Naylor SL and Goeddel DV. (1987). *Cell*, **48**, 137–146.

Lowy DR and Willumsen BM. (1993). *Ann. Rev. Biochem.*, **62**, 851–891.

Marshall MS, Davis LJ, Keys RD, Mosser SD, Hill WS, Scolnick EM and Gibbs JB. (1991). *Mol. Cell. Biol.*, **11**, 3997–4004.

Peterson SN, Trabalzini L, Brtva TR, Fischer T, Altschuler DL, Martelli P, Lapetina EG, Der CJ and White II GC. (1996). *J. Biol. Chem.*, **271**, 29903–29908.

Prendergast GC, Khosravi-Far R, Solski PA, Kurzawa H, Lebowitz PF and Der CJ. (1995). *Oncogene*, **10**, 2289–2296.

Qiu RG, Abo A, McCormick F and Symons M. (1997). *Mol. Cell. Biol.*, **17**, 3449–3458.

Qiu RG, Chen J, Kirn D, McCormick F and Symons M. (1995a). *Nature*, **374**, 457–459.

Qiu RG, Chen J, McCormick F and Symons M. (1995b). *Proc. Natl. Acad. Sci. USA*, **92**, 11781–11785.

Quilliam LA, Khosravi-Far R, Huff SY and Der CJ. (1995). *Bioassays*, **17**, 395–404.

Reynolds SH, Stowers SJ, Patterson RM, Maronpot RR, Aaronson SA and Anderson MW. (1987). *Science*, **237**, 1309–1316.

Rodriguez-Viciana P, Warne PH, Khwaja A, Marte BM, Pappin D, Das P, Waterfield MD, Ridley A and Downward J. (1997). *Cell*, **89**, 457–467.

Rubin JS, Chan AML, Bottaro DP, Burgess WH, Taylor WG, Cech AC, Hirschfield DW, Wong J, Miki T, Finch PW and Aaronson SA. (1991). *Proc. Natl. Acad. Sci. USA*, **88**, 415–419.

Ruoslahti E. (1996). *Ann. Rev. Cell. Dev. Biol.*, **12**, 697–715.

Saez R, Chan AML, Miki T and Aaronson SA. (1994). *Oncogene*, **9**, 2977–2982.

Spaargaren M and Bischoff JR. (1994). *Proc. Natl. Acad. Sci. USA*, **91**, 12609–12613.

Tanaka S, Morishita T, Hashimoto Y, Hattori S, Nakamura S, Shibuya M, Matuoka K, Takenawa T, Kurata T, Nagashima K and Matsuda M. (1994). *Proc. Natl. Acad. Sci. USA*, **91**, 3443–3447.

Tang Y, Chen Z, Ambrose D, Liu J, Gibbs JB, Chernoff J and Field J. (1997). *Mol. Cell. Biol.*, **17**, 4454–4464.

Urano T, Emkey R and Feig LA. (1996). *EMBO J.*, **15**, 810–816.

Van Aelst L, Barr M, Marcus S, Polverino A and Wigler M. (1993). *Proc. Natl. Acad. Sci. USA*, **90**, 6213–6217.

Vossler MR, Yao H, York RD, Pan MG, Rim CS and Stork PJ. (1997). *Cell*, **89**, 73–82.

White MA, Nicolette C, Minden A, Polverino A, Van Aelst L, Karin M and Wigler MH. (1995). *Cell*, **80**, 533–541.

White MA, Vale T, Camonis JH, Schaefer E and Wigler MH. (1996). *J. Biol. Chem.*, **271**, 16439–16442.

Wigler M, Silverstein S, Lee LS, Pellicer A, Cheng YC and Axel R. (1977). *Cell*, **11**, 223–232.

Wolthuis RM, Bauer B, van't-Veer LJ, de-Vries-Smits AM, Cool RH, Spaargaren M, Wittinghofer A, Burgering BM and Bos JL. (1996). *Oncogene,* **13,** 353–362.

Yamamoto T, Matsui T, Nakafuku M, Iwamatsu A and Kaibuchi K. (1995). *J. Biol. Chem.,* **270,** 30557–30561.

Zhang Z, Vuori K, Wang HG, Reed JC and Ruoslahti E. (1996). *Cell,* **85,** 61-69.

THE JOURNAL OF BIOLOGICAL CHEMISTRY
Vol. 273, No. 26, Issue of June 26, pp. 16325–16331, 1998
Printed in U.S.A.

The Effect of Me^{2+} Cofactors at the Initial Stages of V(D)J Recombination*

(Received for publication, March 5, 1998, and in revised form, April 21, 1998)

Sandro Santagata, Vassilis Aidinis, and Eugenia Spanopoulou‡

From the Mount Sinai School of Medicine, Howard Hughes Medical Institute, Ruttenberg Cancer Center, New York, New York 10029

V(D)J site-specific recombination mediates the somatic assembly of the antigen receptor gene segments. This process is initiated by the recombination activating proteins RAG1 and RAG2, which recognize the recombination signal sequences (RSS) and cleave the DNA at the coding/RSS junction. In this study, we show that RAG1 and RAG2 have the ability to directly interact in solution before binding to the DNA. RAG1 forms a homodimer, which leads to the appearance of two distinct RAG1·RAG2 complexes bound to DNA. To investigate the properties of the two RAG1·RAG2 complexes in the presence of different Me^{2+} cofactors, we established an *in vitro* Mg^{2+}-based cleavage reaction on a single RSS. Using this system, we found that Mg^{2+} confers a specific pattern of DNA binding and cleavage. In contrast, Mn^{2+} allows aberrant binding of RAG1·RAG2 to single-stranded RSS and permits cleavage independent of binding to the nonamer. To determine the contribution of Me^{2+} ions at the early stages of V(D)J recombination, we analyzed specific DNA recognition and cleavage by RAG1·RAG2 on phosphorothioated substrates. These experiments revealed that Me^{2+} ions directly coordinate the binding of RAG1·RAG2 to the RSS DNA.

Diversity of the immunoglobulin and T cell receptor repertoire is generated by site-specific rearrangement of V, D, and J gene segments in a process termed V(D)J recombination (1). Each antigen receptor coding segment is flanked by highly conserved recombination signal sequences (RSS),[1] which direct the site of reciprocal recombination (2). The consensus RSS consists of a heptamer sequence (CACAGTG) directly adjacent to the coding element and an A/T-rich nonamer site (ACAAAAACC) separated from the heptamer by a spacer of either 12 or 23 base pairs (3–5). Recombination typically occurs between a 12-base pair and a 23-base pair RSS, a phenomenon referred to as the 12/23 rule (1, 4). V(D)J recombination is initiated by two lymphoid-specific proteins RAG1 and RAG2 (6, 7) that bind to the RSS with specificity (8–10). Recognition of the nonamer motif is mediated by a region of RAG1 that exhibits distinct homology to homeodomain proteins (8, 9, 11) whereas the heptamer DNA binding domain of RAG1·RAG2 remains to be identified. Upon binding, RAG1, RAG2, and other as yet unidentified cellular activities mediate synaptic complex formation that brings together a pair of 12RSS and 23RSS signals (12–14). Subsequently, RAG1 and RAG2 cleave the DNA at the junction between the coding/heptamer sequences (15–17). After the generation of double-stranded broken ends by RAG1·RAG2, several ubiquitously expressed DNA repair proteins are engaged in the reaction including Ku70, Ku80, and DNA-PK (18, 19). Null mutations in RAG1, RAG2, or any of the three DNA repair genes lead to immunodeficiency, demonstrating that all of the above activities are indispensable for V(D)J recombination to occur (20–28).

The initial stages of V(D)J recombination have been successfully reproduced in *in vitro* assays. Using purified RAG proteins and an oligonucleotide substrate with a single RSS, it was demonstrated that RAG1 and RAG2 mediate site-specific cleavage in a two-step process (15, 16). First, a nick is introduced between the coding flank and the heptamer sequence. Second, a double strand break is generated by the liberated 3′ hydroxyl group, which serves as a nucleophile in a direct S_N2-type transesterification reaction of the lower strand (15–17). The cleavage intermediates are a covalently sealed hairpin coding end and a 5′ phosphorylated blunt signal end, as also observed *in vivo* (29–32). Upon cleavage of the 12/23 pair of signals, RAG1 and RAG2 remain stably bound to the signal ends (33).

A notable aspect of the *in vitro* cleavage system is the differential activity of RAG1·RAG2 in the presence of different Me^{2+} cofactors. It was shown previously that only Mn^{2+} mediates efficient cleavage on a single RSS, whereas coupled 12/23 cleavage happens only in the presence of Mg^{2+} (12–16). In this study, we report that Mg^{2+} does allow efficient cleavage on a single RSS whereas Mn^{2+} accelerates the second phase of the reaction, hairpin formation. The two metals enforce different kinetics of the V(D)J cleavage reaction and differential DNA binding properties of the RAG1·RAG2 complexes. Using phosphorothioated substrates, we find that the binding of RAG1·RAG2 to the RSS is directly coordinated by the Me^{2+} cofactor.

EXPERIMENTAL PROCEDURES

Protein Expression and Purification—Glutathione *S*-transferase (GST) fusion recombinant forms of the RAG1 and RAG2 active cores (GST-RAG1 1ΔN, amino acids 330–1040; GST-RAG2 2ΔC, amino acids 1–383) (34–37) were overexpressed in 293T cells and purified as described previously (8). Proteins were dialyzed in storage buffer (25 mM Tris (pH 8.0), 150 mM KCl, 2 mM DTT, and 20% glycerol) and quantified by Coomassie Blue staining following SDS-polyacrylamide gel electro-

* This work was supported in part by Medical Scientist Training Grant T32-GM07280-21, DOA/DOD Breast Cancer Predoctoral Training Program Grant DAMD17-94-J-4111S. S. (to S. S.), and National Institutes of Health Grant 1R01 AI40191-01A1 (to E. S.). The costs of publication of this article were defrayed in part by the payment of page charges. This article must therefore be hereby marked "*advertisement*" in accordance with 18 U.S.C. Section 1734 solely to indicate this fact.

‡ Howard Hughes Medical Institute Assistant Investigator. To whom correspondence should be addressed: Mount Sinai School of Medicine, Howard Hughes Medical Institute, Ruttenberg Cancer Center, 1425 Madison Ave., East Bldg., Box 1130, New York, NY 10029. Tel.: 212-824-8120; Fax: 212-849-2446; E-mail: eugenia_spanopoulou@smtplink.mssm.edu.

[1] The abbreviations used are: RSS, recombination signal sequence; GST, glutathione *S*-transferase; DTT, dithiothreitol; aa, amino acid(s); MOPS, 4-morpholinepropanesulfonic acid; ds, double-stranded; ss, single-stranded.

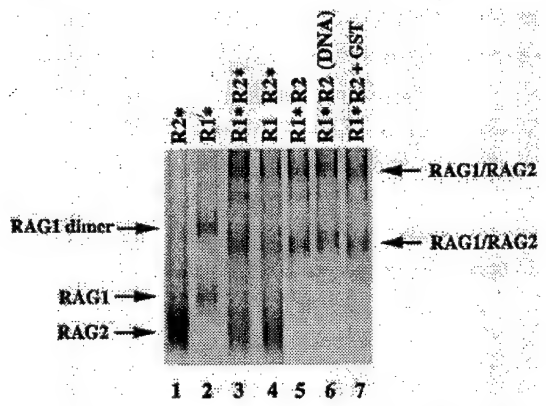

FIG. 1. **RAG1 and RAG2 interactions in solution.** RAG1 and RAG2 were purified as ^{35}S-labeled proteins, mixed together, cross-linked with glutaraldehyde, and resolved on a 5% native polyacrylamide gel. *Lanes 1* and *2* represent purified ^{35}S-labeled RAG2 and RAG1, respectively, after cross-linking. *Lane 3* contains ^{35}S-labeled RAG1 and RAG2, *lane 4* contains ^{35}S-RAG2·RAG1, *lane 5* contains ^{35}S-RAG1·RAG2, and *lane 6* contains ^{35}S-RAG1·RAG2 in the presence of the 12RSS probe. In *lane 7*, RAG1 and RAG2 were mixed with purified GST protein.

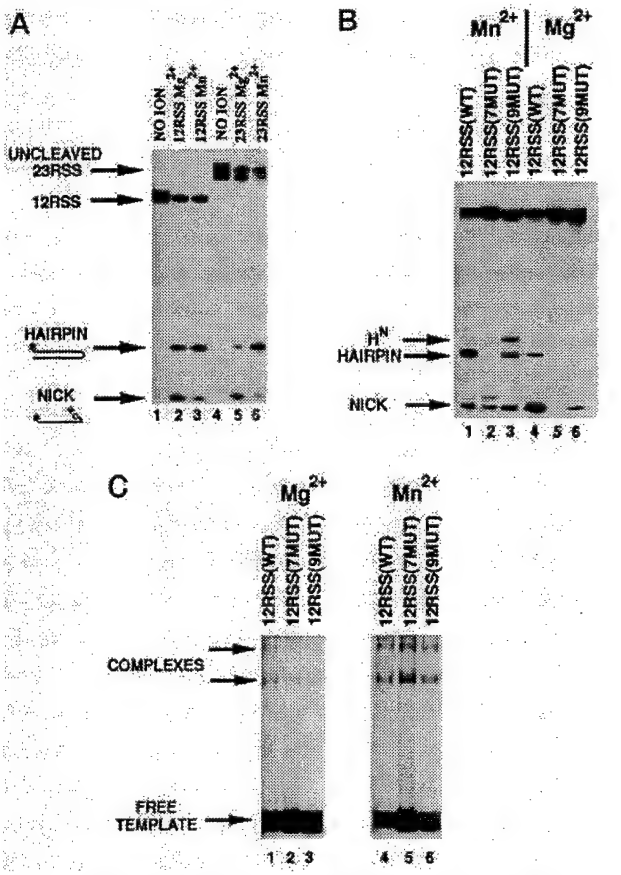

FIG. 2. **RAG1 and RAG2 mediate efficient nicking and transesterification in either Mn^{2+} or Mg^{2+}.** *A*, Mg^{2+}- and Mn^{2+}-based V(D)J cleavage on a single RSS. The 12RSS or 23RSS substrates were ^{32}P 5′ end-labeled to visualize exclusively the nicked products. Purified RAG1 and RAG2 were incubated with the substrates for 60 min. *B*, the effect of heptamer and nonamer mutations on V(D)J cleavage in the presence of Mn^{2+} or Mg^{2+}. Mutant substrates are described under "Experimental Procedures." *C*, mobility shift assays on the heptamer or nonamer mutant substrates. Note that the intensity of the shifted complexes is also dependent on the efficiency of cleavage. A low exposure is purposely shown to reveal the effects of the different mutant templates.

phoresis. ^{35}S-Labeled proteins were transiently expressed in 293T cells. The transfected cells were methionine-deprived for 30 min and subsequently incubated in the presence of [^{35}S]methionine for 2 h prior to harvest.

In Vitro Cleavage Reactions—Standard reaction conditions were modifications of the reactions developed by McBlane *et al.* (16). 50 ng of each protein, RAG1 and RAG2, were incubated with 0.01–0.05 pmol of ^{32}P end-labeled cleavage substrate in 25 mM MOPS-KOH (pH 7.0), 10 mM Tris-HCl (pH 7.0), 95 mM KCl, 2.2 mM DTT, 4% glycerol (no Me_2SO conditions), 1 mM $MgCl_2$, or 1 mM $MnCl_2$ in a 20-μl final volume. Reactions were incubated at 37 °C for the indicated time points. 10% Me_2SO cleavage reactions were conducted in: 25 mM MOPS-KOH (pH 7.0), 5 mM Tris-HCl (pH 7.0), 120 mM KOAc, 18 mM KCl, 10% Me_2SO, 2.2 mM DTT, 0.5 μM nonspecific single-stranded DNA with 50 ng of each protein and 0.01–0.05 pmol of ^{32}P end-labeled probe in a final volume of 20 μl. Reactions were stopped by the addition of 0.1% SDS and loading buffer. Samples were resolved on 16% polyacrylamide denaturing gels.

DNA Cleavage Substrates—The upper strand sequences of cleavage substrates are as follows.

12RSS-up:	5′-ACGCGTCGACGTCTTACACAGTGATACAGCCCTGAACAAAAACCGGATCCGCG-3′
23RSSup:	5′-ACGCGTCGACGTCTTACACAGTGATGCAGGCCAAGTGTGAAGCCATACAAAAACCGGATCCGCG-3′
12RSS(7mut)up:	5′-ACGCGTCGACGTCTTA**ACG**AGTGATACAGCCCTGAACAAAAACCGGATCCGCG-3′
12RSS(9mut)up:	5′-ACGCGTCGACGTCTTACACAGTGATACAGCCCTGAACAA**CCG**CCGGATCCGCG-3′
ICP(1-16):	5′-ACGCGTCGACGTCTTA-3′
ICP(17-53):	5′-CACAGTGATACAGCCCTGAACAAAAACCGGATCCGCG-3′

SEQUENCES 1–6

Standard cleavage reactions employed ^{32}P 5′ end-labeled upper strands annealed to unlabeled, complementary lower strand oligonucleotides. The substrate ssRSS was generated by hybridizing end-labeled ICP(1–16) to the unlabeled 12RSS-lower strand. dsRSS was created by annealing end-labeled ICP(1–16), unlabeled 5′-phosphorylated ICP(17–53) and unlabeled 12RSS-lower strand. The spacers for substrate 12RSS and 23RSS were optimized to include the most frequently occurring nucleotides as determined by data base analysis of multiple loci from numerous species (5). Phosphorothioated oligonucleotides (Genelink) maintained the 12RSS nucleotide sequence but had nonbridging oxygens replaced by sulfurs at the indicated positions.

Electrophoretic Mobility Shift Assays—Conditions were based on the previously published protocol (10). 50 ng of each protein were incubated for 10 min at 30 °C with 0.01–0.05 pmol of 5′ end-labeled probe in 25 mM MOPS-HCl (pH 8.0), 1 mM $MgCl_2$ or 1 mM $MnCl_2$, 2.2 mM DTT, 1 μg of bovine serum albumin, 0.5 μM nonspecific primer (5′-CCTCGAGCTCATCAGCTTGCCTGTGGGCAGCTCGATCTCTTTGTCG-3′), 20% Me_2SO, and 120 mM potassium acetate. Cross-linking was achieved by glutaraldehyde (final concentration 0.1%, v/v) treatment for 10 min at 30 °C. Complexes were resolved on a 4.0% native polyacrylamide gel.

RESULTS

Detection of RAG1·RAG2 Complexes in Solution—The ability of RAG1 and RAG2 to bind and cleave the DNA is dependent on the simultaneous presence of both proteins (15, 16, 31). This implies that RAG1 and RAG2 might interact either in the presence or absence of the RSS DNA. Although *in vivo* the two proteins have been found in the same complex (38, 39), *in vitro* RAG1 and RAG2 have only been observed together in the stable complex formed upon cleavage of the DNA (33). The ability of RAG1 and RAG2 to interact in solution was probed in mixing experiments using ^{35}S-labeled proteins (Fig. 1). After incubation, protein complexes were cross-linked with glutaral-

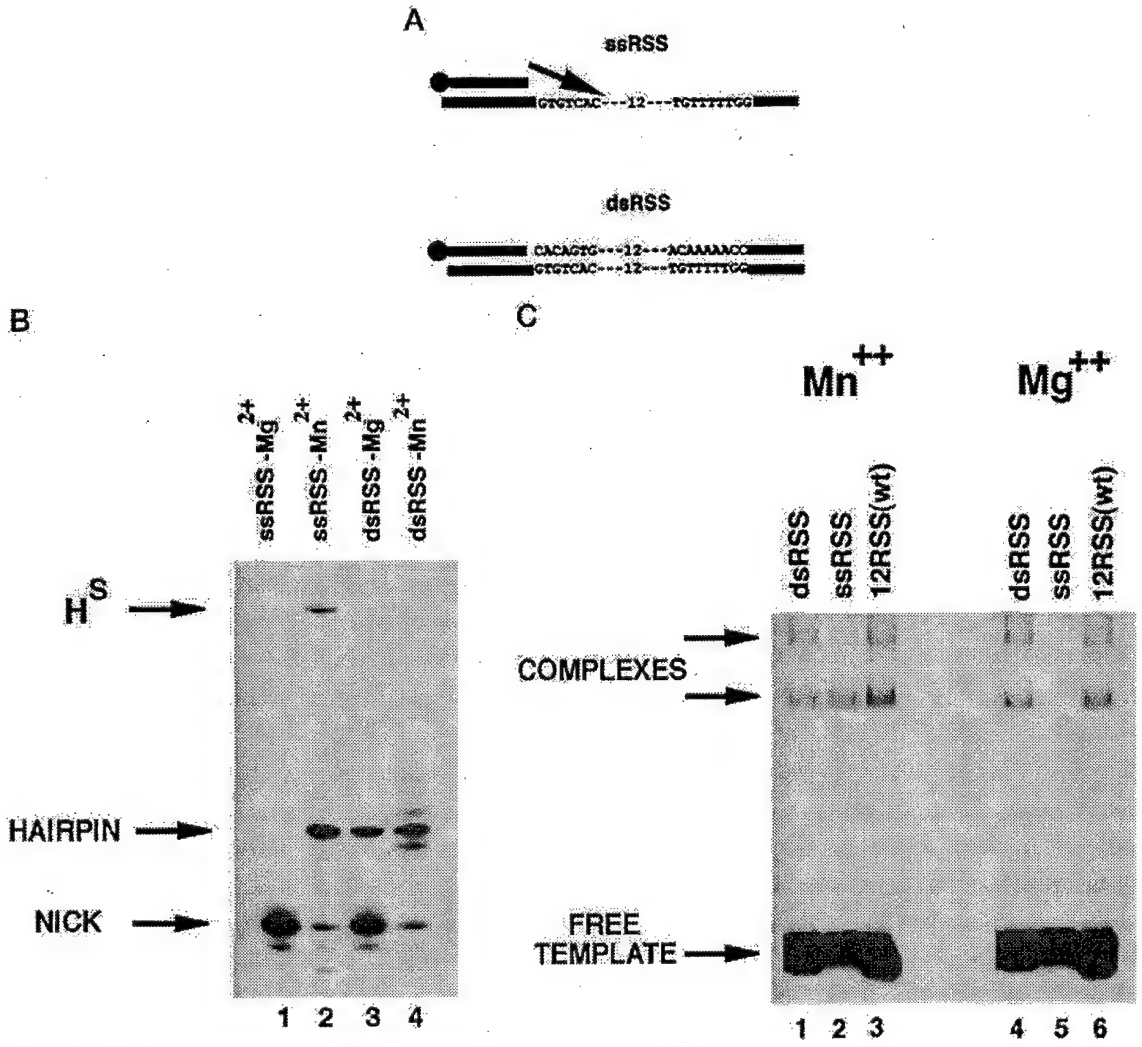

FIG. 3. **Mn^{2+} but not Mg^{2+} allows DNA binding and transesterification on single-stranded RSS.** *A*, single-stranded RSS cleavage substrates (ssRSS) were generated by annealing ^{32}P 5′ end-labeled upper strand coding nucleotides 1–16 with the full-length lower strand (12RSS-lo). The prenicked double-stranded RSS cleavage substrate (dsRSS) was synthesized from ^{32}P 5′ end-labeled ICP(1–16), unlabeled 5′ phosphorylated ICP(17–53), and 12RSS-lo. *B*, cleavage assays. ssRSS was incubated with RAG1 and RAG2 in Mg^{2+} (*lane 1*) and Mn^{2+} (*lane 2*). *H** represents aberrant hairpin production stemming from inappropriate nucleophilic attack at the 5′ end of the lower strand heptamer (40). dsRSS was incubated with RAG1 and RAG2 in Mg^{2+} (*lane 3*) and Mn^{2+} (*lane 4*). *C*, binding of RAG1·RAG2 to dsRSS (*lanes 1* and *4*), ssRSS (*lanes 2* and *5*), and wild type 12RSS (*lanes 3* and *6*) in either Mn^{2+} (*lanes 1–3*) or Mg^{2+} (*lanes 4–6*).

dehyde and resolved on a native polyacrylamide gel. RAG2 alone produces one complex that migrates at the apparent molecular weight for the protein (Fig. 1, *lane 1*). However, RAG1 produced two complexes that corresponded to a monomeric and dimeric form of the protein (Fig. 1, *lane 2*). RAG1 homodimerization is mediated by the homeodomain part of the protein.[2] Incubation of RAG1 with RAG2 produces two new complexes that contain both proteins (Fig. 1, *lanes 3–5*). The observed RAG1·RAG2 interaction is independent of the presence of RSS DNA (Fig. 1, compare *lanes 5* and *6*). In addition, formation of the two complexes is specific to the RAG1·RAG2 interaction because addition of GST protein does not change the stoichiometry of the complexes (Fig. 1, *lane 7*).

Mn^{2+} Relaxes DNA Binding and Cleavage Specificity by RAG1·RAG2—To test the effect of Me^{2+} cofactors at the initial stages of V(D)J recombination, cleavage reactions were performed in the presence of either Mn^{2+} or Mg^{2+} (Fig. 2). The active cores of purified RAG1 (aa 330–1040) and RAG2 (aa 1–383) were incubated with ^{32}P-labeled 12RSS or 23RSS substrates. Surprisingly, in contrast to previous reports (12, 16), we found substantial cleavage of a single RSS substrate in the presence of Mg^{2+} (Fig. 2*A*, *lanes 2* and *5*), whereas Mn^{2+} accelerated hairpin formation by severalfold (Fig. 2*A*, *lanes 3* and *6*). Identical results were obtained on oligonucleotide templates used in the previous reports (12, 16, 40, 41) (data not shown) indicating that these differences are not due to the DNA composition of the substrates. One major factor that could account for the observed differences is the use of RAG1 and RAG2 proteins expressed in mammalian cells that may carry posttranslational modifications required for their cleavage activity.

The availability of an *in vitro* assay that allows single-site cleavage in the presence of Mg^{2+} prompted us to study the effect of Me^{2+} on the specificity of DNA binding and cleavage by RAG1·RAG2. To that extent, specificity of the cleavage reaction was tested by analyzing mutations of nucleotides that have

[2] V. Aidinis and E. Spanopoulou, manuscript in preparation.

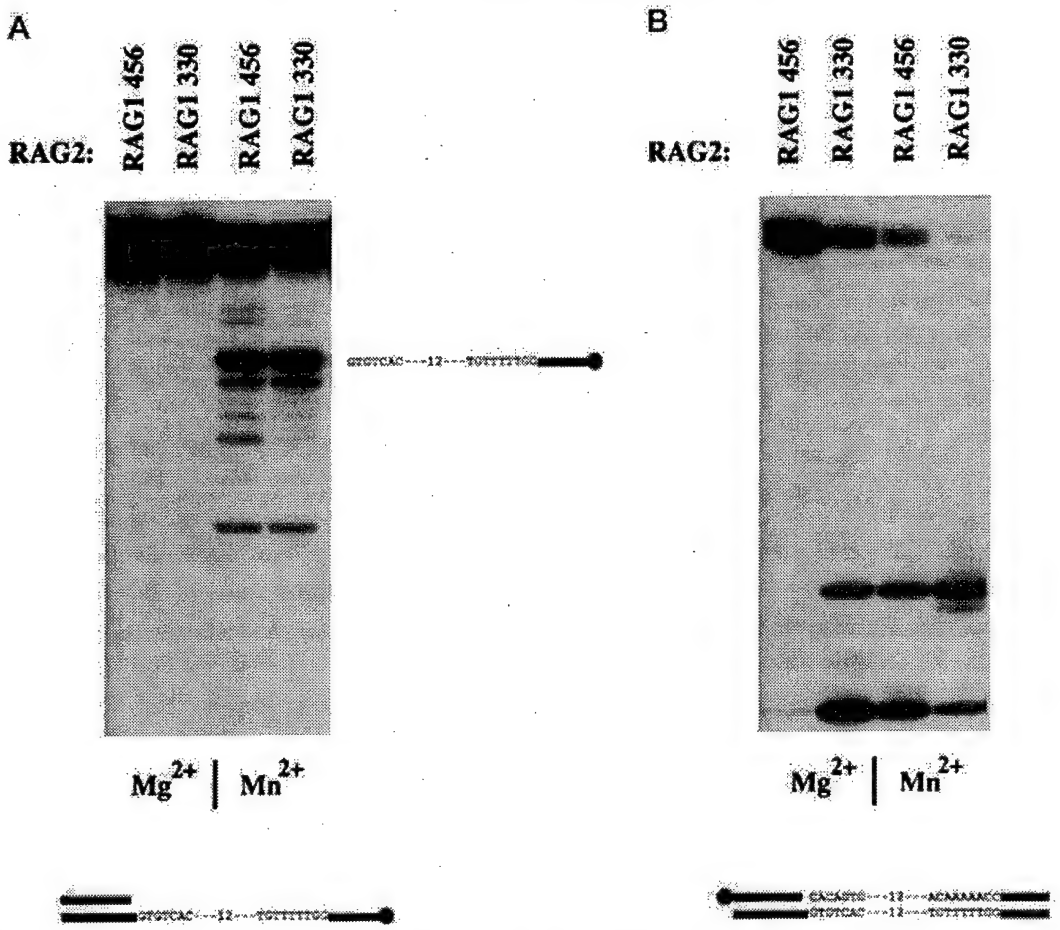

FIG. 4. **RAG1 aa 384–456 are not part of the RAG1·RAG2 active center.** The RAG1 homeodomain is not required for heptamer-mediated cleavage. *A*, RAG1 456–1040 can mediate hairpin formation on ssRSS in the presence of Mn^{2+}. Note that the ssRSS probe was labeled in the lower strand. *B*, RAG1 deletion mutants 456–1040 and RAG1 330–1040 were incubated with RAG2 and a radiolabeled 12RSS substrate for 120 min.

been shown to be critical for the function of the heptamer and nonamer elements of the RSS (40, 41) (Fig. 2*B*). Mutation of the first two residues of the heptamer abolish hairpin formation as reported previously (40, 41). However, RAG1·RAG2 can mediate nicking of the mutant heptamer substrate in the presence of Mn^{2+} but not in Mg^{2+} (Fig. 2*B*, *lanes 2* and *5*). Similarly, mutations in the nonamer element have a profound effect with Mg^{2+} as a cofactor, whereas Mn^{2+} permits efficient nick/hairpin formation on the mutant nonamer substrate (Fig. 2*B*, *lanes 3* and *6*).

The differential effect of the two metals on the cleavage reaction is also reflected on the DNA binding specificity of RAG1·RAG2. Gel retardation assays with purified RAG1·RAG2 and a single RSS probe show two complexes that both contain RAG1 and RAG2 interacting in solution (Fig. 2). In Mn^{2+}, both complexes bind avidly to the DNA despite mutations in the heptamer or nonamer motifs (Fig. 2*C*, *lanes 4–6*). In contrast, Mg^{2+} reduces binding of RAG1·RAG2 to the heptamer mutant by 2-fold and to the nonamer mutant by 5-fold (Fig. 2*C*, *lanes 1–3*).

Mn^{2+} but Not Mg^{2+} Allows DNA Recognition and Cleavage of a Single-stranded RSS—It was shown previously that in the presence of Mn^{2+} RAG1 and RAG2 can form hairpins utilizing a substrate with a double-stranded coding flank and a single-stranded lower strand RSS (40, 41). This finding suggested that RAG1 and RAG2 unwind the RSS providing the DNA distortion required for hairpin formation. The question arose however, as to how RAG1 and RAG2, unlike other DNA-binding proteins, can recognize ssDNA by establishing specific contacts only with nucleotides of the lower strand. We thus examined the ability of RAG1·RAG2 to mediate the transesterification reaction on a single-stranded RSS substrate (Fig. 3*A*) in the presence of either Mg^{2+} or Mn^{2+}. Fig. 3*B* shows that RAG1 and RAG2 are unable to mediate hairpin formation in the presence of Mg^{2+} but they could effectively do so when Mn^{2+} was used as the cofactor. When the upper strand of the RSS was replaced to recreate a double-stranded substrate with a nick remaining in the upper strand (Fig. 3*B*, *dsRSS*), the capacity of RAG1·RAG2 to mediate hairpin formation was reconstituted irrespective of the divalent cation employed. Mobility shift assays were performed to assess whether the basis of this differential usage of a single-stranded RSS resulted from modified DNA recognition in Mn^{2+} or Mg^{2+}. Fig. 3*C* reveals essentially equivalent levels of Mn^{2+} induced DNA recognition of templates dsRSS, ssRSS, and 12RSS (wild type). However, in Mg^{2+}, RAG1 and RAG2 can form a stable ternary complex only with the wild type 12RSS and the nicked dsRSS but are unable to recognize ssRSS.

ssRSS Recognition and Catalytic Activity of RAG1 Is Mediated by aa 456–1040—Given the ability of RAG1·RAG2 to mediate nonamer-independent cleavage and ssRSS recognition when assayed in Mn^{2+} (Figs. 2*B* and 3, *B* and *C*), RAG1 456–1040, which lacks the homeodomain region of the protein, was assayed for its ability to recognize the heptamer and mediate hairpin formation on the ssRSS substrate. As shown in Fig. 4*A*, in the presence of Mn^{2+} RAG1Δ456/RAG2-mediated efficient

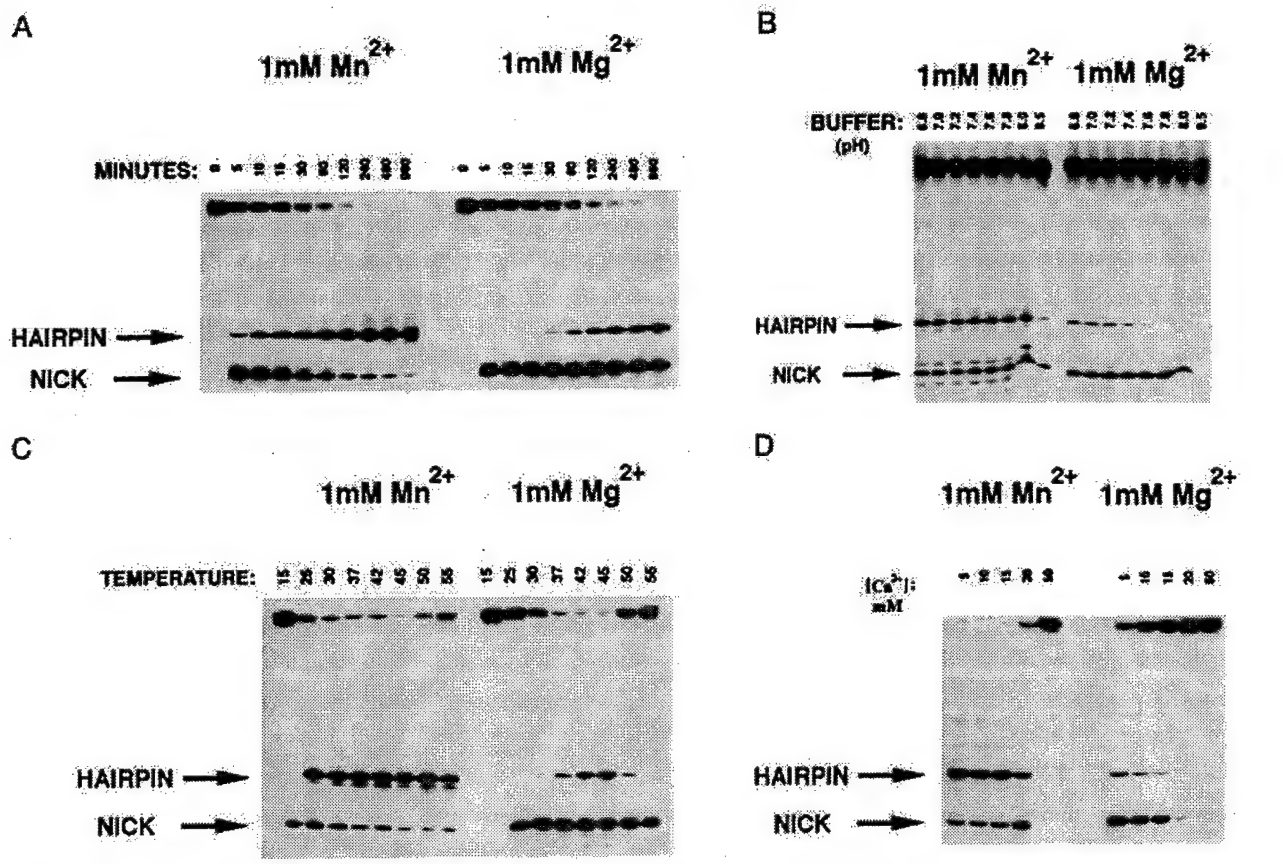

FIG. 5. **Comparison of the kinetics of Mn^{2+}- *versus* Mg^{2+}-based V(D)J cleavage reactions.** *A*, time dependence of the formation of cleavage intermediates. *B*, pH dependence of the transesterification reaction. *C*, temperature (°C) dependence of cleavage intermediate formation. *D*, relative Me^{2+} affinity of RAG1·RAG2 determined by Ca^{2+} titration. Reactions in *B*, *C*, and *D* were allowed to proceed for 60 min.

transesterification of the ssRSS template. The same protein was also capable of mediating DNA recognition and cleavage of the wild type 12RSS substrate in Mn^{2+} but not in Mg^{2+} (Fig. 4*B*). Thus, recognition of the heptamer motif and the subsequent transesterification reaction does not require aa 330–456 of RAG1 including the homeodomain region.

Mg^{2+}- but Not Mn^{2+}-based Reactions Follow Physiological Parameters—Given the differential activity of RAG1·RAG2 in the presence of different divalent ions, we studied the effect of Mn^{2+} and Mg^{2+} on the kinetics of the initial stages of V(D)J recombination. Cleavage of a 12RSS was analyzed by altering various physiological parameters. A time course of the reaction (Fig. 5*A*) revealed that total substrate conversion into cleavage intermediates (either nick or hairpin) is virtually equivalent between reactions conducted in 1 mM Mn^{2+} and in 1 mM Mg^{2+}. However, the kinetics of nick conversion into hairpin is accelerated at least 12-fold by Mn^{2+}. The biochemical requirements for Mn^{2+}- and Mg^{2+}-based cleavage were analyzed through a range of pH and temperature. In Mn^{2+}, nicking and transesterification were efficient within a wide pH range (Fig. 5*B*). However, Mg^{2+}-driven transesterification exhibited a strong pH dependence. Hairpin generation was eliminated above pH 7.6 (Fig. 5*B*), whereas nicking was virtually unaffected. Thus, the transesterification reaction can only occur within a narrow window of pH. A differential profile for Mn^{2+}- *versus* Mg^{2+}-based reactions was also observed by ranging temperature points (Fig. 5C). Mn^{2+}-driven reactions were not inhibited by temperature variations from 25 °C to 55 °C, whereas hairpin formation in Mg^{2+} was most effective at more physiological temperatures, 37 °C to 45 °C, and was repressed below 37 °C and above 50 °C. Interestingly, although total substrate cleavage is equivalent at 37 °C, 42 °C, and 45 °C in Mg^{2+}, the amount of hairpin formation is increased 3-fold over this temperature range. Conceivably, this effect could be due to more efficient melting of the DNA required for hairpin conversion.

To estimate the relative affinities of Mn^{2+} and Mg^{2+} for their binding sites, Me^{2+} binding was titrated out by increasing concentrations of Ca^{2+}. The latter is known to inhibit the cleavage activity of several restriction endonucleases (42) and transposases (43), as well as that of RAG1·RAG2 (10). Although 20 mM Ca^{2+} inhibits the Mn^{2+}-based reaction by only 5%, the same Ca^{2+} concentration almost completely arrests the Mg^{2+}-based reaction.

Phosphorothioate Substitutions Reveal a Role for Divalent Cations in DNA Recognition—The role of divalent cations during site-specific cleavage by RAG1 and RAG2 was explored using phosphorothioated oligonucleotides in which non-bridging oxygens around the site of cleavage were individually replaced by sulfurs. The differential coordination of metal-oxygen and metal-sulfur interactions (44) maintains that coordination of sulfur by Mn^{2+} is stronger than coordination by Mg^{2+}. Hence, involvement of a divalent cation at the catalytic site results in reduced cleavage of a phosphorothioated substrate in Mg^{2+} while leaving Mn^{2+}-based cleavage predominantly uninhibited. Exploration of the catalytic mechanisms of ribozymes using phosphorothioated methodology has demonstrated a role for metal ions in transition state stabilization during sequence-specific endonuclease cleavage (45–47).

Two phosphorothioated oligonucleotides were synthesized

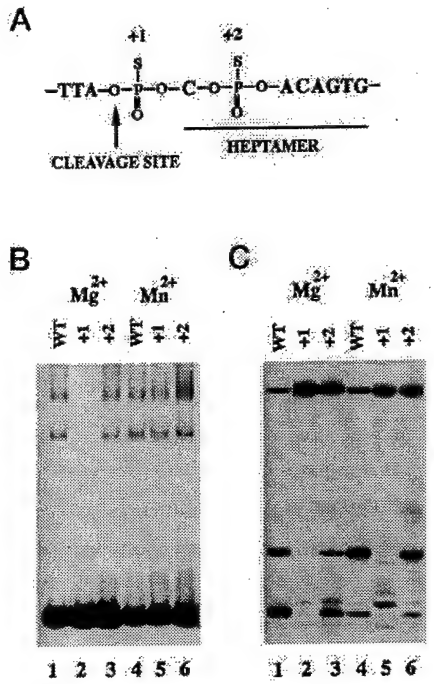

FIG. 6. **Phosphorothioated interference.** *A*, non-bridging oxygens were replaced by sulfurs in the upper strand of the standard cleavage substrate at and around the site of cleavage. The replaced positions are *numbered*. *B*, mobility shift assays were performed with RAG1 and RAG2 in Mn^{2+} or Mg^{2+} using the two phosphorothioated substrates. *C*, cleavage analysis of phosphorothioated substrates. Assays were performed in either Mn^{2+} or Mg^{2+} for 30 min.

with sulfur modifications at the indicated positions (Fig. 6*A*) and analyzed in DNA binding and cleavage assays. Substitution of the non-bridging oxygen at the cleavage site (+1) had a dramatic effect on the DNA binding and cleavage activities of RAG1·RAG2. DNA binding was severely compromised in Mg^{2+} but reconstituted by Mn^{2+} (Fig. 6*B*, *lanes 2* and *5*) or Ca^{2+} (data not shown). However, nicking and transesterification reactions by RAG1·RAG2 were severely reduced on the +1 thiosubstrate (Fig. 6*C*, *lane 2*) and Mn^{2+} only poorly resuscitated the nicking reaction (Fig. 6*C*, *lane 5*). Interestingly, sulfur substitution at the +1 position shifts the nicked product by one nucleotide (Fig. 6*C*, *lane 5*). It should be noted that phosphorothioated substrates were assayed as mixtures of the R_p and S_p forms (48). Thus, both S_p and R_p forms at the +1 position interfere with Mg^{2+}-mediated binding and cleavage by RAG1·RAG2. On the other hand, substitution of the non-bridging oxygen in the heptamer site, +2, reduced overall cleavage activity by 40% but it did not affect the efficiency of hairpin conversion (Fig. 6*C*, *lanes 3* and *6*) or that of DNA binding (Fig. 6*B*, *lanes 3* and *6*).

DISCUSSION

In this study, we analyzed the effect of Me^{2+} cofactors in the function of RAG1·RAG2 during the initial stages of V(D)J recombination. The results show that divalent ions not only modulate the cleavage activity of the complex but they also directly coordinate the binding of the complex to the RSS DNA. In general, Mg^{2+}-based reactions follow more physiological parameters of pH, temperature, and dependence on the heptamer/nonamer RSS motifs. In contrast, Mn^{2+}-mediated assays show relaxed specificity in which RAG1 and RAG2 are able to recognize a ssRSS element and DNA binding and cleavage is independent of nonamer binding. The tolerant phenotype induced by Mn^{2+} has also been observed for other proteins such as restriction endonucleases, retroviral integrases, and transposases. In the presence of Mn^{2+} several of these proteins exhibit relaxed DNA target specificity (49–54). In addition, Mn^{2+} resuscitates the activity of IS10 and Mu transposase and *Eco*RV endonuclease mutants that are catalytically inactive in Mg^{2+} (48, 50–52).

Direct Interaction of RAG1 and RAG2—Using direct mixing experiments we found that RAG1 and RAG2 interact in the absence of DNA to form two complexes that are generated by RAG1 homodimerization. The functional significance of RAG1 homodimerization is currently under study. The two RAG1·RAG2 complexes are formed in the absence of DNA, demonstrating that the two proteins interact directly. Although previous experiments had revealed that RAG1 and RAG2 can be co-precipitated from lymphoid extracts (37, 38), a direct interaction between the two proteins had not been shown. This is perhaps because of the transient nature of the interaction, which can, however, be stabilized by glutaraldehyde cross-linking. The latter also stabilizes the RAG1·RAG2·DNA ternary complexes formed during gel-retardation assays (10).

Mg^{2+}-mediated Cleavage on a Single RSS—Using RAG1 and RAG2 expressed in mammalian cells, we found that the two proteins are able to mediate efficient cleavage on a single RSS in the presence of Mg^{2+}. This is in contrast to the previous notion that single-site cleavage is only permitted by Mn^{2+} (12). It is therefore possible that, under physiological conditions, RAG1 and RAG2 have the ability to cleave on a single RSS. Presumably their 12/23 mode action (1, 13) might be regulated by additional cellular activities that prohibit uncontrolled cleavage on a single RSS. The involvement of such cellular activities has been indicated by previous experiments (13, 14).

The Nonamer Motif Modulates Efficiency of the V(D)J Cleavage Reaction—In vivo V(D)J recombination is critically dependent upon the integrity of both the heptamer and nonamer RSS motifs (3, 56, 57). The role of these two elements has been addressed in *in vitro* DNA binding and cleavage assays. The nonamer motif mediates recognition of the RSS by RAG1 (8, 9) whereas the heptamer stabilizes binding of the complex to the DNA (9, 10) and guides the subsequent transesterification reaction (8, 40, 41). Using Mn^{2+}-based cleavage assays, it was shown previously that mutations in the nonamer motif permit reduced but substantial nicking and hairpin formation (40, 41). These results raised the issue about the importance of the nonamer element during the initial stages of V(D)J recombination. Sequence comparison of RSS motifs from the Ig and T cell receptor loci has shown that in contrast to the heptamer motif the nonamer element is not as highly conserved (5). Collectively, these observations suggested that the nonamer might affect the efficiency of V(D)J recombination whereas the heptamer is essential for the catalysis of the reaction. The results of our *in vitro* assays support this hypothesis. Both the DNA binding and cleavage assays demonstrate that, although the heptamer is indispensable for the cleavage reaction, the nonamer modulates the efficiency of RAG1·RAG2 binding to DNA. When tested in Mg^{2+}-based assays, mutation of the nonamer impairs the DNA binding potential of RAG1·RAG2 and consequently drastically reduces their cleavage activity but mutation of the heptamer eliminates cleavage by RAG1·RAG2. In further support of the hypothesis that the nonamer modulates the efficiency of V(D)J cleavage, elimination of the nonamer DNA binding domain of RAG1 does not affect the cleavage activity of the protein when assayed in Mn^{2+}. Thus, the RAG1 homeodomain seems to affect efficiency and perhaps topology of the initial stages of V(D)J recombination, but it does not participate in the subsequent nicking and

transesterification reactions. These data might account for the reduced frequency of V(D)J recombination observed for truncated mutants of RAG1 that lack the homeodomain region (58) and in human patients carrying missense mutations in the Rag-1 homeodomain region.[3]

Mg^{2+} Directly Coordinates DNA Binding of RAG1·RAG2—The analysis of thiosubstrate +1 revealed that Me^{2+} ions directly coordinate the binding of RAG1·RAG2 to the DNA. Sulfur substitution at the site of cleavage severely reduced the DNA binding activity of RAG1·RAG2 in Mg^{2+}. However, binding was reconstituted to wild type levels by Mn^{2+} or Ca^{2+}. The differential behavior of this substrate in Mg^{2+} or Mn^{2+} strongly indicates that Mg^{2+} directly mediates DNA recognition by RAG1·RAG2 through its coordination with the nonbridging oxygens. Thus, the site of cleavage not only coordinates the nicking and transesterification reactions but also guides the binding of RAG1·RAG2 to DNA via coordination of Mg^{2+}. Given that the two proteins specifically recognize the heptamer sequence and cleave in its vicinity, it is possible that a single, Me^{2+}-coordinated, domain in proximity with the heptamer might execute both DNA recognition and subsequent cleavage. Such a mechanism has been implicated in Tn*10* transposition, where mutations in the active center of the transposase cancel target DNA capture (55). The role of Me^{2+} ions in mediating the binding of proteins to the DNA is poorly characterized with the exception of zinc-finger proteins. In one case, it has been shown that Mg^{2+} maintains the structure of the DNA binding domain of transcription factor HNF3 (59). Mg^{2+} also binds to a Me^{2+} binding site of *Eco*RV distinct from the catalytic center of the enzyme and determines specificity of DNA binding (60). It can be envisaged that the mode of RAG1·RAG2 binding to the DNA through the coordination of Mg^{2+} ions is not restricted to this class of proteins but constitutes a global mode by which transcription factors bind to DNA.

Acknowledgment—We thank Dr. Kenji Adzuma for insightful suggestions.

REFERENCES

1. Tonegawa, S. (1983) *Nature* **302,** 575–581
2. Lewis, S., and Gellert, M. (1989) *Cell* **59,** 585–588
3. Hesse, J. E., Lieber, M. R., Mizuuchi, K., and Gellert, M. (1989) *Genes Dev.* **3,** 1053–1061
4. Lewis, S. M. (1994) *Adv. Immunol.* **56,** 27–150
5. Ramsden, D. A., Baetz, K., and Wu, G. E. (1994) *Nucleic Acids Res.* **22,** 1785–1796
6. Schatz, D. G., Oettinger, M. A., and Baltimore, D. (1989) *Cell* **59,** 1035–1048
7. Oettinger, M. A., Schatz, D. G., Gorka, C., and Baltimore, D. (1990) *Science* **248,** 1517–1523
8. Spanopoulou, E., Zaitseva, F., Wang, F.-H., Santagata, S., Baltimore, D., and Panayotou, G. (1996) *Cell* **87,** 263–276
9. Difilippantonio, M. J., McMahan, C. J., Eastman, Q. M., Spanopoulou, E., and Schatz, D. G. (1996) *Cell* **87,** 253–262
10. Hiom, K., and Gellert, M. (1997) *Cell* **88,** 65–72
11. Nagawa, F., Ishiguro, K.-I., Tsuboi, A., Yoshida, T., Ishikawa, A., Takemori, T., Otsuka, A. J., and Sakano, H. (1998) *Mol. Cell. Biol.* **18,** 655–663
12. van Gent, D. C., Ramsden, D. A., and Gellert, M. (1996) *Cell* **85,** 107–113
13. Eastman, Q. M., Leu, T. M. J., and Schatz, D. G. (1996) *Nature* **380,** 85–88
14. Sawchuk, D. J., Weis-Garcia, F., Malik, S., Besmer, E., Bustin, M., Nussenzweig, M. C., and Cortes, P. (1997) *J. Exp. Med.* **185,** 2025–203
15. van Gent, D. C., McBlane, J. F., Ramsden, D. A., Sadofsky, M. J., Hesse, J. E., and Gellert, M. (1995) *Cell* **81,** 925–934
16. McBlane, J. F., van Gent, D. C., Ramsden, D. A., Romeo, C., Cuomo, C. A., Gellert, M., and Oettinger, M. A. (1995) *Cell* **83,** 387–395
17. van Gent, D. C., Mizuuchi, K., and Gellert, M. (1996) *Science* **271,** 1592–1594
18. Jackson, S. P, and Jeggo, P. A. (1995) *Trends Biochem Sci.* **20,** 412–415
19. Bogue, M., and Roth, D. B. (1996) *Curr. Opin. Immunol.* **8,** 175–180
20. Mombaerts, P., Iacomini, J., Johnson, R. S., Herrup, K., Tonegawa, S., and Papaioannou, V. E. (1992) *Cell* **68,** 869–877
21. Spanopoulou, E., Roman, C. J., Corcoran, L., Schlissel, M. S., Silver, D., Nemazee, D., Nussenzweig, M., Shinton, S. A., Hardy, R. R., and Baltimore, D. (1994) *Genes Dev.* **8,** 1030–1042
22. Shinkai, Y., Rathbun, G., Lam, K.-P., Oltz, E. M., Stewart, V., Medelsohn, M., Charron, J., Datta, M., Young, F., Stall, A. M., and Alt, F. W. (1992) *Cell* **68,** 855–867
23. Schwarz, K., Gauss, G. H., Ludwig, L., Pannicke, U., Li, Z., Linder, D., Friedrich, W., Seger, R. A., Hansen-Hagge, T. E., Desiderio, S., Lieber, M. R., and Bartram, C. R. (1996) *Science* **274,** 97–99
24. Bosma, M. J., and Carroll, A. M. (1991) *Annu. Rev. Immunol.* **9,** 323–350
25. Zhu, C., Bogue, M. A., Lim, D. S., Hasty, P., and Roth, D. B. (1996) *Cell* **86,** 379–390
26. Nussenzweig, A., Chen, C., da Costa Soares, V., Sanchez, M., Sokol, K., Nussenzweig, M. C., and Li, G. C. (1996) *Nature* **382,** 551–555
27. Gu, Y., Seidl, K. J., Rathbun, G. A., Zhu, C., Manis, J. P., van der Stoap, N, Davidson, L., Cheng, H. L., Sekiguchi, J. M., Frank, K., Stanhope-Baker, P., Schlissel, M. S., Roth, D. B., and Alt, F. W. (1997) *Immunity* **7,** 653–665
28. Quyang, H., Nussenzweig, A., Kurimasa, A., da Costa Soares, V., Li, X., Cordon-Cardo, C., Li, W., Cheong, G., Nussenzweig, M., Iliakis, G., Chen, D. J., and Li, G. C. (1997) *J. Exp. Med.* **186,** 921–929
29. Roth, D. B., Nakajima, P. B., Menetski, J. P., Bosma, M. J., and Gellert, M. (1992) *Cell* **69,** 41–53
30. Roth, D. B., Zhu, C., and Gellert, M. (1993) *Proc. Natl. Acad. Sci. U. S. A.* **90,** 10788–10792
31. Schlissel, M., Constantinescu, A., Morrow, T., Baxter, M., and Peng, A. (1993) *Genes Dev.* **7,** 2520–2532
32. Ramsden, D. A., and Gellert, M. (1995) *Genes Dev.* **9,** 2409–2420
33. Agrawal, A., and Schatz, D. G. (1997) *Cell* **89,** 43–53
34. Silver, D. P., Spanopoulou, E., Mulligan, R. C., and Baltimore, D. (1993) *Proc. Natl. Acad. Sci, U. S. A.* **90,** 6100–6104
35. Sadofsky, M. J., Hesse, J. E., McBlane, J. F., and Gellert, M. (1993) *Nucleic Acids Res.* **21,** 5644–5650
36. Sadofsky, M., Hesse, J. E., and Gellert, M. (1994) *Nucleic Acids Res.* **22,** 1805–1809
37. Cuomo, C. A., and Oettinger, M. A. (1994) *Nucleic Acids Res.* **22,** 1810–1814
38. Spanopoulou, E., Cortes, P., Huang, C., Shih, C., Silver, D., Svec, P., and Baltimore, D. (1995) *Immunity* **3,** 715–726
39. Leu, M. J., and Schatz, D. G. (1995) *Mol. Cell. Biol.* **15,** 5657–5670
40. Ramsden, D. A., McBlane, J. F, van Gent, D. C. and Gellert, M. (1996) *EMBO J.* **15,** 3197–3206
41. Cuomo, C. A., Mundy, C. L., and Oettinger, M. A. (1996) *Mol. Cell. Biol.* **16,** 5683–5690
42. Vipond, I. B., and Halford, S. E. (1995) *Biochemistry* **34,** 1113–1119
43. Mizuuchi, M., Baker, T. A., and Mizuuchi, K. (1992) *Cell* **70,** 303–311
44. Pecoraro, V. L., Hermes, J. D., and Cleland, W. W. (1984) *Biochemistry* **23,** 5262–5271
45. Dahm, S. C., and Uhlenbeck, O. C. (1991) *Biochemistry* **30,** 9464–9469
46. Herschlag, D., Piccirilli, J. A., and Cech, T. R. (1991) *Biochemistry* **30,** 4844–4854
47. Piccirilli, J. A., Vyle, J. S., Caruthers, M. H., and Cech, T. R. (1993) *Nature* **361,** 85–88
48. Eckstein, F. (1985) *Annu. Rev. Biochem.* **54,** 367–402
49. Hsu, M., and Berg, P. (1978) *Biochemistry* **17,** 131–138
50. Drelich, M., Wilhelm, R., and Mous, J. (1992) *Virology* **188,** 459–468
51. Engelman, A., and Craigie, R. (1995) *J. Virol.* **69,** 5908–5911
52. Junop, M. S., and Haniford, D. B. (1996) *EMBO J.* **15,** 2547–2555
53. Katzman, M., Katz, R. A., Skalka, A. M., and Leis, J. (1989) *J. Virol.* **63,** 5319–5327
54. Vermote, C. L. M., and Halford, S. E. (1992) *Biochemistry* **31,** 6082–6089
55. Junop, M. S., and Haniford, D. B. (1997) *EMBO J.* **16,** 2646–2655
56. Akamatsu, Y., Tsurushita, N., Nagawa, F., Matsuoka, M., Okazaki, K., Imai, M., and Sakano, H. (1994) *J. Immunol.* **153,** 4520–4529
57. Steen, S. B., Gomelsky, L., Speidel, S. L., and Roth, D. (1997) *EMBO J.* **16,** 2656–2664
58. Kirch, S. A., Sudarsanam, P., and Oettinger, M. A. (1996) *Eur. J. Immunol.* **26,** 886–891
59. Clark, K. L., Halay, E. D., Lai, E., and Burley, S. K. (1993) *Nature* **364,** 412–420
60. Jeltsch, A., Maschke, H., Selent, U., Wenz, C., Kohler, E., Connolly, B. A., Thorngood, H., and Pingoud, A. (1995) *Biochemistry* **34,** 6239–6246

[3] Villa, A., Santagata, S., Bozzi, F., Giliani, S., Frattini, A., Imberti, L., Benerini, L., Ochs, H., Schwarz, K., Notarangelo, L. D., Vezzoni, P., and Spanopoulou, E. (1998) *Cell*, in press.

Cell, Vol. 93, 885–896, May 29, 1998, Copyright ©1998 by Cell Press

Partial V(D)J Recombination Activity Leads to Omenn Syndrome

Anna Villa,[1] Sandro Santagata,[2] Fabio Bozzi,[1] Silvia Giliani,[3] Annalisa Frattini,[1] Luisa Imberti,[4] Luisa Benerini Gatta,[4] Hans D. Ochs,[5] Klaus Schwarz,[6] Luigi D. Notarangelo,[3] Paolo Vezzoni,[1,7] and Eugenia Spanopoulou[2]

[1]Department of Human Genome and Multifactorial Disease
Istituto di Tecnologie Biomediche Avanzate
Consiglio Nazionale delle Ricerche
via Fratelli Cervi 93
20090 Segrate (Milano)
Italy

[2]Howard Hughes Medical Institute
Ruttenberg Cancer Center
Mount Sinai School of Medicine
New York, New York 10029

[3]Department of Paediatrics
Spedali Civili
and University of Brescia
Brescia 25123
Italy

[4]Terzo Laboratorio Analisi
Spedali Civili
Brescia 25123
Italy

[5]Department of Pediatrics
University of Washington
School of Medicine
Seattle, Washington 98195

[6]Department of Transfusion Medicine
University of Ulm, D-89070
Germany

Summary

Genomic rearrangement of the antigen receptor loci is initiated by the two lymphoid-specific proteins Rag-1 and Rag-2. Null mutations in either of the two proteins abrogate initiation of V(D)J recombination and cause severe combined immunodeficiency with complete absence of mature B and T lymphocytes. We report here that patients with Omenn syndrome, a severe immunodeficiency characterized by the presence of activated, anergic, oligoclonal T cells, hypereosinophilia, and high IgE levels, bear missense mutations in either the *Rag-1* or *Rag-2* genes that result in partial activity of the two proteins. Two of the amino acid substitutions map within the Rag-1 homeodomain and decrease DNA binding activity, while three others lower the efficiency of Rag-1/Rag-2 interaction. These findings provide evidence to indicate that the immunodeficiency manifested in patients with Omenn syndrome arises from mutations that decrease the efficiency of V(D)J recombination.

[7]To whom correspondence should be addressed.

Introduction

Diversity of the immune repertoire is generated by somatic assembly of the antigen receptor variable gene segments, in a process termed V(D)J site-specific recombination (Tonegawa, 1983; reviewed by Lewis, 1994). This process is dependent on the activation of two key lymphoid-specific proteins, Rag-1 and Rag-2 (Schatz et al., 1989; Oettinger et al., 1990). Recombination is initiated by the specific binding of Rag-1/Rag-2 to the conserved recombination signal sequences (RSSs) that flank each variable coding element (McBlane et al., 1995; van Gent et al., 1995; Difilippantonio et al., 1996; Spanopoulou et al., 1996; Hiom and Gellert, 1997). Each RSS consists of a highly conserved heptamer (CACAGTG) element and a moderately conserved nonamer motif (ACAAAAACC) separated by a spacer of either 12 or 23 nucleotides (Ramsden et al., 1994). Binding to the nonamer element is mediated by a region of Rag-1 that shows distinct homology to the DNA-binding domain of Hin invertases and that of homeodomain (HD) proteins (Difilippantonio et al., 1996; Spanopoulou et al., 1996; Nagawa et al., 1998). Rag-2 alone has no obvious DNA binding activity (Difilippantonio et al., 1996; Spanopoulou et al., 1996; Hiom and Gellert, 1997).

Upon stable binding to the RSS, the Rag-1/Rag-2 complex cleaves the upper strand at the heptamer/coding sequence junction. The cleavage intermediates are a covalently sealed hairpin coding end and a 5′ phosphorylated blunt signal end (McBlane et al., 1995; van Gent et al., 1995). Following the generation of the two double-strand break (DSB) recombination intermediates by Rag-1/Rag-2, several ubiquitous DNA repair activities, including Ku70, Ku80, and DNA-PK are engaged to process the DSB ends (reviewed by Jackson and Jeggo, 1995; Bogue and Roth, 1996; Agrawal and Schatz, 1997). Additional activities such as XR-1 and ligase IV have been suggested to participate at later stages of V(D)J recombination (Grawunder et al., 1997), which finally leads to joining of the coding ends. Although the complete V(D)J reaction has yet to be reproduced with purified components, fully recombined products can be generated in vitro using Rag-1, Rag-2, and total cell extracts (Cortes et al., 1996; Leu et al., 1997; Ramsden et al., 1997; Weis-Garcia et al., 1997).

Rag-1 and Rag-2, as well as the ubiquitous DNA repair activities Ku70, Ku80, and DNA-PK, are all essential for V(D)J recombination. Disruption of Rag-1 or Rag-2 function blocks initiation of V(D)J recombination and leads to complete absence of mature B and T cells (Mombaerts et al., 1992; Shinkai et al., 1992). Ku70-, Ku80-, or DNA-PK-deficient cells fail to resolve the DSB intermediates generated by Rag-1/Rag-2 (Roth et al., 1992; Jackson and Jeggo, 1995; Bogue and Roth, 1996; Nussenzweig et al., 1996; Zhu et al., 1996; Bogue et al., 1997; Gu et al., 1997). Similarly, in humans, mutations that eliminate the recombination activity of Rag-1 or Rag-2 lead to severe combined immunodeficiency (SCID) due to the absence of antigen receptors (Schwarz et al., 1996).

Table 1. Analysis of OS Patients for Mutations in *Rag-1* or *Rag-2*

Patient	Gene	Nucleotide	Amino Acid Change	Domain
OS1	*Rag-2*	C1324G	C41W	HimA homology
		T2055G	M285R	topoII homology
OS2	*Rag-1*	G1794A	R561H	Rag-2 interaction
OS3	*Rag-1*	C1298T	R396C	Homeodomain, DNA binding
		A2847G	Y912C	Active core
OS4	*Rag-1*	G1299A	R396H	Homeodomain, DNA binding
		deletion 1723–1735		Truncated protein
OS5	*Rag-1*	deletion 368–369		No protein
		A1398G	D429G	Homeodomain, Homodimerization
OS6	*Rag-1*	C1298T	R396C	Homeodomain, DNA binding
OS7	*Rag-1*	C1793T	R561C	Rag-2 interaction
		G2322A	R737H	Active core

Omenn syndrome (OS) is a rare autosomal recessive genetic disorder characterized by symptoms of severe combined immunodeficiency associated with erythrodermia, eosinophilia, hepatosplenomegaly, lymphadenopathy, and elevated serum IgE levels (Omenn, 1965; OMIM 267700). Unless treated by bone marrow transplantation, this disease is invariably fatal (Gomez et al., 1995). At variance with other forms of SCID, OS patients have a variable number of circulating T cells that coexpress activation markers and respond poorly to mitogens and antigens. Previous studies have shown restricted heterogeneity of T cell receptor (TCR) rearrangements in patients with OS (de Saint-Basile et al., 1991; Harville et al., 1997). It has been suggested that the clinical and immunological features of OS could be related to an unbalanced expansion of the T helper 2 (Th2) cell subset as substantiated by increased production of interleukins 4 (IL-4) and 5 (IL-5), reduced synthesis of IL-2 and γ-interferon by in vitro activated lymphocytes (Schandené et al., 1993; Chilosi et al., 1996), and increased numbers of CD30-expressing cells, a surface marker preferentially expressed on Th2 cells (Chilosi et al., 1996). The underlying molecular defect remained unknown although similarities with the murine *scid* model have been described (Cavazzana-Calvo et al., 1993).

We report here the analysis of seven OS patients, all of whom were found to bear recessive mutations in either the *Rag-1* or *Rag-2* genes. All OS mutations lead to reduced V(D)J recombination activity and account for the immunodeficiency observed in OS patients. These findings establish V(D)J recombination deficiencies as the molecular basis of OS.

Results

Detection of Rag Mutations in OS Patients

We studied seven patients fulfilling the criteria for Omenn syndrome, i.e., early-onset generalized erythrodermia, hepatosplenomegaly, lymphadenopathy, hypoproteinemia associated with hypereosinophilia, elevated serum IgE, and presence of activated, anergic T cells. The immunological features of four of them have been previously reported (Chilosi et al., 1996; Brugnoni et al., 1997), while the other three are described in Experimental Procedures. The 7 OS patients were analyzed for mutations in either the *Rag-1* or *Rag-2* genes. The results obtained at the nucleotide level are summarized in Table 1. Six of the patients (OS2–OS7) were found to have an abnormality in the *Rag-1* gene. Two patients were homozygous for a missense mutation, one (OS2) for a G1794A mutation causing an R561H change, the other (OS6) for a C1298T transition leading to an R396C substitution. The four remaining patients were compound heterozygotes bearing missense mutations or deletions. Patient OS5 had a 2 nt deletion (nt 368–369) in the first allele leading to frameshift and premature translational termination and an A1398G transition causing a D429G substitution in the second allele. Patient OS4 had a deletion of 13 nucleotides (nt 1723–1735) in the first allele resulting in frameshift and premature termination and a G1299A transition affecting the same codon of patient OS6, but leading to a different amino acid substitution (R396H). Patient OS3 had two missense mutations, the first (R396C) is identical to the one found in patient OS6, while the second (A2847G) is found near the C terminus of Rag-1 (Y912C). Finally, patient OS7 also had two missense mutations, the first affecting a different nucleotide (C1793T) in the same codon as patient OS2 and causing an R561C change, the second a G2322A transition, which causes an R738H substitution.

Residues R396 and D429 are within the homeodomain region of Rag-1 (Figure 1A) (Spanopoulou et al., 1996). R396 represents the fifth residue of the pentapeptide that shows absolute identity between the Hin and Rag-1 DNA-binding domains and has been proposed to mediate binding of the protein to the nonamer motif of the RSS (Difilippantonio et al., 1996; Spanopoulou et al., 1996). D429 is located at the beginning of helix III of the Rag-1 homeodomain (Spanopoulou et al., 1996), while R561 is within the region of Rag-1 that mediates interaction with Rag-2 (McMahan et al., 1997) (Figure 1A). All three amino acids of Rag-1, R396, D429, and R561 have been conserved throughout evolution (Sadofsky et al., 1993).

The seventh patient (OS1) carried two missense mutations in the *Rag-2* gene, a C1324G transversion and a T2055G transversion, causing a C41W and an M285R substitution, respectively. Both mutations are within the Rag-2 active core (Sadofsky et al., 1994; Cuomo and Oettinger, 1994) and involve amino acids conserved in

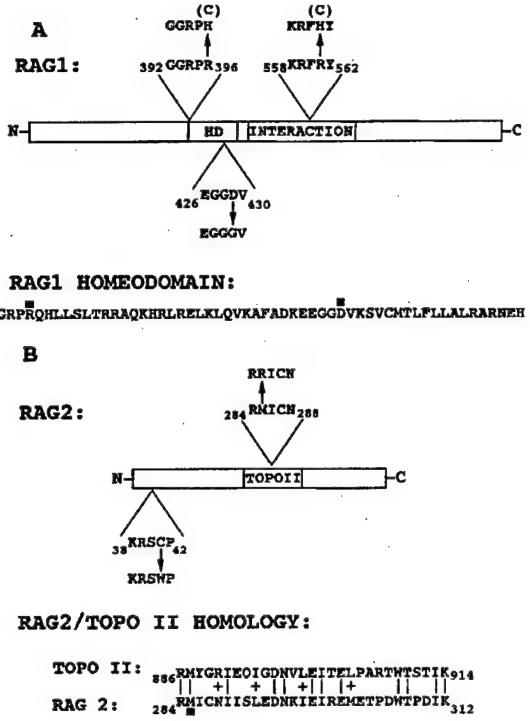

Figure 1. Localization of OS Missense Mutations within the Rag-1 and Rag-2 Proteins

(A) Mutations R396H, R396C, and D429G map within the homeodomain (HD) region of Rag-1 (Spanopoulou et al., 1996). Mutations R561H and R561C map within the Rag-1 domain of interaction with Rag-2 (McMahan et al., 1997).

(B) Rag-2 OS mutations C41W and M285R. The latter localizes within the topoisomerase II homologous region of Rag-2 (Silver, 1994).

all the Rag-2 proteins from mammals, birds, and fish (Sadofsky et al., 1994; Bernstein et al., 1996). M285 maps within a domain of Rag-2 demonstrating high homology to the nonspecific DNA-binding domain of topoisomerase II (Figure 1B) (Silver et al., 1993; Berger et al., 1996).

Mutations of patients OS1 through OS4, for whom parent DNA was available, were traced back to their parents. All parents were heterozygous for the *Rag* mutant alleles and had normal counts of B and T cells. The OS phenotype correlated with the presence of two mutant *Rag-1* or *Rag-2* alleles in their offspring. The possibility that the missense mutations represent rare polymorphisms was excluded by analysis of ethnically matched populations. Rag-1 A2847G and Rag-2 C1324G and T2055G point mutations were from Italian patients and, as they modify a restriction enzyme site, they were analyzed by RFLP analysis of amplified PCR products, in 260 chromosomes from Italian control individuals. The remaining missense mutations were found in Italian (G1794A, C1298T, G1299A), American (C1298T, C1793T, G2322A), and in one case in a Yugoslavian (A1398G) patient. We therefore sequenced 100 chromosomes from American controls; in addition, we performed SSCP analysis on 100 chromosomes from Italian controls. In no case were any of these mutations detected.

Analysis of the TCRβ Repertoire of OS Patients

All seven patients had variable yet detectable numbers of T cells. To investigate the effect of the OS mutations on V(D)J recombination, we determined the TCRβ (TCRB) repertoire. Our study included a global analysis of the variable β (TCRBV) usage and the characterization of TCRBV clonality of individual TCRBV segments, as described elsewhere (Bettinardi et al., 1992; Sottini et al., 1996; Imberti et al., 1997; see also Experimental Procedures). In the OS patients studied (OS1 through OS4), the recombination machinery was sufficiently functional to recombine most TCRBV segments. However, the usage of individual TCRBV segments in OS samples differed from that of unrelated healthy infants of the same ethnic origin with the four OS patients (i.e., Italian) (Figure 2, last panel). In addition, TCRBV rearrangements in OS patients showed restricted heterogeneity, as indicated by heteroduplex analysis of several TCRBV subfamilies prepared from patients OS1 to OS4 (Figure 2, first four panels).

To confirm further the restricted heterogeneity of the TCR repertoire in OS, we cloned and sequenced both the TCRBV segments dominantly expressed in OS (such as TCRBV6 in patient OS1, and TCRBV15 in patient OS4), as well as the least represented OS TCRBV segments (such as TCRBV1 segments) (Table 2). This analysis revealed a predominance of one or a few sequences within each of the TCRBV transcripts analyzed in OS patients (Table 2). In contrast, sequencing of 2 different TCRBV transcripts from a control infant demonstrated that 60 out of 61, and 63 out of 64 clones, respectively, were unique. Similar results were obtained with unfractionated lymphocytes from normal adults (Quirós Roldan et al., 1995). In addition, N nucleotides were present in all sequenced junctions suggesting that these patients do not have deficiencies in terminal deoxynucleotidyl transferase (TdT) activity (Table 2).

Functional Analysis of the OS Rag-1 and Rag-2 Mutations

To determine whether the identified Rag mutations in the OS patients can explain the partial immunodeficiency in OS, we tested the OS mutant Rag proteins for their ability to mediate Rag-1/Rag-2 interaction, specific binding of the complex to the RSS, their cleavage activity and, finally, their potential to mediate recombination of an extrachromosomal recombination substrate.

Effect of OS Mutations on the Rag-1/Rag-2 Interaction

Rag-1/Rag-2 interaction was assayed by coexpression of the wild-type or mutant proteins in 293T cells as previously described (Spanopoulou et al., 1995). Rag-1 OS mutations R396H, D429G, and R561H gst fusion proteins (gst-Rag-1) were transiently expressed along with influenza haemaglutinin (HA)-tagged wild-type Rag-2 (Flu-Rag-2) in 293T cells. Lysed cellular extracts were subjected to affinity precipitation using glutathione beads, and the purified complexes were analyzed by Western blot (Figure 3). Rag-1 homeodomain mutants R396H and D429G maintained efficient interaction with Rag-2, while interaction of Rag-1/R561H with Rag-2 was

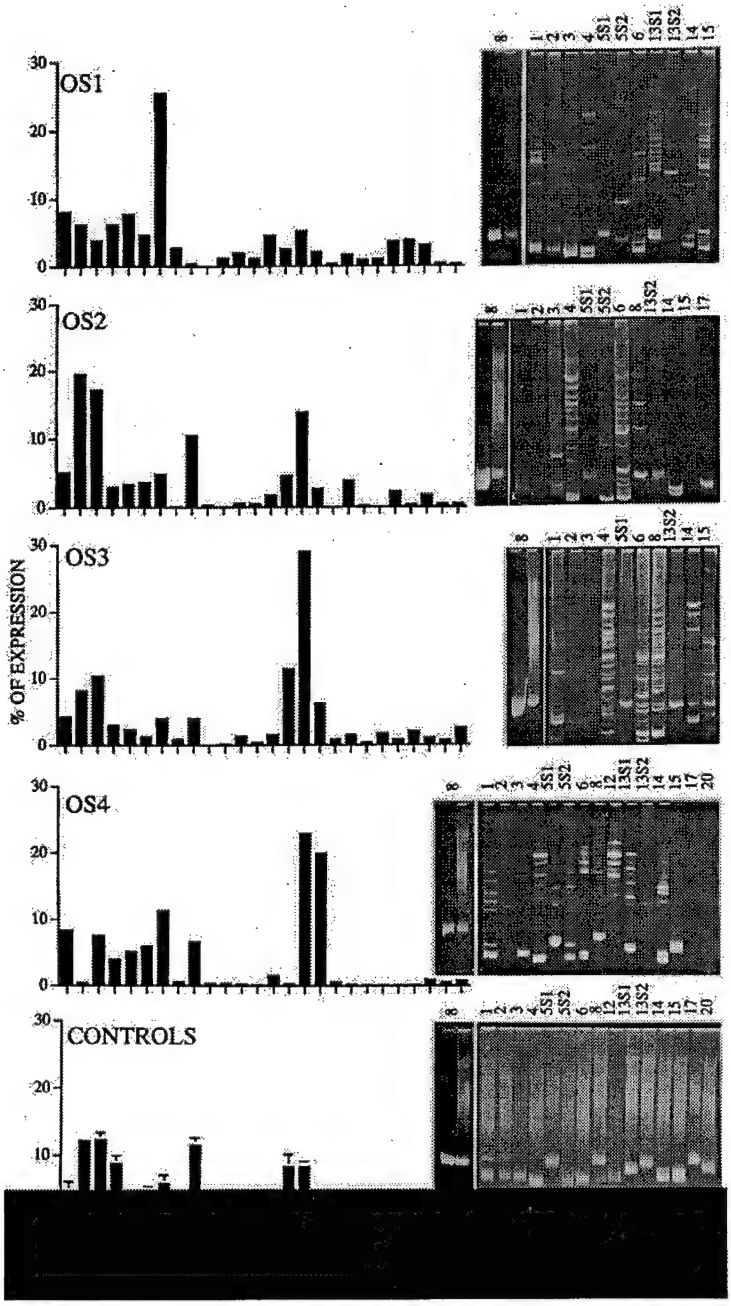

Figure 2. Analysis of the TCRB Repertoire of Total Lymphocytes from OS Patients

(Left) The 4 top graphs indicate the TCRBV usage of peripheral lymphocytes prepared from patients OS1–OS4, while the bottom one represents the mean and standard deviation obtained by analyzing lymphocytes prepared from four unrelated healthy children.

(Right) Heteroduplex analysis of the indicated TCRBV chains obtained by PCR performed with BV family-specific primers on lymphocytes prepared from four OS patients (four top pictures) and from a representative healthy child (bottom). TCRBV8 amplified products, prepared from monoclonal and polyclonal cell preparations, were used as controls and loaded into the first and second lines of each gel.

reduced to about 40% of the wild-type levels (Figure 3A). To test the efficiency of interaction of OS Rag-2 mutants C41W and M285R with Rag-1, gst-Rag-2 proteins were coexpressed with HA-tagged Rag-1 wild-type protein (Figure 3B). Both OS Rag-2 mutations showed reduced interaction with Rag-1 despite the fact that the two mutations are in different parts of the Rag-2 molecule. In all cases, the expression of each individual mutant protein was tested by Western blot analysis of the total cell extract, which revealed that all proteins were expressed at equal levels (Figures 3A and 3B, lower panels).

DNA Binding Activity of the OS Mutants

The effect of OS mutations on the binding of Rag-1/Rag-2 to the RSS was tested by electrophoretic mobility shift assays (EMSAs) (Hiom and Gellert, 1997) using purified recombinant proteins (Spanopoulou et al., 1996). Binding of wild-type Rag-1/Rag-2 to the RSS produces two complexes (Figure 4, lane 1) that both contain Rag-1 and Rag-2 (Santagata et al., 1998). The upper complex results from homodimerization of Rag-1, in part through its homeodomain region (V. Aidinis and E. S., unpublished data), while the lower complex represents the monomeric form of the Rag-1/Rag-2 heterodimer. Muta-

Table 2. Sequences of TCRB Transcript from Omenn Syndrome (OS) Patients

	TCRBV	N[a]	TCRBD[b]	N[a]	TCRBJ[d]		Frequency
OS4	TCRBV1						
	CTGTGCCA.....	CC	GGACAGGGGG	GAGGG	.....ACTGAAG	(1S1)	9/14
	CTGTGCCAGCAG.....	GTC	GACAGGG	AAAA	.....ATACGC	(2S3)	3/14
	CTGTGCCAGCAGCGTAG		GGAGG	ATAGC	.....GACCC	(2S5)	2/14
	TCRBV15						
	CTGTGCCACCAGTGATT..	CATACATCC	GGGACAGGG		.GCACAGATACGC	(2S3)	13/13
OS1	TCRBV1						
	CTGTGCCAGCA.....		GACAGGGG		.....AATTCACCCC	(1S6)	14/28
	CTGTGCCAGCAGCGTAG		GCG	TC	.....GAGACCC	(2S5)	3/28
	CTGTGCCAGCAGCGTAG		GGGG		.....CGAGC	(2S7)	1/28
	CTGTGCCAGCAGCGTAG		GGACTAG		...CTACGAGC	(2S7)	1/28
	CTGTGCCAGCAGCGTAG	A	AGGGGGC	C	..CCTACGAGC	(2S7)	6/28
	CTGTGCCAGCAGC....	CC	GGGG	AA	CTCCTACGAGC	(2S7)	1/28
	CTGTGCCAGCAGC....	CCGG	CAGGG	CCTG	..CCTACGAGC	(2S7)	1/28
	CTGTGCCAGCAGC....	CCCGCCGTAAG[c]			CTCCTACGAGC	(2S7)	1/28
	TCRBV6						
	CTGTGCCAGCA.....	CCCGATTGATC	GGGGC	CCCACAAGT	..CACAGATACGC	(2S3)	1/10
	CTGTGCCAGCAGCT....		GGACAGGGGG		...CTACGAGC	(2S7)	8/10
	CTGTGCCAGCAGCTTA..	ATTGG	TAGCG	AGGG	.....CGAGC	(2S7)	1/10

[a] A few of these nucleotides can be considered as P nucleotides.
[b] The underlined sequences pertain to D1, while the others are from D2.
[c] Two of these nucleotides could be derived from the D sequence.
[d] The specific J segments are indicated in parentheses.

tion R396H decreased the affinity of both complexes (Figure 4, lane 2). The second OS mutation in the Rag-1 homeodomain (D429G) produced a different result. This mutation had little effect on the binding of the lower Rag-1/Rag-2 complex to the RSS but it severely decreased formation of the upper complex (Figure 4, lane 3). Thus, D429G specifically disrupts Rag-1 homodimerization. The third Rag-1 mutation, R561H decreased binding of both the upper and the lower complexes (Figure 4, lane 4). The decreased DNA binding could be due to the lower efficiency of Rag-1 R561H/Rag-2 interaction (Figure 3A). Rag-2 mutants C41W and M285R gave no detectable DNA binding activity (Figure 4, lanes 5 and 6), which could be partly accounted for by their low efficiency of interaction with Rag-1 (Figure 3).

Effect of OS Mutations on the Rag-1/Rag-2 Cleavage Activity

The cleavage activity of the Rag-1 and Rag-2 OS mutants was tested by incubation of purified recombinant Rag proteins with a 12RSS substrate labeled at the 5′ end of the top strand. Conditions for the in vitro cleavage reactions were similar to the DNA binding conditions described by Hiom and Gellert (1997) (see Experimental Procedures and Santagata et al., 1998). The nicking activity of all Rag-1 and Rag-2 OS mutants was directly proportional to their DNA binding activity (compare Figures 4 and 5), while hairpin formation followed a slower rate. Rag-1 R396H had cleavage activity at about 30% of that of the wild-type protein (Figure 5A, lanes 2 and 6) (similar activity was observed for DNA binding, see Figure 3). Rag-1 D429G shows approximately 30% of the wild-type activity (Figure 5A, lanes 3 and 7), while R561H retains only 10% of the wild-type activity (Figure 5A, lanes 4 and 8). OS mutations C41W and M285R in Rag-2 showed no obvious cleavage in accordance with their diminished DNA binding activity (Figure 5B).

Recombination Activity of OS Mutants on Extrachromosomal Substrates

To test the ability of OS mutants to mediate recombination of an extrachromosomal substrate in vivo. Rag-1, Rag-2, and the recombination substrates pJH200 (deletional) and pJH288 (inversional) (Lieber et al., 1988) were cotransfected in NIH 3T3 cells. Recombination products were determined either by PCR analysis (Roman and Baltimore 1996; Spanopoulou et al., 1996) or by $Cam^R.Amp^R$ versus Amp^R (Table 3). OS mutations within the Rag-1 homeodomain drastically reduced the ability of the mutant proteins to mediate recombination of the two substrates (Figure 6, lanes 3 and 4; Table 3). R396H produced only 5%–10% of the wild-type recombination activity whereas D429G impaired recombination on the pJH288 substrate and produced 20% of the wild-type activity on the pJH200 substrate (Figure 6A, lanes 3 and 4; Table 3). The Rag-1 R561H OS mutation that decreases efficiency of Rag-1/Rag-2 interaction reduced overall recombination efficiency to approximately 1/3 of that of the wild-type protein (Figure 6A lane 5; Table 3). All three OS Rag-1 mutations exhibited a similar phenotype when analyzed either in the context of the active core or as full-length proteins, for in vivo recombination (data not shown).

The two OS mutations in Rag-2 showed a differential phenotype. C41W showed diminished recombination activity (Figure 6B, lane 8), in accordance with its DNA binding and cleavage activities (see Figures 4 and 5). However, M285R was able to mediate recombination of the two recombination substrates at 15%–20% of the wild-type levels (Figure 6B, lane 9). Overall, all OS mutant proteins exhibited lower recombination efficiency in mediating inversion of the pJH288 substrate than deletion of the pJH200 substrate (Figure 6). An aliquot of the cells used for the recombination assays was lysed and probed by Western analysis for expression of the various recombinant Rag proteins (Figure 6, lower panel).

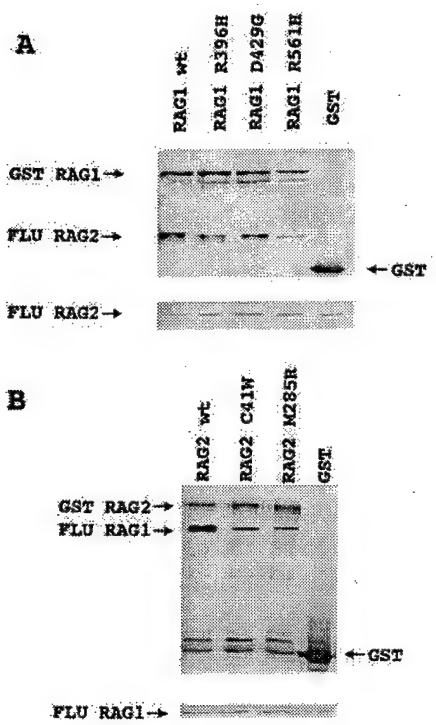

Figure 3. Effect of OS Mutations on the Rag-1/Rag-2 Interaction

Wild-type or mutant proteins were transiently expressed in 293T cells and interaction was evaluated by coprecipitation assays.

(A) Rag-1 OS mutants R396H, D429G and R561H were expressed as gst fusion proteins in the context of the human Rag-1 protein active core (aa 333–1043). Recombinant Rag-1 proteins were coexpressed with HA-tagged Rag-2 active core (aa 1–388).

(B) Rag-2 OS mutants C41W and M285R were expressed as gst fusion proteins in the context of full-length human Rag-2. Recombinant proteins were coexpressed with HA-tagged Rag-1 active core. The lower panels represent Western analysis of the total cell lysates to detect the levels of expression of each recombinant protein.

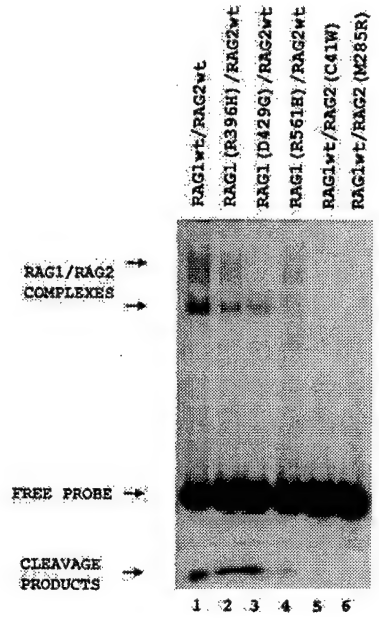

Figure 4. DNA Binding Profile of OS Mutant Rag-1 and Rag-2 Proteins

Purified proteins were incubated with ^{32}P-labeled oligonucleotide containing the 12RSS heptamer-nonamer motifs; ternary complexes were cross-linked with glutaraldehyde and resolved by EMSA as previously described (Hiom and Gellert, 1997). Cleavage products can be visualized at the bottom of the gel.

Discussion

We present evidence that a defect in the *Rag-1* and *Rag-2* genes is responsible for Omenn syndrome, a severe combined immunodeficiency with substantial numbers of activated, oligoclonal T cells. This finding is surprising because previously described Rag mutations led to a complete absence of mature B and T cells, as manifested by the SCID phenotype in both humans and mice (Mombaerts et al., 1992; Shinkai et al., 1992; Schwarz et al., 1996). Three factors demonstrate the link between mutations in the Rag genes and the appearance of the OS phenotype. First, appearance of the OS immunodeficiency correlates with mutations on both *Rag-1* or *Rag-2* chromosomal alleles. Second, analysis of more than 400 chromosomes from healthy individuals, ethnically matched to the OS patients, showed that these mutations do not represent polymorphisms in the general population. Third, all Rag mutations detected in OS patients drastically reduce V(D)J recombination as judged by in vitro and in vivo assays. From the genetic and biochemical data reported in this paper, it can be concluded that the defect in Omenn syndrome is caused by mutations in the *Rag-1* and *Rag-2* genes that confer partial activity and allow only a low degree of V(D)J recombination to occur.

Genotype of OS

Five of the OS missense alleles affect either the 396 or 561 Rag-1 codons, but in four of the cases different nucleotides are involved. This finding, together with the fact that the two patients with the same C1298T transition are of different ethnic origin (OS6 is English-American, while OS3 is Italian), suggests that the mutated codons could represent a hot spot for mutations. An alternative explanation, however, would be that only a limited number of residues in the Rag genes can be altered in order to maintain the partial recombinase activity necessary for the OS phenotype. Previous analyses of B^-T^- SCID patients have shown that the complete lack of mature B and T cells in those patients resulted from either truncations of the Rag genes or missense mutations in the active core of the two proteins that eliminated Rag function (Schwarz et al., 1996). In contrast, the OS mutant Rag proteins retain part of their activity, which appears to account for the recombination events present in the T cells of these patients. The issue then arises as to what level of Rag activity is required for the establishment of a functional immune system. The fact that the parents that are heterozygotes for *Rag-1* deletions 1723–1735 and 368–369 represent healthy individuals with normal counts of B and T cells, suggests that expression of only one allele is sufficient

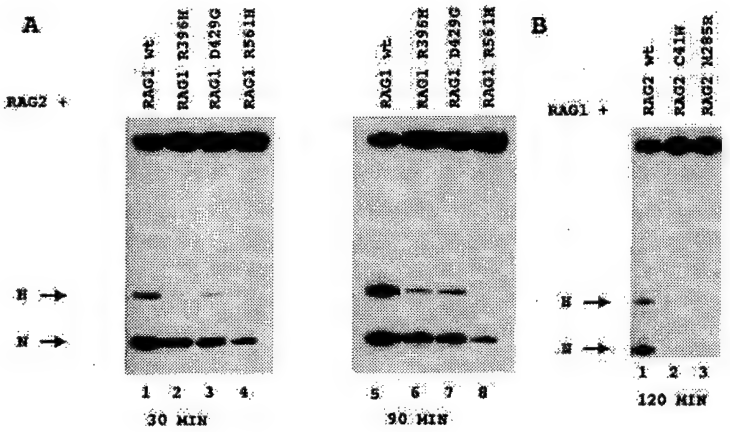

Figure 5. Cleavage Activity of OS Mutant Rag-1 and Rag-2 Proteins

Purified proteins were incubated with the 12RSS substrate labeled on the upper strand, and cleavage products, nicked intermediates, and covalently sealed hairpins were resolved on a denaturing polyacrylamide gel.

for normal V(D)J recombination and immunocompetence. In addition, none of the OS missense mutations have a dominant negative effect since the heterozygous parents have a normal immune system.

OS Mutations that Affect Rag-1/Rag-2 Interaction

Three of the OS mutations, Rag-1 R561H, Rag-2 C41W, and Rag-2 M285R, have a significant effect on the Rag-1/Rag-2 interaction. R561H is within a region of Rag-1 that mediates interaction with Rag-2 (McMahan et al., 1997) and decreases efficiency of interaction by ~80%. Mutations that affect the Rag-1/Rag-2 association might have a more dramatic effect during recombination in lymphocytes than when assayed in the in vitro or fibroblast assays. In lymphocytes, endogenous Rag-1 and Rag-2 are present in limiting amounts, and efficiency of Rag-1/Rag-2 interaction is critical for V(D)J recombination to occur. In contrast, both the in vitro and fibroblast assays are conducted in the presence of high levels of Rag-1 and Rag-2 augmenting the efficiency of their interaction. It is therefore possible that the effect of Rag-1 R561 in lymphocytes is far more pronounced than in the in vitro assays.

OS mutation C41W in Rag-2 provides a radical change by the substitution of a Cys residue with Trp. This mutation shows diminished DNA binding and cleavage activity that might result from a global change of the tertiary structure of the protein. The other OS Rag-2 mutation, M285R, maps within a region of Rag-2 that shows distinct homology to the nonspecific DNA-binding domain of topoisomerase II (Silver, 1994; Berger et al., 1996). The function of this topo II homologous domain of Rag-2 remains to be defined. M285R follows the pattern of C41W in that it interacts with Rag-1 with lower efficiency and has almost undetectable DNA binding and cleavage activity in vitro. However, in vivo the protein retained about 20% of the wild-type activity. This enhanced in vivo activity might be conferred by conformational changes through the interaction with other cellular proteins.

OS Mutations within the Rag-1 Homeodomain

Three of the seven OS patients characterized in this study carried a missense mutation at position R396. R396 is at the N terminal of the Rag-1 homeodomain within the region of Rag-1 (GGRPR, aa 392–396) that shows absolute homology to the DNA-binding domain of the Hin invertase (Difilippantonio et al., 1996; Spanopoulou et al., 1996). We have previously shown that the equivalent positions in mouse Rag-1 are important for binding of the protein to the nonamer motif (Spanopoulou et al., 1996). Mutation of R396 in the human gene reduces binding of the protein to the RSS, while it has no effect on the Rag-1/Rag-2 interaction. Given the effect of this mutation on the repertoire of the OS patients the

Table 3. In Vivo Recombination Activity of OS Mutants

Amino Acid Mutation	PCR Relative Recomb.		pJH288		
	pJH288	pJH200	$Cam^R.Amp^R/Amp^R$	Efficiency	Relative Recomb.
Rag-1 WT	100%	100%	232/26,710	0.86%	100%
Rag-1 R396H	5%	10%	39/28,230	0.14%	16%
Rag-1 #396C	NA	NA	NA	—	—
Rag-1 D429G	5%	20%	18/25,370	0.07%	8%
Rag-1 R561H	23%	34%	63/27,300	0.23%	27%
Rag-1 R561C	NA	NA	NA	—	—
Rag-1 R737H	8%	16%	15/29,840	0.05%	6%
Rag-1 Y912C	NA	NA	NA	—	—
Rag-2 C41W	4%	10%	12/19,740	0.06%	7%
Rag-2 M285R	15%	30%	46/25,680	0.18%	22%

Values represent the average of five independent experiments analyzed by PCR and two analyzed by bacterial transformation. Statistical variation for recombination efficiency by bacterial transformation ranged from 0.01–0.03% depending on the sample.
NA; not analyzed.

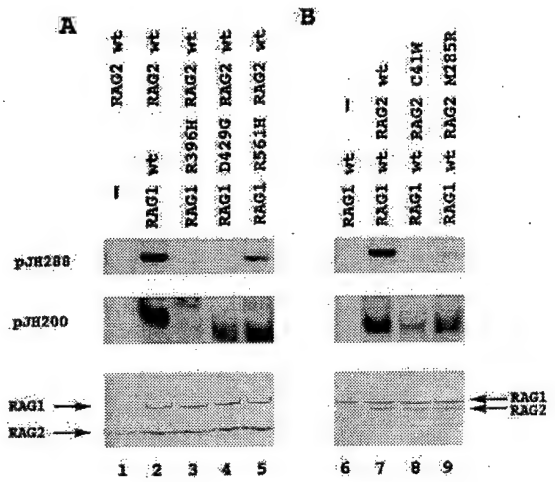

Figure 6. Effect of OS Mutations on V(D)J Recombination Activity

(A) OS human Rag-1 mutants were expressed in the context of the active core protein. Human Rag-2 mutants were expressed as full length form. OS mutant Rag-1 or Rag-2 were expressed from the peBG cassette (Spanopoulou et al., 1996). Plasmids expressing the recombinant proteins were cotransfected along with the recombination substrates pJH200 or pJH288 (Lieber et al., 1988) in NIH 3T3 cells, and 48 hr later recombination products were isolated. Recombination efficiency was detected by PCR analysis using primers that detect the recombined sequences (Roman and Baltimore, 1996). To control for transfection efficiency and production of the recombinant proteins, an aliquot of the cell lysate was analyzed by Western analysis for the expression of the recombinant proteins (bottom panel) detected with an anti-gst antibody.

question becomes whether low-affinity binding of Rag-1 mutants to the nonamer motif might drive preferential recombination of certain nonamer elements and/or heptamer-only dependent rearrangement. The availability of an animal model for the Rag-1 R396 mutation would provide a tool to analyze the repertoire generated by such a mutation and the role of the Rag-1 homeodomain in vivo.

Mutation OS Rag-1/D429G Affects Rag-1 Homodimerization

The other OS mutation within the Rag-1 homeodomain, D429G, maps to the first residue of the putative homeodomain helix III (Spanopoulou et al., 1996). The mutation specifically eliminates formation of the upper Rag-1/Rag-2 complex, which is partly mediated by homodimerization of the homeodomain (V. Aidinis and E. S., unpublished data). Therefore, D429 contributes to Rag-1 homodimerization, which might be crucial for synaptic complex formation. Homodimerization of homeodomain regions has been documented for the *Paired* class of homeodomains. The crystal structure of the *Paired* homeodomain has shown that dimer formation is mediated by a set of amino acids in the interphase of two domains that includes an acidic amino acid, Glu-42, present at the first position of recognition helix III (Wilson et al., 1995). Asp-429 of the Rag-1 homeodomain is present at the equivalent position with Glu-42. In this context, it is interesting to note that mutation of the first residue, E80A, in the recognition helix III of the CRX homeodomain also leads to disease. CRX is a photoreceptor-specific transcription factor that belongs to the *Paired* class of homedomains. Mutation of Glu-80 to Ala leads to cone-rod dystrophy in humans (Freund et al., 1997).

Phenotype of OS

A major question that remains to be answered is why partial V(D)J recombination activity leads to the OS phenotype. OS immunodeficiency is characterized by an overrepresentation of Th2-type cells (as judged by increased secretion of IL-4, IL-5, and IL-10), elevated serum IgE, and eosinophilia (Schandené et al., 1993; Chilosi et al., 1996; Brugnoni et al., 1997). The genetic defect in OS allows productive rearrangement of multiple TCRBV segments, yet the TCR repertoire in peripheral blood T cells is mostly oligoclonal. Selective expansion of TCR clones may be a consequence of either intrathymic selection of specific rearrangements or peripheral expansion in response to infections, or both. In addition, it is possible that mutations in the nonamer DNA-binding domain of Rag-1 could lead to preferential recombination of certain TCRBV segments. Skewing toward Th2 might be the result rather than the cause of the OS phenotype. As observed in other cases, immunedeficient individuals have, by definition, an increased antigen exposure and a defect in antigen clearance that results in persistent high antigen load. If, as in OS, the genetic defect is permissive and allows the development of limited clones of mature T cells, the antigen overload favors prolonged T cell activation that has been associated with increased IL-4 secretion and polarization toward a Th2 phenotype (Hsieh et al., 1993; Hosken et al., 1995).

The high IgE levels and eosinophilia observed in OS patients can be a direct response to the selective expansion of Th2 clones. In several mouse models high levels of IgE production have been associated with the expansion of the NK1.1, IL-4 producing, Th2 cells (Yoshimoto et al., 1995; Bendelac et al., 1996). In addition, elevated serum IgE has been associated with the absence of the TCR$\alpha\beta$ lineage in TCRα-deficient mice (Wen et al., 1994). In all of the above cases, as in OS, there is an imbalance in the T–B network of interactions due to the preferential expansion of certain T cell subsets with consequent altered secretion of particular cytokines and Ig isotypes. This imbalance must be characteristic of only some lymphoid abnormalities. Other immunodeficient organisms, such as the V(D)J recombination-deficient SCID mouse that has low levels of T cells or genetically engineered mice with low numbers of B cells (such as the $\lambda 5^{-/-}$ mice), do not manifest a Th2 phenotype or high levels of IgE. Definitive answers on the pathogenesis of OS will come from the establishment of animal models for the different OS mutations.

V(D)J Recombination Activity in Omenn Syndrome

The data present in this study show that the immunodeficiency in OS arises from missense mutations in the Rag proteins that confer partial V(D)J recombination activity. All of the OS patients (7/7) analyzed in this study carried mutations in the Rag genes that can account for the

"leakiness" of the OS phenotype. However, it is possible that certain mutations in the ubiquitous components of the V(D)J recombination machinery could also lead to an Omenn-like phenotype. For example, in light of the findings that *Ku70*$^{-/-}$ mice have low levels of T cells and develop T cell lymphomas (Gu et al., 1997), it is conceivable that a partial Ku70 function could produce an OS phenotype associated with T cell lymphomas (Mache et al., 1994). V(D)J recombination deficiencies that lead to low-to-normal numbers of T cells in the absence of mature B cells are a recurring theme. When the differentiation defect in *Rag*$^{-/-}$ or SCID mice is rescued by genetic manipulation such as p53 or poly(ADP-ribose) polymerase (PARP) inactivation or by damaging agents, the T cell, but not the B cell compartment, is restored (Danska et al., 1994; Guidos et al., 1995, 1996; Bogue and Roth, 1996; Livak et al., 1996; Nacht et al., 1996; Morrison et al., 1997). The mechanisms underlying these differences between B and T cell development remain to be defined. The elucidation of the molecular basis of the defect in Omenn syndrome will permit the investigation of these mechanisms as well as the clinical features of the disease.

Experimental Procedures

Patients

We studied seven patients with typical signs of OS. The immunological features of four patients have been previously reported. Patient OS1 corresponds to G. M. in Chilosi et al., 1996. Patients OS2, OS3, and OS4 correspond to R. C., C. A., and C.N., respectively, in Brugnoni et al., 1997. Patient OS5, the female child of non consanguineous parents, developed generalized erythrodermia in the neonatal period and chronic diarrhea and failure to thrive at two months of age. At that time, eosinophilia (2024 cells/mm3) and increased serum IgE (500 U/ml) were manifested. Lymphocyte subpopulations (%) were as follows: CD3 = 11, CD19 < 1, CD16 = 57. Virtually all $CD3^+$ cells coexpressed CD45R0, a marker for primed T cells, and 93% of them were also DR^+. In vitro lymphocyte proliferative responses to phytohemagglutinin (PHA) and anti-CD3 monoclonal antibody were abolished. Patient OS6 had eosinophilia (1400/mm^3), normal numbers of peripheral blood lymphocytes (2,750/mm^3), the majority (88%) being $CD16^+$ NK cells, with severely reduced $CD3^+$ cells (4%), and absence of B cells. Virtually all circulating T lymphocytes coexpressed the DR activation antigen. In vitro lymphocyte proliferation to PHA was abolished.

Patient OS7 developed generalized erythrodermia associated with lymphoadenopathy at 3 weeks of age and, subsequently, presented with diarrhea, failure to thrive, splenomegaly, pneumonia, anemia, thrombocytopenia, and eosinophilia (5,200 cells/mm^3). She had elevated serum IgE (800 U/ml at 3 months of age and 45,000 U/ml at 5 months) and an increased lymphocyte count (5,000–13,000/mm^3), with 54% $CD3^+$ T cells, most of which (74%) coexpressed the DR antigen, and 2% B cells. The in vitro proliferative response to PHA was markedly reduced. Patients OS5 and OS7 have died after unsuccessful bone marrow transplantation, and sepsis, respectively. All other patients have been cured by bone marrow transplantation. In all patients, the autologous origin of T lymphocytes (to rule out maternal T cell engraftment) was demonstrated by HLA typing and by molecular analysis with highly polymorphic markers (D1S80, APOB).

Strategy for Mutation Identification in the *Rag-1* and *Rag-2* Genes

Rag-1 and *Rag-2* coding sequences were amplified from genomic DNA. All the patient DNAs were obtained before bone marrow transplantation. DNAs were obtained also from the parents of OS1, OS2, OS3, and OS4 patients. Primers were designed for the amplification of the Rag genes based on the sequences reported in databases (*Rag-1*: a.n. M29474; *Rag-2*: a.n. M94633). *Rag-1* gene was amplified in two segments (94–1852 and 1781–3262) and *Rag-2* in one segment (1201–2922). Sequencing was performed directly on the PCR products purified from the gel with the Thermosequenase kit (Amersham, U. K.). Mutations were confirmed by analysis of several clones from PCR amplification products cloned in TA vector (Invitrogen) and sequenced by the dideoxynucleotide chain termination method using the Sequenase kit (USB), as previously described (Macchi et al., 1995). For the analysis of restriction enzyme sites eliminated or created by the mutations, the pertinent PCR products were digested with the appropriate enzyme according to the suggestions of the manufacturer. Single-stranded chain polymorphism (SSCP) was performed on small PCR products amplified with pertinent primers and run according to standard methods.

Analysis of TCRB Repertoire

Total cytoplasmic RNA and cDNA were prepared from peripheral blood lymphocytes as previously described (Bettinardi et al., 1992), and the cDNA was subjected to enzymatic amplification using a TCRBC primer (βAI: 5′ CCC ACT GTG CAC CTC CTT CC 3′) and a TCRBV degenerated primer: Vβd: 5′ ACG TGA ATT CT(GT) T(ACT) (CT) TGG TA(CT) (AC)(AG)(AT) CA 3′. This amplification generates a product of about 360 bp, which contains one-half of the V region gene and extends through the VDJ junctions until the first 165 bp of the C region. The 40 cycles of PCR were carried out by combining 1 μl of cDNA in 100 μl of reaction volume containing 2.5 U of Taq polymerase, dNTP at the final concentration of 250 μM each and 150 pmol of the Vβd primer and 50 pmol of the βAI primer in a buffer prepared with 67 mM Tris-HCl (pH 8.8), 16.6 mM $(NH_4)_2SO_4$, 10 mM β-mercaptoethanol, 2 mM $MgCl_2$, and 100 μg/ml of BSA. The PCR conditions were as previously described (Imberti et al., 1997).

The specificity of the total amplified products was analyzed using a colorimetric method (Bettinardi et al., 1992) and biotinylated TCRBV-specific probes. The relative percentage of expression of each individual TCRBV segment was calculated by dividing the single TCRBV signals by the sum of the signals for all TCRBV families and multiplying by 100. Subsequently, the TCRBV of interest were individually amplified by 35 cycles of PCR, using TCRBV-specific oligonucleotides and the βAI TCRBC primer, and subjected to heteroduplex analysis as previously described (Sottini et al., 1996). Samples were denaturated at 95°C for 5 min and then kept at 50°C, a temperature that is permissive for the annealing between either homologous (homoduplex) or heterologous DNA strands, which have the same TCRBV family but differ for the N and the TCRBJ regions (heteroduplex). The annealed samples were run on a 12% acrylamide gel, and the gels were stained with ethidium bromide and photographed under UV light. Amplified TRCBV8 products from the T cell line J77 and from lymphocytes stimulated with an anti-TCRBV8 monoclonal antibody were used as monoclonal and polyclonal controls, respectively (Sottini et al., 1996). Specific PCR products of interest were purified, cloned, and sequenced as described (Sottini et al., 1996). The sequences were compared with published data relative to TCRBV, TCRBD, TCRBJ, and TCRBC segments (Arden et al., 1995).

Constructs

PCR products containing the mutations found in OS patients were cloned in TA vector and sequenced. Subsequently, PCR products were cloned in pEBG according to the general strategy of substituting restriction fragments cut with pertinent enzymes to the wild-type genes cloned in this vector. For protein expression, aa 330–1044 of human Rag-1 (Rag-1 active core; Sadofsky et al., 1993; Silver et al., 1993) and aa 1–527 of human Rag-2 or the corresponding fragments from the mutant proteins were subcloned into the mammalian expression vector pEBG, which provides the coding sequences for the glutathione transferase gene (*gst*) (Spanopoulou et al., 1995).

Protein Expression and Purification

Gst-fusion recombinant forms of the human Rag-1 and Rag-2 proteins were overexpressed in 293T cells and purified as previously described (Spanopoulou et al., 1996). Proteins were dialyzed in cleavage buffer and quantified by Coomassie blue staining following SDS–PAGE.

In Vitro Cleavage Reactions

Standard reaction conditions were modifications of previously published protocols (McBlane et al., 1995; Hiom and Gellert, 1997; Santagata et al., 1998). Fifty nanograms of each protein, Rag-1 and Rag-2, was incubated with 0.01–0.05 pmol of ^{32}P end-labeled cleavage substrate in 25 mM MOPS-KOH (pH 7.0), 5 mM Tris-HCl (pH 8.0), 120 mM KOAc, 18 mM KCl, 10% dimethyl sulfoxide (DMSO), 2.2 mM DTT, 1mM Mg^{2+}, 0.5 mM nonspecific single-stranded DNA with 50 ng of each protein and 0.01–0.05 pmol of ^{32}P end-labeled probe in a final volume of 20 μl. Reactions were stopped by the addition of 0.1% SDS and loading buffer. Samples were analyzed on 16% polyacrylamide denaturing gels. The upper strand sequence of 12RSS cleavage substrate is: 5′-ACGCGTCGACGTCTACACAG TGATAAGCCCTGAACAAAAACCGGATCCGCG-3′. Standard cleavage reactions employed ^{32}P 5′ end-labeled upper strand annealed to the unlabeled, complementary lower strand oligonucleotide.

Electrophoretic Mobility Shift Assays

Conditions were based on the previously published protocol (Hiom and Gellert, 1997). Fifty nanograms of each protein was incubated for 10 min at 30°C with 0.01–0.05 pmol of 5′ end-labeled probe in 25 mM MOPS-HCl (pH 7.0), 1 mM $MgCl_2$, 2.2 mM DTT, 1 μg of bovine serum albumin (BSA), 0.5 μM of nonspecific primer (5′-CCTC GAGCTCA TCAGCTTGCCTGTGGGCAGCTCGATCTCTTTGTCG-3′), 20% DMSO, and 120 mM potassium acetate. Cross-linking was achieved by glutaraldehyde (final concentration 0.1% v/v) treatment for 10 min at 30°C. Complexes were resolved on a 4% native polyacrylamide gel.

Rag-1/Rag-2 Protein Interaction Assays

Recombinant proteins, human gst-Rag-1 wild type or OS mutants and mouse influenza HA-tagged Rag-2 (Flu-Rag-2) or mouse HA-tagged active core Rag-1 (Flu-Rag-1) and human gst-Rag-2, were transiently transfected in 293T cells and after 48 hr their interaction potential was assessed by coprecipitation assays as previously described (Spanopoulou et al., 1995).

In Vivo Recombination Assays

Mutant proteins were tested for their recombination activity in NIH 3T3 cells. Human Rag-1 active core (aa 330–1043) was cotransfected with mouse wild-type Rag-2 active core (aa 1–388) whereas human full-length Rag-2 proteins were cotransfected with mouse Rag-1 active core (aa 330–1040). Recombinant constructs were expressed in NIH 3T3 cells along with the recombination substrates pJH288 or pJH200 (Lieber et al., 1988). Cells were transfected by calcium phosphate precipitation and harvested 48 hr later. Recombined products were isolated as described previously (Oettinger et al., 1990) and analyzed for recombination frequency by PCR analysis (Roman and Baltimore, 1996). To ensure that the PCR assays follow a quantitative pattern, reactions were allowed to proceed for 25 cycles and controlled by limited dilutions (1/2, 1/10, 1/100, 1/1000) of a recombined pJH288 plasmid DNA. Oligonucleotides detect the recombined products by annealing to the joined heptamer signal sequences (oligo-RA5) and to the *CAT* gene (oligo-RA14) (RA5: 5′-CCAGTCTGTAGCACTGTGCAC-3′ and RA14: 5′-TCCAGCTGAA CGGTCTGGT-3′). The reactions incorporated [^{32}P]dCTP. Reaction products were analyzed on a 5% polyacrylamide gel and visualized by autoradiography. Relative recombination activity was estimated by phosphoimaging (Biorad). Alternatively, efficiency of recombination was estimated by transformation of the recovered plasmid DNA into electrocompetent MC1061 bacteria (Biorad) and analysis of the CamR/AmpR versus AmpR ratio (Lieber et al., 1988).

Acknowledgments

We are grateful to Prof. R. Dulbecco and Prof. L. Rossi Bernardi for their encouragement. We thank Prof. A. Ugazio and Drs. F. Facchetti, D. Brugnoni, R. Medzhitov, A. Hodtsev, and V. Aidinis for useful comments. The technical assistance of Dario Strina and typing of the manuscript by S. Bevan is thankfully acknowledged. This work was supported by NIH grant AI40191 to E. S. and HD17427 to H. D. O., and DOA/DOD Breast Cancer Predoctoral Training Program grant DAMD17-94-J-4111 to S. S. Partially supported by grants from Telethon, Italy (no. E.495 to A. V. and no. E.668 to L. D. N.) and MURST (to L. D. N.). E. S. is a Cancer Research Institute Clinical Investigator and Howard Hughes Medical Institute Assistant Investigator. This work is manuscript no. 19 of the Genoma 2000/ITBA Project funded by CARIPLO.

Received January 26, 1998; revised April 24, 1998.

References

Agrawal, A., and Schatz, D.G. (1997). RAG-1 and RAG-2 form a stable postcleavage complex with DNA containing signal ends in V(D)J recombination. Cell *89*, 43–53.

Arden, B., Clark, S.P., Kabelitz, D., and Mak, T.W. (1995). Human T-cell receptor variable gene segment families. Immunogenetics *42*, 455–500.

Bendelac, A., Hunziker, R.D., and Lantz, O. (1996). Increased interleukin-4 and immunoglobulin E production in transgenic mice overexpressing NK1 T cells. J. Exp. Med. *184*, 1285–1293.

Berger, J.M., Gamblin, S.J., Harrison S.C., and Wang, J.C. (1996). Structure and mechanism of DNA topoisomerase II. Nature *379*, 225–232.

Bernstein, R.M., Schluter, S.F., Bernstein, H., and Marchalonis, J.J. (1996). Primordial emergence of the recombination activating gene 1 (RAG-1): sequence of the complete shark gene indicates homology to microbial integrases. Proc. Natl. Acad. Sci. USA *93*, 9454–9459.

Bettinardi, A., Imberti, L., Sottini, A., Primi, D. (1992). Analysis of amplified T cell receptor VB transcripts by a non-isotopic immunoassay. J. Immunol. Methods *146*, 71–80.

Bogue, M., and Roth, D.B. (1996). Mechanism of V(D)J recombination. Curr. Opin. Immunol. *8*, 175–180.

Bogue, M.A., Wang, C., Zhu, C., and Roth, D.B. (1997). V(D)J recombination in Ku86-deficient mice: distinct effects on coding, signal and hybrid joint formation. Immunity *7*, 37–47.

Brugnoni, D., Airo, P., Facchetti, F., Blanzuoli, L., Ugazio, A.G., Cattaneo, R., and Notarangelo, L.D. (1997). In vitro cell death of activated lymphocytes in Omenn's syndrome. Eur. J. Immunol. *27*, 2765–2773.

Cavazzana-Calvo, M., Le Deist, F., de Saint-Basile, G., Papadopoulo, D., De Villartay, J.P., and Fisher, A. (1993). Increased radiosensitivity of granulocyte macrophage colony-forming units and skin fibroblasts in human autosomal recessive severe combined immunodeficiency. J. Clin. Invest. *91*, 1214–1218.

Chilosi, M., Facchetti, F., Notarangelo, L.D., Romagnani, S., Del Prete, G., Almerigogna, F., De Carli, M., and Pizzoli, G. (1996). CD30 cell expression and abnormal soluble CD30 serum accumulation in Omenn's syndrome: evidence for a T helper 2-mediated condition. Eur. J. Immunol. *26*, 329–334.

Cortes, P., Weis-Garcia, F., Misulovin, Z., Nussenzweig, A., Lai, J.S., Li, G., Nussenzweig, M.C., and Baltimore, D. (1996). In vitro V(D)J recombination: signal joint formation. Proc. Natl. Acad. Sci. USA *93*, 14008–14013.

Cuomo, C.A., and Oettinger, M.A. (1994). Analysis of regions of Rag-2 important for V(D)J recombination. Nucleic Acids Res. *22*, 1810–1814.

Danska, J.S., Pflumio, F., Williams, C.J., Huner, O., Dick, J.E., and Guidos, C.J. (1994). Rescue of T cell-specific V(D)J recombination in *scid* mice by DNA damaging agents. Science *266*, 450–455.

de Saint-Basile, G., Le Deist, F., de Villartay, J.P., Cerf-Bensussan, N., Journet, O., Brousse, N., Griscelli, C., and Fischer, A. (1991). Restricted heterogeneity of T lymphocytes in combined immunodeficiency with hypereosinophilia (Omenn's syndrome). J. Clin. Invest. *87*, 1352–1359.

Difilippantonio, M., McMahan, C.J., Eastman, Q.M., Spanopoulou, E., and Schatz, D.G. (1996). RAG-1 mediates signal sequence recognition and recruitment of RAG-2 in V(D)J recombination. Cell *87*, 253–262.

Freund, C.L., Gregory-Evans, C.Y., Furukawa, T., Papaioannou, M., Looser, J., Ploder, L., Bellingham, J., Ng, D., Herbrick, J.-A.S., Duncan, A., et al. (1997). Cone-rod dystrophy due to mutations in a

novel photoreceptor-specific homeobox gene (*CRX*) essential for maintenance of the photoreceptor. Cell *91*, 543–553.

Gomez, L., Le Deist, F., Blanche, S., Cavazzana-Calvo, M., Griscelli, C., and Fischer, A. (1995). Treatment of Omenn syndrome by bone marrow transplantation. J. Pediatr. *127*, 76–81.

Grawunder, U., Wilm, M., Wu, X., Kulesza, P., Wilson, T.E., Mann, M., and Lieber, M.R. (1997). Activity of DNA ligase IV stimulated by complex formation with XRCC4 protein in mammalian cells. Nature *388*, 492–495.

Gu, Y., Seidl, K.J., Rathbun, G.A., Zhu, C., Manis, J.P., van der Stoap, N., Davidson, L., Cheng, H.L., Sekiguchi, J.M., Frank, K., Stanhope-Baker, P., Schliesel, M., Roth, D.B., and Alt, F.W. (1997). Growth retardation and leaky SCID phenotype of Ku70-deficient mice. Immunity *7*, 853–865.

Guidos, C.J., Williams, C.J., Wu, G.E., Paige, C.J., and Danska, J.S. (1995). Development of $CD4^+$, $CD8^+$ thymocytes in RAG-deficient mice through a T cell receptor beta chain-independent pathway. J. Exp. Med. *181*, 1187–1195.

Guidos, C.J., Williams, C.J., Grandal, I., Knowles, G., Huang, M.T.F., and Danska, J.S. (1996). V(D)J recombination activates a p53-dependent DNA damage checkpoint in scid lymphocyte precursor. Genes Dev. *10*, 2038–2054.

Harville, T.O., Adams, D.M., Howard, T.A., and Ware, R.E. (1997). Oligoclonal expansion of $CD45RO^+$ T lymphocytes in Omenn syndrome. J. Clin. Immunol. *17*, 322–332.

Hiom, K., and Gellert, M. (1997). A stable RAG-1-RAG-2-DNA complex that is active in V(D)J cleavage. Cell *88*, 65–72.

Hosken, N.A., Shibuya, K., Heath, A.W., Murphy, K.M., and O'Garra, A. (1995). The effect of antigen dose on $CD4^+$ T helper cell phenotype development in a T cell receptor-alpha and beta-transgenic model. J. Exp. Med. *182*, 1579–1584.

Hsieh, C.S., Macatonia, S.E., Tripp, C.S., Wolf, S.F., O'Garra, A., and Murphy, K.M. (1993). Development of TH1 $CD4^+$ T cells through IL-12 produced by Listeria-induced macrophages. Science *260*, 547–549.

Imberti, L., Sottini, A., Signorini, S., Gorla, R., and Primi, D. (1997). Oligoclonal $CD4^+$ $CD57^+$ T-cell expansions contribute to the imbalanced T-cell receptor repertoire of rheumatoid arthritis patients. Blood *89*, 2822–2832.

Jackson, S.P., and Jeggo, P.A. (1995). DNA double strand break repair and V(D)J recombination: involvement of DNA-PK. Trends Biochem. Sci. *20*, 412–415.

Leu, T.M.J., Eastman, Q.M., and Schatz, D.G. (1997). Coding joint formation in a cell-free V(D)J recombination system. Immunity *7*, 303–314.

Lewis, S.M. (1994). The mechanism of V(D)J joining: lessons from molecular, immunological and comparative analyses. Adv. Immunol. *56*, 27–150.

Lieber, M.R., Hesse, J.E., Lewis, S., Bosma, G.C., Rosenberg, N., Mizuuchi, K., Bosma, M.J., and Gellert, M. (1988). The defect in murine severe combined immunodeficiency: joining of signal sequences but not coding segments in V(D)J recombination. Cell *55*, 7–16.

Livak, F., Welsh, S.C., Guidos, C.J., Crispe, I.N., Danska, J.S., and Schatz, D.G. (1996). Transient restoration of gene rearrangement at multiple T cell receptor loci in gamma-irradiated scid mice. J. Exp. Med. *184*, 419–428.

Macchi, P., Villa, A., Giliani, S., Sacco, M.G., Frattini, A., Porta, F., Ugazio, A.G., Johnston, J.A., Candotti, F., O'Shea, J.J., et al. (1995). Mutations of Jak-3 gene in patients with autosomal severe combined immune deficiency (SCID). Nature *377*, 65–68.

Mache, C.J., Slavc, I., Schmid, C., Hoefler, G., Urban, C.E., Schwinger, W., Winter, E., Hulla, W., Zenz, W., and Holter, W. (1994). Familial hemophagocytic lymphokistiocytosis associated with disseminated T cell lymphoma: a report of two siblings. Ann. Hematol. *69*, 85–91.

McBlane, J.F., van Gent, D.C., Ramsden, D.A., Romeo, C., Cuomo, C.A., Gellert, M., and Oettinger, M.A. (1995). Cleavage at a V(D)J recombination signal requires only RAG-1 and RAG-2 proteins and occurs in two steps. Cell *83*, 387–395.

McMahan, C.J., Sadofsky, M.J., and Schatz, D.G. (1997). Definition of a large region of Rag-1 that is important for coimmunoprecipitation of Rag-2. J. Immunol. *158*, 2202–2210.

Mombaerts, P., Iacomini, J., Johnson, R.S., Herrup, K., Tonegawa, S., and Papaioannou, V.E. (1992). RAG-1-deficient mice have no mature B and T lymphocytes. Cell *68*, 869–877.

Morrison, C., Smith, G.C.M., Stingl, L., Jackson, S.P., Wagner, E., and Wang, Z.Q. (1997). Genetic interaction between PARP and DNA-PK in V(D)J recombination and tumorigenesis. Nature Genet. *17*, 479–482.

Nacht, M., Strasser, A., Chan, Y.R., Harris, A.W., Schlissel, M., Bronson, R.T., and Jacks, T. (1996). Mutations in the p53 and SCID genes cooperate in tumorigenesis. Genes Dev. *10*, 2055–2066.

Nagawa, F., Ishiguro, K.-I., Tsuboi, A., Yoshida, T., Ishikawa, A., Takemori T., Otsuka, A.J., and Sakano, H. (1998). Footprint analysis of the RAG protein recombination signal sequence complex for V(D)J type recombination. Mol. Cell. Biol. *18*, 655–663.

Nussenzweig, A., Chen, C., da Costa Soares, V., Sanchez, M., Sokol, K., Nussenzweig, M.C., and Li, G.C. (1996). Requirement for Ku80 in growth and immunoglobulin V(D)J recombination. Nature *382*, 551–555.

Oettinger, M.A., Schatz, D.G., Gorka, C., and Baltimore, D. (1990). RAG-1 and RAG-2, adjacent genes that synergistically activate V(D)J recombination. Science *248*, 1517–1523.

Omenn, G.S. (1965). Familial reticuloendotheliosis with eosinophilia. N. Engl. J. Med. *273*, 427–432.

Quirós Roldan, E., Sottini, A., Bettinardi, A., Imberti, L., and Primi, D. (1995). Different TCRBV genes generate biased patterns of V-D-J diversity in human T cells. Immunogenetics *41*, 91–100.

Ramsden, D.A., Baetz, K., and Wu, G.E. (1994). Conservation of sequence in recombination signal sequence spacers. Nucleic Acids Res. *22*, 1785–1796.

Ramsden, D.A., Paull, T.T., and Gellert, M. (1997). Cell-free V(D)J recombination. Nature *388*, 488–491.

Roman, C.A.J., and Baltimore, D. (1996). Genetic evidence that the Rag-1 protein directly participates in V(D)J recombination through substrate recognition. Proc. Natl. Acad. Sci. USA *93*, 2333–2338.

Roth, D.B., Menetski, J.P., Nakajima, P.B., Bosma, M.J., and Gellert, M. (1992). V(D)J recombination: broken DNA molecules with covalently sealed (hairpin) coding ends in scid mouse thymocytes. Cell *70*, 983–991.

Sadofsky, M.J., Hesse, J.E., McBlane, J.F., and Gellert, M. (1993). Expression and V(D)J recombination activity of mutated Rag-1 proteins. Nucleic Acids Res. *21*, 5644–5650.

Sadofsky, M.J., Hesse, J.E., and Gellert, M. (1994). Definition of a core region of RAG-2 that is functional in V(D)J recombination. Nucleic Acids Res. *22*, 1805–1809.

Santagata, S., Aidinis, V., and Spanopoulou, E. (1998). The effect of Me^{2+} cofactors at the initial stages of V(D)J recombination. J. Biol. Chem., in press.

Schandené, L., Ferster, A., Mascart-Lemone, F., Crusiaux, A., Gerard, C., Marchant, A., Lybin, M., Velu, T., Sariban, E., and Goldman, M. (1993). T helper type 2-like cells and therapeutic effects of interferon-gamma in combined immunodeficiency with hypereosinophilia (Omenn's syndrome). Eur. J. Immunol. *23*, 56–60.

Schatz, D.G., Oettinger, M.A., and Baltimore, D. (1989). The V(D)J recombination activating gene *RAG-1*. Cell *59*, 1035–1048.

Schwarz, K., Gauss, G.H., Ludwig, L., Pannicke, U., Li, Z., Lindner, D., Friedrich, W., Seger, R.A., Hansen-Hagge, T.E., Desiderio, S., et al. (1996). Rag mutations in human B cell-negative SCID. Science *274*, 97–99.

Shinkai, Y., Rathbun, G., Lam, K.-P., Oltz, E.M., Stewart, V., Mendelsohn, M., Charron, J., Datta, M., Young, F., Stall, A.M., and Alt, F. (1992). Rag-2-deficient mice lack mature lymphocytes owing to inability to initiate V(D) rearrangement. Cell *68*, 855–867.

Silver, D.P. (1994). Functional analysis of the Rag-1 protein. Ph.D. Thesis, Massachusetts Institute of Technology, Cambridge, MA.

Silver, D.P., Spanopoulou, E., Mulligan, R.C., and Baltimore, D. (1993). Dispensable sequence motifs in the Rag-1 and Rag-2 genes for plasmid V(D)J recombination. Proc. Natl. Acad. Sci. USA *90*, 6100–6104.

Sottini, A., Quirós-Roldan, E., Albertini, A., Primi, D., and Imberti, L. (1996). Assessment of T-cell receptor beta-chain diversity by heteroduplex analysis. Hum. Immunol. *48*, 12–22.

Spanopoulou, E., Cortes, P., Huang, E., Shih, C., Silver, D., Svec, P., and Baltimore, D. (1995). Localization, interaction and RNA-binding properties of the V(D)J recombination activating proteins Rag-1 and Rag-2. Immunity *3*, 715–726.

Spanopoulou, E., Zaitseva, F., Wang, F-H., Santagata, S., Baltimore, D., and Panayotou, G. (1996). The homeodomain region of Rag-1 reveals the parallel mechanisms of bacterial and V(D)J recombination. Cell *87*, 263–276.

Tonegawa, S. (1983). Somatic generation of antibody diversity. Nature *302*, 575–581.

van Gent, D.C., McBlane, J.F., Ramsden, D.A., Sadofsky, M.J., Hesse, J.E., and Gellert, M. (1995). Initiation of V(D)J recombination in a cell-free system. Cell *81*, 925–934.

Weis-Garcia, F., Besmer, E., Sawchuk, D.J., Yu, W., Hu, Y., Cassard, S., Nussenzweig, M.C., and Cortes, P. (1997). V(D)J recombination: in vitro coding joint formation. Mol. Cell. Biol. *17*, 6379–6385.

Wen, L., Roberts, S.J., Viney, J.L., Wong, F.S., Mallick, C., Findly, R.C., Peng, Q., Craft, J.E., Owen, M.J., and Hayday, A.C. (1994). Immunoglobulin synthesis and generalized autoimmunity in mice congenitaly deficient in αβ(+) T-cells. Nature *369*, 654–658.

Wilson, D.S., Guenther, B., Desplan, C., and Kuriyan, J. (1995). High resolution crystal structure of a Paired (Pax) class cooperative homeodomain binding on DNA. Cell *82*, 709–719.

Yoshimoto, T., Bendelac, A., Watson, C., Hu-Li, J., and Paul, W.E. (1995). Role of NK1.1$^+$ T cells in a T_H2 response and in immunoglobulin E production. Science *270*, 1845–1847.

Zhu, C., Bogue, M.A., Lim, D.S., Hasty, P., and Roth, D.B. (1996). Ku86-deficient mice exhibit severe combined immunodeficiency and defective processing of V(D)J recombination intermediates. Cell *86*, 379–390.

Proc. Natl. Acad. Sci. USA
Vol. 95, pp. 2648–2652, March 1998
Pharmacology

Expression of Q227L-Gα_s in MCF-7 human breast cancer cells inhibits tumorigenesis

JIANGHAO CHEN†, JEFFRY A. BANDER, TARA ANN SANTORE, YIBANG CHEN, PRAHLAD T. RAM, MARTINE J. SMIT, AND RAVI IYENGAR‡

Department of Pharmacology, Mount Sinai School of Medicine, New York, NY 10029

Communicated by Lutz Birnbaumer, University of California School of Medicine, Los Angeles, CA, November 3, 1997 (received for review September 24, 1997)

ABSTRACT **The effects of expression of mutant (Q227L)-activated Gα_s and elevation of cAMP on mitogen-activating protein kinase (MAPK) activity and the transformed phenotype were studied in the MCF-7 human mammary epithelial cell line. Elevation of cAMP partially inhibited the epidermal growth factor-stimulated DNA synthesis and the intrinsic MAPK (ERK-1 and ERK-2) of serum-starved MCF-7 cells. Addition of 8Br-cAMP or expression of mutant (Q227L)-activated Gα_s in MCF-7 cells blocked the ability of these cells to grow in an anchorage-independent manner, as assessed by colony formation in soft agar. 8Br-cAMP in the culture medium also blocked estrogen stimulation of MCF-7 cell proliferation *in vitro*. MCF-7 cells expressing Q227L-Gα_s grew very slowly *in vitro*, and when these cells were injected s.c. into athymic mice implanted with estrogen pellets, the frequency of tumor formation was reduced greatly and the sizes of the tumors formed were much smaller than those in mice injected with MCF-7 cells that had been transfected with the empty vector. These results indicate that the intracellular levels of cAMP in transformed mammary epithelial cells can be a crucial factor in determining the expression of the transformed phenotype. Interactions between the G_s/adenylyl cyclase and MAPK-1,2 signaling pathways could be one mechanism by which expression of the transformed phenotype in mammary epithelial cells are regulated.**

Interactions between signaling pathways regulate many cellular processes, including proliferation and transformation. It is now well established that many growth factors that bind receptor-tyrosine kinases use Ras as the signal transducer to activate a cascade of protein kinases, including Raf and MEK-1,2, resulting in the activation of mitogen-activated protein kinase (MAPK) 1 and 2 (1, 2). In fibroblast-derived cell lines such as NIH 3T3, Ras directly interacts with Raf (3) and Raf activates MEK, which activates MAPK 1 and 2 (1, 2). Constitutively activated MEK induces transformation of NIH 3T3 cells (4, 5). These observations have indicated that activation of the Raf/MEK/MAPK may be sufficient to trigger transformation in at least fibroblasts. A number of studies also have shown that elevation of cAMP blocks signaling through the Ras/Raf/MEK pathway (6–9) and blocks Ras-induced transformation through protein kinase A (9). Regulation at the level of Raf appears to be a major site where protein kinase A modulates signal transmission to MAPK-1 and -2 (7, 8, 10).

We sought to extend our observations that mutant-activated Gα_s and elevation of cAMP block Ras-induced MAPK activity and transformation (9) to other systems. The human breast cancer cell lines appeared to be a particularly attractive system because many studies indicated that signaling from receptor and nonreceptor tyrosine kinases play a crucial role in the transformation of mammary epithelia (11–13). If signaling through the MAPK pathway were involved in maintaining the transformed state in mammary epithelia, then expression of activated Gα_s could be useful in blocking the expression of the transformed phenotype *in vivo*. To examine this hypothesis, we developed stably transfected MCF-7 mammary epithelial cell lines expressing activated Gα_s and tested their capability to proliferate in soft agar and to form tumors in athymic mice.

MATERIALS AND METHODS

Materials. DMEM and phenol red-free DMEM were from GIBCO/BRL. Fetal bovine serum and charcoal-treated fetal bovine serum were from HyClone. Recombinant human insulin from Novo-Nordisk (Copenhagen) was obtained from the Mount Sinai Pharmacy. The 17β-estradiol used in tissue culture experiments was from Sigma. The 17β-estradiol pellets (0.72-mg pellet, 60-day release) was from Innovative Research of America. MAPK antibodies were from New England Biolabs. Sources of others reagents have been described previously (9).

Cell Culture. Human breast cancer MCF-7 cells were purchased from American Type Culture Collection. The cells were grown in DMEM supplemented with 2 μg/ml insulin, 1 mM sodium pyruvate, 1 mM nonessential amino acids, 4 mM glutamine, 10% fetal calf serum, and antibiotics (penicillin/streptomycin). For routine culture, cells were grown in phenol red containing medium. When required, 1 week before experiments cells were grown in phenol red-free medium supplemented with 5% dextran-coated, charcoal-stripped fetal calf serum.

Transfections and Establishment of Clonal Cell Lines. For establishment of clonal cell lines, 20 μg of pRc/cytomegalovirus (CMV) or 20 μg of pRc/CMV-α_s* (9) were diluted into 220 μl of 0.1× TE (10 mM Tris·HCl, pH 8.0/1 mM EDTA) and mixed with 250 μl of 2× Hepes-buffered saline in a sterile 15-ml tube to which 31 μl of 2 M $CaCl_2$ was added slowly. The transfection mixtures then were distributed evenly over subconfluent MCF-7 cells for 24 h. The transfection medium was removed, and the cells were then fed with fresh medium (DMEM supplemented with 2 μg/ml insulin and 10% fetal calf serum). One day later, medium containing 0.8 g/liter G-418 was added to the cells, and neomycin-resistant cells were selected for 10 days. The individual neomycin-resistant cells were allowed to grow for another 2 weeks to form colonies. The colonies were picked by placing cloning cylinders around clearly separated colonies. A cAMP accumulation assay was used to select the α_s*-expressing MCF-7

The publication costs of this article were defrayed in part by page charge payment. This article must therefore be hereby marked "*advertisement*" in accordance with 18 U.S.C. §1734 solely to indicate this fact.

Abbreviations: MAPK, mitogen-activated protein kinase; CMV, cytomegalovirus; EGF, epidermal growth factor.

†Present address: Department of Medicine, Columbia University College of Physicians and Surgeons, New York, NY 10032.
‡To whom reprint requests should be addressed. e-mail: iyengar@msvax.mssm.edu.

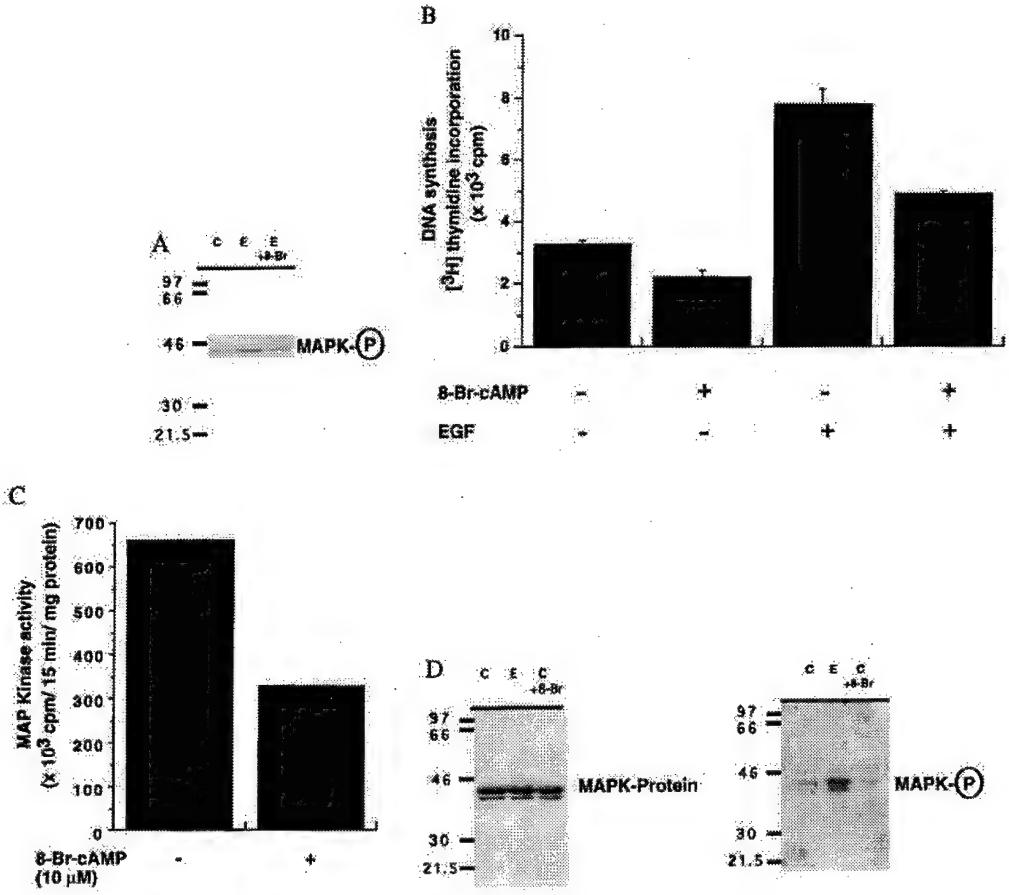

FIG. 1. Effects of 8Br-cAMP on the activities of MAPK-1,2 and DNA synthesis in MCF-7 cells. (*A*) Immunoblot of phospho-MAPK-1,2 in extracts from cells treated with or without (*C*) EGF (10 ng/ml) after incubation with 8Br-cAMP (10 mM). (*B*) EGF stimulated DNA synthesis in cells incubated with and without 8Br-cAMP. Serum-starved cells were incubated with or without 8Br-cAMP (10 mM) for 12 h and then with 1 mCi [^{3}H]-thymidine, without or with EGF (10 ng/ml), for another 16 h. Cells then were washed and extracted with trichloroacetic acid, and the trichloroacetic acid precipitate was counted (9). Values are mean ± SD of triplicate determinations. (*C*) Effect of 8Br-cAMP on the basal MAPK activity of serum-starved MCF-7 cells. Cell extracts were resolved on Mono-Q columns by using fast protein liquid chromatography. Aliquots of column fractions were assayed. Total counts under the peak are plotted as a bar graph. For controls, extracts that had been heat inactivated were resolved on Mono-Q columns by fast protein liquid chromatography and assayed. Control activity was 50–75 per column aliquot. (*D*, left) Immunoblot of total ERK1 and ERK2 from serum-starved cells treated without any additives (*C*) or with EGF (10 ng/ml) or 8Br-cAMP (10 mM). (*D*, right) Immunoblot of phospho-MAPK-1,2 in extracts from serum-starved cells treated without any additives (*C*) or with EGF (10 ng/ml) or 8Br-cAMP (10 mM). Equal aliquots were used in both assays.

clonal cell lines. For this, cells were labeled with [^{3}H]-adenine and cAMP accumulation was measured in the presence of 0.1 mM 3-isobutylmethylxanthine. Clones displaying 50–100% increases in basal cAMP levels were used for further studies.

MAPK Assays. The subconfluent MCF-7, vector CMV, or the α_s*-expressing MCF-7 clonal cell lines were maintained in serum-free DMEM (without phenol red). After 24 h, various concentrations of 8Br-cAMP, as indicated, were added to the MCF-7 cells. Twelve hours later, the cells were extracted and the extract was resolved on Mono-Q columns by using fast protein liquid chromatography. MAPK activity in column fractions was measured by using peptide substrate $EGFR_{662-681}$ (9).

Phosphorylation of MAPK-1,2. MCF-7 cells were serum-starved for 24 h. Then, 12 h before the start of the experiments, 8Br-cAMP was added to the required plates. When needed, cells were stimulated with epidermal growth factor (EGF) for 15 min. After treatment, cells were extracted in RIPA buffer (0.15 mM NaCl/0.05 mM Tris·HCl, pH 7.2/1% Triton X-100/1% sodium deoxycholate/0.1% SDS) containing protease and phosphatase inhibitors and lysed by sonication. Aliquots of cell extracts were resolved electrophoretically and transferred to Immobilon-P (Millipore) membrane. The membranes were blotted with antibodies to phospho-ERK-1,2 or antibodies that recognize ERK1,2 proteins irrespective of their phosphorylation state. Bands were visualized by chemiluminescence by using alkaline phosphatase-coupled secondary antibody.

Colony Formation in Soft Agar. MCF-7 cells were incubated with various concentrations of 8Br-cAMP for 1 week, and then aliquots were plated onto soft agar plates. Wild-type, empty vector pRc/CMV or the α_s*-expressing clonal cells were assayed for colony formation in soft agar. Cells (5×10^4) were suspended in 3 ml of medium (DMEM supplemented with 2 μg/ml insulin and 10% fetal calf serum) containing 0.3% agar. The mixture was added over a layer of 0.5% agar in DMEM on a 60-mm plate. Plates were fed weekly with 2 ml of DMEM with 10% fetal calf serum, 0.3% agar, 2 μg/ml insulin, and 8Br-cAMP if needed. Three weeks later, plates were stained with the vital stain 2-(*p*-isodophenyl)-3-(*p*-nitrophenyl)-5-phenyltertazolium chloride hydrate for 2 days. Colonies larger then 0.15 mm in diameter were scored.

Tumorigenesis in Athymic Mice. 17-β-estradiol pellets (0.72 mg) were implanted s.c. in athymic mice. One day later, 10^6 control (neo^r) or α_s*-expressing MCF-7 clonal MCF-7 cells

were injected. Mice showing tumors were counted, and the tumor sizes were measured initially after 1 month and subsequently on a weekly basis for another 4 weeks. Final measurements after 8 weeks are given. All experiments were repeated at least twice, most three or more times. Qualitatively similar results were obtained. Typical experiments are shown.

RESULTS

MCF-7 cells have EGF receptors (14) that are known to signal through Ras and Raf to MAPK-1,2 (1, 2). MAPK-1,2 are activated by phosphorylation (15), and phospho-MAPK-1,2 immunoblots are widely used as an indicator of their state of activation. (16). Elevation of cAMP and activation of protein kinase A block signal transmission at the level of Raf (8, 10). Hence, we determined whether EGF stimulated the phosphorylation of MAPK-1,2 and whether this stimulation was blocked by cAMP. For this, serum-starved MCF-7 cells were incubated with and without 8Br-cAMP and then stimulated with EGF. Cell extracts then were resolved electrophoretically on SDS/polyacrylamide gels, transferred to Immobilon membranes, and blotted with phospho-MAPK-1,2-specific antibodies. EGF stimulated the phosphorylation of MAPK-1,2, and 8Br-cAMP greatly reduced this stimulation (Fig. 1*A*). We then checked whether 8Br-cAMP also inhibited EGF-stimulated DNA synthesis. When serum-starved MCF-7 cells were incubated with 8Br-cAMP and then tested for EGF-stimulated [^{3}H]-thymidine incorporation, it was found that 8Br-cAMP significantly inhibited EGF-stimulated [^{3}H]-thymidine incorporation (Fig. 1*B*). In this experiment, we also noticed that treatment with 8Br-cAMP significantly inhibited basal [^{3}H]-thymidine incorporation. Hence, we checked whether there was any effect of 8Br-cAMP on the basal MAPK activity of serum-starved MCF-7 cells. In initial experiments, MAPK activities were measured in fast protein liquid chromatography fractions by using $EGFR_{662-681}$ peptide as a substrate. It was found that incubation of serum-starved MCF-7 cells with 8Br-cAMP resulted in a 50% inhibition of the basal MAPK activity (Fig. 1*C*). This result was unusual in comparison with our data from NIH 3T3 fibroblasts in which no measurable basal MAPK activity was seen in serum-starved cells. To further verify this effect of 8Br-cAMP, we checked the phosphorylation state of MAPK-1 and -2 in MCF-7 cells. Treatment did not result in any change in total ERK-1,2 protein levels (Fig. 1*D*, left). Measurable levels of phosphorylated MAPK-1,2 were observed in serum-starved MCF-7 cells. (Fig. 1*D*, right), and as expected, EGF stimulated the phosphorylation of MAPK-1,2. 8Br-cAMP decreased basal phosphorylation in serum-starved MCF-7 cells (Fig. 1*D*, right).

In NIH 3T3 cells, we had observed that a partial suppression of Ras-stimulated MAPK activity and DNA synthesis resulted in a full inhibition of Ras-induced transformation (9). Hence, we decided to check whether 8Br-cAMP blocked expression of the transformed phenotype in MCF-7 cells as well. For this, we assessed the anchorage-independent growth of MCF-7 cells by measurement of colony formation in soft agar in the presence of varying concentrations of 8Br-cAMP. Increasing concentrations of cAMP suppressed colony formation by MCF-7 cells (Fig. 2). Although in long term experiments such as this a full effect was observed with 1 mM 8Br-cAMP, complete inhibition was not seen reproducibly at this concentration in acute MAPK experiments. Therefore, we used 10 mM 8Br-cAMP for the acute experiments.

We were interested in determining whether the effects of cAMP elevation that were observed in these *in vitro* experiments also occurred *in vivo*. Because it is not possible to selectively elevate cAMP levels in MCF-7 cells for prolonged periods *in vivo*, we decided to express stably the mutant-activated $G\alpha_s$ in MCF-7 cells. For this, MCF-7 cells were transfected with the vector pRc/CMV without any insert or

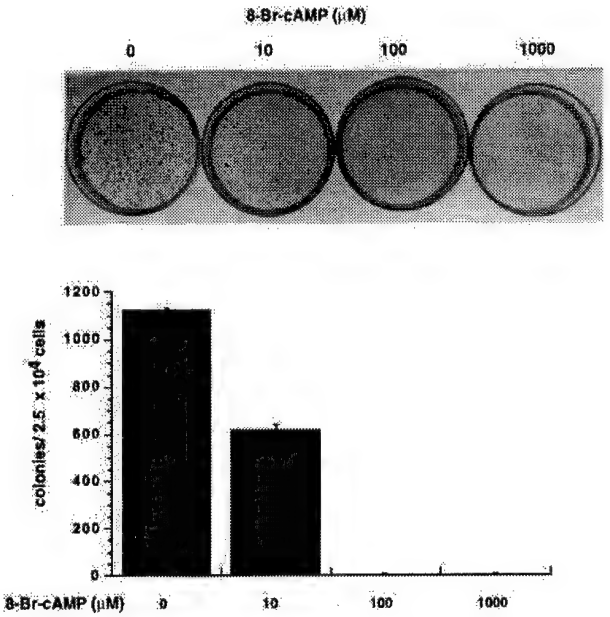

FIG. 2. Effect of varying concentrations of 8Br-cAMP on soft agar colony formation by MCF-7 cells. Cells were seeded and colony formation was assayed as described in *Material and Methods*. Four plates per condition were counted for each 8Br-cAMP concentration. Values are mean ± SD. A picture of a typical plate at each concentration of 8Br-cAMP also is shown.

with Q227L-$G\alpha_s$ (α_s*). Neomycin-resistant stable clonal lines were selected. The α_s*-expressing lines were identified by their elevation of basal cAMP levels. Under standard culture conditions, the α_s*-expressing lines grew slower (Fig. 3*A*). Under conditions in which the vector-transfected cell line formed over 500 colonies, the α_s*-expressing line formed under 50 colonies (Fig. 3*B*). To verify that the observed effect of α_s* was not caused by clonal variation, we compared three control (neo^r) and three α_s*-expressing lines. All three α_s*-expressing lines showed markedly reduced capability to form colonies in soft agar (Fig. 3*C*).

Because the α_s*-expressing MCF-7 cells did not show a transforming phenotype *in vitro*, we next determined whether the expression of α_s* reduced the capability of MCF-7 cells to form tumors in athymic mice. For MCF-7 cells to grow and form tumors in athymic mice, estrogen is required (17), and hence, we first checked the effect of 8Br-cAMP on estrogen regulation of MCF-7 cell proliferation in culture. For this, MCF-7 cells were cultured in phenol red-free medium-supplemented charcoal-stripped serum. Under these conditions, estrogen (10 nM) stimulated the proliferation of MCF-7 cells. Inclusion of 8Br-cAMP in the medium inhibited the estrogen effect (Fig. 4).

Athymic mice were implanted with estrogen pellets and 24 h later injected with either control or α_s*-expressing lines. Animals were scored for tumor formation initially after 1 month and then weekly for another 4 weeks. In three separate experiments, we found that the α_s*-expressing MCF-7 cell lines had a greatly reduced capability of forming tumors in athymic mice and the tumors that formed were much smaller in size after 8 weeks (Table 1). Two mice, one from the control (CMV-1) cell group and one from the CMV-α_s*-2 cell-injected group, are shown in Fig. 5.

DISCUSSION

The role of cAMP in regulating mammary carcinoma proliferation has been studied for some time (18–20). Initial studies

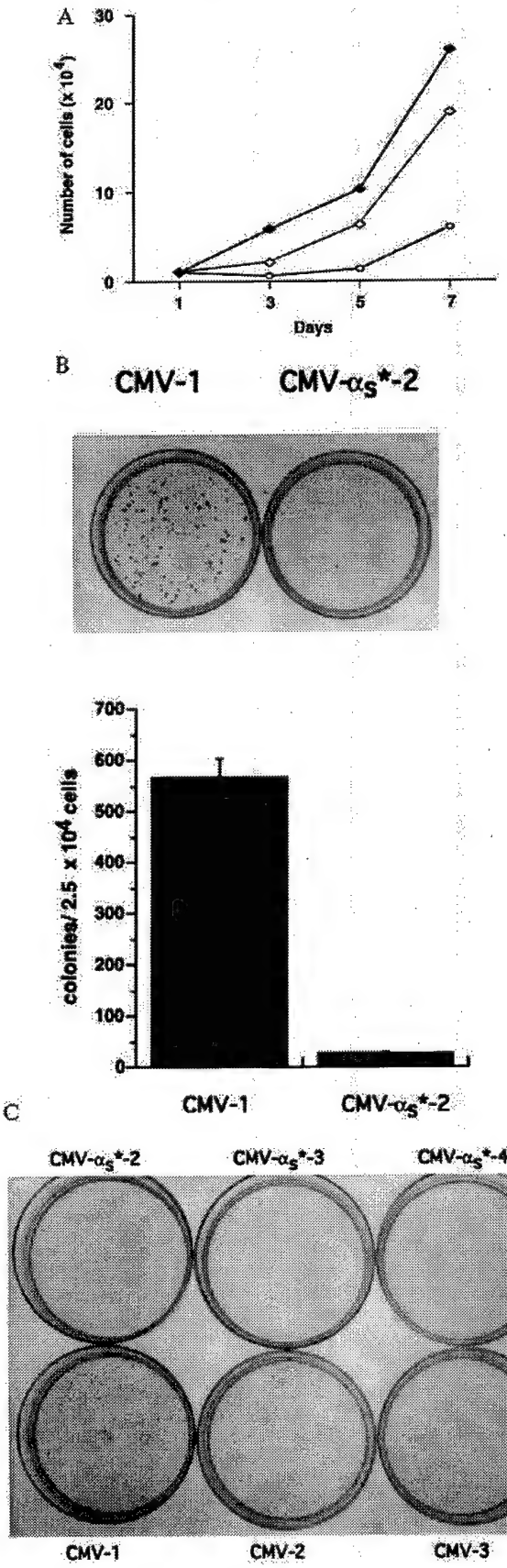

FIG. 3. Effect of α_s* expression on proliferation and soft agar colony formation by MCF-7 cells. (*A*) Wild-type (◆), vector-transfected (◇), and α_s*-expressing cells (○) were grown for 7 days. Cells were counted in duplicate every other day. Values are average of duplicate determinations, which were within 10%. (*B*) Cells were seeded and colony formation was assayed as described in *Material and Methods*. Four plates for the vector-transfected cell line and the α_s*-expressing cell line were counted. Values are mean ± SD. Pictures of a typical vector-transfected cell line and α_s*-expressing cell line are shown. (*C*) Three different vector-transfected and α_s*-expressing cell lines were compared for ability to form colonies in soft agar. Plating was carried out in triplicate. A typical plate for each condition is shown.

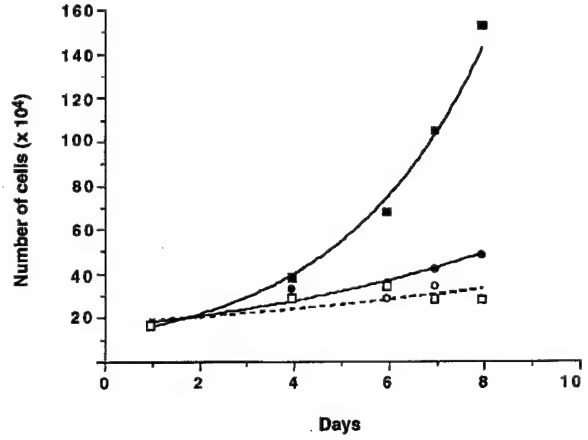

FIG. 4. Effect of 8Br-cAMP or α_s* expression on estrogen-stimulated proliferation of MCF-7 cells. Cells were incubated without (closed symbols) and with (open symbols) 8Br-cAMP (1 mM) in the absence (○, ●) and presence (□, ■) of 10 nM estrogen. Values are mean of triplicate determinations. Coefficient of variance was <10%.

indicated that dibutryl-cAMP in conjunction with arginine suppressed the proliferation of MCF-7 cells (18). Subsequently chloro-derivatives of adenosine were reported to be potent inhibitors of MCF-7 cell proliferation (19). A recent evaluation of the chloro-derivatives of cAMP indicated that their growth inhibitory effects were not related to their ability to activate protein kinase A. Their effects appear rather to be caused by toxicity of their breakdown products (20). Nevertheless, even in that study, elevation of cAMP by forskolin was found to inhibit proliferation of MCF-7 cells. In the results presented here, we show that elevation of cAMP levels has substantial effects on expression of the transformed phenotype of MCF-7 cells. 8Br-cAMP also inhibited EGF-stimulated MAPK-1,2 in MCF-7 cells and more interestingly inhibited the "basal" MAPK activity in serum-starved MCF-7 cells. This elevated MAPK activity may be caused by autocrine factors secreted by MCF-7 cells that stimulate this pathway. Such factors have long been postulated to sustain the proliferation of MCF-7 cells (21). It is noteworthy that our observations in MCF-7 cells are similar to those we had with NIH 3T3 cells (9), suggesting that the Raf to MAPK-1,2 signal transmission may be important for the expression of the transformed phenotype in mammary epithelia. Of course, activation of this pathway alone may not be sufficient for transformation as has been demonstrated for rat intestinal epithelial cells (22).

For the *in vitro* experiments, we were able to use 8Br-cAMP. However, this approach would not be feasible for *in vivo* experiments such as tumor formation in athymic mice. To elevate cAMP constitutively in MCF-7 cells, we expressed α_s*. Expression of α_s* in MCF-7 cells such that ambient cAMP levels were raised 50–100% did not kill the cells; rather, under standard culture conditions, these cells grew slower than normal MCF-7 cells. The growth rate of the α_s*-expressing cells was similar to that seen with wild-type cells in the

Table 1. Effect of α_s* expression on MCF-7-induced tumors in Na/Na mice

Experiment	MCF-7 clone	Animals showing tumors, *n*	Mean tumor diameter, mm
1	CMV-1	4/5	5.6 ± 0.8
	CMV-α_s-2	0/5	
	CMV-α_s-3	1/5	0.4
2	CMV-1	9/10	6.9 ± 0.5
	CMV-α_s-2	0/10	
	CMV-α_s-4	2/10	3.8, 4.5
3	CMV-1	4/4	6.8 ± 0.3
	CMV-α_s-2	2/5	1.6, 2.5
	CMV-α_s-3	2/5	1.9, 3.1

Indicated MCF cell clonal lines were injected into mice that had been implanted with estrogen pellets. Tumor diameter was measured with calipers. Both length and width were measured, and diameter for each tumor was calculated as length + width/2.

presence of 8Br-cAMP. Addition of 8Br-cAMP or expression of α_s* caused a partial inhibition of MAPK-1,2 and DNA synthesis. However, the α_s*-expressing cells have a greatly diminished capability to display a transformed phenotype. This was visible both in *in vitro* assays such as soft agar colony formation and in *in vivo* assays such as tumor formation in athymic mice. The tumorigenesis assays are important because they show for the first time that interactions between signaling pathways may be useful in inhibiting tumor formation *in vivo*. Up to now, it had not been certain that the interactions between the cAMP and MAPK signaling pathways that regulate proliferation *in vitro* would work *in vivo* or whether there would be compensatory mechanisms *in vivo* that would negate the anti-proliferative and anti-transforming effects of the cAMP pathway. The experiments presented here show that targeted continuous elevation of cAMP can be used to block tumor formation. In these experiments, we introduced the α_s* cDNA by transfection; however it may be possible to deliver this gene by the use of viral vectors by using approaches that currently are used in gene therapy. Further experiments are needed to ascertain whether interactions between signaling pathways can be used as a basis for therapeutic intervention in proliferative disorders.

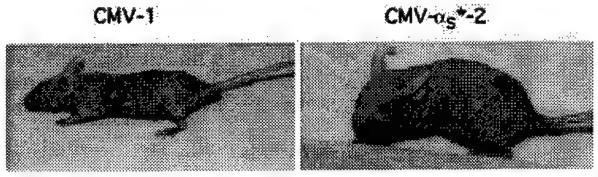

FIG. 5. Pictures of mice injected with either vector-transfected or α_s*-expressing MCF-7 cells. Animals were implanted with the estrogen pellet and injected with the indicated cell line. Tumor after 8 weeks is shown.

We thank Dr. Rafael Mira-Y-Lopez for help with the early tumorigenesis experiments. This research was supported by a grant from the American Cancer Society and by National Institutes of Health Grant GM-54508. M.J.S. was supported by a fellowship from the Netherlands Organization for Scientific Research, T.S. was a predoctoral fellow on the U.S. Army Breast Cancer Training Grant, and P.T.R. is supported by the Molecular Endocrinology Training Grant DK-0745.

1. Egan, S. E. & Wienberg, R. A. (1993) *Nature (London)* **365,** 781–783.
2. Schlessinger, J. (1993) *Trends Biochem Sci.* **18,** 273–275.
3. Moodie, S. A., Willumsen, B. M., Weber, M. J. & Wolfman, A. (1993) *Science* **260,** 1658–1661.
4. Crowley, S., Paterson, H., Kemp, P. & Marshall, C. J. (1993) *Cell* **77,** 841–852.
5. Mansour, S. J., Matten, W. T., Hermann, A. S., Candia, J. M., Rong, S., Fukasawa, K. , VandeWoudw, G. F. & Ahn, N. G. (1994) *Science* **265,** 966–970.
6. Svetson, B. R., Kong, X. & Lawrence, J. C. (1993) *Proc. Natl. Acad. Sci. USA* **90,** 10305–10309.
7. Cook, S. J. & McCormick, F. (1993) *Science* **262,** 1069–1072.
8. Wu, J., Dent, P., Jelink, T., Wolfman, A., Weber, M. & Sturgill, T. W. (1993) *Science* **262,** 1065–1069.
9. Chen, J. H. & Iyengar, R. (1994) *Science* **263,** 1278–1281.
10. Hafner, S., Adler, H. S, Mischak, H., Janosch, P., Heidecker, G., Wolfman, A., Pippig, S., Lohse, M., Ueffing, M. & Kolch, W. (1994) *Mol. Cell Biol.* **14,** 6696–6703.
11. Dickson, R. B. & Lippmann, M. E. (1986) *Endocr. Rev.* **8,** 29–43.
12. King, C. R., Kraus, M. H. & Aaronson, S. A. (1985) *Science* **229,** 974–976.
13. Slamon, D. J., Clark, G. M., Wong, S. G., Levin, W. J., Ullrich, A. & McGuire, W. L. (1987) *Science* **244,** 702–712.
14. Godden, J, Leake, R. & Kerr, D. J. (1992) *Anticancer Res.* **12,** 1683–1688.
15. Marshall, C. J. (1995) *Cell* **80,** 179–185.
16. Sturgill, T. W., Ray, L. B., Erickson, E. & Maller, J. L. (1988) *Nature (London)* **334,** 715–718.
17. Shafie, S. M. & Grantham, F. H. (1980) *Cancer Lett.* **10,** 177–189.
18. Cho-Chung, Y.-S., Clair, T., Bodwin, J. S. & Berghoffer, B. (1981) *Science* **214,** 77–79.
19. Cho-Chung, Y.-S., Clair, T., Tortora, G. & Yokozaki, H. (1991) *Pharmacol. Ther.* **50,** 1–33.
20. Karsten, O., Vintermyr, R. B., Brustugun, O. D., Maronde, E., Aakvaag, A. & Doskeland, S. O. (1995) *Endocrinology* **136,** 2513–2520.
21. Dickson, R. B., Mcmanaway, M. E. & Lippmann, M. E. (1986) *Science* **232,** 1540–1543.
22. Oldham, S. M., Clark, G. J., Gangarosa, L. M., Coffey, R. J. & Der, C. J. (1996) *Proc. Natl. Acad. Sci. USA* **93,** 6924–6928.

Identification of a novel class of genomic DNA-binding sites suggests a mechanism for selectivity in target gene activation by the tumor suppressor protein p53

Lois Resnick-Silverman,[1] Selvon St. Clair,[1] Matthew Maurer,[1] Kathy Zhao,[1] and James J. Manfredi,[1–3]

[1]Derald H. Ruttenberg Cancer Center and the [2]Brookdale Center for Molecular and Developmental Biology, Mount Sinai School of Medicine, New York, New York 10029 USA

There are two response elements for p53 in the promoter of the gene for the cyclin-dependent kinase inhibitor p21. The binding of p53 to the 5′ site was enhanced by incubation with monoclonal antibody 421, whereas the binding of p53 to the 3′ site was inhibited. Mutational analysis showed that a single-base change caused one element to behave like the other. A response element in the human *cdc25C* promoter is bound by p53 with properties similar to the 3′ site. These results identify two classes of p53-binding sites and suggest a mechanism for target gene selectivity by p53.

Received March 25, 1998; revised version accepted May 27, 1998.

The tumor suppressor protein p53 has been implicated in the cellular response to DNA damage and mediates either growth arrest or apoptosis, depending on particular cellular conditions (see Gottlieb and Oren 1996; Ko and Prives 1996; Levine 1997). It has also been implicated in a spindle checkpoint (Cross et al. 1995) and in the induction of either differentiation (Shaulsky et al. 1991; Aloni-Grinstein et al. 1993; Soddu et al. 1994) or senescence (Sugrue et al. 1997). The p53 protein is a transcription factor that binds in a sequence-specific manner to particular sites in the genome and activates transcription of target genes (for review, see Gottlieb and Oren 1996; Ko and Prives 1996; Levine 1997). Utilizing immunobinding assays involving the monoclonal antibody 421, a consensus binding site for p53 has been defined and consists of four pentameric repeats of RRRCW in which R is a purine and W represents either an A or T residue (El-Deiry et al. 1992; Funk et al. 1992; Halazonetis et al. 1993). Two palindromic pentamers (half-site) are juxtaposed to a second set of two palindromic pentamers, the two half-sites being separated by no insert or insertions from 1–13 bp (El-Deiry et al. 1992). Such a consensus site is consistent with the fact that p53 exists in solution and binds to DNA as a tetramer (Friedman et al. 1993). It has been proposed that to accommodate a symmetrical tetrameric p53 on such a site, the DNA must bend (Balagurumoorthy et al. 1995; Nagaich et al. 1997a,b). Studies to date have implicated the C residue at position 4 of each pentamer as essential for the binding of p53 to DNA (Halazonetis et al. 1993; Nagaich et al. 1997b).

The structure of p53 is consistent with its role as a transcription factor with identified domains that are responsible for transcriptional activation, sequence-specific DNA binding, and oligomerization as a tetramer. Previous studies have implicated the carboxy-terminal 30 amino acids of p53 as exerting a negative regulatory effect on the DNA-binding activity of the protein. Deletion of these carboxy-terminal 30 amino acids, phosphorylation of sites within this region by casein kinase II and protein kinase C, and the binding of bacterial DnaK in this region all will activate the DNA-binding activity of p53 (Hupp et al. 1992; Takenaka et al. 1995). Consistent with this, the mAb 421, which has an epitope in this carboxy-terminal region, activates the ability of p53 to bind to DNA (Funk et al. 1992; Hupp et al. 1992; Halazonetis et al. 1993; Mundt et al. 1997). Finally, a peptide derived from the carboxyl end of p53 has also been shown to stimulate the ability of p53 to interact with DNA, although not to the same extent as the activators identified previously (Hupp et al. 1995).

DNA damage induces expression of p53 protein which, in turn, transcriptionally activates expression of particular genes, most notably those that encode the cyclin-dependent kinase inhibitor p21. Consistent with this, cells that lack p21 expression have an impaired p53-dependent response to DNA damage (Brugarolas et al. 1995; Deng et al. 1995). The human *p21* promoter has been shown to contain two p53-responsive elements. Deletion analysis of reporter constructs containing the sequence of the human *p21* promoter identified a distal element located 2.3–2.5 kb and a proximal element located 1.1–1.5 kb from the start site of transcription (El-Deiry et al. 1993,1995; Macleod et al. 1995).

In this report we have confirmed the existence of two p53-responsive elements in the human *p21* promoter. One of these, the 3′ site, matches the consensus sequence for p53 DNA binding at 18 of 20 positions. Notably, there is a G residue in place of the C residue in the fourth position of the first pentamer (Fig. 1). In contrast to other known p53-binding sites, the binding of p53 to this 3′ site in the *p21* promoter is inhibited by mAb 421. This suggests the existence of a new class of genomic sites in which the binding of p53 may be regulated differentially. Because p53 has been implicated in a variety of cellular responses, an understanding of the mechanism for selection of target genes by p53 is central to understanding its biological functions. The results pre-

[*Key Words:* Tumor suppressor; DNA binding; sequence specificity; p53 protein; transcriptional activation; binding sites]
[3]Corresponding author.
E-MAIL jmanfredi@smtplink.mssm.edu; FAX (212) 849-2446.

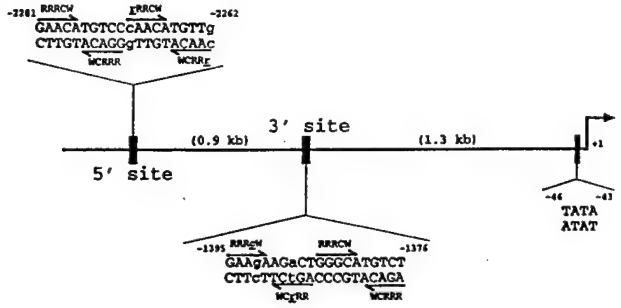

Figure 1. Schematic of *p21* promoter. Shown is 2.5 kb of the upstream sequence of the human *p21* promoter; 2.2 kb from the start site of transcription is a well-documented p53-binding site at positions –2281 to –2262. It matches the published consensus sequence for a p53 DNA binding site in 18 of 20 positions; the variations from the consensus are shown by lowercase letters. A second site with similarity to the consensus sequence is 1.3 kb upstream from the start site of transcription. Contained within positions –1395 to –1376, this sequence also matches the consensus at 18 of 20 positions. Note that in this 3′ site, the fourth position of the first pentamer contains a G rather than a C residue (shown in lowercase and boldface type). The position of the TATA box of the promoter is also indicated.

sented here suggest one potential mechanism for such site selection by p53.

Results

Two p53-responsive elements are present in the human p21 *promoter*

Using a series of deletion constructs, two p53-response elements had been identified previously in the human *p21* promoter (Macleod et al. 1995). A well-characterized element was located 2.4 kb upstream from the start site of transcription, and a second element had been suggested to be present 1.1–1.5 kb from the start of transcription (Fig. 1). We demonstrate that both a 20-bp 5′ element, located between –2262 and –2281, and a 20-bp 3′ element, located between –1376 and –1395, are each sufficient to transactivate a reporter gene in a p53-dependent manner (Fig. 2). Double-stranded synthetic oligonucleotides containing either one copy of the 5′ site or two copies of the 3′ site were inserted into a reporter vector, pGL3–E1bTATA, containing the *E1b* promoter upstream of a luciferase reporter gene. Although a single copy of the 3′ site conferred p53-dependent transcriptional activation on the minimal promoter (see Fig. 5B, below), two copies of the 3′ site showed a more pronounced effect and were used in the experiments described here (Fig. 2). Each reporter construct was cotransfected into p53-negative Saos-2 cells with empty vector or a plasmid expressing either human wild-type p53 or the human temperature-sensitive mutant $p53^{Ala143}$. The temperature-sensitive mutant $p53^{Ala143}$ is in a mutant conformation at 37°C. At this temperature, it is unable to activate p53-response elements. However, when shifted to 32°C, this mutant can assume a wild-type conformation and has been shown to activate some p53-responsive promoters (such as *p21*) but not others (such as Bax) (Friedlander et al. 1996). Cells were maintained at 37°C or shifted to 32°C, 17 hr prior to lysis. At 37°C, a luciferase reporter containing a single copy of the 5′ site was activated 1730-fold by wild-type p53, but only 2-fold by $p53^{Ala143}$. The reporter plasmid containing two copies of the 3′ site was activated 380-fold by wild-type p53, but again only 2-fold by $p53^{Ala143}$. The reporter vector lacking either response element was minimally activated by expression of either the wild-type or mutant p53 (Fig. 2A). At 32°C, the luciferase reporter containing a single copy of the 5′ site was activated 1154-fold by wild-type p53 and 792-fold in the presence of $p53^{Ala143}$. The reporter plasmid containing two copies of the 3′ site was activated 362-fold by wild-type p53 and 96-fold by the mutant $p53^{Ala143}$. A luciferase reporter plasmid containing the full-length *p21* promoter p21P was activated 16-fold by wild-type p53 and ninefold by the mutant $p53^{Ala143}$. At 32°C, the reporter vector lacking either response element was not activated by either wild-type or mutant p53 (Fig. 2B). These data confirm that there are two p53-response elements in the human *p21* promoter, each of which is sufficent to confer p53-dependent transcriptional activation on a luciferase reporter gene containing the minimal adenovirus *E1b* promoter. Additionally, neither the 5′ nor the 3′ site is activated by the temperature-sensitive mutant $p53^{Ala143}$ at 37°C, whereas at 32°C both sites are activated, although less so than by wild-type p53.

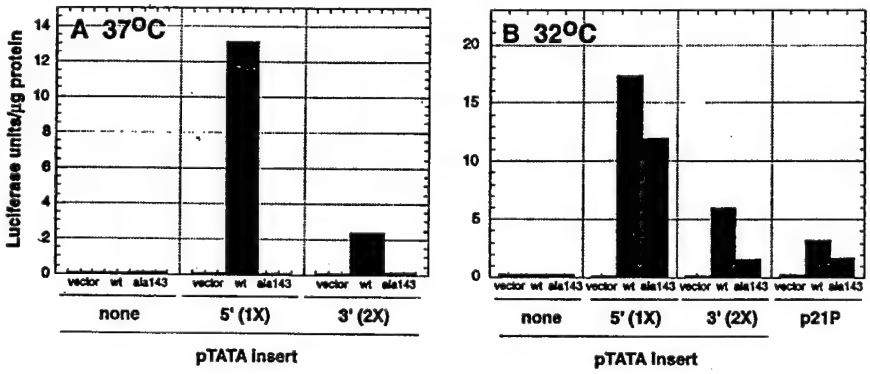

Figure 2. Two p53-response elements are present in the *p21* promoter. Saos-2 cells were transfected as described in Materials and Methods with 2 µg of the indicated reporter constructs in the absence or presence of either 50 ng of pCMV–p53wt, an expression vector encoding human wild-type p53 under the control of the CMV promoter (light and dark bars, respectively), or 50 ng of $pCMV–p53^{ala143}$, an expression vector encoding the temperature-sensitive mutant $p53^{Ala143}$ (solid bars). Cells were either maintained at 37°C (*A*) or shifted to 32°C 17 hr prior to lysis (*B*) and then were assayed for luciferase activity and total protein levels as described in Materials and Methods. The indicated values are the average of three (37°C) or four (32°C) independent experiments that had been performed in duplicate.

Two p53-binding sites are present in the human p21 promoter

Double-stranded oligonucleotides that contain the sequence of the 5′ and 3′ sites were synthesized and used in electrophoretic mobility shift assays (EMSAs). The 5′ site was bound by purified p53, and this binding was competed by an excess of unlabeled 5′ site (Fig. 3A, lanes 2–4), as well as an excess of the 3′ site (Fig. 3A, lanes 8–10), but not by an unlabeled oligonucleotide containing a mutated sequence of the 5′ site in which the C residue in the fourth position of each pentamer has been mutated to a T residue (Fig. 3A, lanes 5–7). The 3′ site competes approximately threefold less well than the 5′ site for the binding of p53 protein to a labeled 5′ site (Fig. 3A, lanes 2–4, and 8–10). The mAb 1801 supershifts the p53–5′ site complex effciently, demonstrating the presence of p53 in that complex (Fig. 3A, lane 11). As has been reported previously for a p53 consensus site (Funk et al. 1992), mAb 421 also efficiently supershifts the p53–5′ site complex and in so doing enhances the binding that is seen (Fig. 3A, lane 12).

The 3′ site also was bound by purified p53, and the binding of p53 to a labeled 3′ site was effectively competed by the unlabeled 3′ site (Fig. 3B, lanes 2–4), as well as the unlabeled 5′ site (Fig. 3B, lanes 8–10) but not the mutated 5′ site with all four C residues altered (Fig. 3B, lanes 5–7). Consistent with the results of the competition analysis using the labeled 5′ site, the unlabeled 5′ site competed threefold better for binding to the labeled 3′ site as the unlabeled 3′ site (Fig. 3B, lanes 2–4, and 8–10). mAb 1801 again supershifted the p53–3′ site complex (Fig. 3B, lane 11) efficiently. Surprisingly, in contrast to the result with the labeled 5′ site, mAb 421 appeared to inhibit the binding of p53 to the 3′ site and supershifted what little DNA-binding complex that was detected only poorly (Fig. 3B, lane 12). This latter result suggests the intriguing possibility that the optimal binding of p53 to each of these sites may require different conformations of the p53 tetramer.

Mutation of a C residue affects responsiveness to mAb 421

The 3′ site diverges from the published consensus for p53-binding sites in two positions. The residue in position 4 of the first pentamer is a G (instead of a C residue), and the residue in position 3 of the second pentamer is an A residue (instead of a pyrimidine). The binding of p53 to the labeled 3′ site is inhibited in the presence of mAb 421 (Fig. 4, lanes 9–12). However, when a 1-bp change, G^4 to C residue, was engineered in this sequence and used as the labeled probe, the binding to p53 was enhanced in the presence of mAb 421 (Fig. 4, lanes 13–16). Thus, mutation of G^4 to a C, thereby creating a site with four consensus pentamers, allowed the binding of p53 to this site to be enhanced by mAb 421.

The reverse effect could be achieved through mutagenesis of the 5′ site. This site conforms to the consensus sequence in that a C residue is present in the fourth position of each pentamer. A labeled 5′ probe bound to increasing amounts of p53 (Fig. 4, lanes 1–2) and this binding could be enhanced in the presence of mAb 421 (Fig. 4, lanes 3,4). When mutated 5′ (C^{14} to G) was labeled and used in this EMSA, its binding to p53 was inhibited in the presence of 421 (Fig. 4, lanes 5–8) just like the 3′ site (Fig. 4, lanes 9–12). Therefore, the primary sequence of the response element can determine

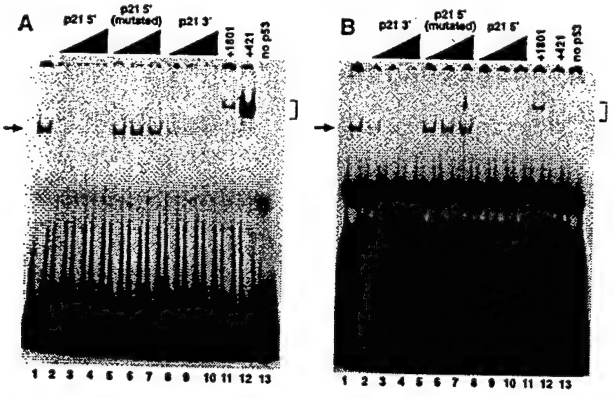

Figure 3. Monoclonal antibody enhances the binding of p53 to the 5′ site but inhibits the binding of p53 to the 3′ site. (*A*) An EMSA using as labeled probe the 5′ p53-binding site; (*B*) an EMSA using as labeled probe the 3′ p53-binding site. Five nanograms of purified p53 protein was incubated alone (lane *1*), in the presence of a 17-, 33-, or 50-fold excess of each unlabeled competitor, as indicated (lanes *2–10*), or in the presence of a 4 µl of mAb 1801 (lane *11*) or 4 µl of mAb 421 (lane *12*). p21 5′ (mutated) refers to a 5′ site in which the fourth postion of each pentamer has been mutated to a T residue. A sample that does not contain any p53 protein is shown in lane *13*. (→) The position of the p53–DNA complex; (■) the position of the supershifted p53–DNA antibody complex.

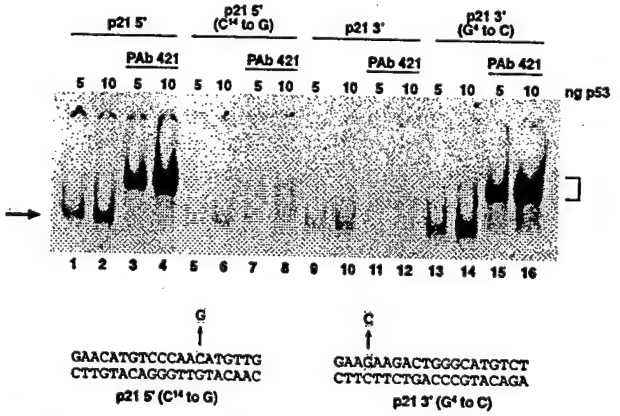

Figure 4. Mutational analysis demonstrates the importance of the C residue in the fourth position of a pentamer in responsiveness to mAb 421. Purified p53 (5 or 10 ng as indicated) was incubated with labeled probes containing the 5′ site (lanes *1–4*), the 5′ site with the residue at position 14 mutated to a G (C^{14} to G) (lanes *5–8*), the 3′ site (lanes *9–12*), or the 3′ site with the residue at position 4 mutated to a C (G^4 to C) (lanes *13–16*). The labeled probes had equivalent specific activities. Reactions were performed either in the absence (lanes *1,2,5,6,9,10,13,14*) or presence (lanes *3,4,7,8,11,12,15,16*) of mAb 421. The arrow (→) position of the p53–DNA complex; position of the supershifted p53–DNA–antibody complex.

whether the binding by p53 is enhanced or inhibited by antibody 421.

There is a p53-response element in the promoter of the human cdc25C *gene with properties similar to the 3′ site*

A search in the human genome database for other variant p53-binding sites that consist of four pentamers, only three of which contain C residues in the fourth position, was performed. A site in the promoter of the *cdc25C* gene, which encodes a cell cycle-regulated protein phosphatase that is necessary for progression into mitosis, was subjected to further analysis. A radiolabeled synthetic oligonucleotide containing a sequence from the human *cdc25C* promoter is bound by purified human p53 in an EMSA (Fig. 5A, lane 7). mAb 1801 supershifts this complex efficiently, whereas mAb 421 inhibits the binding of p53 to this site (Fig. 5A, lanes 8,9). Similar results were obtained with a radiolabeled oligonucleotide containing the sequence of the 3′ site of the *p21* promoter (Fig. 5A, lanes 4–6). These results are in contrast to the ability of mAb 421 to enhance and supershift the complex of p53 with a radiolabled oligonucleotide containing the 5′ site from the *p21* promoter (Fig. 5A, lanes 1–3). These results demonstrate that the site from the *cdc25C* promoter binds to p53 in the presence of mAb 421 with similar properties as the 3′ site from the *p21* promoter.

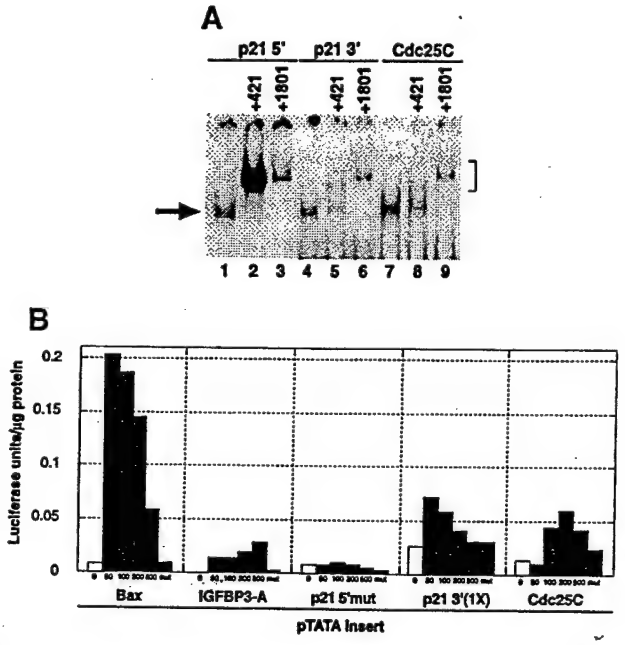

Figure 5. The p53-response element in the promoter of the human *cdc25C* gene has properties similar to the 3′ site. (*A*) An EMSA using as radiolabeled probe the 5′ site (lanes *1–3*), the 3′ site (lanes *4–6*), or the site from the *cdc25C* promoter (lanes *7–9*). The probes had an equivalent specific activity of labeling. Five nanograms of purified p53 was incubated in the absence (lanes *1,4,7*) or presence of either 4 μl of mAb 421 (lanes *2,5,8*) or the presence of 4 μl of mAb 1801 (lanes *3,6,9*). (→) The position of the p53–DNA complex, (■) position of the supershifted p53–DNA–antibody complex. (*B*) Saos-2 cells were transfected as described in Materials and Methods with 2 μg of the indicated reporter constructs in the absence (open bars) or presence of increasing amounts of pCMV–p53wt (50, 100, 200, or 500 ng, shaded bars), or 500 ng of pCMV–p53ala143 (solid bars). Appropriate amounts of the vector pCMV were added to each transfection mixture to maintain a total level of plasmid DNA of 2.5 μg. Cells were maintained at 37°C and assayed for luciferase activity and total protein levels as described in Materials and Methods. The indicated values are from a representative experiment that had been performed in duplicate.

To determine whether this p53-binding site from the *cdc25C* promoter can act as a p53-response element in cells, an oligonucleotide containing a single copy of the sequence of this site was inserted adjacent to the adenovirus *E1b* minimal promoter in a luciferase reporter plasmid. This construct was compared to constructs containing two previously characterized p53-response elements, namely one from the human bax promoter, and one of the two intronic sites found in the *IGFBP3* gene, the so-called box A site (Buckbinder et al. 1995; Miyashita and Reed 1995; Friedlander et al. 1996; Ludwig et al. 1996). These reporter constructs were compared to a plasmid containing a single copy of the 3′ site from the *p21* promoter and a plasmid containing a single copy of the 5′ site that contains all four C residues altered. Saos-2 cells were transfected with increasing amounts of the wild-type p53 expression vector in the presence of these various reporter constructs. Wild-type p53 activated reporters containing the Bax, IGFBP3-A, 3′ site, and Cdc25C sites, but not a reporter containing the mutated 5′ site (Fig. 5B). This demonstrates that the site from the *cdc25C* promoter is sufficient to confer p53-dependent transcriptional activation on a heterologous luciferase reporter construct. Thus, mAb 421 differentially affects the binding of p53 to two different genomic binding sites that can mediate p53-dependent transcriptional activation.

Discussion

The binding of the mAb 421 to p53 stimulates the ability of p53 to bind to one set of genomic sites that conform to a previously identified consensus sequence and inhibits its ability to bind to another set of genomic sites that deviate from that consensus. This ability to regulate the sequence selectivity of DNA binding by a transcription factor, even in an in vitro setting, is a novel finding. A provocative unanswered question is whether the inhibition seen in the presence of mAb 421 has a physiological counterpart in the cell such that the sequence-specific binding of p53 to elements such as the 3′ site is regulated. The relevance of the mAb 421 effect will remain an open question until cellular conditions are identified that produce selective inhibition of these variant p53-response elements. Previous studies suggest some possible mechanisms, including regulation by the coactivator p300 and phosphorylation by particular kinases. The coactivator p300 recently has been shown to stimulate the sequence-specific DNA-binding activity of p53 (Gu and Roeder 1997), and the DNA-binding activity of p53 can also be stimulated by phosphorylation by casein ki-

nase II, protein kinase C, and cyclin-dependent kinase (Meek et al. 1990; Takenaka et al. 1995; Wang and Prives 1995). Studies to examine the role of these different kinases, as well as p300, in the regulation of the ability of p53 to interact with elements such as the 3′ site in the *p21* promoter are essential to address these possibilities.

Depending on particular cellular conditions, the tumor suppressor protein p53 has been reported to induce growth arrest in both the G_1 and G_2 phases of the cell cycle, mediate an apoptotic response, or trigger alternatively a differentiation or a senescence pathway (see Gottlieb and Oren 1996; Ko and Prives 1996; Levine 1997; Sugrue et al. 1997). Because the DNA-binding activity of p53 appears to play a role in each of these physiological responses, the ability of p53 to select among various target genes to elicit a particular cellular response is central to the regulation of its biological function. To date, the identification of a mechanism for the regulation of target gene selectivity by p53 has been elusive. The results presented here, albeit under nonphysiological conditions, suggest one potential mechanism by which such selectivity may be achieved. It will be important to determine whether such a mechanism occurs during any of the various cellular responses to p53 and to identify the target genes that are relevant in each situation.

Materials and methods

Plasmids

The expression plasmids pCMV–$p53^{wt}$ and pCMV–$p53^{Ala143}$, encode the indicated human p53 protein under the control of the CMV promoter. These plasmids were referred originally to as pCMV–SN3 and pCMV–CX3, respectively. The reporter plasmid, pGL3–E1bTATA, was constructed by digesting a synthetic double-stranded oligonucleotide, GCGCGGTACCCTCGAGATGCATG AATTCGCTAGCGAGCTCAGGGTATATAATGAAGCTTGGCC, with *KpnI* and *HindIII* and cloning it into the pGL3–Basic vector (Promega), which had been double-digested with *KpnI* and *HindIII*. The resulting plasmid contains a multiple cloning region with the unique restriction sites, *KpnI*, *XhoI*, *NsiI*, *EcoRI*, *NheI*, and *SacI* upstream of the minimal adenovirus *E1b* promoter sequence and the coding region for firefly luciferase.

The following synthetic double-stranded oligonucleotides were digested with *KpnI* and either *NheI* [5′, 3′(1×), 3′(2×), Cdc25C, and Bax] or *SacI* (5′ mut and IGFBP3-A] and cloned into pGL3–E1bTATA, which had been double-digested with *KpnI* and either *NheI* or *SacI* to produce the appropriate reporter plasmids: 5′-AATTGGTACCGAACATGTCCCAACATGTTGGCTAGCGAATT; 3′-(1×)-AATTCGGTACCGAAGAAGACTGGGCATGTCTGCTAGCGAATT; 3′(2×)-AATTCGGTACCGAAGAACACTGGGCATGTCTGAAGAAGACTGGGCATGTCTGCTAGCGAATT; 5′ mut–AATTCGGTACCGAATATATCCCAATATATTGGAGCTCGAATT; Cdc25C–AATTCGGTACCGGGCAAGTCTTACCATTTCCAGAGCAAGCACGCTAGCGAATT; Bax–AATTCGGTACCTCACAAGTTAGAGACAAGCCTGGGCGTGGGCTATATTGCTAGCGAATT; and IGFBP3-A–AATTCGGTACCAAACAAGCCACCAACATGCTTTGGAGCTCGAATT.

Transfection of reporter constructs

Saos-2 cells were transfected using the DOTAP liposomal transfection reagent (Boehringer Mannheim) according to the manufacturer's instructions. Lysates were prepared, total protein concentration was determined, and luciferase assays were quantitated using a TD-20e Luminometer (Turner).

Purification and quantitation of human p53 protein

Sf9 cells that were infected with recombinant baculovirus were lysed in 20 mM HEPES (pH 7.4) containing 20% glycerol, 10 mM NaCl, 0.2 mM EDTA, 0.1% Triton X-100, 1 mM DTT, 1 mM PMSF, 50 μM leupeptin, and 50 μg/ml aprotinin (lysis buffer). Nuclei were pelleted by centrifugation at 2300 rpm and then resuspended in lysis buffer containing 500 mM NaCl. Extracts were diluted to 100 mM NaCl, applied to a 0.5-ml Ni-NTA-agarose column (Qiagen) that was equilibrated with 20 mM HEPES containing 100 mM NaCl, and eluted with 200 mM imidazole containing 10 mM HEPES, (pH 7.4) and 5 mM NaCl. Fractions of 0.5-ml were collected, dialyzed against 10 mM HEPES (pH 7.4), 5 mM NaCl, 0.1 mM EDTA, 20% glycerol, and 1 mM DTT, aliquoted, and stored at −70°C.

EMSAs

Complementary single-stranded oligonucleotides were annealed, and ends were filled using the Klenow fragment of DNA polymerase to produce the following double-stranded oligonucleotides: p21 5′-AATTCTCGAGGAACATGTCCCAACATGTTGCTCGAGAATT; p21 3′-AATTCTCGAGGAAGAAGACTGGGCATGTCTTCTACCTCGAGAATT; p21 5′ (mutated)–AATTCTCGAGGAATATATCTTGAATTCTTCCTCGAGAATT; p21 5′ (C^{14} to G)–AATTCTCGAGGAACATGTCCCAAGATGTTGCTCGAGAATT; p21 3′ (G^4 to C)–AATTCTCGAGGAACAAGACTGGGCATGTCTTCTACCTCGAGAATT; and Cdc25C–AATTCTCGAGGGGCAAGTCTTACCATTTCCAGAGCAAGCACCTCGAGAATT.

Purified p53 protein, 3 ng of labeled double-stranded oligonucleotide, and hybridoma supernatant where appropriate, were incubated in a total volume of 30 μl of DNA binding buffer containing 20 mM HEPES (pH 7.5), 83 mM NaCl, 0.1 mM EDTA, 12% glycerol, 2 mM $MgCl_2$, 2 mM spermidine, 0.7 mM DTT, 133 μg/ml BSA, and 25 μg/ml poly[d(I–C)] for 30 min at room temperature. Samples were loaded on a native 4% acrylamide gel in 0.5× TBE and electrophoresed at 4°C at 200 V for 2 hr. The gel was dried and exposed to Kodak XAR-5 film using an intensifying screen at −70°C. Bands were quantitated using the Molecular Analyst Phosphorimaging system (Bio-Rad).

Acknowledgments

We thank Bert Vogelstein for the p53 expression plasmids, and Zéev Ronai for the recombinant baculovirus expressing His-tagged human p53. Ron Magnusson is thanked for help with the recombinant baculovirus infections. Helpful discussions with Avrom Caplan, Robert Krauss, Jonathan Licht, Leslie Pick, Serafin Piñol-Roma, and, especially, Zhen-Qiang Pan are gratefully acknowledged. Members of the Manfredi laboratory are thanked for their help and support: Yvette Tang, Edward Thornborrow, Michelle Denberg, and Joyce Meng. These studies were supported by grants from the National Cancer Institute (CA69161) and the Breast Cancer Program of the U.S. Army Medical Research and Materiel Command (U.S. AMRMC; DAMD-17-97-1-7336 and DAMD-17-97-1-7337). S.S.C. was supported by a training grant from the Breast Cancer Program of the U.S. AMRMC (DAMD-17-94-J-4111).

The publication costs of this article were defrayed in part by payment of page charges. This article must therefore be hereby marked "advertisement" in accordance with 18 USC section 1734 solely to indicate this fact.

References

Aloni-Grinstein, R., I. Zan-Bar, I. Alboum, N. Goldfinger, and V. Rotter. 1993. Wild type p53 functions as a control protein in the differentiation pathway of the B-cell lineage. *Oncogene* 8: 3297–3305.

Balagurumoorthy, P., H. Sakamoto, M.S. Lewis, N. Zambrano, G.M. Clore, A.M. Gronenborn, E. Appella, and R.E. Harrington. 1995. Four p53 DNA-binding domain peptides bind natural p53-response elements and bend the DNA. *Proc. Natl. Acad. Sci.* 92: 8591–8595.

Brugarolas, J., C. Chandrasekaran, J.I. Gordon, D. Beach, T. Jacks, and G.J. Hannon. 1995. Radiation-induced cell cycle arrest compromised by p21 deficiency. *Nature* 377: 552–557.

Buckbinder, L., R. Talbott, S. Velasco-Miguel, I. Takenaka, B. Faha, B.R. Seizinger, and N. Kley. 1995. Induction of the growth inhibitor IGF-binding protein 3 by p53. *Nature* 377: 646–649.

Cross, S.M., C.A. Sanchez, C.A. Morgan, M.K. Schimke, S. Ramel, R.L. Izerda, W.H. Rashkind, and B.J. Reid. 1995. A p53-dependent mouse spindle checkpoint. *Science* 267: 1353–1355.

Deng, C., P. Zhang, J.W. Harper, S.J. Elledge, and P. Leder. 1995. Mice

lacking $p21^{CIP1/WAF1}$ undergo normal development, but are defective in G1 checkpoint control. *Cell* **82:** 675–684.

El-Deiry, W.S., S.E. Kern, J.A. Pietenpol, K.W. Kinzler, and B. Vogelstein. 1992. Definition of a consensus binding site for p53. *Nature Genet.* **1:** 45–49.

El-Deiry, W.S., T. Tokino, V.E. Velculescu, D.B. Levy, R. Parsons, J.M. Trent, D. Lin, W.E. Mercer, K. Kinzler, and B. Vogelstein. 1993. WAF1, a potential mediator of p53 tumor suppression. *Cell* **75:** 817–825.

El-Deiry, W.S., T. Tokino, T. Waldman, J.D. Oliner, V.E. Velculescu, M. Burrell, D.E. Hill, E. Healy, J.L. Rees, S.R. Hamilton, K.W. Kinzler, and B. Vogelstein. 1995. Topological control of $p21^{WAF1/CIP1}$ expression in normal and neoplastic tissues. *Cancer Res.* **55:** 2910–2919.

Friedlander, P., Y. Haupt, C. Prives, and M. Oren. 1996. A mutant p53 that discriminates between p53-responsive genes cannot induce apoptosis. *Mol. Cell. Biol.* **16:** 4961–4971.

Friedman, P.N., X. Chen, J. Bargonetti, and C. Prives. 1993. The p53 protein is an unusually shaped tetramer that binds directly to DNA. *Proc. Natl. Acad. Sci.* **90:** 3319–3323.

Funk, W.D., D.T. Pak, R.H. Karas, W.E. Wright, and J.W. Shay. 1992. A transcriptionally active DNA-binding site for human p53 protein complexes. *Mol. Cell. Biol.* **12:** 2866–2871.

Gottlieb, T.M. and M. Oren. 1996. p53 in growth control and neoplasia. *Biochim. Biophys. Acta* **1287:** 77–102.

Gu, W. and R.G. Roeder. 1997. Activation of p53 sequence-specific DNA binding by acetylation of the p53 C-terminal domain. *Cell* **90:** 595–606.

Halazonetis, T.D., L.J. Davis, and A.N. Kandil. 1993. Wild-type p53 adopts a "mutant"-like conformation when bound to DNA. *EMBO J.* **12:** 1021–1028.

Hupp, T.R., D.W. Meek, C.A. Midgely, and D.P. Lane. 1992. Regulation of the specific DNA binding function of p53. *Cell* **71:** 875–886.

Hupp, T.R., A. Sparks, and D.P. Lane. 1995. Small peptides activate the latent sequence-specific DNA binding function of p53. *Cell* **83:** 237–245.

Ko, L.J. and C. Prives. 1996. p53: Puzzle and paradigm. *Genes & Dev.* **10:** 1054–1072.

Levine, A.J. 1997. p53, the cellular gatekeeper for growth and division. *Cell* **88:** 323–331.

Ludwig, R.L., S. Bates, and K.H. Vousden. 1996. Differential activation of target cellular promoters by p53 mutants with impaired apoptotic function. *Mol. Cell. Biol.* **16:** 4952–4960.

Macleod, K.F., N. Sherry, G. Hannon, D. Beach, T. Tokino, K. Kinzler, B. Vogelstein, and T. Jacks. 1995. p53-dependent and independent expression of p21 during cell growth, differentiation, and DNA damage. *Genes & Dev.* **9:** 935–944.

Meek, D.W., S. Simon, U. Kikkawa, and W. Eckhart. 1990. The p53 tumour suppressor protein is phosphorylated at serine 389 by casein kinase II. *EMBO J.* **9:** 3253–3260.

Miyashita, T. and J.C. Reed. 1995. Tumor suppressor p53 is a direct transcriptional activator of the human bax gene. *Cell* **80:** 293–299.

Mundt, M., T. Hupp, M. Fritsche, C. Merkle, S. Hansen, D. Lane, and B. Groner. 1997. Protein interactions at the carboxyl terminus of p53 result in the induction of its in vitro transactivation potential. *Oncogene* **15:** 237–244.

Nagaich, A.K., E. Appella, and R.E. Harrington. 1997a. DNA bending is essential for the site-specific recognition of DNA response elements by the DNA binding domain of the tumor suppressor protein p53. *J. Biol. Chem.* **272:** 14842–14849.

Nagaich, A.K., V.B. Zhurkin, H. Sakamoto, A.A. Gorin, G.M. Clore, A.M. Gronenborn, E. Appella, and R.E. Harrington. 1997b. Architectural accommodation in the complex of four p53 DNA binding domain peptides with the p21/waf1/cip1 DNA response element. *J. Biol. Chem.* **272:** 14830–14841.

Shaulsky, G., N. Goldfinger, A. Peled, and V. Rotter. 1991. Involvement of wild-type p53 in pre-B-cell differentiation in vitro. *Proc. Natl. Acad. Sci.* **88:** 8982–8986.

Soddu, S., G. Blandino, G. Citro, R. Scardigli, G. Piaggio, A. Ferber, B. Calabretta, and A. Sacchi. 1994. Wild-type p53 gene expression induces granulocytic differentiation of HL-60 cells. *Blood* **83:** 2230–2237.

Sugrue, M.M., D.Y. Shin, S.W. Lee, and S.A. Aaronson. 1997. Wild-type p53 triggers a rapid senescence program in human tumor cells lacking functional p53. *Proc. Natl. Acad. Sci.* **94:** 9648–9653.

Takenaka, I., F. Morin, B.R. Seizinger, and N. Kley. 1995. Regulation of the sequence-specific DNA binding function of p53 by protein kinase C and protein phosphatases. *J. Biol. Chem.* **270:** 5405–5411.

Wang, Y. and C. Prives. 1995. Increased and altered DNA binding of human p53 by S and G2/M but not G1 cyclin-dependent kinases. *Nature* **376:** 88–91.

Grant Number: DAMD17-94-J-4111
Principal Investigator: Stuart A. Aaronson, M.D.

Supplement 1
Bibliography

A. Publications

Feinleib, J. L., and Krauss, R. S. (1996) Dissociation of ras oncogene-induced gene expression and anchorage- independent growth in a series of somatic cell mutants. Mol. Carcinog. 16: 139-148.

Kang, J. S., Gao, M., **Feinleib, J. L.**, Cotter, P. D., Guadagno, S. N., and Krauss, R. S. (1997) CDO: an oncogene-, serum-, and anchorage-regulated member of the Ig/fibronectin type III repeat family. J. Cell. Biol. 138: 203-213.

Fang, Y., **Fliss, A. E.**, Robins, D. M., and Caplan, A. J. (1996) Hsp90 regulates androgen receptor hormone binding affinity in vivo. J. Biol. Chem. 271: 28697-28702.

Fliss, A. E., Fang, Y., Boschelli, F., and Caplan, A. J. (1997) Differential In Vivo Regulation of Steroid Hormone Receptor Activation by Cdc37p. Mol. Biol. Cell 8: 2501-2509.

Fang, Y., **Fliss, A.E.**, Rao, J., and Caplan, A.J. (1998) SBA1 encodes a yeast hsp90 cochaperone that is homologous to vertebrate p23 proteins. Mol. Cell. Biol. 18:3727-3734.

Somasundaram, K., Zhang, H., Zeng, Y. X., **Houvras, Y.**, Peng, Y., Zhang, H., Wu, G. S., Licht, J. D., Weber, B. L., and El-Deiry, W. S. (1997) Arrest of the cell cycle by the tumour-suppressor BRCA1 requires the CDK-inhibitor p21WAF1/CIP1. Nature 389: 187-190.

Kimmelman, A., Tolkacheva, T., Lorenzi, M.V., **Osada, M.**, and Chan, A.M.-L. (1997) Identification and characterization of R-ras3: a novel member of the RAS gene family with a non-ubiquitous pattern of tissue distribution Oncogene 15: 2675 - 2686.

Spanopoulou, E., Zaitseva, F., Wang, F. H., **Santagata, S.**, Baltimore, D., and Panayotou, G. (1996) The homeodomain region of Rag-1 reveals the parallel mechanisms of bacterial and V(D)J recombination. Cell 87: 263-276.

Santagata, S., Aidinis, V., and Spanopoulou, E. (1998) The effect of Me2+ cofactors at the initial stages of V(D)J recombination. J. Biol. Chem. 273: 16325-16331.

Villa, A., **Santagata, S.**, Bozzi, F., Giliani, S., Frattini, A., Imberti, L., Benerini Gatta, L., Ochs, H.D., Schwarz, K., Notarangelo, L.D., Vezzoni, P., and Spanopoulou, E. (1998) Partial V(D)J recombination activity leads to Omenn syndrome. Cell 93: 885-896

Chen, J., Bander, J. A., **Santore, T. A.**, Chen, Y., Ram, P. T., Smit, M. J., and Iyengar, R. (1998) Expression of Q227L-galphas in MCF-7 human breast cancer cells inhibits tumorigenesis. Proc. Natl. Acad. Sci. USA 95: 2648-2652.

Resnick-Silverman, L., **St. Clair, S.**, Maurer, M., Zhao, K., and Manfredi, J.J. (1998) Identification of a novel class of genomic DNA binding sites suggests a mechanism for selectivity in target gene activation by the tumor suppressor protein p53. Genes Dev. 12:2102-2107.

B. Presentations

None.

C. Meeting Abstracts

Gao, M., Kang, J.-S., Fenleib, J.L., Guadagno, S.N. and Krauss, R.S. (1996) CDO: a serum-, oncogene-, and anchorage-regulated gene that encodes a novel member of the immunoglobulin superfamily. 6th International Congress on Cell Biology and 36th American Society for Cell Biology Annual Meeting (San Fransisco, CA). Mol. Biol. Cell 7(Suppl.):172a.

Osada, M., Tolkacheva, T., Li, W., and Chan, A.M. (1997) The role of R-ras in cellular transformation and cell adhesion. The 13th Annual Meeting on Oncogenes (Frederick, MD).

Resnick-Silverman, L., **St. Clair, S.**, Zhao, K., Meng, J., and Manfredi, J.J. (1998) Identification of a novel class of genomic DNA binding sites suggests a mechanism for selectivity in target gene activation by the tumor suppressor protein p53. Ninth p53 Workshop (Crete, Greece).

St. Clair, S., Kaelin, W.G., Jr., and Manfredi, J.J. (1998) The p53-related protein p73 activates transcription via p53 binding sites. Ninth p53 Workshop (Crete, Greece).

Resnick-Silverman, L., **St. Clair, S.**, Maurer, M., Zhao, K., Denburg, M., Meng, J., and Manfredi, J.J. (1998) Identification of a novel class of genomic DNA binding sites suggests a mechanism for selectivity in target gene activation by the tumor suppressor protein p53. 63rd Symposium: Mechanisms of Transcription (Cold Spring Harbor, NY).

St. Clair, S., Denburg, M., Kaelin, W.G., and Manfredi, J.J. (1998) The tumor suppressor p53 mediates sequence-specific repression via an element derived from the human cdc25c promoter. Meeting on Cancer Genetics and Tumor Suppressor Genes (Cold Spring Harbor, NY).

Supplement 2
Personnel Receiving Pay

Trainee	Dates of Support				Total Months of Support
	Year One	Year Two	Year Three	Year Four	
Jessica Feinlieb		7/1/95-6/30/96	7/1/96-6/30/97	7/1/97-6/30/98	36
Albert Fliss			10/1/96-6/30/97	7/1/97-6/30/98	21
Maxim Fonarev	7/1/94-6/30/95	7/1/95-6/30/96			24
Ulrich Hermanto	7/1/94-6/30/95	7/1/95-6/30/96	7/1/96-8/31/96		26
Yariv Houvras			7/1/96-6/30/97	7/1/97-6/30/98	24
Wei Li		7/1/95-6/30/96	7/1/961/31/97		19
Masako Osada			9/1/96-6/30/97	7/1/97-6/30/98	22
Selvon St. Clair			2/1/97-6/30/97	7/1/97-6/30/98	17
Sandro Santagata			7/1/96-6/30/97	7/1/97-6/30/98	24
Tara Santore	7/1/94-6/30/95	7/1/95-6/30/96	7/01/96-9/30/96		27

Supplement 3
Graduate Degrees Resulting from Grant Award

Ph.D., Albert Fliss